Bulletin
of
The Geological Society of America

VOLUME 66 September 1955 NUMBER 9

CONTENTS

	Pages
Crustal structure of the Arctic regions from the L_g phase. By Jack Oliver, Maurice Ewing, and Frank Press	1063–1074
Sphericity and roundness of quartz grains in sediments. By J. R. Curray and J. C. Griffiths	1075–1096
Spilitic intrusion near Ladron Peak, Socorro County, New Mexico. By Robert W. Duschatko and Arie Poldervaart	1097–1108
Violent mud-volcano eruption of Lake City hot springs, northeastern California. By Donald E. White	1109–1130
Isotopic composition and distribution of lead, uranium, and thorium in a Precambrian granite. By George R. Tilton, Claire Patterson, Harrison Brown, Mark Inghram, Richard Hayden, David Hess, and Esper Larsen, Jr.	1131–1148
Deformation of the Northeastern Pacific basin and the west coast of North America. By Henry W. Menard	1149–1198
Short Notes	
Interpretation of Gutenberg's low-velocity lithosphere channel. By M. H. P. Bott	1199–1202
Low-velocity lithosphere channel. By B. Gutenberg	1203–1204
Canons of landscape evolution—a discussion. By H. D. Thompson	1205
Reply to comment by H. D. Thompson. By Lester C. King	1205–1206
Canons of landscape evolution—a discussion. By John R. Schultz	1207–1212
Peneplanation and pediplanation. By C. A. Cotton	1213–1214
Reply to Professor Cotton. By L. C. King	1214

Subscription $15.00 per year.

Printing Office: Mt. Royal & Guilford Aves., Baltimore 2, Md.

Communications for publications should be addressed to The Geological Society of America, Dr. H. R. Aldrich, Secretary, 419 West 117 Street, New York, N. Y.

Please give notice of change of address 4 weeks in advance. Claims for non-receipt of the Bulletin of a given month must be sent to the Secretary of the Society before the end of the second succeeding month.

Entered as second-class matter at the Post Office at Baltimore, Md., under the Act of Congress of July 16, 1894.
Accepted for mailing at special rate of postage provided for in Section 1103 Act of October 3, 1917, authorized on July 8, 1918.

PAPERS IN PRESS FOR FORTHCOMING ISSUES

Welded Tuffs of Chiricahua National Monument, Arizona. By Harold E. Enlows

Geology of the Blue Ridge near Harpers Ferry, West Virginia. By Richard P. Nickelsen

Experimental Deformation of Hasmark Dolomite. By John Handin and H. W. Fairbairn

Geology of the Bridger Range, Montana. By William J. McMannis

Precambrian Monazite and Zircon from the Mountain Pass Rare-earth District, San Bernardino County, California. By Howard W. Jaffe

Experimental Study of the Strength of Rocks. By Eugene C. Robertson

Origin of Playa Stone Tracks, Racetrack Playa, Inyo County, California. By George M. Stanley

BULLETIN OF THE GEOLOGICAL SOCIETY OF AMERICA
VOL. 66, PP. 1063-1074, 1 FIG., 3 PLS. SEPTEMBER 1955

CRUSTAL STRUCTURE OF THE ARCTIC REGIONS FROM THE L_g PHASE

BY JACK OLIVER, MAURICE EWING, AND FRANK PRESS

ABSTRACT

The presence of the L_g earthquake surface-wave phase, which is indicative of continental structure between the epicenter and recording station, is used in the exploration of Arctic regions. Water-covered areas of continental structure include the Canadian archipelago, parts of Baffin Bay and Davis Strait, the Barents Sea, Bering Strait, and the shallow parts of the Bering and Greenland seas. Areas of noncontinental structure include the Arctic Ocean, Beaufort Sea, Norwegian Sea, and the deep parts of the Bering and Greenland seas.

CONTENTS

TEXT

	Page
Introduction	1063
Procedure	1070
Results	1071
Summary	1073
References cited	1073

ILLUSTRATIONS

Figure	Page
1. Rayleigh-wave dispersion across the Arctic Ocean Basin	1072

Plate	Facing page
1. Seismograms: L_g across Barents Sea to Copenhagen	1070
2. Seismograms	1071
3. Paths across Arctic regions	1074

TABLE

Table	Page
1. Master list of shocks used in Arctic study	1064

INTRODUCTION

In a recent paper Press and Ewing (1952, p. 219) described a seismic surface wave of unusually large amplitudes and characteristic appearance traveling only over paths of continental structure. Although an adequate theory for this phase is not yet available, discrimination of crustal columns other than that typical of continents against the phase suggested the possibility of using its presence or absence to explore regions of unknown crustal structure. The Gulf of Mexico was cited (Press and Ewing 1952, p. 228) as an area through which L_g did not propagate; this indicated a non-continental structure for the underlying rocks, a conclusion subsequently borne out by seismic-refraction work. This paper presents the results of a similar study for the Arctic regions.

Press and Ewing assigned the symbol L_g to the phase $-L$ because the particle motion was predominantly of the *SH* or Love type, and *g* because the waves were thought to be the surface-wave counterpart of S_g, propagated to great distances by a wave-guide mechanism in the silicic crust. They presented experimental data for paths across North America, largely using earthquakes along the west coast recorded at Palisades.

Some sample seismograms illustrating the L_g phase are shown in Plates 1 and 2. Its distinctive characteristics are:

(1) Sharp commencements with periods usually from ½ to 4 seconds, but occasionally as high as 7 seconds. In general, earthquakes slightly offshore or those at very great distances do not produce the shorter periods.

(2) Amplitudes far larger than those of any other phase in the same period range for continental paths.

(3) Approximately equal amplitudes on all components at the beginning of the phase, but greater amplitudes on the transverse horizontal component after a few cycles.

(4) A velocity of about 3.5 km/sec. for the beginning. This velocity may vary slightly over different paths but it is very close to the shear-wave velocity in the upper 15 km of continental crust (Katz, 1954, p. 1343).

TABLE 1.—MASTER LIST OF SHOCKS USED IN ARCTIC STUDY

Berkeley group (B); College (C); Copenhagen (G); Sitka (K); Palisades (P); Lund (L); Resolute Bay (R); Scoresby Sound (S); Uppsala (U); Ivigtut (V).

No.	Date D-M-Y	Hour	Lat.	Long.	Geographical loc.	Depth	Mag.	Δ in km	Lg	Lg Vel. in km/sec	Comp	Remarks
B1	22–4–51	12 36 16	76°N	73°W	Baffin Bay	.....	...	4500	Yes	3.5	Z	Mineral—poor data for Lg
								4810	Yes	3.45	Z	Mt. Hamilton—poor data for Lg
B2	6–6–51	16 10 52	71½N	8°W	Jan Mayen	60	7	..	No	..	....	Mineral
									No	..	....	Fresno
C1	2–2–50	23 33 38	22N	100½E	S. Yunnan Prov. China	.....	6¾	..	No	..	....	.....
C2	3–2–50	16 45 29*	54N	162W	Aleutians	.....	...	1440	Yes	3.23	E	Excellent Lg—Long Period Preceding
C3	4–2–50	02 07 53*	54N	162W	Aleutians	.....	...	1440	Yes	3.27	E	Same as above
C4	7–2–50	10 37 22	46N	152E	Kurile Isl.	.....	...	..	No	..	....	.....
C5	18–2–50	14 39 30	54N	164W	Aleutians	.....	...	1500	Yes	3.26	E	.....
C6	27–3–50	13 04 04	53½N	173E	Aleutians	.....	...	..	No	..	....	.....
C7	4–4–50	18 44 10	52N	101E	Border USSR & Outer Mongolia	.....	6½	..	No	..	....	S.P. Benioff only
C8	5–4–50	01 17 15	52N	177W	Aleutians	.....	...	..	No	..	....	S.P. Benioff only
C9	26–4–50	12 18 28	53N	170W	Aleutians	60	...	..	Possibly	..	Z, E	No H.F.
C10	5–6–50	11 16 12	87N	45E	No. Polar Region	.....	...	..	No	..	....	Good dispersed train of surface waves
C11	27–6–50	15 41 54	45½N	140E	Off Hokkaido	.....	6½	..	No	..	....	.....
C12	9–7–50	16 09 55	36N	72E	Pakistan	.....	...	..	No	..	....	.....
C13	12–7–50	11 09 15	53N	166W	Aleutians	.....	6¼	1400	Yes	3.48	E	.....
C14	14–7–50	12 06 45	52N	171W	Aleutians	.....	...	..	No	..	....	.....
C15	8–8–50	05 12 00	55N	134½W	S.E. Alaska	.....	...	1250	Possibly	..	E	Not a good Lg
C16	15–8–50	14 09 30 Aftershocks	28½N	97E	CBI Border	.....	8½	..	No	..	....	.....
C17	22–8–50	07 40 07	53N	160E	Off Kamchatka	Deeper than normal	...	..	No	..	....	.....
C18	2–9–50	02 47 23	52½N	169W	Aleutians	100	6¾	1820	Yes	3.52	E	.....
C19	10–9–50	03 21 20	35N	140E	Near Honshu	.....	6¾	..	No	..	....	.....

						than normal						
C18	2–9–50	02 47 23	52½N	169W	Aleutians	100	6¾	1820	Yes	3.52	E	.....
C19	10–9–50	03 21 20	35N	140E	Near Honshu	.....	6¾	..	No	..	....	.....
C20	16–9–50	21 58 15	52½N	178E	Aleutians	100	6.6	2180	No	..	....	.....
C21	28–9–50	21 47 01	54½N	134½W	Qu. Charlotte Isl.	.....	...	5900	Possibly	..	E	.....
C22	5–11–50	17 37 25	33N	134½E	Off Shikoku, Japan	.....	...	..	No	..	....	.....
C23	22–11–50	10 16 26*	51N	176W	Aleutians	.....	...	..	No	..	....	.....
C24	9–1–51	16 00 24	81N	122E	Arctic Ocean	.....	6¾–6½	..	No	..	....	Good dispersed train of surface waves
C25	15–1–51	01 50 36 02 29 46	51N	178½E	Aleutians	.....	...	..	No	..	....	.....
C26	18–1–51	21 15 50	52N	177W	Aleutians	.....	...	..	No	..	....	.....
C27	24–1–51	07 17 01	33N	115¾W	California	.....	6	..	No	..	....	.....
C28	12–2–51	17 22 02	66N	136E	Siberia	.....	...	..	No	..	....	.....
C29	5–3–51	14 46 00	53N	163W	S. of Alaska Pen.	.....	...	..	No	..	....	.....
C30	5–3–51	20 11 45	29N	128E	Ryukyu Isl.	150	7	..	No	..	....	.....
C31	19–3–51	20 28 55	57N	160E	Kamchatka	.....	...	..	No	..	....	.....
C32	14–4–51	13 32 59	61N	136E	Siberia	.....	...	..	No	..	....	.....
C33	22–4–51	12 36 16	76N	73W	Baffin Bay	.....	...	2790	Doubtful	3.27	E	Weak
C34	29–4–51	07 35 46	80½N	121E	Arctic Ocean	.....	...	..	No	..	....	Good dispersed train of surface waves
C35	25–4–51	21 59 35	81N	121E	Arctic Ocean	.....	...	..	No	..	....	.....
C37	10–3–51	19 44 52 19 47 14	51N	180W	Aleutians	60	...	..	No	..	....	.....
C38	5–6–51	16 57 47	30N	132E	Kyushu	100	6¾–7	..	No	..	....	.....
C39	6–6–51	16 10 52	71½N	8W	Jan Mayen	60	7	4640	Doubtful	3.34	E	No H.F.
C40	9–7–51	01 30 28	32½N	139E	Off Honshu, Japan	.....	...	..	No	..	....	.....
C41	14–7–51	07 18 12	47N	154½E	Kuriles	.....	...	..	No	..	....	.....
C42	19–7–51	20 41 25 21 07 07	51½N	177½W	Aleutians	60	6	..	No	..	....	.....
C43	22–7–51	09 01 02	51N	178½W	Aleutians	60	...	..	No	..	....	.....
C44	26–7–51	10 00 00	41N	143E	Hokkaido	600	6¼	..	No	..	....	.....
C45	28–7–51	23 04 33	37N	143E	Honshu	.....	6	..	No	..	....	.....
C46	11–8–51	09 54 20	55N	163E	Off Kamchatka	.....	...	..	No	..	....	.....

TABLE 1—*Continued*

No.	Date D-M-Y	Hour	Lat.	Long.	Geographical loc.	Depth	Mag.	Δ in km	Lg	Lg Vel. in km/sec	Comp	Remarks
C47	13–8–51	18 33 40	43N	32½E	Black Sea	.....	6½	..	No	..	....	.....
C48	24–8–51	14 21 15	47N	151E	Kuriles	.....	6½	..	No	..	....	.....
C49	12–9–51	15 10 18	45½N	151E	Kuriles	.....	...	..	No	..	....	.....
C50	1–10–51	10 11 40	55N	166W	Aleutians	.....	...	1480	Yes	3.57	E	.....
C51	15–10–51	21 01 57	33N	134E	Shikoku	.....	...	..	No	..	....	.....
C52	18–10–51	08 26 23	42N	142E	Hokkaido	100	6¾	..	No	..	....	.....
C53	21–10–51	22 07 55	44½N	151E	Kuriles	.....	...	..	No	..	....	.....
C54	6–11–51	16 40 02	47N	154E	Kuriles	.....	7¼	..	No	..	....	.....
C55	8–11–51	13 45 39	54½N	160W	Off Alaska Pen.	.....	6½	..	No	..	....	.....
C56	12–11–51	08 09 26	47N	154E	Kuriles	.....	6½	..	No	..	....	.....
C57	15–11–51	19 42 12	52½N	160½E	Kamchatka	60	6¼	..	No	..	....	.....
C58	18–11–51	09 35 43	31N	90½E	E. Tibet	.....	7½	..	No	..	....	.....
C59	24–11–51	04 30 24	57½N	176½W	Aleutians	60	...	..	No	..	....	.....
C60	21–12–51	08 37 28	26½N	100E	Yunnan, China	.....	...	..	No	..	....	.....
C61	25–12–51	15 58 28	49N	155½E	Kuriles	60	...	..	No	..	....	.....
C62	12–3–52	12 13 10	64N	22W	W. Coast of Iceland	.....	...	..	No	..	....	.....
C63	19–3–52	09 04 18	41N	125E	Korea	.....	...	..	No	..	....	.....
C64	1–4–52	00 37 41.5	48.0N	113.8W	N.W. Montana	.....	...	2750	Yes	3.50	E	Weak
C65	19–6–52	12 12 56	23N	100E	S. Yunnan Prov., China	.....	6½	..	No			
C66	17–8–52	16 02 05	30½N	91½E	Tibet	.....	7¼	..	No	..	....	.....
C67	14–9–52	09 34 10	34N	93½E	Shanghai, China	.....	...	..	No	..	....	.....
C68	30–9–52	12 52 00	28½N	102E	China	.....	6½	8030	Yes	3.66	E	No H.F. Also recorded at Uppsala
C69	10–10–52	18 47 37	30½N	69E	Cent. Pakistan	.....	...	..	No	..	....	.....
C70	8–12–52	15 09 30	23N	99½E	CBI Border	.....	...	..	No	..	....	.....
C71	10–12–52	05 58 06	71N	7W	Jan Mayen Isl.	.....	...	..	No	..	....	Looks slightly deep, perhaps 100 km
C72	23–11–47	09 46 05.5	47°47′N	112°02′W	S. W. Montana	.....	...	3120	Yes	3.59	N, E	Excellent Lg
C73	28–1–48	15 51.3	38N	68E	Turkistan	.....	...	..	No	..	....	.....
C74	18–2–48	20 29.8	82N	43E	Arctic Region	.....	6¾	..	No	..	....	.....
C75	25–5–48	07 11.3	30N	99½E	Siking Prov. China	.....	7¼	..	No	..	....	.....
C76	28–9–48	21 36.6	23N	94E	Burma	.....	...	..	No	..	....	.....

C73	28–1–48	15 51.3	38N	68E	Turkistan	.....	...	..	No	..	....	.....
C74	18–2–48	20 29.8	82N	43E	Arctic Region	.....	6¾	..	No	..	....	.....
C75	25–5–48	07 11.3	30N	99½E	Siking Prov. China	.....	7¼	..	No	..	....	.....
C76	28–9–48	21 36.6	23N	94E	Burma	.....	...	..	No	..	....	.....
G1	18–2–48	20 29.8	82N	43E	Arctic Region	.....	...	3080	Yes	3.68	....	Excellent Lg
G2	26–4–48	09 32 20	51N	34W	N. Atlantic	.....	...	3070	No	..	....	Good Rayleigh wave dispersion
G3	8–7–48	12 34.6	71N	6W	Near Jan Mayen Land	.....	...	1920	No	..	....	.....
G4	28–8–48	02 27.8	57N	161E	Kamchatka	.....	...	7170	No	..	....	.....
G5	2–3–49	06 54.6	72N	3W	Arctic Ocean	.....	...	2290	No	..	....	.....
G6	19–4–49	15 19.2	48N	154E	Kuriles	.....	...	7950	No	..	....	.....
G7	27–9–49	15 30 43	60N	149W	S. Alaska	.....	...	4930	No	..	....	.....
G8	6–6–51	16 10 52	71½N	8W	Jan Mayen	60	7	2600	No	..	....	.....
G9	12–2–51	17 22 02	66N	136E	Siberia	.....	...	5675	Doubtful	3.27	N	Weak if present
G10	14–4–51	13 32 39	61N	136E	Siberia	.....	...	6120	Yes	3.38	N, E, Z	No H.F.
K1	2–2–50	23 33 38	22N	100½E	S. Yunnan Prov. China	.....	6¾	..	No	..	....	.....
K2	4–4–50	18 44 10	52N	101E	Border USSR & Outer Mongolia	.....	6½	..	No	..	....	.....
K3	5–6–50	11 16 12	87N	45E	N. Polar Region	.....	...	..	No	..	....	.....
K4	9–7–50	16 09 53	36N	72E	Pakistan	.....	...	..	No	..	....	.....
K5	26–8–50	04 39 27	65N	162W	150 mi. NW of Nome	.....	6½	..	No	..	....	.....
K6	12–2–51	17 22 02	66N	136E	Siberia	.....	...	..	No	..	....	.....
K7	14–4–51	13 32 59	61N	136E	Siberia	.....	6¾	3650	No	..	....	.....
K8	22–4–51	12 36 16	76N	73W	Baffin Bay	.....	...	3200	Yes	3.30	N, E	
K9	6–6–51	16 10 52	71½N	8W	Jan Mayen	60	7	..	No	..	....	.....
K10	13–8–51	18 33 40	43N	32½E	Black Sea	.....	6½	..	No	..	....	.....
K11	18–11–51	09 26 33 09 35 43	31N	90½E	E. Tibet	.....	7½	..	No	..	....	.....
K12	21–12–51	08 37 28	26½N	100E	Yunnan, China	.....	...	..	No	..	....	.....
K13	31–10–35	18 37 49	46½N	112W	Helena, Mont.	.....	...	1790	Yes	3.55	....	Periods less than 4 sec

TABLE 1—*Continued*

No.	Date D-M-Y	Hour	Lat.	Long.	Geographical loc.	Depth	Mag.	Δ in km	Lg	Lg Vel. in km/sec	Comp	Remarks
L1	12–2–51	17 22 02	66N	136E	Siberia	.....	...	5650	Doubtful	3.23	NW	Very weak
L2	14–4–51	13 32 59	61N	136E	Siberia	.....	...	6100	Yes	3.44	NW, NE	No H.F.
P1	19–6–52	12–12–56*	23N	100E	S. Yunnan Prov. China	.....	6½	12950	No	..	....	.....
P2	17–8–52	16 02 05*	30½N	91½E	Eastern Tibet	.....	...	11950	No	..	....	.....
P3	14–9–52	09 34 10*	34N	93½E	Shanghai Prov.	.....	...	11600	No	..	....	.....
P4	30–9–52	12 52 00*	28½N	102E	Szechwan Prov. China	.....	6½	12300	No	..	....	.....
P5	27–11–52	07 20 13*	37N	70E	N. Afghanistan	.....	...	10600	No	..	....	Weak at Palisades
P6	8–12–52	15 09 30*	23N	99½E	China-Burma Border	.....	...	12800	No	..	....	.....
P7	12–2–51	17 22 02	66N	136E	Near Verkhoyanski Mts., Siberia	.....	6½	..	No	..	....	Poor records
P8	14–4–51	13 32 59*	61N	136E	Near Verkhoyanski Mts., Siberia	.....	6¾	8350	No	..	....	.....
P9	22–4–51	12 36 16*	76N	73W	Baffin Bay	.....	...	3900	Yes	3.58	Z	.....
P10	29–4–51	07 35 46*	80½N	121E	Arctic Ocean	.....	...	6430	No	..	....	.....
P11	6–6–51	16 10 52	71½N	8W	Jan Mayen	60	7	4900	No	..	....	.....
P12	12–2–53	04 31 16*	65N	133W	Yukon, Canada	.....	...	4550	Yes	3.57	N	Excellent Lg
R1	22–4–51	12 36 16	76N	73W	Baffin Bay	.....	...	610	Yes	3.76	....	Velocity doubtful
R2	6–6–51	16 10 52	71½N	8W	Jan Mayen	60	7	2600	Doubtful	3.60	Z	Only fair at Resolute. No H.F.
R3	27–9–51	19 24 12	49N	129W	Off Vancouver, B.C.	.....	...	3200	Yes	3.54	Z	.....
R4	20–9–51	12 38 40	65N	154W	Central Alaska	.....	...	2350	Yes	3.46	E	.....
R5	12–2–51	17 22 02	66N	136E	Siberia	.....	6½	..	No	..	....	.....
S1	1–3–29	07 31 0	50.2N	130.7W	Off Vancouver Island	.....	...	5440	Doubtful	3.63	E	No H.F.—not a good Lg

S1	1–3–29	07 31 0	50.2N	130.7W	Off Vancouver Island	.....	...	5440	Doubtful	3.63	E	No H.F.—not a good Lg
S2	4–7–29	04 28 28	63.2N	147.3W	Central Alaska	.....	...	4550	No	..	....	.....
S3	4–7–29	07 14 18	55.7N	35.5W	N. Atlantic Ocean	.....	...	1770	No	..	....	Good train of dispersed surface waves
S4	4–7–29	07 31 10	55.7N	35.5W	N. Atlantic Ocean	.....	...	1770	No	..	....	Good train of dispersed surface waves
S5	4–7–29	05 56 32	55.7N	35.5W	N. Atlantic Ocean	.....	...	1770	No	..	....	Good train of dispersed surface waves
S6	25–3–32	23 58 39	62.5N	153.3W	Near Anchorage, Alaska	.....	...	4760	Doubtful	3.53	E	Not a sharp Lg
S7	28–7–34	21 37 04	55N	156.8W	Off Alaska Peninsula	.....	...	5490	No	..	....	.....
S8	24–9–35	22 12 25	49.3N	129.2W	Off Vancouver Island	.....	...	5490	Yes	3.32	....	S.P. missing—L.P. insts. may have missed beginning
S9	22–3–38	15 22 11	57.6N	132.1W	Off. Qu. Charlotte Islands	.....	...	5270	Yes	3.55	E	S.P. missing
S10	29–5–40	01 57 46	66.6N	135.4W	Near MacKenzie River	.....	...	3990	Yes	3.42	Z	Excellent—very H.F. some L.P.
S11	30–7–41	01 51.5	60.9N	149.2W	Near Anchorage	.....	...	4870	No	..	....	.....
S12	28–2–48	01 58 05	53.5N	133W	Qu. Charlotte Islands	.....	...	5450	No	..	....	.....
S13	27–6–48	21 39.2	56N	158W	S. of Alaska Peninsula	.....	...	5520	No	..	....	.....
S14	23–8–49	20 24 32	53N	132W	Off Brit. Columbia	.....	...	5210	Yes	3.52	N	Good Lg
S15	31–10–49	01 39 32	56N	135W	Sitka, Alaska	.....	...	5000	Yes	3.49	E	Good Lg but not very H.F.
S16	27–3–50	13 04 04	53.5N	173E	Aleutians	.....	...	6290	No	..	....	.....
S17	6–4–50	21 48 02	49N	129W	Vancouver, B.C.	.....	...	5530	No	..	....	.....
S18	5–6–50	11 16 16	87N	50E	North Polar Region	.....	...	2080	No	..	....	.....
S19	20–6–50	14 11 45	74.5N	80E	Jan Mayen	.....	...	1080	No	..	....	Good train of dispersed waves
S20	12–7–50	11 09 15	53N	166W	Aleutians	.....	...	5990	No	..	....	.....
S21	12–2–51	17 22 02	66N	136E	Siberia	.....	...	..	No	..	....	.....
S22	14–4–51	13 32 59	61N	136E	Siberia	.....	...	..	No	..	....	.....

TABLE 1—*Concluded*

No.	Date D-M-Y	Hour	Lat.	Long.	Geographical loc.	Depth	Mag.	Δ in km	Lg	Lg Vel. in km/sec	Comp	Remarks
U1	6–6–51	16 10 52	71½N	8W	Jan Mayen	60	7	2600	No	..	....	Poor records for Lg
V1	15–4–45	02 35.2	56N	164E	Off Kamchatka	.....	...	5840	No	..	....	.....
V2	8–11–45	09 05 41	81N	7W	Greenland Sea	.....	...	2560	Yes	3.73	N	Good H.F.
V3	8–11–45	10 62.5	81N	7W	Greenland Sea	.....	...	2560	Yes	3.66	N	.....
V4	12–1–46	20 25.7	59N	147.5W	Gulf of Alaska	.....	...	4970	No	..	....	.....
V5	1–4–46	12 28.9	54N	164W	Aleutians	.....	...	6040	No	..	....	.....
V6	16–10–47	02 09 45	64.5N	148.8W	40 mi. S.W. of Fairbanks	.....	...	4660	Yes	3.68	Z	Good H.F.

(5) Reverse dispersion, *i.e.*, the shorter periods have the higher group velocities. Periods increase to about 10–15 seconds. Dispersion is not as regular as that of Rayleigh waves over oceanic paths.

(6) Superposition occasionally on the classical long-period Love waves.

(7) A duration far longer than might be expected for the short-period segment of classical Love waves.

(8) Occurrence only when the entire path is continental. Insertion of a 100 km segment of oceanic crustal structure is sufficient to prevent the appearance of L_g on the seismogram.

This sensitivity of L_g to horizontal variations in the crustal column forms the basis of this paper. The capacity to distinguish between areas of continental and noncontinental structure is limited only by the geographical distribution of suitable epicenters and recording stations.

This research was made possible through support and sponsorship extended by the Geophysics Research Division of the Air Force Cambridge Research Center under Contract AF 19(122)441.

PROCEDURE

The Arctic was chosen for the first application of the method because it includes several interesting localities of uncertain structure and because many seismograms with Arctic paths are available. Stations that supplied records from the following instruments were: College—Wenner EW, Benioff short period Z, McComb-Romberg NS and EW; Sitka—Wenner NS and EW; Resolute Bay—Sprengnether NS, EW, Z, Columbia Z; Palisades—Columbia NS, EW, Z, Benioff long and short period NS, EW, Z; Scoresby Sund—Galitzin-Wilip NS, EW, Z; Ivigtut—Wiechert NS, EW, Grenet Z; Copenhagen—Galitzin-Wilip, NS, EW, Z, Benioff short period Z; Uppsala—Wiechert NS, EW, Grenet Z; Lund—Wiechert NE-SW, NW-SE; Berkeley—Galitzin NS, EW, Z; Fresno—Sprengnether NS, EW, Z.

Table 1 lists all the paths studied. Each path is designated by a letter which indicates the recording station and a number which indicates the particular shock as listed at that

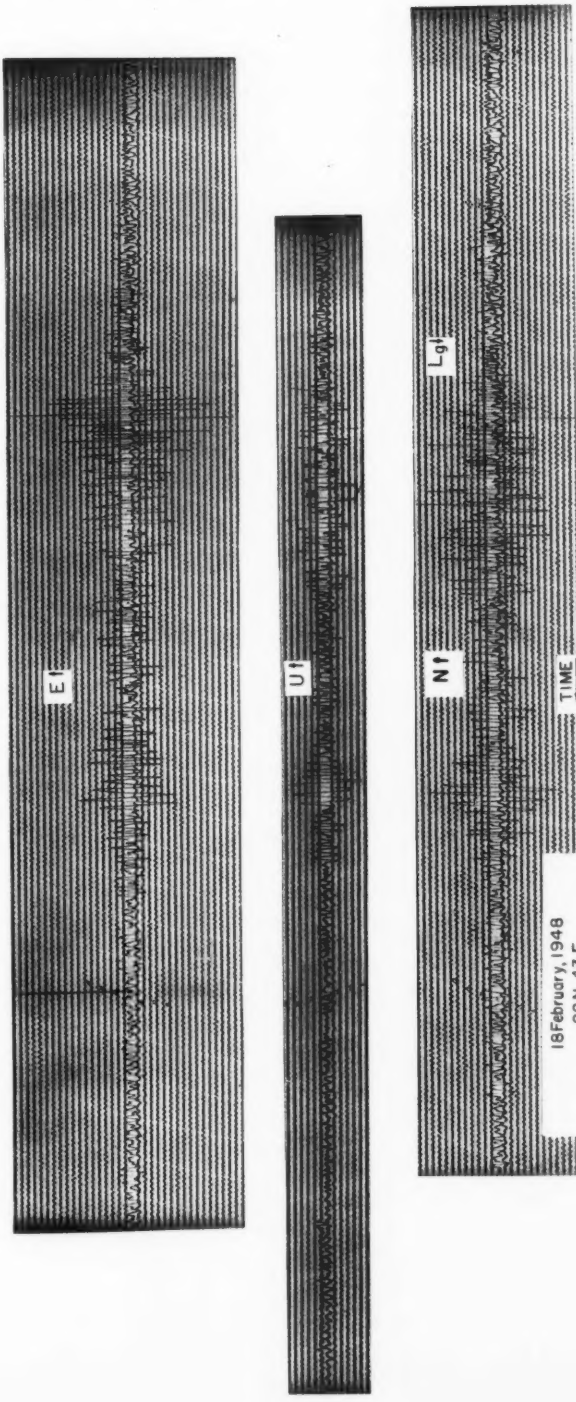

SEISMOGRAMS: Lg ACROSS BARENTS SEA TO COPENHAGEN

FIGURE 1. L_g, ALEUTIANS TO COLLEGE, ALASKA

FIGURE 2. L_g, SOUTHWEST MONTANA TO COLLEGE, ALASKA

SEISMOGRAMS

station. With this system the same shock recorded at different stations will have more than one path symbol, *e.g.*, the shock of 12 February 1951 has path symbols P7 to Palisades, C28 to College and K6 to Sitka.

All records were carefully examined for L_g, and the velocity of the commencement of the phase was calculated. When considerable energy was recorded at the expected arrival time for L_g but the distinctive characteristics of L_g, primarily the high frequencies, were absent, the path was labeled doubtful. No attempt was made to study variations in velocity, primarily because many of the records do not show good high-frequency beginnings. Furthermore, many of the velocities printed here may be approximate because of possible errors in epicentral location. This is especially true for the shorter paths, like the Alaskan peninsula shocks to College where a small error would be a significant portion of the path.

Some difficulties in applying the method are:

(1) The location of many epicenters near shore and offshore, which prohibits exploration of other segments of the path since L_g excitation is always in doubt. To circumvent this, two or more recording stations can be used to span the segment in question, in which case the station nearer the epicenter will determine the degree of L_g excitation and the farther one the effect of the intervening segment on the phase.

(2) Excitation effects at the source, especially the depth of the shock. L_g excitation varies for shocks listed as normal depth.

(3) The discrimination of various instruments against parts of the frequency spectrum of L_g.

(4) The effect of mountainous terrain on L_g, a factor not thoroughly understood at present. Meager evidence indicates that L_g will travel a considerable distance through a mountainous region such as the Rocky Mountains (path C72, Pl. 2, fig. 2).

(5) Azimuthal effects at the source. No qualitative data are available on this at present.

It is then apparent that although the presence of L_g is indisputable proof of continental structure[1] along the entire path, the absence of L_g, particularly the high frequencies, cannot be used without caution to deduce the existence of a segment of noncontinental structure along the path. In short, the presence of L_g is sufficient proof of continental structure along the entire path. The absence of L_g is necessary but not sufficient proof of the presence of a segment of noncontinental structure.

Results

Plates 3A and 3B are maps of the Arctic regions with the great circle paths from epicenter to recording station superimposed. Solid lines indicate that no L_g was recorded, crossed lines that L_g was recorded, and dashed lines that the presence of L_g on the record is doubtful.

It is evident from the maps that the water-covered areas of the Canadian archipelago, Baffin Bay, and Davis Strait overlie continental structure, although in the case of the latter no good data are available for the southern part of the strait where it joins with the North Atlantic Ocean, nor is there conclusive evidence for the small deep areas of Baffin Bay. The results are in agreement with geologic interpretations of the area (Eardley, 1951, p. 538). A good L_g path across Greenland extends about 2° off the northeast coast into shallow water. Because of the nature of the L_g phase, this is not likely to shed any light on the current theories (Nye 1952, p. 529) of the elevation of the rock floor of Greenland other than to indicate that whatever the elevation of its surface, the crustal column beneath is continental.

Path G1 to Copenhagen traverses the broad continental shelf underlying the Barents Sea, a clear indication of continental structure.

In no case is L_g recorded for paths that traverse the Arctic Ocean basin proper. This evidence highly favors a crustal structure other than continental for the Arctic Ocean basin. To supplement this information, records exhibiting Rayleigh-wave dispersion across the Arctic Ocean were examined. In such a study it is highly advantageous to choose a path which

[1] Continental structure as used here refers to a silicic crust having a thickness of about 35 km as determined by seismic refractions and near earthquake data, although the L_g-wave guide need be no larger than about 15 km, for the short period oscillations. In areas of typical oceanic structure, sub-crustal material is 10–12 km deep.

has as small a continental segment and as large an oceanic segment as possible. College, Alaska, is at present the best station from this point of view, but the only long-period instrument

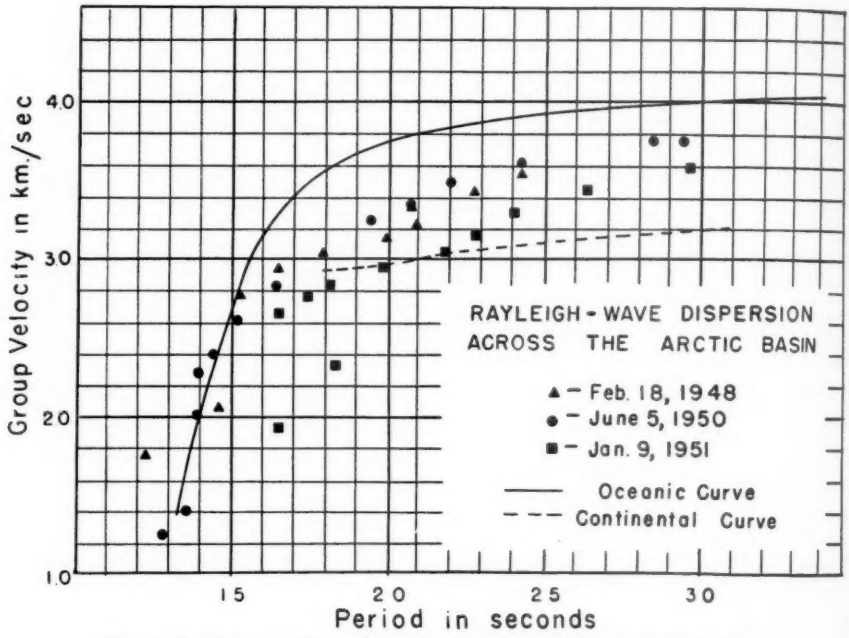

FIGURE 1.—RAYLEIGH-WAVE DISPERSION ACROSS THE ARCTIC OCEAN BASIN

there measures the east-west or primarily transverse component of ground motion for most Arctic quakes. However, one set of records is available for which north-south and east-west long-period instruments were recording. The dispersion curve of this quake, path C74, as well as some points from waves tentatively identified as the Rayleigh type on the east-west component for paths C24 and C10 are shown in Figure 1. Corrections have been made from the curve of Brilliant and Ewing (1954, p. 157) for the land-travel time in Alaska and the Alaskan continental shelf. Although there is considerable scatter, the curve falls below the oceanic curve of Ewing and Press (1950, p. 275) but above the continental curve of Brilliant and Ewing (1954, p. 149). This apparently indicates a structure of intermediate nature for the Arctic Ocean basin, but the Rayleigh-wave data are so poor that a final decision is not warranted here. Furthermore, recent sounding data in the Arctic by Crary *et al.* (1952) show that considerable changes need to be made in the map of Emery (1949) on which the continental corrections are based. The Arctic basin most certainly is not underlain by a continental column of rocks. Its identification with the oceanic column of the Atlantic and Pacific or with some intermediate structure awaits further evidence. Eardley (1951, p. 538) has interpreted a continental structure underlying the Arctic Ocean from geological evidence. Such evidence, he admits, is quite scanty. Gutenberg and Richter (1941, p. 27), from PP/P ratios, found the Arctic Ocean floor to be similar to that of the Pacific, although Byerly, *et al.* (1949, p. 269) and Mei (1943, p. 149) have pointed out that supplemental studies on the radiation pattern of the source are desirable.

No L_g phases were recorded for any of the paths crossing the Greenland Sea-Norwegian Sea area in the vicinity of Jan Mayen, with the possible exception of a doubtful one at Resolute

Bay. Although the Jan Mayen shocks are suspected of slightly greater than normal depth, additional evidence for paths G5 and S19 favors a noncontinental structure for this area.

No L_g phases were recorded from the North Atlantic shocks.

The shocks along the Alaskan peninsula and the Aleutian arc exhibit a very consistent set of data. From the easternmost shock on the peninsula clockwise in azimuth around College to path C9 most shocks made the L_g phase. Two did not but they are far enough from shore to be inefficient in L_g excitation. Path C9 which is approximately on the margin of the deep part of the Bering Sea made a doubtful L_g. The remainder of the shocks to the west whose paths cross the deep Bering Sea did not make L_g at College. The consistency of the results indicates with certainty that the crustal structure of the deep Bering Sea is markedly different from that of the continent.

The large group of Japanese, Kurile, and Kamchatka shocks failed to produce an L_g at College. However, the complicated nature of the path does not permit any specific conclusions to be drawn since most of the paths cross either the Pacific Ocean or the Okhotsk Sea in addition to the Bering Sea.

Most of the shocks whose paths cross the Bering Strait did not make an L_g at College. One shock, C68, did, although the very high frequencies are missing. In an effort to isolate the reason for the missing L_g phases, shocks corresponding to paths C28, L1, and G9, and to paths C32, L2, and G10 were examined at Copenhagen and Lund. Neither made an L_g at College. The former made a very doubtful L_g at both European stations, the latter made a weak one. This evidence indicates that the reason for the missing L_g at College was inefficient excitation at the source rather than a structural anomaly at the Bering Strait. Furthermore, for shock C68 which did send an L_g to College, Uppsala also reports L_g in its station bulletin. On the other hand, Uppsala does not report L_g for shock C67, nor is it recorded at College. The conclusion, then, is that continental structure is continuous, at least across the narrow part of the Bering Strait. This is in agreement with the geologic interpretations of the area (Eardley, 1951, p. 532).

There is an excellent correlation between water depth and areas through which L_g will not propagate. In no case is there L_g propagation beneath water deeper than 1000 fathoms for any great distance. The possibility that the absence of L_g over these paths might be due to the water column rather than the underlying rocks is ruled out because, although it is present on all three components, L_g is primarily a shear wave polarized horizontally. This component of motion could not be affected by the water. Thus it appears that water depths actually reflect changes of the crustal column. Indeed, geophysical methods of any sort have yet to detect an area where a continental structural column underlies oceanic depths.

Summary

The L_g surface-wave phase was used to distinguish areas of continental crustal structure from areas of noncontinental structure in the Arctic regions. Water-covered areas of continental structure include the Canadian archipelago, parts of Baffin Bay and Davis Strait, the shallow parts of the Bering Sea and of the Greenland Sea, the Barents Sea and Bering Strait. Areas of noncontinental structure include the Arctic Ocean, Beaufort Sea, Greenland Sea, Norwegian Sea and the deep Bering Sea. Nowhere is a continental structural column detected beneath oceanic depths.

References Cited

Brilliant, R., and Ewing, M., 1954, Dispersion of Rayleigh waves across United States: Bull. Seismol. Soc. America, v. 44, p. 149–158.

Byerly, P., Mei, A. I., S. J., and Rommey, Carl, 1949, Dependence on Azimuth of the amplitudes of P and PP: Bull. Seismol. Soc. America, v. 39, p. 269–284.

Crary, A. P., Cotell, R. D., and Sexton, T. F., 1952, Preliminary report on scientific work on Fletcher's Ice Island, T3: Arctic, v. 5, no. 4, p. 211–223.

Eardley, A. J., 1951, Structural geology of North America: N. Y., Harper and Bros., 538 p.

Emery, K. O., 1949, Topography and sediments of the Arctic basin: Jour. Geology, v. 57, p. 512–521.

Ewing, M., and Press, F., 1950, Crustal structure and surface wave dispersion, Part I: Bull. Seismol. Soc. America, v. 40, p. 271–280.

Gutenberg, B., and Richter, C. F., 1941, Seismicity

of the earth: Geol. Soc. America Special Paper 34, p. 94.

Katz, Samuel, 1954, Seismic study of crustal structure in Pennsylvania and New York (Abstract): Geol. Soc. America Bull., v. 65, p. 1343.

Mei, A. I., S. J., 1943, The amplitude ratio PP/P as recorded by the Galitzin seismographs: Bull. Seismol. Soc. America, v. 33, p. 149–195.

Nye, J. F., 1952, A method of calculating the thickness of ice sheets: Nature, v. 169, p. 529–530.

Press, F., and Ewing, M., 1952, Two slow surface waves across North America: Bull. Seismol. Soc. America, v. 42, p. 219–228.

LAMONT GEOLOGICAL OBSERVATORY (COLUMBIA UNIVERSITY), PALISADES, NEW YORK

MANUSCRIPT RECEIVED BY THE SECRETARY OF THE SOCIETY, AUGUST 23, 1954

LAMONT GEOLOGICAL OBSERVATORY CONTRIBUTION NO. 165

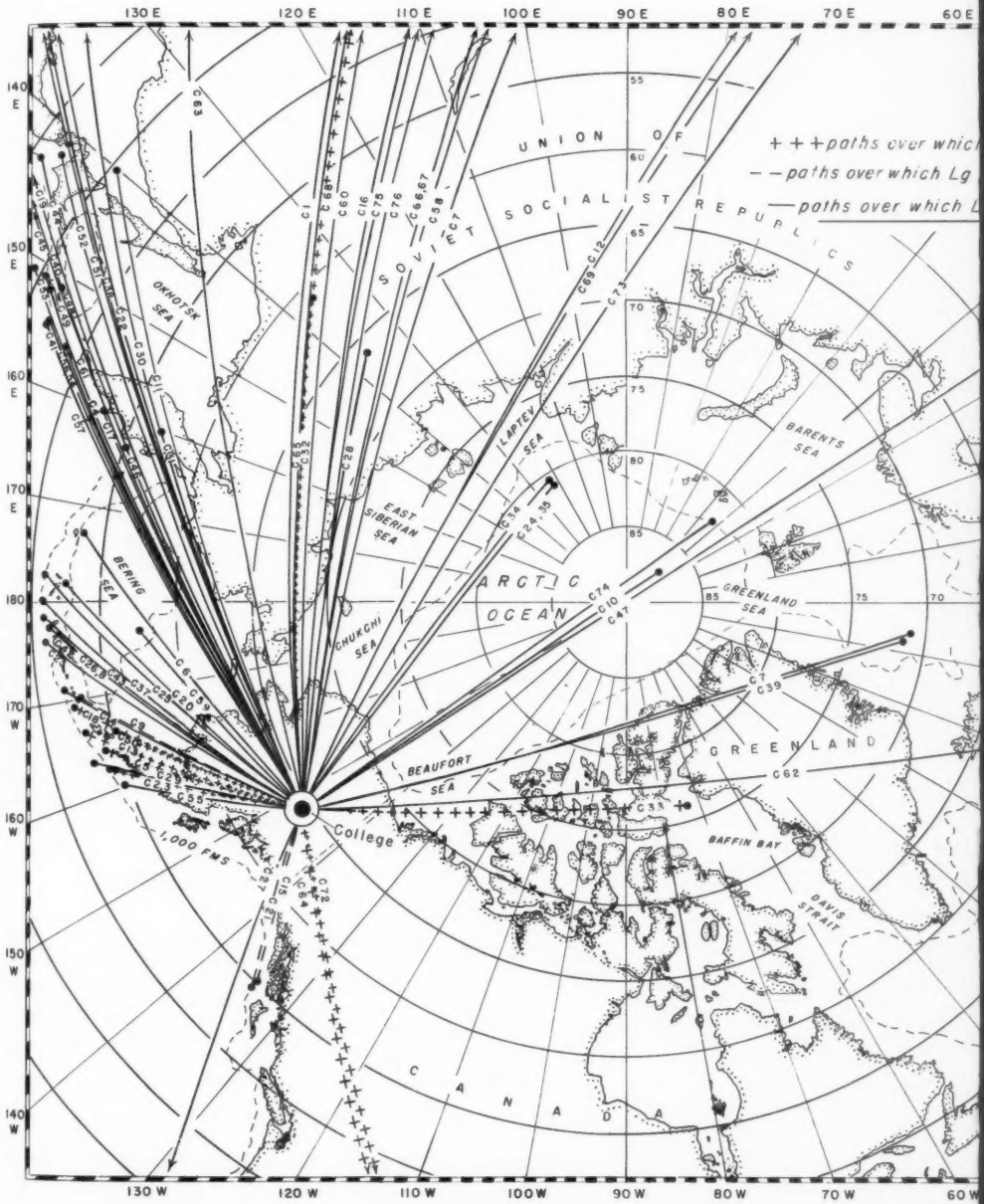

A. Paths across Arctic Regions to College, Alaska

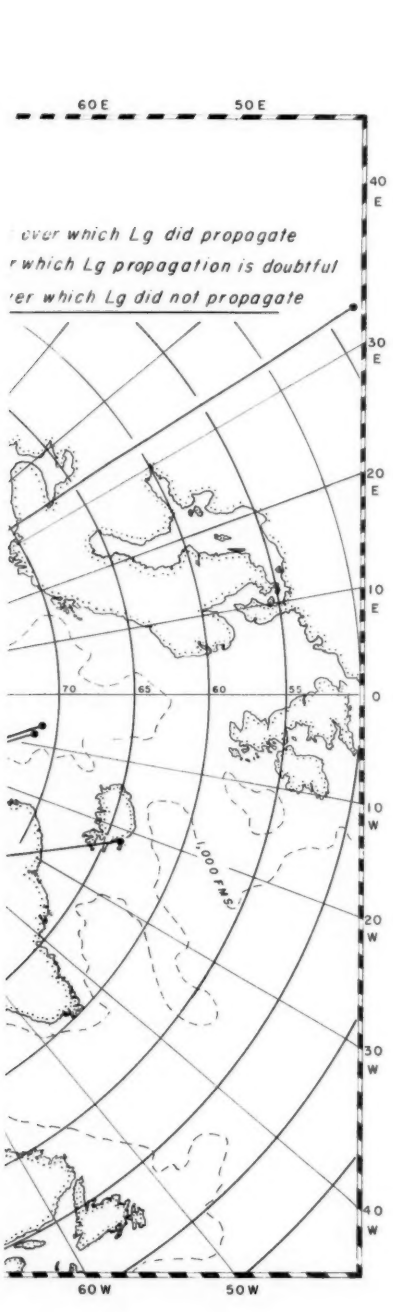

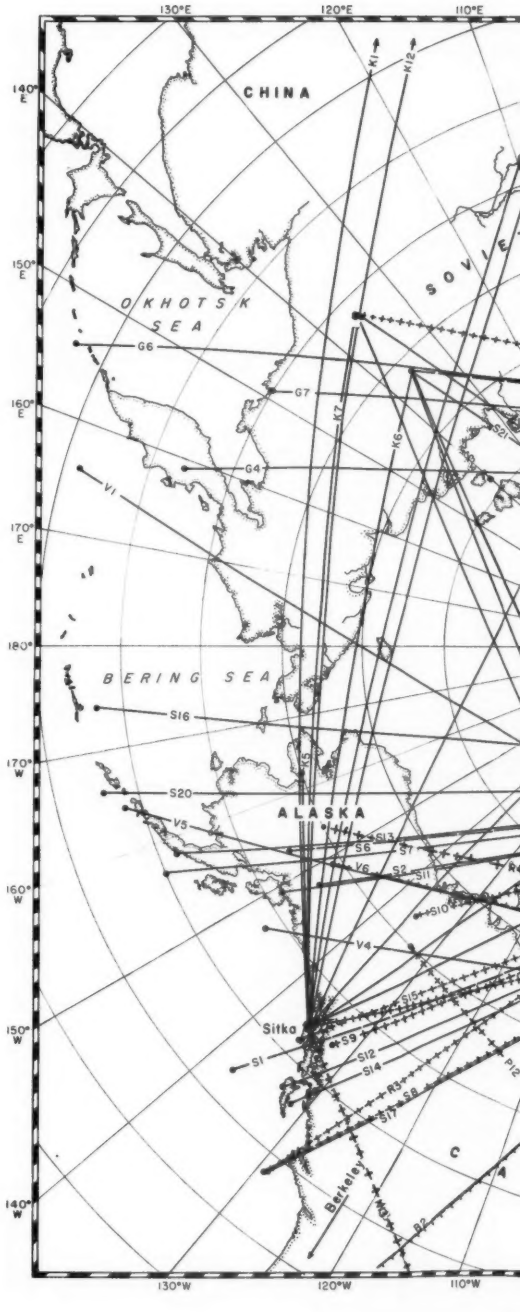

B.

PATHS ACROSS ARCTIC REGIONS

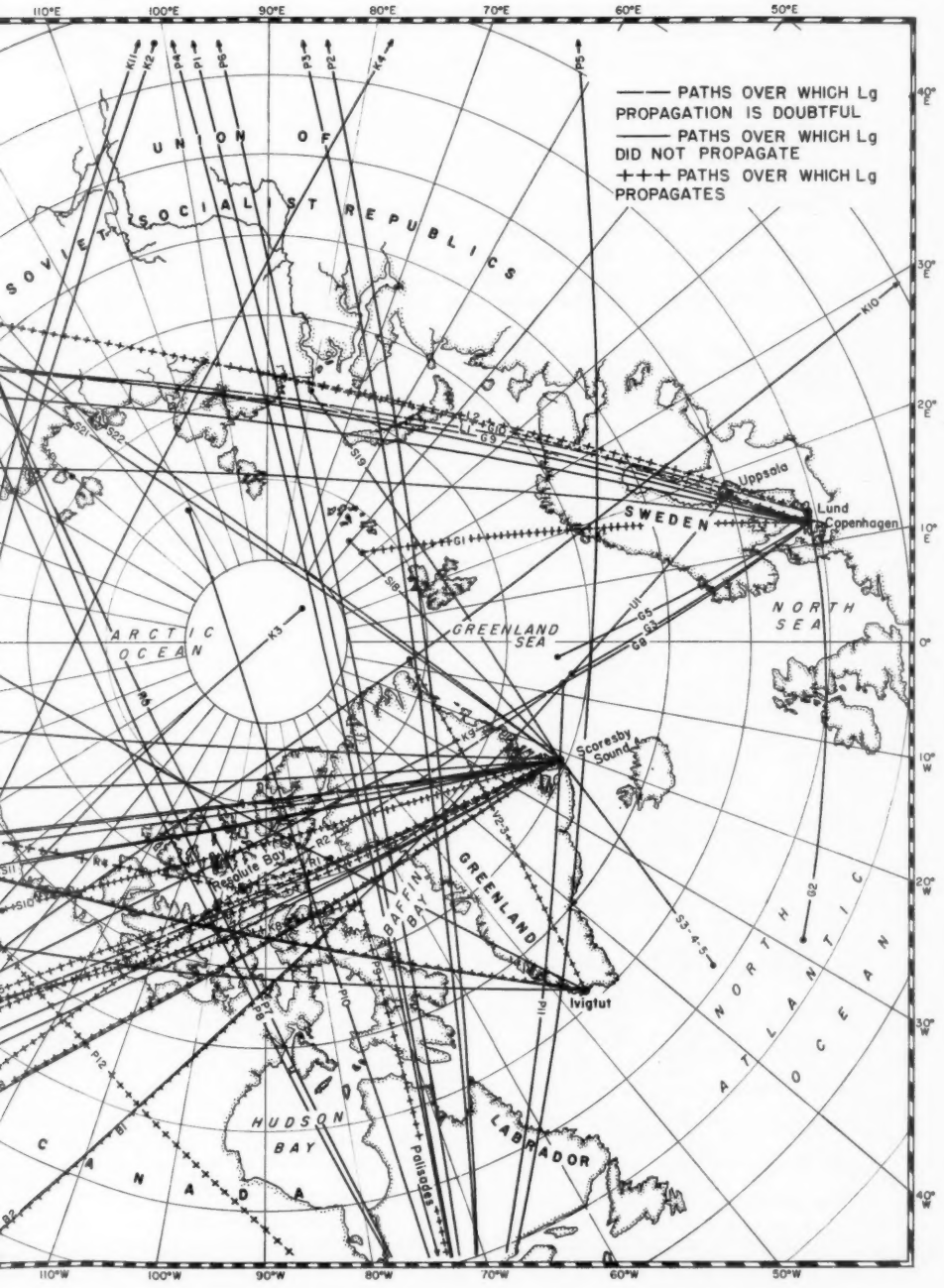

B. Paths across Arctic Regions to all Stations except College, Alaska

SPHE

Introdu
Acknow
Samplin
Techni
Experi
Descrip
Analysi
Descrip
Analysi
Interre
roun
Conclu
Refere

Figure
1. Fre
q
2. Fre
q
3. Fre
q
4. Spl
f
s
5. Me
f
6. Fr
c
s
7. Fr
c

BULLETIN OF THE GEOLOGICAL SOCIETY OF AMERICA
VOL. 66, PP. 1075-1096, 9 FIGS. SEPTEMBER 1955

SPHERICITY AND ROUNDNESS OF QUARTZ GRAINS IN SEDIMENTS

BY J. R. CURRAY AND J. C. GRIFFITHS

ABSTRACT

Sphericity of quartz grains in sediments determined by three dimensional measurement varies from 0.5 to 1.0 around a mean of 0.75 sphericity units and is approximately normally distributed. Differences in sphericity of quartz grains between arkoses, graywackes, and quartzites are not large and arkoses are least spherical, graywackes intermediate, quartzites most spherical; the differences are not statistically significant on the basis of these 2700 measured grains.

The roundness determined by visual comparison of quartz grains from 125 micron size-grade shows a similar trend from least round in arkoses to most round in quartzites, but the frequency distribution of roundness is markedly nonnormal and the conclusions based on statistical analysis are approximate.

The magnitude of variation in sphericity and roundness in arkoses is greatest among grains and least among samples, in low rank graywackes it is moderate in both, whereas in quartzites it is least among grains and greatest among samples; this difference requires a sampling plan specifically designed for each rock type if the analysis of shape of quartz grains is to lead to significant differences at the formation level.

CONTENTS

TEXT

	Page
Introduction	1076
Acknowledgments	1076
Sampling plan	1076
Technique and procedure	1076
Experimental design	1077
Description of sphericity measurements	1079
Analysis of sphericity measurements	1082
Description of roundness measurements	1086
Analysis of roundness measurements	1088
Interrelationship between sphericity and roundness	1091
Conclusion	1094
References cited	1095

ILLUSTRATIONS

Figure	Page
1. Frequency distribution of sphericity of quartz grains in different rock types	1078
2. Frequency distribution of sphericity of quartz grains in different size grades	1080
3. Frequency distribution of sphericity of quartz grains in sediments	1081
4. Sphericity means and least significant differences; three formations and two sizes from each rock type	1084
5. Mean sphericity for each sample, size, formation, and rock type	1087
6. Frequency distribution of roundness of quartz grains in 120-mesh (125 micron) size grade of sediments	1088
7. Frequency distribution of roundness of quartz grains in three rock types	1089
8. Mean roundness for samples and rock types (120-mesh)	1092
9. Mean sphericity compared with mean roundness of quartz grains in 125-micron grain size	1093

TABLES

Table	Page
1. Sampling plan for estimation of sphericity of quartz grains in sediments	1077
2. Sphericity of quartz grains in different rock types	1079
3. Sphericity of quartz grains in different size grades	1079
4. Analysis of variance of sphericity measurements ignoring formations and rock types and using two size grades (60 and 120 mesh)	1082
5. Mean sphericity for each sample, size, formation, and rock type	1083
6. Analysis of variance of sphericity measurements: arkoses	1083
7. Analysis of variance of sphericity measurements: graywackes	1083
8. Analysis of variance of sphericity measurements: quartzites	1084
9. Analysis of variance of sphericity measurements: arkoses	1086
10. Analysis of variance of sphericity measurements: graywackes	1086
11. Analysis of variance of sphericity measurements: quartzites	1086
12. Means, error-standard deviations, and coefficients of variation of sphericity data for rock types	1088

Table Page
13. Roundness of quartz grains in 125-micron grain size of sedimentary rocks 1089
14. Analysis of variance of roundness measurements: arkoses 1090
15. Analysis of variance of roundness measurements: graywackes 1090
16. Analysis of variance of roundness measurements: quartzites 1090
17. Means, error-standard deviations, and coefficients of variation of roundness data for rock types 1091
18. Analysis of variance of roundness variation between rock types 1091

Introduction

The five fundamental properties of sedimentary rocks are mineral compostion, size, shape, orientation, and packing (Griffiths, 1952b, p. 1256). Before using these properties for interpretation, one should understand how they vary and how they are interrelated. This study is an attempt to evaluate the magnitude of variation in shape of quartz grains in sedimentary rocks. To pinpoint the problem, the mineral composition variable has been rendered constant by confining attention to quartz grains; fabric, orientation, and packing have been eliminated by using loose grains; and, finally, while shape is considered to comprise sphericity, roundness, and surface texture, the last has been given no special consideration.

These restrictions have been adopted so that the experiment might be more comprehensive, particularly of the wide variety of sedimentary rock types. Such limitations are perhaps necessary in a reconnaissance investigation in order to cover the range in magnitude of the variables. Of course this approach cannot supply final answers which would require a study of all properties simultaneously if we are to understand the meaning of the variations in sedimentary rocks.

Acknowledgments

The writers thank Miss Irene Waraksa for drafting the figures, and Dr. J. A. Hipple, Director of the Mineral Industries Experiment Station, and Professor P. D. Krynine, Head of the Department of Mineralogy, both of the Pennsylvania State University, for critical reading of the manuscript.

Sampling Plan

Three of Krynine's four detrital rock types were selected for sampling: namely, arkose, low-rank graywacke, and quartzite (Krynine, 1948, p. 149). These account for an estimated 90 per cent of all detrital sediments. The three rock types are represented by three formations, and two samples were arbitrarily chosen from each formation. As the shape of quartz grains is thought to be related to their size, three sizes, determined by sieving the disaggregated samples, were selected for study. The sphericity of 50 grains from each of the three sizes was measured; however it was soon found impossible to select exactly the same sizes for all samples. The two sizes, 120 mesh (125 microns) and 60 mesh (250 microns), were common to all samples and the 35 mesh (500 microns) was used for 11 samples. The remaining seven samples were too fine-grained to supply sufficient material for study of the 35-mesh size, so the 80 mesh (177 microns) was used as a third size fraction. The sphericity of 50 quartz grains was determined for each size, 150 for each sample, 300 for each formation, and 900 for each rock type, a total of 2700 sphericity measurements (Table 1).

An early difficulty in determining roundness led to a decision to use only one size, the 120 mesh (125 microns), for this part of the analysis. The 18 samples resulted in 900 measurements of roundness, 50 measurements (or grains) per sample for each formation and rock type.

Technique and Procedure

Each sample was crushed in a mortar and the residue sieved into size fractions. Three size fractions were chosen, and each fraction was split to between 50 and 100 grains by an Otto microsplit (Otto, 1933, p. 30); each split was mounted on a glass slip and the 50 quartz grains nearest the long edge of the slide permanently mounted with gum arabic (Plumley, 1948, p. 562) for grains of 250 microns and finer, but a fluid mixture of acetone and Duco cement was more satisfactory for mounting the

coarser grains. The long and intermediate axes were determined from tracings of the projected grain images; to measure the short axes the mount was turned on edge (perpendicular to the maximum projected area of the grains) by means of a clip support.

The short (*c*) axis was measured directly from the projected image, whereas the long (*a*) and intermediate (*b*) axis were measured on the tracings of the grain images. The intermediate *b* axis was first determined as the distance between the two most closely spaced parallel lines tangent to the maximum projection outline of the grain by means of calibrated parallel rules, and the long *a* axis was taken as the longest axis perpendicular to the intermediate axis (Griffiths and Rosenfeld, 1950, p. 205). The Krumbein intercept sphericity was determined from a modified Zing chart using the axial ratios c/b and b/a (Krumbein, 1941, Pl. 1, p. 168).

Experimental Design

Initially, all sources of variation were to be included in a single comprehensive analysis of variance by use of a randomized-blocks design (Snedecor, 1946, p. 253) composed of the several subdivisions, rock types, formations, samples, sizes, and grains, but two difficulties arose: first, samples differed greatly within formations, and because only two samples per formation were used, the wide variation obscured differences between formations and rock types; also the size sample interaction or inconsistency gave rise to very large magnitude variation. Any attempt, therefore, to compute a general sum of squares or a correction term for the analysis of variance embracing the entire set of data meant including heterogeneous variance in the analysis. It is more informative in such cases to divide the data into homogeneous groups.

Table 1.—Sampling Plan for Estimation of Sphericity of Quartz Grains in Sediments

Rock types		Formations	Sample number	Mesh (microns)			
				35 500	60 250	80 177	120 125
Arkose		Roslyn, Eocene	R_1	....	x	x	x
		Washington	R_2	x	x	....	x
		Sespe, Oligocene	S_1	x	x	....	x
		California	S_2	x	x	....	x
		Fountain, Pennsylvanian	F_1	x	x	....	x
		Colorado	F_2	x	x	....	x
Low-rank graywacke		Miocene	M_1	....	x	x	x
		Trinidad, B.W.I.	M_2	....	x	x	x
		Bradford Sand, Devonian	B_1	....	x	x	x
		Pennsylvania	B_2	....	x	x	x
		Oswego, Ordovician	T_1	x	x	....	x
		Pennsylvania	T_2	x	x	....	x
Ortho-quartzite		Oriskany, Devonian	O_1	x	x	....	x
		Pennsylvania	O_2	x	x	....	x
		Homewood, Pennsylvanian	H_1	....	x	x	x
		Pennsylvania	H_2	....	x	x	x
		Gatesburg, Cambrian	G_1	x	x	....	x
		Pennsylvania	G_2	x	x	....	x
Total	3	9	18	11	18	7	18

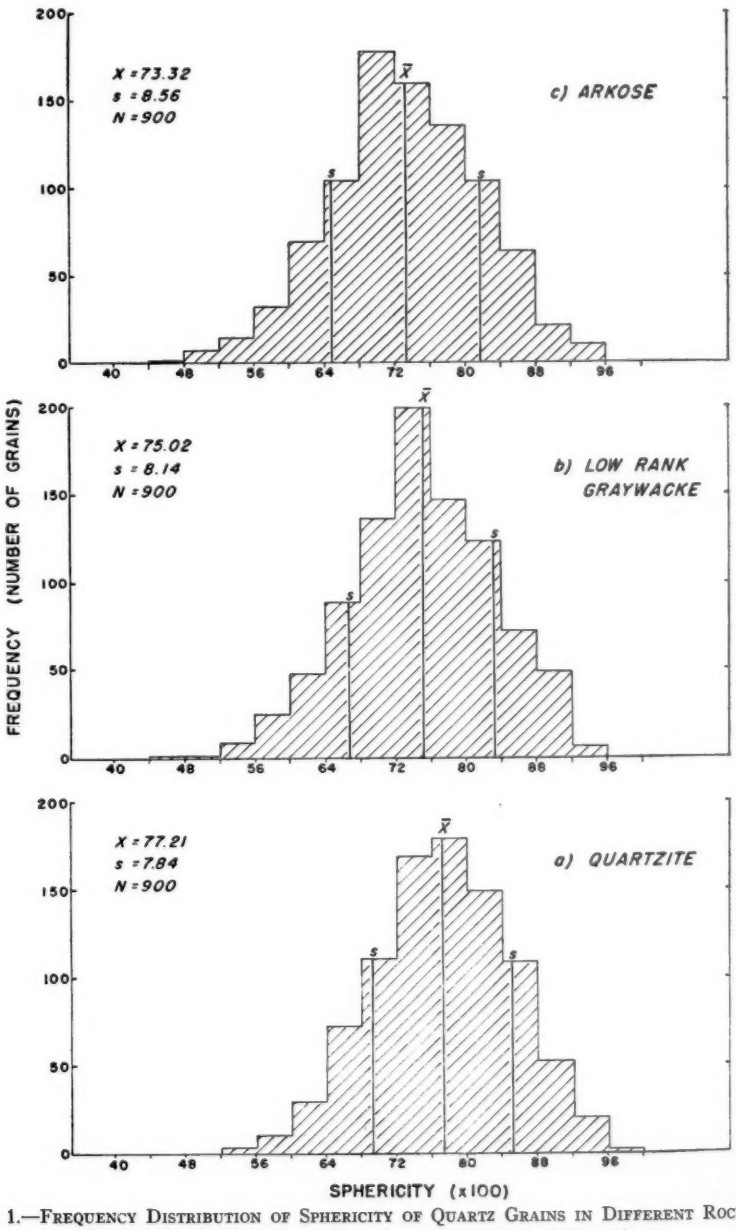

FIGURE 1.—FREQUENCY DISTRIBUTION OF SPHERICITY OF QUARTZ GRAINS IN DIFFERENT ROCK TYPES
$\bar{X}$ = arithmetic mean; s = standard deviation; N = number of items

For roundness similar difficulties arose and although only one size fraction was included, the peculiar form of the frequency distribution suggests that these data should also be considered in homogeneous subdivisions rather than one comprehensive unit.

The data is grouped in different ways and subjected to statistical analysis by use of a

completely randomized design except where several sizes are common to all samples, in which case the design that includes the size-sample interaction is a randomized-blocks arrangement. Analysis of variance with completely randomized and randomized-block designs is explained elsewhere (Snedecor, 1946, p. 214–317; Cochran and Cox, 1950, p. 86–102; Griffiths and Rosenfeld, 1950, 1953; Griffiths, 1953; Rosenfeld and Griffiths, 1950, 1953).

TABLE 2.—SPHERICITY OF QUARTZ GRAINS IN DIFFERENT ROCK TYPES

Rock type	Grains N	Arithmetic mean $\bar{x}$	Variance s^2	Standard deviation s	Coefficient of variation Cv *per cent*	Chi-square against normalcy χ^2	Probability P
Arkose	900	73.32	73.19	8.56	11.69	9.58	$<30 > 20$
Low-rank graywacke	900	75.02	66.25	8.14	10.85	8.05	$<30 > 20$
Quartzite	900	77.21	61.52	7.84	10.15	4.45	$<80 > 70$
All types	2700	75.18	69.52	8.34	11.09	15.571	$<0.05 > 0.02$

Coded sphericity (ψ): $X = 100\,\psi$.

TABLE 3.—SPHERICITY OF QUARTZ GRAINS IN DIFFERENT SIZE GRADES

Sieve mesh	Size in microns	No. of grains N	Arithmetic mean $\bar{x}$	Variance s^2	Standard deviation s	Coefficient of variation Cv *per cent*	Chi-square against normalcy χ^2	Probability P
35	500	550	76.50	58.50	7.65	10.00	4.68	$<50 > 30$
60	250	900	74.65	67.36	8.21	10.99	3.46	$<95 > 90$
80	177	350	75.79	71.61	8.46	11.62	3.04	$<90 > 80$
120	125	900	74.67	75.86	8.71	11.66	9.44	$<50 > 30$
All meshes	All sizes	2700	75.18	69.52	8.34	11.09	15.571	$<0.05 > 0.02$

Coded sphercity (ψ): $X = 100\,\psi$.

DESCRIPTION OF SPHERICITY MEASUREMENTS

One of the fundamental features of any variable is its frequency-distribution function and until its form is defined, use of the variable is considerably restricted. Sometimes it is possible to predict the form of the distribution function a priori, but usually the empirical approach is more reliable, and it is always advisable to confirm a priori analysis by means of empirical data before final acceptance of the conclusions. The present sampling plan facilitates the empirical establishment of the frequency distribution of sphericity; however this frequency function applies only where the present procedure is used. With these qualifications in mind we may describe the frequency-distribution function of sphericity as follows:

The 2700 sphericity estimates are first subdivided into groups of 900 measurements for each rock type. Each set of 50 grains from each size fraction of each rock sample can be considered a random sample from the parent populations of sphericity measurements of each rock type. Each frequency distribution (Fig. 1; Table 2) is compared with the theoretical normal distribution with the same mean and variance, and a chi-square test (Smith and Duncan, 1945, p. 139), shows that there is no evidence of departure from normalcy.

The data may now be combined in terms of sizes, and the 2700 measurements broken down into samples. In this case each set of 50 grains is considered a random sample from the parent population of each size grade, and differences between rock types, formations, and samples are ignored (Table 3). Once more, from the chi-square test against the respective normal distributions, the frequency distributions for size fractions show no significant departure from normalcy.

These tests give some assurance of the suitability of the data for analysis of variance and support the assumption of normal distri-

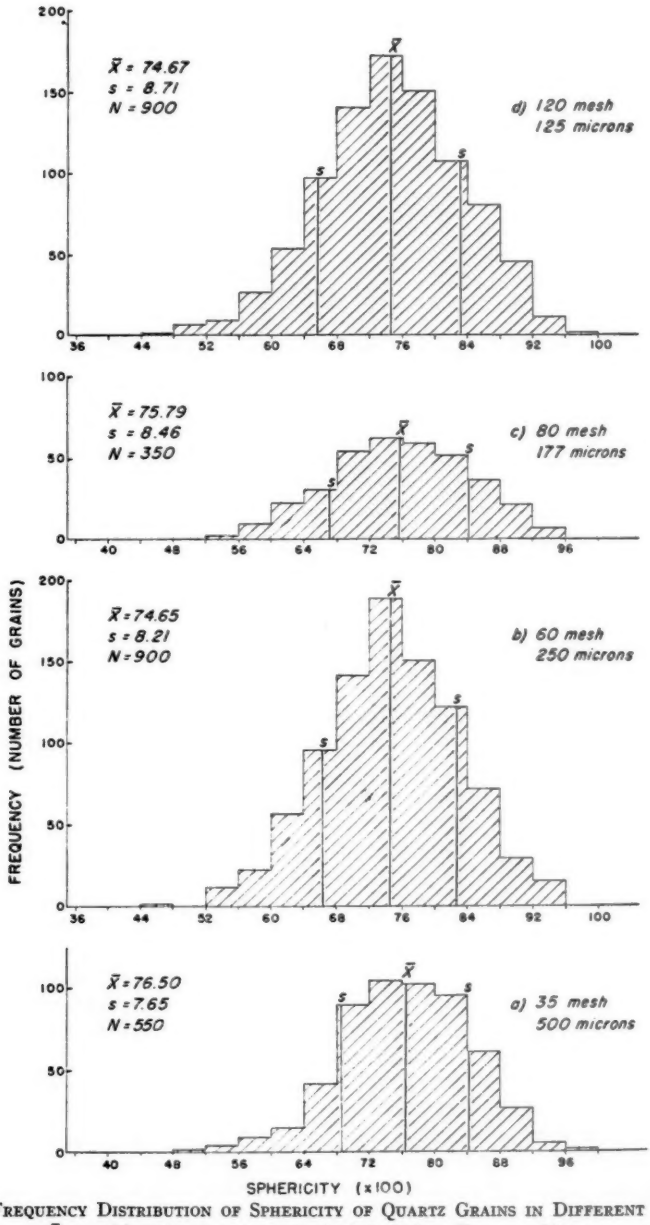

FIGURE 2.—FREQUENCY DISTRIBUTION OF SPHERICITY OF QUARTZ GRAINS IN DIFFERENT SIZE GRADES
$\bar{X}$ = arithmetic mean; s = standard deviation; N = no. of items

bution necessitated for full efficiency in this procedure. When all 2700 grains are totaled into a single homogeneous frequency distribution, a chi-square test shows a significant departure from the normal ($P < 0.05 > 0.02$; Fig. 3; Tables 2, 3). The departure from normalcy is not large, but because of the large sample size it is statistically significant. The

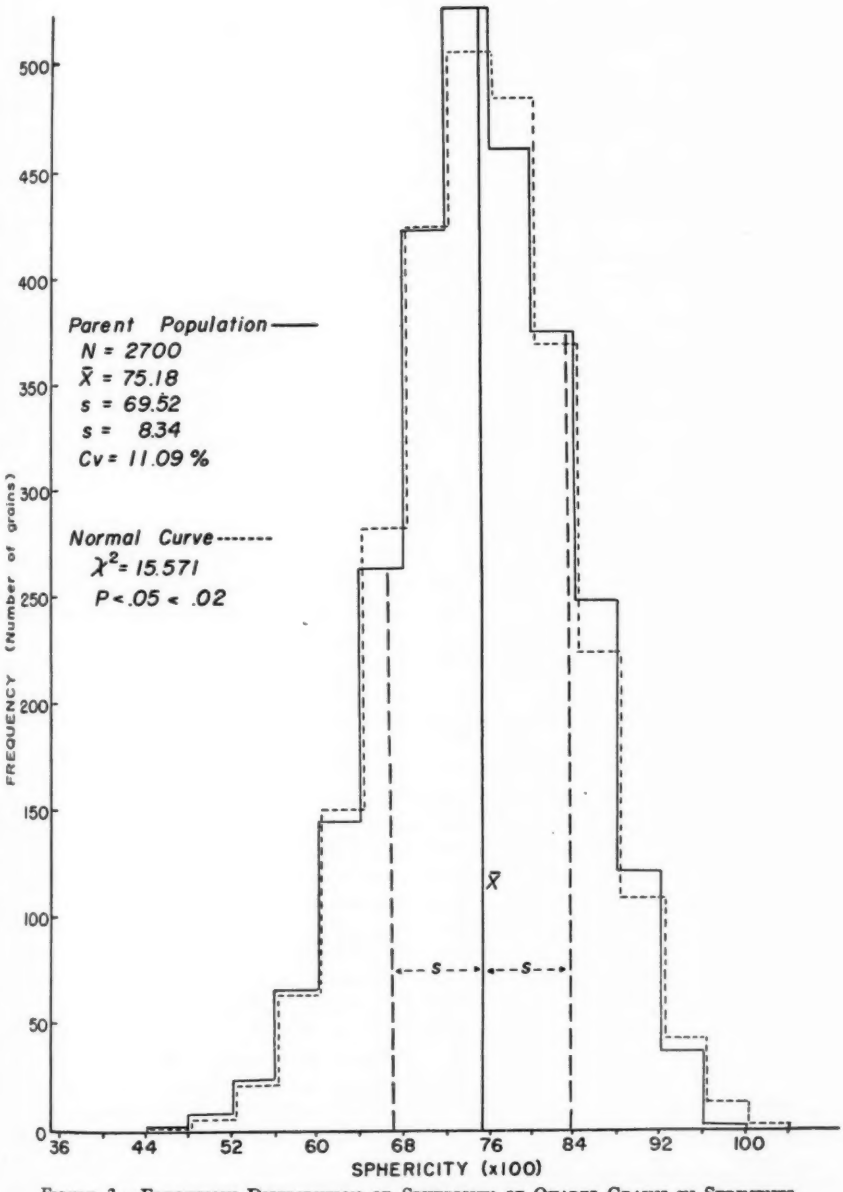

FIGURE 3.—FREQUENCY DISTRIBUTION OF SPHERICITY OF QUARTZ GRAINS IN SEDIMENTS
$\bar{X}$ = arithmetic mean; s^2 = variance; s = standard deviation; N = no. of items; Cv = coefficient of variation = $(s/\bar{X}) \times 100$; x^2 = chi square

skewness and kurtosis of this frequency distribution were tested for significance by the Fisher g statistics and their standard errors (Fisher, 1948, p. 75): the results are:

$g_1 = -0.1526 \quad s_{g1} = 0.04712 \quad P < 0.01$

$g_2 = +0.0181 \quad s_{g2} = 0.0942 \quad P > 0.75$

where g_1 is a measure of skewness, and g_2 a

measure of kurtosis; s = the respective standard errors and P = probability.

The kurtosis is not significant but the skewness is at the 1-per cent level. The negative value indicates deficiency of high-sphericity values. The writers believe this skewness has been induced by sampling only three sizes and so introducing unequal weighting of sphericity in terms of size. Fortunately, the departure is not large enough to affect the significance levels of the analysis of variance.

The differences between the mean sphericity for rock types are not large and the order—arkose least spherical, graywackes intermediate, and quartzite most spherical—is consistent. In the case of size fractions the range in means is both small and inconsistent. The standard deviation for both rock types and sizes is similar, and the coefficients of variation, close to 10 per cent, indicate good experimental control.

As the set of 2700 measurements is approximately normal, the population mean may be estimated:

Sphericity Units

0.7486–0.7550 with 95 per cent probability

0.7469–0.7566 with 95 per cent probability

If this set is representative of the sphericity-frequency distribution of quartz grains in sedimentary rocks, then almost the entire range of sphericity should be encompassed in the interval

$$\bar{X} \pm 3s = 0.7518 \pm 0.2502$$

or approximately 0.50–1.00 sphericity units.

Analysis of Sphericity Measurements

The lack of certain size grades in some samples has precluded a single comprehensive analysis. After various arrangements were attempted, it was decided that the analysis could be performed in four stages. A general idea of the magnitude of subsidiary effects of sample and size differences may be found by confining attention to the two sizes, 60 and 120 mesh, common to all samples and by ignoring differences between rock types and formations. Such an analysis leads to the randomized-blocks design summarized in Table 4 (Snedecor, 1946, p. 275).

Table 4.—Analysis of Variance of Sphericity Measurements Ignoring Formations and Rock Types and Using Two Size Grades (60 and 120 Mesh)[1]

Source of variation	Degrees of freedom	Sum of squares	Mean square	F[2]
Between samples	17	8468.26	498.133	3.313**
Between sizes	1	1.33	1.33	<1
Sizes and samples	17	2556.26	150.368	2.28**
Grains (within sizes and samples)	1764	116,457.26	66.019	....
Total	1799	127,483.11	....	....

[1] Data in all analysis-of-variance tables coded as follows: $100\psi = X$ where ψ = sphericity value; X = coded value.

[2] Asterisks in all analysis-of-variance tables signify * = significant at the 5-per cent level; ** = significant at the 1-per cent level; *** = significant at the 0.1-per cent level.

Two difficulties arise from incorrect arrangement of the experiment: (1) Since the difference between samples is large, two samples will not be sufficient. (2) Contrary to expectations based on the literature, there is no significant difference in sphericity between size grades, but there is a highly significant interaction between sizes and samples. This underlines the fact that there is no consistent difference in sphericity between sizes and indicates that there is an inconsistent difference in sphericity from size to size over different samples (Table 5).

From a petrographical point of view, differences between rock types are of major interest. The analysis of Table 4 suggests that it would be advantageous to treat each rock type separately in order to offset both the size-sample interaction and sample differences which may not be characteristic of all three rock types; hence the succeeding steps will consider the

TABLE 5.—MEAN SPHERICITY FOR EACH SAMPLE, SIZE, FORMATION AND ROCK-TYPE

Rock-type	Arkose						Graywacke						Quartzite					
Formation	Roslyn		Fountain		Sespe		Miocene		Bradford		Oswego		Oriskany		Homewood		Gates-burg	
Sample	1	2	1	2	1	2	1	2	1	2	1	2	1	2	1	2	1	2
Size	$\bar{x}$	$\bar{x}$	$\bar{x}$	$\bar{x}$	$\bar{x}$	$\bar{x}$	$\bar{x}$	$\bar{x}$	$\bar{x}$	$\bar{x}$	$\bar{x}$	$\bar{x}$	$\bar{x}$	$\bar{x}$	$\bar{x}$	$\bar{x}$	$\bar{x}$	$\bar{x}$
35	..	7372	7564	7274	7324	7492	..	..	..	..	7710	7788	7624	7618	..	..	7978	7960
60	7080	7180	7016	7304	7452	7394	7434	7172	7198	7842	7528	7396	7790	7640	7560	7954	7360	7296
80	7050	..	..	..	..	..	7298	7590	7310	7522	..	..	..	..	7826	6142	..	..
120	7298	6962	7394	7440	7338	7292	7450	7510	7300	7688	7128	7294	7028	7686	7802	7964	7506	7238

Each $\bar{x}$ is coded = 10,000 (observed value in sphericity units).

TABLE 6.—ANALYSIS OF VARIANCE OF SPHERICITY MEASUREMENTS: ARKOSES
(3 formations; 2 samples; 50 grains; 120- and 60-mesh sizes)

Source of variation	Degrees of freedom	Sum of squares	Mean square	F
Formations	2	591.490	295.745	3.85*
Sizes	1	37.001	37.001	<1
Sizes over formations	2	351.564	175.782	2.30
Samples (within formations)	3	222.585	74.195	<1
Sizes over samples	3	311.005	103.668	1.357
Grains (within all classes)	588	44,924.980	76.403	....
Total	599	46,438.625	....	....
Pooled error	596	45,810.134	76.86	....

$\bar{X}_G = 72.625$; $s_e = 8.741$; Cv = 12.04 per cent.

TABLE 7.—ANALYSIS OF VARIANCE OF SPHERICITY MEASUREMENTS: GRAYWACKES
(3 formations; 2 samples; 50 grains; 120- and 60-mesh sizes)

Source of variation	Degrees of freedom	Sum of squares	Mean square	F
Formations	2	302.91	151.455	<1
Sizes	1	16.67	16.67	<1
Sizes over formations	2	458.36	229.18	<1
Samples	3	1383.73	461.243	7.20**
Sizes over samples	3	322.53	107.51	1.68
Grains (within all classes)	588	37,534.64	63.83	....
Total	599	40,018.84	....	....
Pooled error	591	37,857.17	64.06	....

$\bar{X}_G = 74.116$; $s_e = 8.296$; Cv = 11.19 per cent.

data for each rock type separately. Because certain sizes were lacking in some formations, (*see* Table 1), it was decided to use the two common sizes and these analyses are summarized in Tables 6–8.

In the arkoses no significant differences were found between samples or either interaction term, samples over sizes and formations over sizes. When sums of squares for these items are pooled, the differences between formations are significant at the 5-per cent level. It is surprising to find no differences in sphericity between sizes and such a small mean square; similarly there is no difference in sphericity between samples, which confirms the necessity for breakdown of the analysis into rock types.

The analysis of the data for low-rank graywackes yields an entirely different result (Table 7). Here the size-sample interaction is not significantly greater than error (grains), and

TABLE 8.—ANALYSIS OF VARIANCE OF SPHERICITY MEASUREMENTS: QUARTZITES
(3 formations; 2 samples; 50 grains; 120- and 60-mesh sizes)

Source of variation	Degrees of freedom	Sum of squares	Mean square	F
Formations	2	2209.21	1104.61	5.189*
Sizes	1	16.00	16.00	<1
Sizes over formations	2	432.18	216.09	1.020
Samples	3	658.68	219.56	1.075
Sizes over samples	3	612.28	204.09	3.53*
Grains (within all classes)	588	33,997.64	57.82	....
Total	599	37,925.99	....	....
Pooled error	8	1703.14	212.89	....

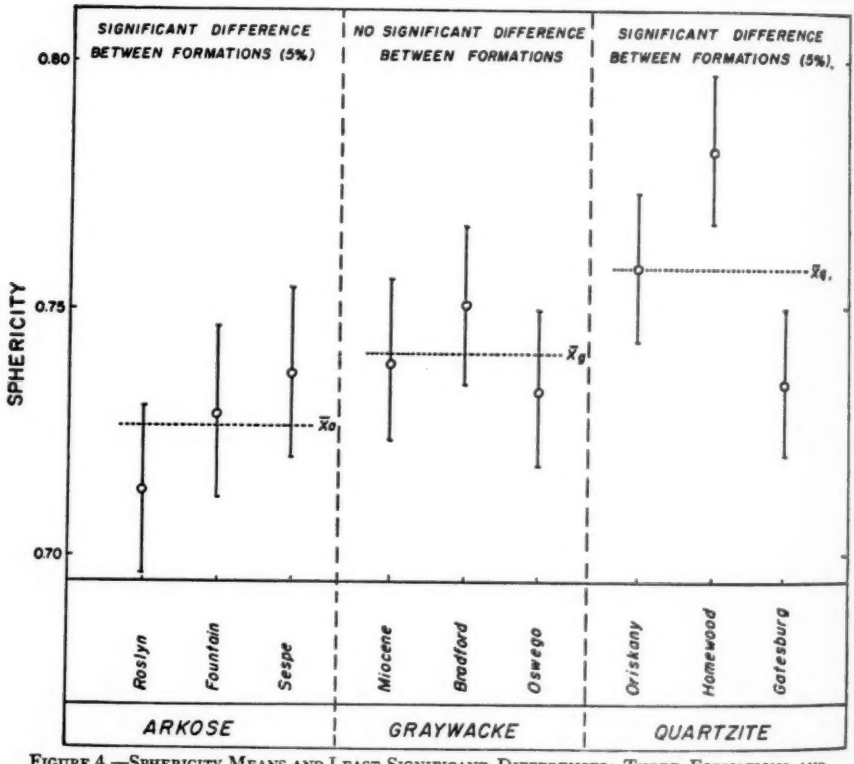

FIGURE 4.—SPHERICITY MEANS AND LEAST SIGNIFICANT DIFFERENCES; THREE FORMATIONS AND TWO SIZES FROM EACH ROCK TYPE

$\bar{X}$ = arithmetic mean; a = arkose; g = graywacke; q = quartzite

when these two sources are pooled and the differences between samples tested against the pooled error, there is a highly significant difference in sphericity between samples. In fact, the variation in sphericity between samples is so large that neither the size-formation interaction nor the main effects, sizes and formations are significantly greater. Evidently in this case it is necessary to analyze more samples in order to reduce this source of variation. Again, differences between sizes is surprisingly small and the interaction or inconsistency is larger.

In the case of the quartzites, the analysis (Table 8) reveals that the size-sample interaction is significantly greater (at the 5-per cent level) than the error term. The differences between samples is not significantly greater than this interaction and neither is the size-formation interaction. The variance from these three items is therefore pooled and used to test sizes and formations. Once again the differences in sphericity for different sizes are not significant and the mean square is small. Differences between formations are significant at the 5-per cent level.

On the basis of these analyses it is impossible to find significant differences in sphericity among the rock types here represented. Figure 4 exemplifies the variation due to error[1] (the residual or grains source of variation of Tables 6, 7, 8) around each formation mean. The differences between the formation means are small, the error variation large; sample differences or interaction add to this variation and hence no statistically significant differences could be established between mean sphericities for rock types. Figure 4 shows that the trend in sphericity is from least spherical in the arkoses to most spherical in the quartzites, the graywackes being intermediate; this trend would be expected but the difference is too small to be positively confirmed.

Further analyses were performed utilizing the data for two formations within each rock type which possessed three sizes in common. Again the results were disappointing; the arkoses showed no significant differences for any factor or interaction. The graywackes again yielded significant differences at the 5-per cent level among samples and no other significant differences. The quartzites possessed a highly significant (0.1-per cent level) interaction between sizes and formations.

For the graywackes and quartzites, the data for the formation not used in the last analyses could be arranged for an individual analysis by use of three sizes for the two samples available. Again no further information was forthcoming.

The sample differences and size-sample or size-formation interactions contribute rather large-magnitude variation in most cases, and as the size differences are exceedingly small and inconsistent (interactions significant) the data can be rearranged and each size grade looked upon as a subsample of each sample. In this way, all the data could be utilized in a single analysis, but rock types should be treated separately and hence the 900 sphericity measurements for each rock type were analyzed as a completely randomized design (Snedecor, 1946, p. 236; Tables 9–11).

Successive testing of the variation of each term against the preceding led to significant differences between sizes for the arkose data. However, previous analyses have shown that this size difference is not consistent and may be neglected from a petrographical viewpoint. As the samples yielded such small differences, the differences between samples and between sizes (*i.e.*, subsamples of the same sample) were pooled and the differences among formations were then significant at the 5-per cent level when tested against the pooled error term. This merely confirms previous findings based on Table 7.

From analysis of the graywacke data, the sizes again proved significantly different at the 0.1-per cent level, but the inconsistency of sphericity differences of size over samples suggests no important petrographical implications. The differences between formations is insignificant.

In the case of the quartzite data, the only significant differences occurred between sizes, as already and repeatedly pointed out, this is not to be taken as implying consistent change of sphericity with size (*see* Fig. 5) and hence is to be looked upon as differences between subsamples of the same sample.

Summarizing more samples and subsamples are needed; size may be ignored. This set of 2700 measurements indicates that the sampling plan was incorrectly devised. Also this data does not corroborate claims in the literature that sphericity and size are related.

Figures 4 and 5 suggest that the variation between samples and sizes (subsamples) around the rock-type means increases from arkoses through graywackes to a maximum in quartzites. The least variation between samples and sizes and the greatest variation between grains occurs in the arkose; the graywackes are intermediate; the quartzites have the greatest variation between samples and sizes and the least

[1] In terms of the 5-per cent least significant differences (Johnson, 1950, p. 123).

variation among grains (*see also* Table 13). This feature was not evaluated separately, and the differences are not statistically significant, but frequency distribution is definitely not normal as both the skewness and kurtosis are highly significant. (*See* Table 13; Fig. 6.) The skewness

TABLE 9.—ANALYSIS OF VARIANCE OF SPHERICITY MEASUREMENTS: ARKOSES
(3 formations; 2 samples; 3 sizes; 50 grains)

Source of variation	Degrees of freedom	Sum of squares	Mean square	*F*
Formations	2	837.50	418.75	3.854*
Samples	3	11.19	3.73	<1
Sizes	12	1618.40	134.86	1.886*
Grains	882	63,068.50	71.51	....
Total	899	65,535.59	....	....
Pooled error (samples and sizes)	15	1629.59	108.64	....

TABLE 10.—ANALYSIS OF VARIANCE OF SPHERICITY MEASUREMENTS: GRAYWACKES
(3 formations; 2 samples; 3 sizes; 50 grains)

Source of variation	Degrees of freedom	Sum of squares	Mean square	*F*
Formations	2	88.11	44.05	<1
Samples	3	1306.82	435.606	2.157
Sizes	12	2423.16	201.93	3.251***
Grains	882	54,780.98	62.11	....
Total	899	58,599.07	65.18	....

TABLE 11.—ANALYSIS OF VARIANCE OF SPHERICITY MEASUREMENTS: QUARTZITES
(3 formations; 2 samples; 3 sizes; 50 grains)

Source of variation	Degrees of freedom	Sum of squares	Mean square	*F*
Formations	2	1813.67	906.835	3.309
Samples	3	822.14	274.046	<1
Sizes	12	3891.92	324.326	6.03***
Grains	882	47,444.52	53.79	....
Total	899	53,972.25	60.04	....
Pooled errors (samples and sizes)	15	4714.06	314.271	....

the presence of similar features with greater magnitude differences in roundness suggest that a more efficient experimental arrangement, particularly with regard to apportionment of samples, would establish this trend.

DESCRIPTION OF ROUNDNESS MEASUREMENTS

The 900 measurements of roundness may also be considered a sample from a parent population, namely, the roundness of quartz grains in 120-mesh (125 micron) size sediments; this is positive, *i.e.*, there are more values of higher roundness than the average in a symmetrical distribution. Similarly the frequency distribution is leptokurtic indicating more roundness values in and around the modal class than would be expected in a normal distribution.

If these 900 measurements are subdivided into 300 for each rock type they again yield nonnormal distributions (Fig. 7; Table 13). All three distributions are positively skewed (g_1 positive) and the quartzites and graywackes are leptokurtic whereas the arkoses yield a nonsignificant value for kurtosis (g_2). The differ-

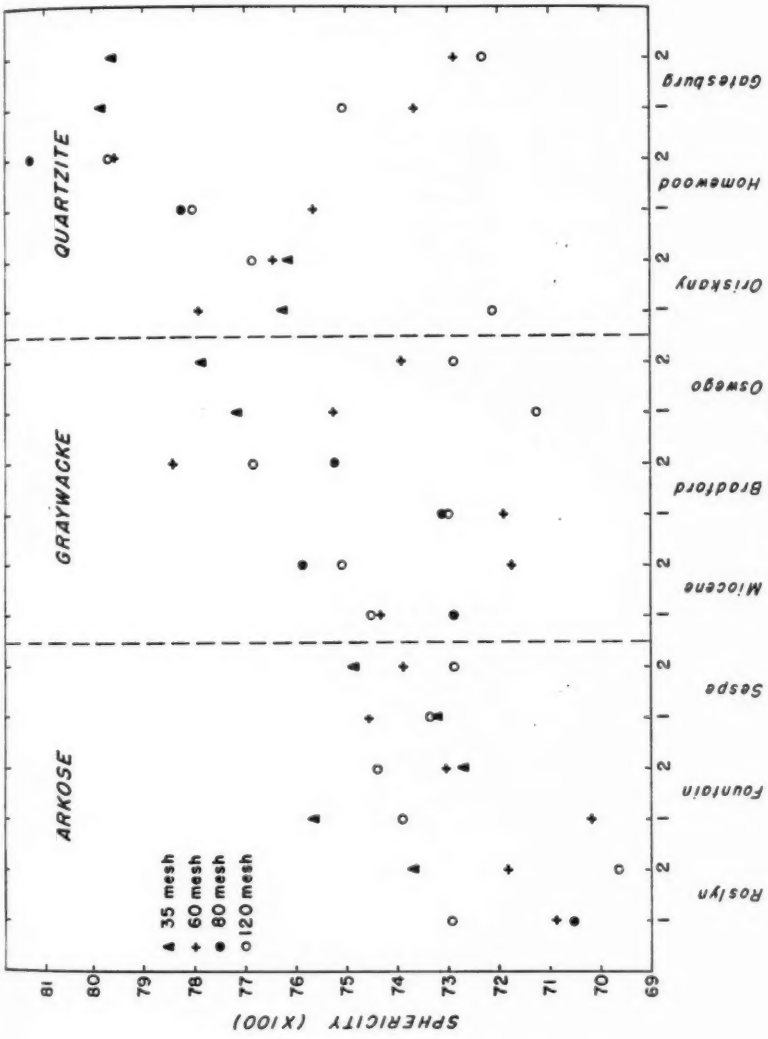

FIGURE 5.—MEAN SPHERICITY FOR EACH SAMPLE, SIZE, FORMATION, AND ROCK TYPE

TABLE 12.—MEANS, ERROR-STANDARD DEVIATIONS AND COEFFICIENTS OF VARIATION OF SPHERICITY DATA FOR ROCK TYPES

(Based on analysis of variance of Tables 7, 8, and 9)

Rock type	Grand mean $\bar{X}_g$	Error standard deviation s_e	Coefficient of variation per cent
Arkose	0.726	0.087	12.04
Graywacke	0.741	0.083	11.19
Quartzite	0.758	0.076	10.03

from arkoses through graywackes to quartzites.

These distributions are not suitable for statistical analysis in their present form, but until further data for different sizes are collected it is not worthwhile transforming the data; it should be remembered, that the probability levels in the analysis of variance will be affected to an unknown degree by the skewed and leptokurtic distributions, and the results are therefore only approximate.

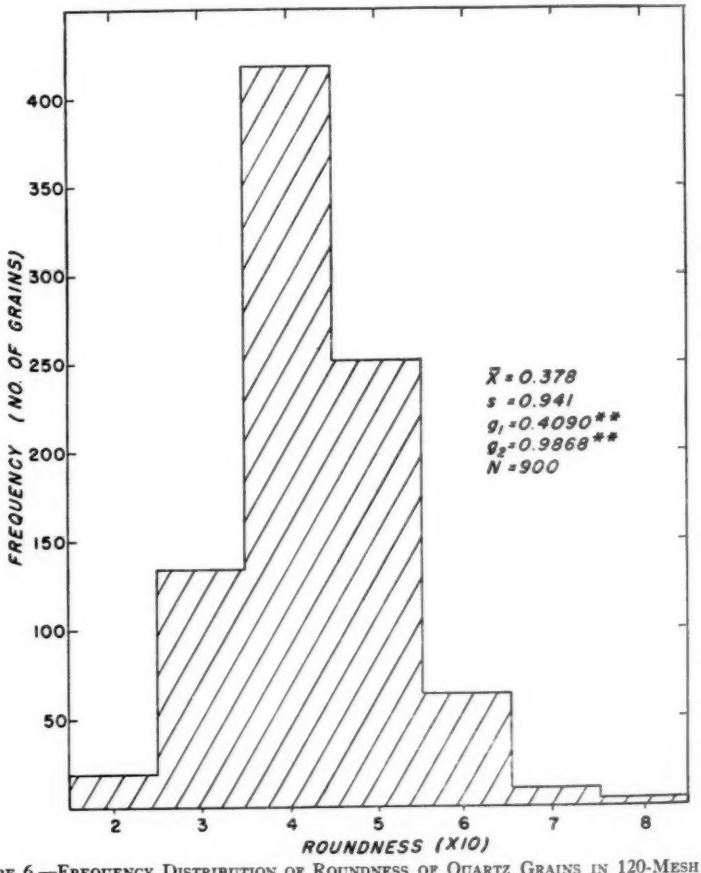

FIGURE 6.—FREQUENCY DISTRIBUTION OF ROUNDNESS OF QUARTZ GRAINS IN 120-MESH (125 MICRON) SIZE GRADE OF SEDIMENTS

$\bar{X}$ = arithmetic mean; s = standard deviation; g_1 = estimate of skewness; g_2 = estimate of kurtosis; N = no. of items; asterisks** indicate significance at the 1-per cent level.

ences between the mean roundnesses for rock types are larger than in the case of sphericity, and the mean roundness progressively increases

ANALYSIS OF ROUNDNESS MEASUREMENTS

As in the case of the sphericity measurements, it is preferable to treat each rock type sepa-

TABLE 13.—ROUNDNESS OF QUARTZ GRAINS IN 125-MICRON GRAIN SIZE OF SEDIMENTARY ROCKS

Rock type	Number of grains	$\bar{x}$	s^2	s	Cv per cent	x^2	P
Arkose	300	3.777	0.553	0.744	19.70	8.55	<0.01 > .001
Low-rank graywacke	300	4.180	0.721	0.849	20.31	6.36	<.02 > .01
Quartzite	300	4.883	0.756	0.870	17.82	14.91	<0.001
All rock types	900	3.780	0.8860	0.9413	24.90	227.57	<<0.001

Coded roundness (P); $X = 10\,P$.

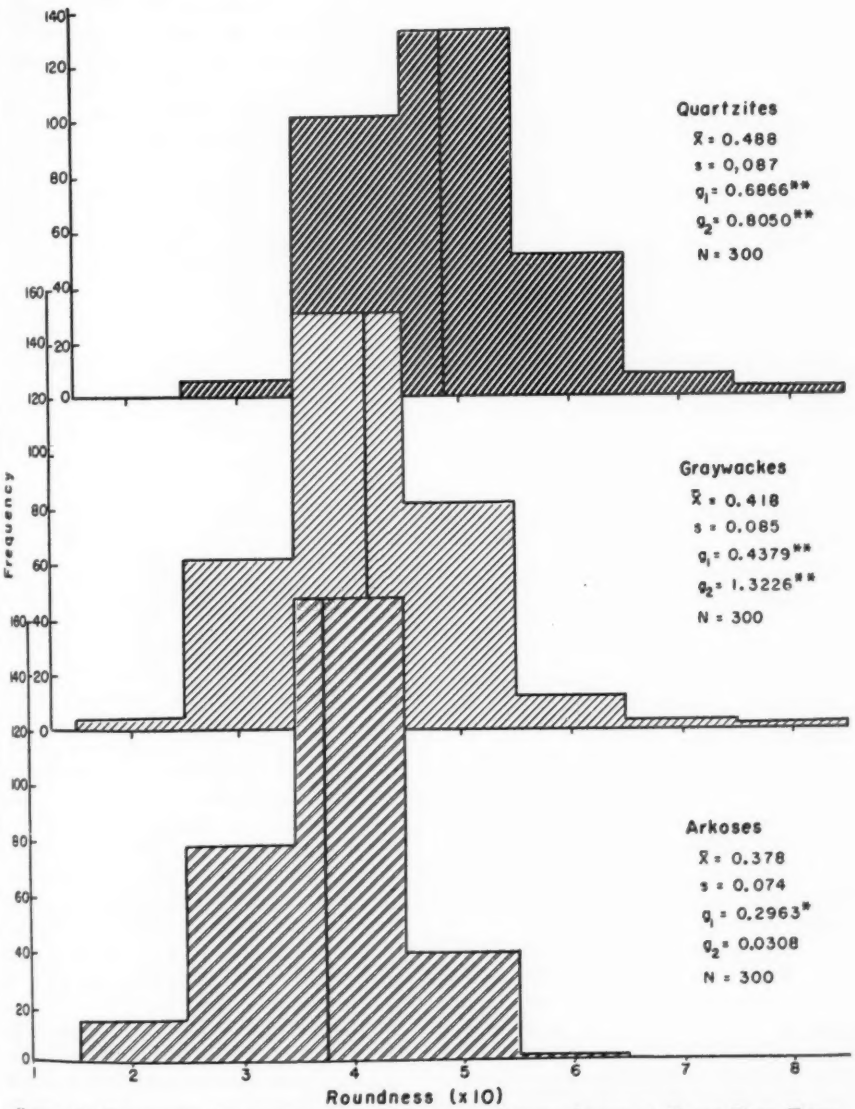

FIGURE 7.—FREQUENCY DISTRIBUTION OF ROUNDNESS OF QUARTZ GRAINS IN THREE ROCK TYPES

$\bar{X}$ = arithmetic mean; s = standard deviation; g_1 = estimate of skewness; g_2 = estimate of kurtosis; N = no. of items; asterisks indicate level of significance: * significant at 5-per cent level, ** significant at 1-per cent level.

TABLE 14.—ANALYSIS OF VARIANCE OF ROUNDNESS MEASUREMENTS: ARKOSES

Source of variation	Degrees of freedom	Sum of squares	Mean square	F
Between formations	2	0.41	0.2050	<1
Between samples	3	2.61	0.870	1.58
Between grains	294	163.02	0.5544	
Total	299	166.04		

$\bar{X}$ = 3.78; s_e = .7446; Cv = 19.70 per cent.

a suitable estimate of the population value as no significant difference occurs in the different classes.

The results of analysis of the roundness data for low-rank graywackes are summarized in Table 15, and here again no significant differences were found. If, however, the pooled variation (*i.e.*, variation between samples and among grains) is used, differences in mean roundness for different graywacke formations is significant at the 5-per cent level. This suggests that variation among mean roundnesses for formations is significantly greater than the variation be-

TABLE 15.—ANALYSIS OF VARIANCE OF ROUNDNESS MEASUREMENTS: GRAYWACKES

Source of variation	Degrees of freedom	Sum of squares	Mean square	F
Between formations	2	31.38	15.69	25.2*
				18.82
Between samples within formations	3	2.50	0.83	1.343
Between grains within samples	294	182.40	0.6204	....
Total	299	216.28	.....	....
Pooled error	297	184.90	0.6225	....

$\bar{X}$ = 4.18; s_e = .7876; Cv = 18.84 per cent.

TABLE 16.—ANALYSIS OF VARIANCE OF ROUNDNESS MEASUREMENTS: QUARTZITES

Source of variation	Degrees of freedom	Sum of squares	Mean square	F
Between formations	2	52.907	26.453	6.072
Between samples within formations	3	13.070	4.356	7.958***
Between grains within samples	294	160.940	0.5474	....
Total	299	226.917	0.7589	....

$\bar{X}$ = 4.88; s_e = .7399; Cv = 15.16 per cent.

rately. When analyses were combined into one design the rock type means differed significantly (Curray, 1951, M.S. thesis, the Pa. State Univ., p. 65).

Analysis of the roundness data for arkoses is summarized in Table 14; no significant differences were found, and it is clear that variation between samples within formations is large. In this case, the variation between samples is not significantly greater than the error variation (grains); the variation from these two sources could be pooled but the differences between formations would still not be significant. The mean roundness for arkoses is

tween grains (residual) and samples within formations combined.

The analysis of roundness data for quartzites is illustrated in Table 16; here there are significant differences between samples within formations, clearly indicating that two samples are insufficient to characterize these rock types. Despite this difference, the variation between quartzite formations is larger than that between samples but is statistically significant only at the 10-per cent level. This suggests that more information, *i.e.* more samples, would suffice to distinguish between quartzite formations in roundness and this in turn suggests that varia-

tion in roundness of quartzites is larger than that of arkoses or graywackes. It appears then that the quartzite group is heterogeneous in terms of roundness.

The roundness means, error-standard deviations, and coefficients of variation for each rock type are listed in Table 17, and the order of increase of roundness from arkose through graywacke to quartzite matches expectations; the variation in the error-standard deviation is, however, small. The coefficient of variation is noticeably larger here than in the sphericity measurement, suggesting less experimental control.

TABLE 17.—MEANS, ERROR-STANDARD DEVIATIONS AND COEFFICIENTS OF VARIATION OF ROUNDNESS DATA FOR ROCK TYPES

(Based on analysis of variance of Tables 14, 15, 16)

Rock type	Grand mean $\bar{x}_g$	Error standard deviation s_e	Coefficient of variation Cv per cent
Arkose	0.378	0.074	19.70
Graywacke	0.418	0.079	18.84
Quartzite	0.488	0.074	15.16

In all these analyses, the differences between formations in mean roundness are overshadowed by differences in mean roundness for samples within each formation. Therefore formations may be ignored and sample differences used as a test for differences between rock types in mean roundness. In Table 18 differences between mean roundness for each rock type are significantly greater than differences between samples. For future experiments it is necessary to obtain more data, if differences in roundness between different rock types are to be established; specifically, it is necessary to increase the number of samples in order to reduce the relative variation arising from this source (Fig. 8). The scatter of sample means around rock type means is least in the arkoses, intermediate in the graywackes, and greatest in the quartzites.

This graphically illustrates the implication of the analysis of variance; the means for samples and formations in the arkose group are similar, hence there are no significant differences. These arkoses in terms of samples and formations are homogeneous in roundness. The graywackes show greater differences both between sample means within formations and between formations, and when sample differences are pooled with differences between grains within samples, the comparison with formation means leads to significant differences. The quartzites show the greatest differences both between sample means within formations and between formations, but the sample differences are so large that no difference between formations is significant. Any attempt to combine the information from different rock types is difficult because variation at the formation, sample, and grain level differs in the different rock types.

TABLE 18.—ANALYSIS OF VARIANCE OF ROUNDNESS VARIATION BETWEEN ROCK TYPES

Source of variation	Degrees of freedom	Sum of squares	Mean square	F
Between rock types	2	188.20	94.10	2.316
Between samples within rock types	15	609.24	40.616	....
Total	17	797.44	....	....

These conclusions are of fundamental importance in planning future experiments, particularly in determining the sampling plan of the experiment. Equal sampling of different rock types is one of the problems; the sampling pattern for arkoses, graywackes, and quartzites must be fundamentally different; the ideal is to choose the numbers of samples in proportion to the magnitude of variability at each stage. This sampling plan is an obvious derivative of the processes of sedimentation which lead to differences between samples, formations and rock types.

INTERRELATIONSHIP BETWEEN SPHERICITY AND ROUNDNESS

Examination of the relationship between sphericity and roundness is possible only on the data for the 125-micron, 120-mesh grade size, and the data for sample, formation, and rock-

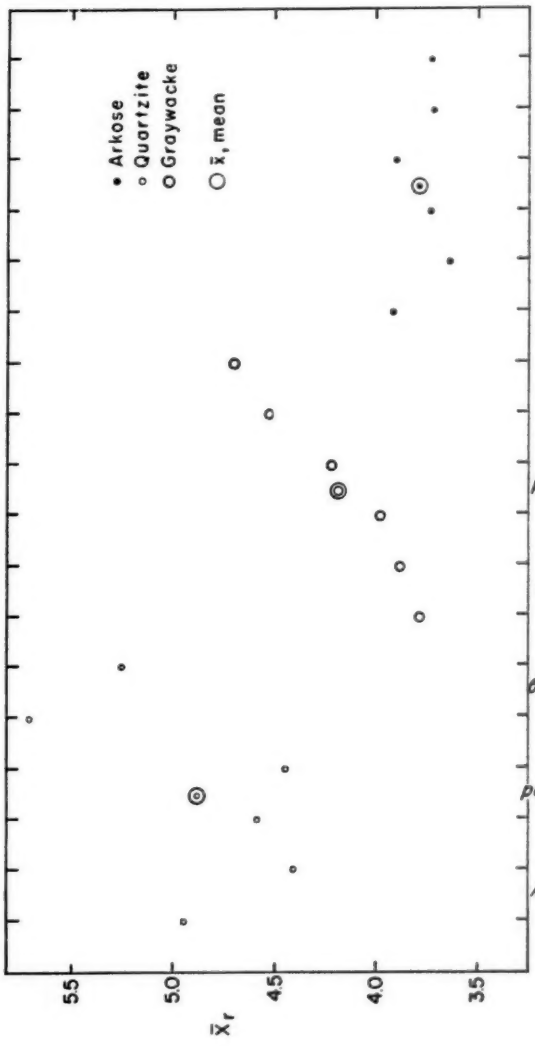

FIGURE 8.—MEAN ROUNDNESS FOR SAMPLES AND ROCK TYPES (120 MESH)

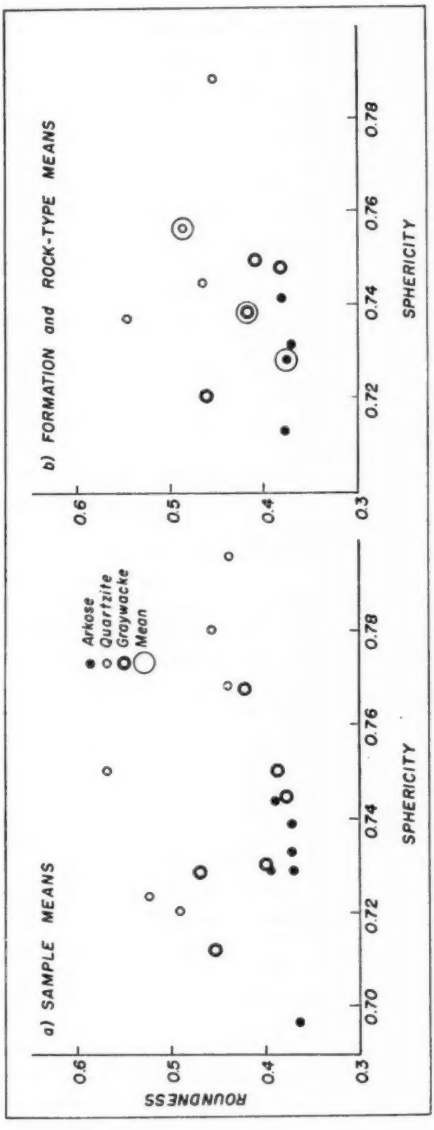

FIGURE 9.—MEAN SPHERICITY COMPARED WITH MEAN ROUNDNESS OF QUARTZ GRAINS IN 125-MICRON GRAIN SIZE

type means are plotted in Figure 9. It is difficult to decide on the basis of these plots whether a real relationship exists, and as the differences between sample means, formation means, and rock-type means are not significant in most cases, no attempt has been made to analyze the data for a trend. The arkoses do tend to possess lower sphericity and roundness than the graywackes and quartzites as shown by the rock-type means. However, the formation means show a wide spread, and the sample means an even wider spread; presumably the grains would show an even greater spread. Much more data will be necessary to establish a possible trend.

The spread between samples (Fig. 9a) and between formations (Fig. 9b) increases from arkoses through graywackes to quartzites. This suggests that the fundamental basis for comparison may be the variance and not the means, a feature which has emerged from a number of our recent investigations of sediments, e.g., size versus sorting (Griffiths, 1951, p. 241), and orientation of grains in sediments (Griffiths, 1952a, p. 48; Griffiths and Rosenfeld, 1950, p. 220; 1953, p. 204).

The graphs emphasize the fact that the range of variation in sphericity is much less than the range of variation in roundness, and this implies that greater precision is necessary to estimate sphericity than roundness if real differences are to be defined. This was pointed out in an earlier experiment (Rosenfeld and Griffiths, 1953, p. 583), and from the results of these investigations it seems advisable to use measuring techniques and avoid comparison standards in so far as possible.

Conclusions

On the basis of this experiment, when three-dimensional intercept sphericity is measured by the procedure described, the distribution of sphericity measurements is approximately normal with mean 0.7518 and standard deviation 0.0834 sphericity units. The interval 0.5–1.0 sphericity units includes 99.7 per cent of the area of a normal distribution with these parameters, which implies that this range includes the entire scale likely to occur in sediments. The mean sphericity of quartz grains in quartzites appears to exceed that in low-rank graywackes, and the quartz grains of graywackes are more spherical than those of arkoses, although on the basis of this experiment the differences are not statistically significant.

The investigation of petrographic properties of sediments by the use of sieves to determine size can result in confusion. No consistent relationship exists between size and sphericity, and the dividing of samples of sediments into sieve fractions introduces a large and inconsistent variation between size fractions. The theoretical uncertainty of the size-shape relationship has been commented on by Griffiths, (1952b, p. 1256), and this experiment justifies that view.

Because the range of variation in sphericity is small, and differences between different samples of the same formation large, it will be necessary to design a sampling plan with care to establish differences in mean sphericity among formations; the variation of sphericity within samples, *i.e.*, between grains—and between samples and formations is different in the different rock types and the sampling program must take this into account. Variation tends to be greater among grains than between samples in arkoses, whereas in quartzites the reverse is more common. The efficient apportionment of numbers of grains per sample, numbers of samples per formation, and numbers of formations per rock type will, therefore, vary from one rock type to another.

The roundness of quartz grains in the 125-micron size determined by visual comparison with charted standards yields skewed distributions, and in low-rank graywackes and quartzites the distributions are leptokurtic. These distributions are difficult to manipulate and may necessitate a transformation of the variable before roundness can be efficiently analyzed. It has often been noted that variation in roundness is greater than that of sphericity but the implications of this fact are obscure. In the present case, the roundness means appear to be related to the variances in a complicated fashion, and unless this feature can be offset by suitable sampling statistical analysis will yield only approximate results.

The mean roundness is least in arkoses and greatest in quartzites, but once again the differences may not be statistically significant. Indeed, because the mean roundness for formations and samples is correlated with the respec-

tive variances in graywackes and quartzites, no precise comparison of rock type means is possible. Variation within the sample tends to be large, and that between samples and between formations small in arkoses; the reverse occurs in the quartzites. This once more emphasizes the need for a suitably designed sampling program which will be differently arranged for the different rock types.

The interrelationship between sphericity and roundness is obscure for the 125-micron grade size, and although the rock type means are aligned as would be expected—increasing sphericity and roundness from arkose through graywacke to quartzite—the wide scatter of formation means and sample means suggest that the data from this experiment cannot establish the interrelationship.

Perhaps the most fundamental conclusion suggested by these data is that more knowledge is needed before a suitable experiment may be designed. The problem of sampling sediments has been paramount throughout the analysis and, unless this problem is satisfactorily solved, no experiment will be capable of establishing unambiguous conclusions about variation in petrographic properties of sedimentary rocks. Significantly all the properties investigated by measurement have shown similar variation. Solution of the sampling problem for a single variable will probably lead to a general solution of the entire problem.

References Cited

Cochran, W. G., and Cox, G. M., 1950, Experimental designs: N. Y., Wiley and Sons, p. 1–454.

Fisher, R. A., 1948, Statistical methods for research workers: London, Oliver and Boyd, 10th ed., p. 1–354.

Griffiths, J. C., 1951, Size versus sorting in some Caribbean sediments: Jour. Geology, v. 59, p. 211–243.

—— 1952a, A review of dimensional orientation of quartz grains in sediments: The Pa. State Univ., Min. Industries Expt. Sta. Bull. 60, p. 47–55.

—— 1952b, Measurement of the properties of sediments (abstract): Geol. Soc. America, Bull. v. 63, p. 1256.

—— 1953, Estimation of error in grain-size analysis: Jour. Sed. Petrology, v. 23, p. 75–84.

Griffiths, J. C., and Rosenfeld, M. A., 1950, Progress in measurement of grain orientation in Bradford sand: The Pa. State Univ., Min. Industries Expt. Sta. Bull., v. 56, p. 202–236.

—— 1953, A further test of dimensional orientation of quartz grains in Bradford sand: Am. Jour. Sci., v. 251, p. 192–214.

Johnson, L. P. V., 1950, Applied biometrics: Minneapolis, Burgess Publ. Co., p. 1–165.

Krumbein, W. C., 1941, Measurement and geological significance of shape and roundness of sedimentary particles: Jour. Sed. Petrology, v. 11, p. 64–72.

Krynine, P. D., 1948, The megascopic study and field classification of sedimentary rocks: Jour. Geology, v. 56, p. 130–165.

Otto, G., 1933, Comparative tests of several methods of sampling heavy-mineral concentrates: Jour. Sed. Petrology, v. 3, p. 30–39.

Plumley, W. J., 1948, Black Hills terrace gravels; a study in sediment transport: Jour. Geology, v. 56, p. 526–577.

Rosenfeld, M. A., and Griffiths, J. C., 1950, A new approach to the problem of porosity measurement: The Pa. State Univ., Min. Industries Expt. Sta. Bull., v. 56, p. 163–201.

—— 1953, An experimental test of visual comparison technique in estimating two dimensional sphericity and roundness of quartz grains: Am. Jour. Sci., v. 251, p. 553–585.

Smith, J. G., and Duncan, A. J., 1945, Sampling statistics and applications: N. Y., McGraw-Hill, p. 1–498.

Snedecor, G. W., 1946, Statistical methods; Ames, Iowa State College, p. 1–485.

Scripps Institute of Oceanography, La Jolla, Calif.; Pennsylvania State University, University Park, Pa.

Manuscript Recieved by the Secretary of the Society, January 15, 1954.

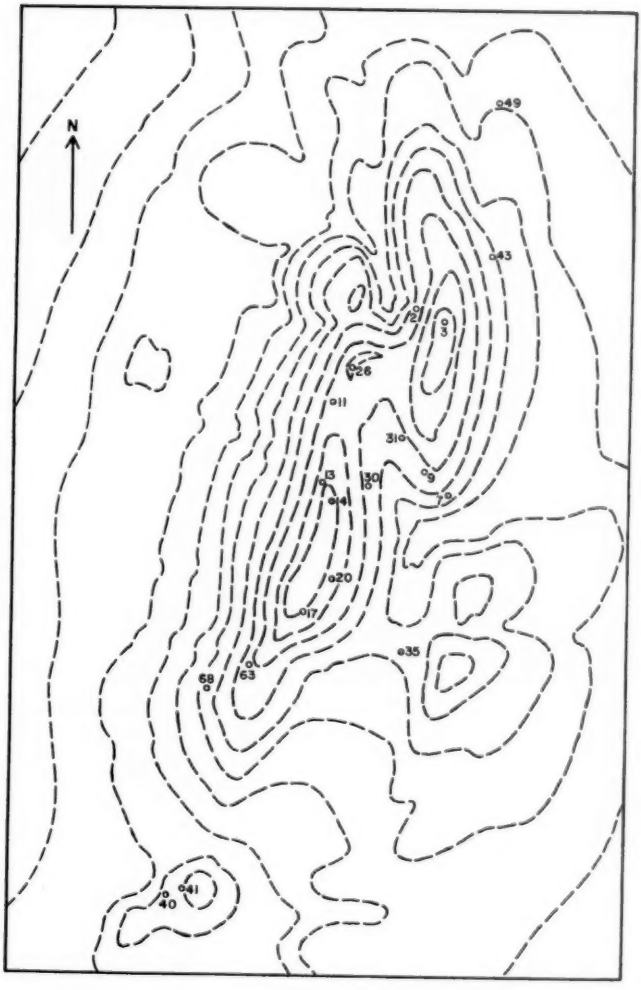

GEOLOGIC MAP
S

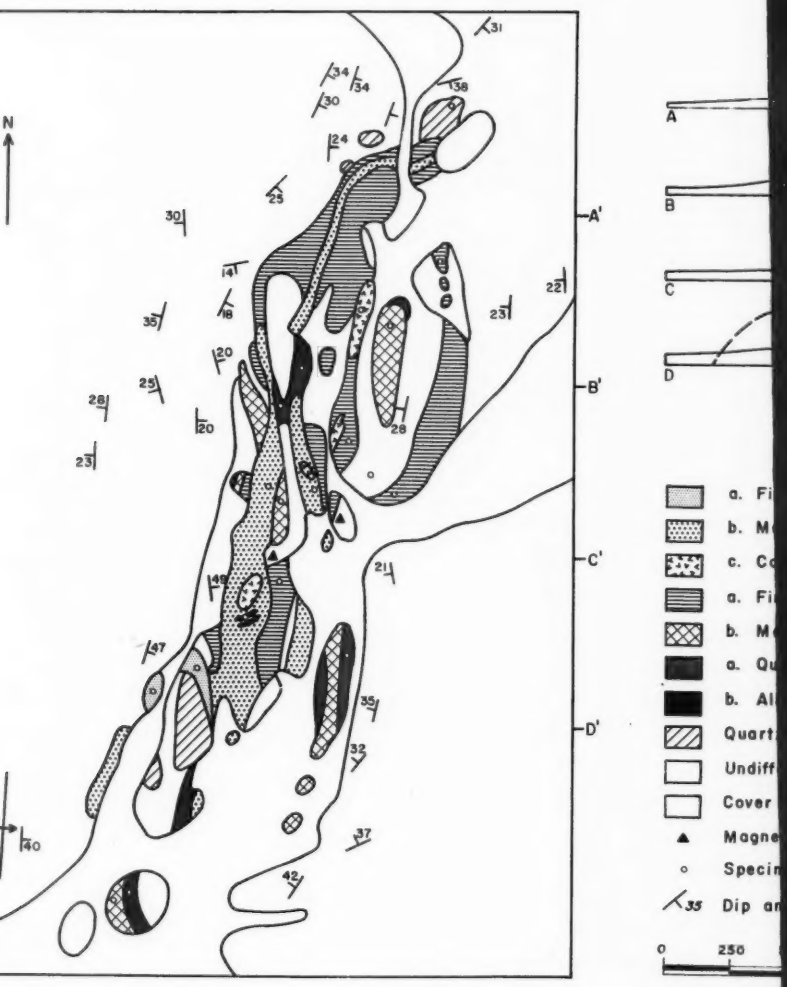

OGIC MAP AND CROSS SECTIONS OF SPILITIC INTRUSION, SOCORRO COUNTY, NEW MEXICO

Contour interval 20 feet

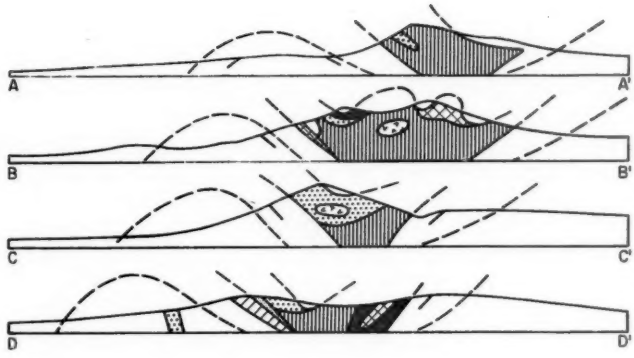

LEGEND

a. Fine-grained, porphyritic	Group 1	
b. Medium-grained	color index 40-50	
c. Coarse-grained		
a. Fine-grained, non-porphyritic	Group 2	
b. Medium-grained	color index 20-30	
a. Quartz-albitites	Group 3	
b. Albitites	color index 1-10	

Quartzofeldspathic rocks

Undifferentiated sediments, including contact quartzites

Cover

▲ Magnetite

○ Specimen locality referred to in text

35 Dip and strike of sediments

0 250 500 1000 feet

BULLETIN OF THE GEOLOGICAL SOCIETY OF AMERICA
VOL. 66, PP. 1097-1108, 5 FIGS., 1 PL. SEPTEMBER 1955

SPILITIC INTRUSION NEAR LADRON PEAK, SOCORRO COUNTY, NEW MEXICO

BY ROBERT W. DUSCHATKO AND ARIE POLDERVAART

ABSTRACT

A suite of highly altered spilitic rocks from an intrusion 100-150 feet thick in the Yeso formation is described. There are many similar intrusions throughout the region. The alteration process is traced in detail. With falling temperatures each metallic element tends to form its own mineral or minerals with Si and Al as the only other cations. Deuteric alteration probably has been accentuated by distillation of hyperfusibles, especially sulphate radicles, from the country rocks which include much gypsum. Fine- to medium-grained albitites are the end products of differentiation, and zircon studies indicate that these rocks are partly of magmatic, partly of metasomatic origin. Five chemical analyses and results of 10 spectrographic analyses are given.

CONTENTS

TEXT

	Page
Introduction	1097
Field characteristics	1098
Petrography	1099
Group 1. Basaltic to doleritic rocks with color index 40–50	1099
Group 2. Basaltic to doleritic rocks with color index 20–30	1100
Group 3. Fine- to medium-grained albitites with color index 1–10	1100
Mixed rocks	1100
Petrology	1101
General	1101
Zircons	1102
Alteration	1106
Petrogenesis	1106
Igneous rocks	1106
Metasomatic and mixed rocks	1107
Conclusions	1107
References cited	1108

ILLUSTRATIONS

Figure	Page
1. Index map of New Mexico showing location of the intrusion	1098
2. Metasomatic quartz-feldspar rocks and intrusion breccia—Magnification ×10	1100
3. Stages in the recrystallization of quartz observed in metasomatic quartz-feldspar rocks—Magnification ×5	1101
4. Composite triangular diagram of chemical variation of the spilitic rocks and albitites	1104
5. Zircons of the spilitic and associated rocks—Magnification ×40	1105

Plate	Facing page
1. Geologic map and cross sections of spilitic intrusion, Socorro County, New Mexico	1097

TABLES

Table	Page
1. Modes	1102
2. Chemical analyses	1103
3. Spectrographic analyses	1104

INTRODUCTION

The intrusion is located 5¾ miles west of Ladron Peak at the south end of the Lucero Uplift in Socorro County, New Mexico (Fig. 1). During field work for a research project of the Atomic Energy Commission, Duschatko found many similar intrusions in the region, chiefly in the Permian upper Yeso formation. During a short stay of Poldervaart, a number of these intrusions were visited and one was selected for further study. The present body was chosen because it appeared thoroughly representative of this type of intrusion in the region and exposures seemed slightly better than encountered elsewhere.

The emphasis of this account is on results obtained, and in the opinion of the writers further work on other bodies of similar character is required before the petrogenesis of the rocks can be understood fully. It is hoped that the present paper will stimulate such further studies.

The field work formed part of a study of the

Lucero Uplift, financed by the Atomic Energy Commission. Chemical analyses were done by Dr. H. B. Wiik, of Helsinki, Finland, and funds for the analyses were made available through a grant from the Kemp Fund of Columbia University. Miss Irene H. Sribny did the spectrographic work under the able guidance of Mr. Karl Turekian, both of the Department of Geology, Columbia University. The writers gladly and gratefully acknowledge this assistance.

FIGURE 1.—INDEX MAP OF NEW MEXICO SHOWING LOCATION OF THE INTRUSION

FIELD CHARACTERISTICS

The area studied is about three-quarters by one-half mile, with a central long hill about 150–200 feet above the surrounding plain (Pl. 1). The topography can be attributed to the more resistant character of the igneous and contact metamorphic rocks, as compared with the rather friable sediments which make up the country rocks. Regionally the latter form a broad lowland consisting of sandstones, siltstone, limestones, and gypsum of the Permian Yeso formation, with total thickness of about 1100 feet. Siltstones and gypsum predominate in the section, with interspersed sandstone and limestone beds, in individual units rarely more than 20–50 feet thick. Exposures of the sediments are poor. Along the crest of the hill in the mapped area exposures are fairly continuous, but rubble and soil commonly cover lower parts of slopes.

Associated intrusions are emplaced in Triassic sediments and in places are covered by Quaternary pediment gravels which contain pebbles of the spilitic rocks. The intrusions are therefore post-Triassic, pre-Quaternary, and have been mapped as Tertiary by Kelley and Wood (1951). The cover of the intrusions at the time of emplacement was less than 3000 feet, probably around 1500 feet.

The igneous rocks were classified in the field on lithologic characters, especially megascopically identifiable mineral composition, color index, and grain-size. Subsequent laboratory work corroborated and simplified the field classification, with corresponding simplification of the map. Three major groups have been defined:

Group 1. Melanocratic, basaltic and doleritic rocks; subdivided into (a) fine-grained, porphyritic, (b) medium-grained, and (c) coarse-grained rocks
Group 2. Mesocratic, basaltic to doleritic rocks; subdivided into (a) fine-grained, nonporphyritic, and (b) medium-grained rocks
Group 3. Leucocratic, fine- to medium-grained albitites; subdivided into rocks (a) with small amounts of quartz, and (b) without quartz.

It was apparent in the field and later confirmed in laboratory studies that all the rocks had suffered severe alteration which could not be attributed to atmospheric weathering alone.

Poor exposures have prevented the differentiation of sediments on Plate 1. In the vicinity of the igneous body the sediments include white, fine-grained quartzites flecked by opaque iron ores. At both the northern and southern end of the intrusion there are areas of coarse-grained glassy quartzites, quartzofeldspathic rocks, and quartz-feldspar breccias with feldspathic veinlets cementing the angular quartzitic fragments. Exposures in these areas are poor, and most of the material is indigenous float. The feldspathic veinlets of the breccias are fine-grained albitite, but the sodic plagioclase of the quartzofeldspathic rocks is of larger grain size. At two localities small outcrops of recrystallized limestone have been found associated with coarsely crystalline magnetite.

Absence of definite marker horizons makes detailed structural interpretation difficult. In general the sediments strike north with moderate east or west dips, the regional dip being toward the west. Considerable variations in strike and dip within distances of a few hundred feet suggest local folding and possibly faulting. Contact exposures of the intrusive are few and limited to a few square feet in each instance. Small patches of sandstone and quartzite on the upper slopes of the hill are discordant, but this relation could not be established elsewhere, and topographic relief is inadequate to determine the dip of boundary surfaces with certainty. The intrusion may be shaped as a partly discordant sheet or as a dikelike body, probably emplaced along the axis of a doubly plunging syncline (Pl. 1). Contacts are shown on the map as solid lines only for clarity, but they are generally transitional within the igneous rocks and largely inferred along the outer boundaries of the body.

Petrography

Group 1. Basaltic to Doleritic Rocks with Color Index 40–50

The texture of the rocks is subophitic to subhedral. Basaltic varieties contain phenocrysts of plagioclase and augite, set in a fine-grained groundmass. Plagioclase and augite are major constituents of all the rocks. Biotite is absent in some of the specimens, a minor constituent in others, but prominent in a few rocks. Quartz and potash feldspar are absent in all the rocks. Plagioclase is oligoclase ranging to albite at crystal margins. Most plagioclase laths (50–80 per cent) exhibit complex twinning. Augite generally is lime-rich, iron-poor, with a range of 2V (+) 50°–55°, and β values 1.680–1.685, but augite phenocrysts in basaltic varieties have a range of 2V (+) 46°–50°. Biotite is a magnesian variety with β 1.635. Skeletal crystals of titaniferous iron ore and small apatite needles are accessories in all the rocks.

Alteration is pronounced in all specimens, but the distribution of alteration products is patchy and irregular, as if effected by solutions which migrated through the rocks and altered the minerals in their paths. Plagioclase has been partly replaced by aggregates of prehnite in all the rocks. The aggregates form irregular patches and are associated with calcite, chlorite, and zeolites, especially thomsonite. Much of the remaining plagioclase is intensely sericitized and kaolinized, but many of the albitic outer rims of the crystals have remained clear. Part of the sericitization may have occurred earlier than kaolinization of plagioclase, especially since some sericite flakes are well developed. Alteration of augite is curious and indicates a tendency toward separation of calcium from magnesium in the minerals formed. Calcium contributed to the formation of very pale-green or pale-brown calciferous hornblendes, tremolite, prehnite, calcic zeolites, or calcite, roughly in that order of crystallization. Magnesium formed biotite, of later formation than the amphiboles, and finally chlorite (penninite). Chlorite may be pseudomorphous after biotite or, like prehnite, may be found in irregular patches of erratic distribution. Sphene in some specimens occurs as narrow rims around opaque ore.

Group 2. Basaltic to Doleritic Rocks with Color Index 20–30

Rocks of this group are petrographically similar to those of Group 1, but contain larger amounts of sodic plagioclase. The basaltic varieties are nonporphyritic. Alteration of plagioclase to prehnite may be found in rocks of this group. Alteration of augite is to pale-green or pale-brown hornblendes rather than tremolite, and the amphiboles have a characteristic prismatic habit with ragged terminations. Rims of sphene around opaque ore are more conspicuous than in Group 1, and in several rocks sphene has been replaced by rutile, calcium presumably being used in calcic zeolites or calcite. Penninite is still the dominant chlorite, but in addition clinochlore is found. One of the basaltic specimens (locality 43) contains barely distinguishable subangular fragments of an even finer-grained, nonporphyritic, extremely altered rock with more ferromagnesian minerals, although opaque ores are sprinkled evenly throughout the enclosed and enclosing rock.

Group 3. Fine- to Medium-grained Albitite Color Index 1–10

Small albite laths are the main constituent of all rocks of this group. Crystals are generally turbid through pronounced sericitization and kaolinization, but may have narrow clear outer rims of pure albite. The majority of the laths show simple Carlsbad twinning, but complex twins and untwinned crystals are also encountered. Some sections show a tendency toward porphyritic development of albite, though grain sizes are seriate rather than inequigranular. One specimen (locality 41) shows minute quartz-albite intergrowths associated with interstitial quartz. Prehnite and zeolites are absent in all rocks of this group, but small amounts of calcite may be found. Quartz is present in most of the rocks and occurs as small, interstitial, anhedral crystals. Rocks without quartz are probably only locally developed (locality 17). Colorless diopside is found in minor amounts and shows alteration to tremolite, which in turn may be partly replaced by calcite. Chlorite and sericite are found as interstitial tufts or minute flakes. Titaniferous iron ore is also a minor constituent and is found associated with sphene and rutile which is quite conspicuous in some rocks (locality 17). Biotite is of erratic occurrence, but is the dominant minor constituent in one specimen (locality 35). Apatite and zircon are ubiquitous accessory minerals. Potash feldspar is absent from all the rocks. One specimen (locality 11) contains ovoidal patches of an even finer-grained rock of essentially the same mineralogical composition as the enclosing rock.

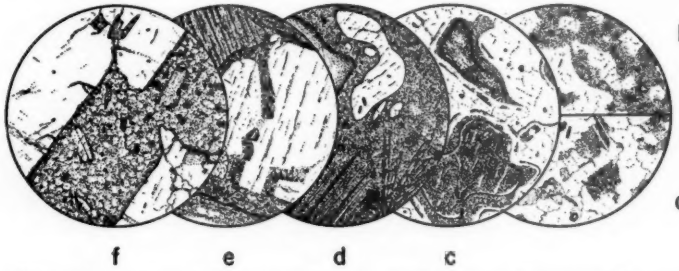

FIGURE 2.—METASOMATIC QUARTZ-FELDSPAR ROCKS AND INTRUSION BRECCIA—MAGNIFICATION X10

a, b—fine-grained, recrystallized Yeso siltstones with interstitial oligoclase.
c, d, e—coarse-grained quartz-feldspar rocks; *note* narrow albite rims around oligoclase in *c*, with rims of minute granules (magnetite?) in surrounding quartz; large albitite patch in *d*, with variolitic development of albite, and evident corrosion and resorption of both quartz and oligoclase; narrow veinlets of albitite in quartz, issuing from albitite rims around oligoclase in *e*.
f—veinlet of magmatic albitite in quartz-feldspar breccia.

Mixed Rocks

Thin sections were made of recrystallized Yeso siltstones found near contacts and of the

peculiar quartzitic rocks at the north and south ends of the intrusion. The recrystallized siltstones are fine-grained and show small, interlocking quartz crystals with interstitial, subhedral, turbid sodic plagioclase (Fig. 2a, b). The glassy quartzites consist of interlocking larger individuals. The breccias consist of similar quartzofeldspathic material, sharply cut by veinlets of fine-grained albitite in which there are irregular remnants of larger quartz and feldspar crystals with diffuse borders (Fig. 2f).

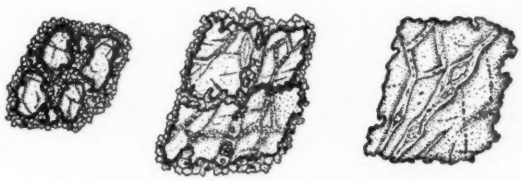

FIGURE 3.—STAGES IN THE RECRYSTALLIZATION OF QUARTZ OBSERVED IN METASOMATIC QUARTZ-FELDSPAR ROCKS—MAGNIFICATION ×5

large quartz crystals with minor opaque ore dust which in one sample is concentrated in a network enclosing areas of clear quartz. This network appears to represent sealed fractures since rutile is also concentrated here along with magnetite granules. Similar large quartz mosaic units with blocky extinction are found in the quartzofeldspathic rocks, in addition to smaller quartz crystals and large crystals of oligoclase. Each plagioclase crystal is surrounded by a rim of extremely fine-grained turbid albite with a little or no quartz, and tongues of this material may also protrude between adjacent quartz crystals (Fig. 2c, d, e). Some of these rims are flanked by narrow, discontinuous bands of a concentration of opaque particles sharply delineated outwards and located within the quartz but wholly outside the albitite rims (Fig. 2c). Wider rims, found in the same specimens, show evidence of reaction and resorption of both earlier plagioclase and quartz. In these rims variolitic new growths of turbid albite may also be found (Fig. 2d).

The recrystallization of quartz can be traced in the sections, from the small interlocking crystals which characterize the recrystallized siltstones to the larger mosaic units with blocky extinction which represent the end-products of this process. Various stages are shown in Figure 3. The irregular extinction of the larger units is attributed not to strain but to imperfections in orientation of the smaller crystals which merged upon recrystallization into the

PETROLOGY

General

Estimated mineralogical compositions are given in Table 1. Table 2 shows the results of chemical analysis of five rocks, with calculated norms.

The analyses have been plotted in figure 4 on triangular (atomic) Mg-(total)Fe-(Na + K); (atomic) Ca-Na-K, and Q-L-M von Wolff diagrams superimposed on one another.

Chemical variations are obviously highly irregular. The rock from locality 68, although basaltic and porphyritic, is considerably albitized, presumably through absorption of sodium in the groundmass. The most mafic rock of the suite is No. 2, but it is coarser-grained than Nos. 68 and 13. Sample No. 13 has Ca equivalent to No. 2, but is further advanced in the ferromagnesian reaction series. Rock No. 7 is equally advanced with respect to Mg-Fe fractionation as samples Nos. 13 and 68, but is as highly albitized as specimen No. 68. The albitite No. 11 is evidently the most advanced rock in the differentiation series of this igneous suite.

Table 3 shows the spectrographic results. Ba, Sr, Ni, Cr, and Co were determined by mixing one part of sample with two parts of graphite buffer and arcing 10 mgs of the mixture to completion in a platform electrode at 16 amperes. Cu, Pb, and Ga were measured with centerpost electrodes at 7 amperes (DC

arc). Arcing was terminated after the sodium burning was completed, usually 60 seconds for a 10-mg sample. All samples were compared with synthetic standards in which the matrix was similar to the samples studied.

(Poldervaart, 1955). Four specimens of Groups 1 and 2 (spilitic basalts and dolerites; localities 2, 3, 7, 13) contained only a few zircons, but from two others (localities 14, 20) more crystals were recovered. The majority of the

TABLE 1.—MODES

	Spilitic basalts and dolerites							Albitites		
Locality reference	68	13	30	2	7	3	40	11	26	17
Classification	1a	1b	1b	1c	2a	2b	2b	3a	3a	3b
Quartz	–	–	–	–	–	–	–	4	3	–
Plagioclase	12*	48	47	51	75	72	76	90	94	95
Prehnite	+	3	5	1	1	–	–	–	–	–
Zeolites	–	1	2	1	3	–	–	–	–	–
Calcite	+	+	½	½	½	½	+	+	+	1
Augite	3*	25	19	1	½	½	–	3	½	–
Amphiboles	+	+	½	42	2	14	12	½	½	½
Biotite	1	9	12	½	3	+	–	–	+	–
Chlorite	+	4	5	1	5	2	1	½	½	½
Sericite	+	+	+	+	+	+	+	+	+	+
Opaque ores	10	9	8	1	10	10	10	2	1	1
Sphene	+	+	+	+	+	+	1	+	½	+
Rutile	–	–	–	–	–	–	–	+	+	2
Apatite	1	1	1	1	+	1	+	+	+	+
Groundmass	73	–	–	–	–	–	–	–	–	–
Color index	50	47	44	45	20	26	24	6	3	4
Average length plagioclase (mm)	1.3* 0.2†	0.9	0.5	2.5	0.3	0.9	1.0	0.4	0.8	0.2

* Phenocrysts.
† Groundmass.

The spectrographic results emphasize the irregular distribution of Ba in the igneous rocks. Sr concentrations remain about the same in the basaltic and doleritic phases and show a maximum in the magmatic albitite No. 17, only to decrease sharply in the albitite of mixed origin No. 11, the quartzofeldspathic rock, and the siltstone. The distribution of Ni and Cr is irregular, but both elements show a maximum concentration in the pegmatitic dolerite from locality 2. Co, Pb, and Ga throughout remain near or below the limits of detection. Cu concentrations are about the same throughout the intrusion, but vary irregularly in the surrounding rocks.

Zircons

Attempts have been made to separate zircons from selected samples of the main rock types

zircons are jagged chips or irregular skeletal crystals, with very few of the simple bipyramidal prisms which characterize zircons of granitic rocks (Fig. 5a). All the crystals are small and short, crystal edges and points are sharp, and crystal surfaces are smooth or slightly striated. One sample (locality 7) yielded an abundant heavy residue consisting almost exclusively of barite. The slide of this rock shows barite associated with prehnite, zeolites, and calcite.

Three specimens of Group 3 (albitites; localities 11, 17, 35) returned small amounts of zircons, approximately equivalent to the amounts recovered from the two specimens of Groups 1 and 2. Zircons of two specimens are sharply euhedral, but of a variety of habits, including many highly elongated crystals (Fig. 5b, c). Those of one albitite (locality 11) are mostly small and well rounded, with

TABLE 2.—CHEMICAL ANALYSES

Analyst H. B. Wiik

Locality reference Classification	68 1a	13 1b	2 1c	7 2a	11 3a	A	B .....
SiO_2	51.47	51.06	48.55	49.23	68.65	50.3	50.9
TiO_2	1.77	1.45	1.23	1.60	1.00	1.5	3.3
Al_2O_3	15.46	15.24	16.94	14.95	14.79	15.7	13.6
Fe_2O_3	4.73	5.69	1.12	6.17	0.73	4.4	2.8
FeO	5.11	4.82	2.59	5.47	0.50	4.5	9.1
MnO	0.06	0.11	0.05	0.07	0.01	0.1	0.2
MgO	4.08	4.03	7.02	5.50	1.41	5.2	4.5
CaO	5.59	6.99	9.89	4.72	2.85	6.8	6.9
Na_2O	6.05	4.50	5.28	4.69	8.82	5.2	4.9
K_2O	1.09	2.34	1.63	1.89	0.94	1.7	0.7
P_2O_5	0.88	0.85	0.37	0.39	0.24	3.6	1.9
H_2O^+	3.32	2.57	3.88	3.95	0.26	0.6	0.3
H_2O^-	0.04	0.04	0.15	0.29	0.11		
CO_2	nil	nil	1.03	0.72	0.10	0.4	0.9
Totals	99.65	99.69	99.73	99.64	100.41	100.0	100.0
Sp. gr.	2.80	2.88	2.74	2.79	2.64	.....	.....

Norms

Qu	.....	.....	.....	.....	10.39
Or	6.46	13.80	9.63	11.19	5.56
Ab	50.96	38.06	24.96	39.69	70.83
An	11.82	14.49	17.72	14.16	.....
Ne	0.11	.....	10.68	.....	.....
Na_2SiO_3	.....	.....	.....	.....	0.32
Acm	.....	.....	.....	.....	2.12
Di Wo	4.48	6.33	9.47	1.02	4.41
Di En	3.22	4.76	7.53	0.77	3.51
Di Fs	0.86	0.94	0.86	0.15	.....
Hy En	.....	3.88	.....	9.27	.....
Hy Of	.....	0.77	.....	1.66	.....
Ol Fo	4.87	0.97	6.98	2.56	.....
Ol Fa	1.39	0.22	0.79	0.49	.....
Il	3.37	2.75	2.34	3.04	1.08
Mt	6.85	8.24	1.62	8.94	.....
Ti	.....	.....	.....	.....	1.06
Ap	1.92	1.86	0.81	0.84	0.53
Cc	.....	.....	2.34	1.64	0.23
H_2O	3.36	2.61	4.03	4.24	0.37
Totals	99.67	99.68	99.76	99.66	100.41

68, 1a—melanocratic, porphyritic, spilitic basalt.
13, 1b—melanocratic, medium-grained, spilitic dolerite.
2, 1c—melanocratic, coarse-grained, spilitic dolerite.
7, 2a—mesocratic, nonporphyritic, spilitic basalt.
11, 3a—albitite with accessory quartz.
A—average first four analyses.
B—average spilite (Sundius, 1930, p. 9).

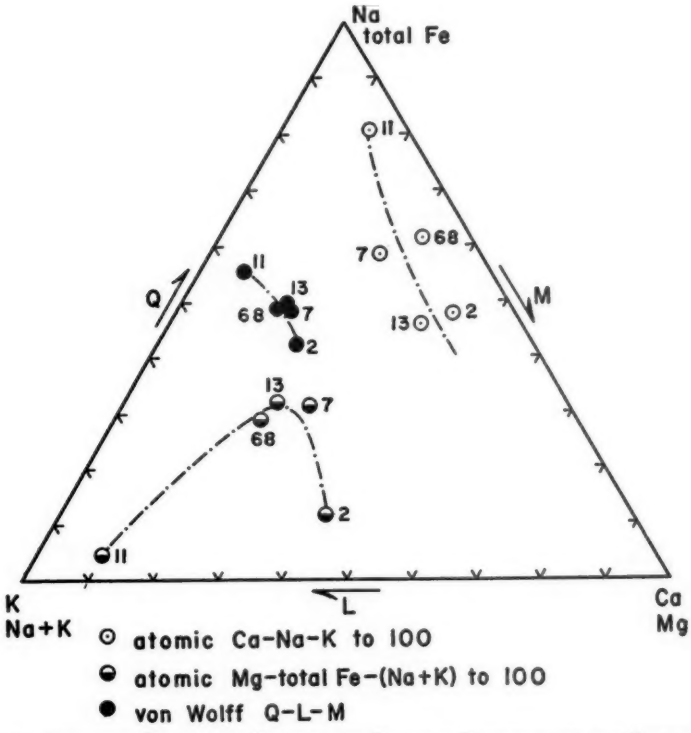

FIGURE 4.—COMPOSITE TRIANGULAR DIAGRAM OF CHEMICAL VARIATION OF THE SPILITIC ROCKS AND ALBITITES

TABLE 3.—SPECTROGRAPHIC ANALYSES

Locality references	Classification	Ba	Sr	Ni	Cr	Co	Cu	Pb	Ga
68*	1a	*2*	*3*	∼.008	*	*	*3*	*	*
63	1a	*4*	*3*	*	*	*	*3*	*	*
13*	1b	*3*	*3*	*	*	*	*3*	*	*
2*	1c	*3*	*3*	.1	.01	*	*2*	*	*
7*	2a	*4*	*3*	∼.008	*	*	*2*	*	*
37	2b	*3*	*3*	∼.008	*	*	*2*	*	*
11*	3a	*1*	*2*	*	*	*	*2*	*	*
17	3b	*2*	*4*	*	*	*	*2*	*	*
49	quartz-feldspar rock	*2*	*2*	∼.008	*	*	*2*	*	*
67	Yeso siltstone	*2*	*1*	*	*	*	*1*	*	*

Numbers used for concentrations of Ba and Sr indicate increasing intensities from *1* to *4*: *1* ∼ 0.01 per cent, *4* ∼ 0.1 per cent. Those used for Cu are: *1* ∼ 0.0005 per cent, *3* ∼ 0.005–0.01 per cent.

Asterisks indicate amounts near or below limit of detection but without marked variation; for Ni 0.008, Cr 0.01, Co 0.0036, Pb 0.0025, and Ga 0.002 per cent.

* Chemically analyzed rocks.

elongation ratios well below 2.0, and with strongly pitted surfaces, but a minority of crystals are sharply euhedral (Fig. 5d).

Heavy residues were also obtained from two quartzites, a sandstone, and a siltstone from the Yeso formation. In all four samples, zircons were abundant. Zircons of the quartzites and the sandstone are small, well rounded, most have elongation ratios well below 2.0, and show strongly pitted surfaces (Fig. 5e). Zircons of the siltstone are of two varieties: the majority are similar to those of the quartzites and sandstone; a minority are thin with elongation ratios exceeding 2.0, smooth surfaces, and rounded terminations. Anatase is also present in these heavy residues. A sample of gypsum from the Yeso formation was examined, but contained no zircons.

Five samples from the north and south ends of the intrusion were examined. Few zircons were recovered from a specimen of a glassy quartzite. A small amount of zircons was obtained from a sample of breccia, but two quartzofeldspathic rocks gave abundant well-rounded zircons with pitted surfaces. One sample shows a majority of grains with elongation ratios more than 2.0 (Fig. 5f) which resemble those found in the one siltstone examined, but the other sample is normal also with regard to elongation of grains. The breccia contains rounded zircons with pitted surfaces and a few, small, sharply euhedral crystals (Fig. 5g).

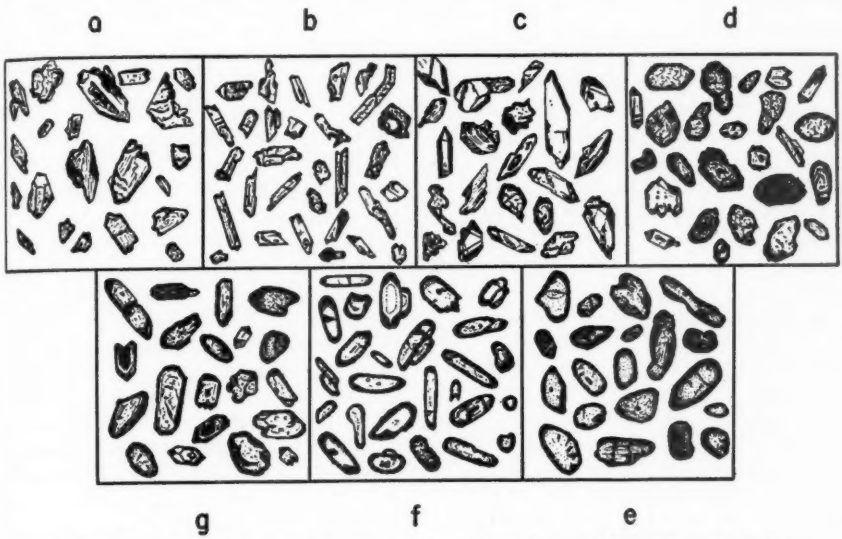

FIGURE 5.—ZIRCONS OF THE SPILITIC AND ASSOCIATED ROCKS—MAGNIFICATION ×40

a—typical zircons of rocks of groups 1 and 2.
b, c—zircons of two magmatic albitites.
d—zircons of albitite of mixed origin (locality 11), with a majority of rounded grains and a minority of euhedral crystals.
e—zircons of a Yeso siltstone, showing high degree of rounding.
f—zircons of coarse-grained quartz-feldspar rock showing rounding of terminations, and a majority of elongated grains.
g—zircons of the intrusion breccia; a few euhedral crystals amidst many rounded grains.

Observations on zircons obtained from the rocks are not conclusive in all cases. Zirconium apparently enters into ferromagnesian minerals at high temperatures (Wager and Mitchell, 1951, p. 192–193), but zircon is formed in the intermediate temperature ranges. The irregular shapes of the zircons yielded by rocks of Groups 1 and 2 are attributed to initiation of growth as skeletal crystals. Most normal basaltic rocks yield no zircons at all or small amounts of zircons which characteristically are

of irregular or skeletal forms. Most of the zircons of the analyzed albitite (locality 11) are identical with the rounded grains recovered from arenites of the Yeso formation, but a few are euhedral and clearly of igneous crystallization (Poldervaart, 1955). Zircons of the other two albitites are all euhedral and of magmatic origin. The writers interpret this as indicating that, with falling temperatures and rising concentrations of hyperfusibles, magmatic albitite melts formed from which euhedral zircons crystallized. However, the melts eventually graded into aqueous solutions containing Na and Al which metasomatized the adjacent Yeso arenites, yielding nearly identical albitites, but with many of the mechanically worn zircons of the sediments.

Sample No. 11 shows small, ovoidal patches of fine-grained albitite, which may further indicate a mixed origin. Heavy residues of mixed rocks from the northern and southern ends of the intrusion yield little information concerning their origin. The absence of zircons from the glassy quartzite may indicate that it is not a simple recrystallization product of arenaceous sediment, but a result of silica replacement, perhaps of gypsum or limestone. Zircons of the quartzofeldspathic rocks are rounded, but those of the breccia include a few small euhedral crystals; these indicate brecciation and intrusion by magmatic albitite melts. These samples may represent a feldspathic horizon in the sedimentary sequence, but the microscopic features (Fig. 2) and the absence of potash feldspar suggest that oligoclase was introduced metasomatically during the early magmatic phases of crystallization

Alteration

The simplification of minerals crystallizing with falling temperatures is one of the most striking features of the alteration process. Each metallic element tends to form a mineral, or a succession of minerals, in which it alone is represented, without "sharing favors" with other metallic ions except Si and Al. It is of interest to trace the stage at which combinations of the main metallic elements cease. Fe at first unites with Ti in ilmenite, or with Ca and Mg in pyroxene, but these combinations are superseded by simple iron oxides. The amount of iron in the igneous rocks decreases rapidly, which perhaps indicates migration of iron into the country rocks. This is also suggested by the magnetite rocks found in recrystallized limestone at two contacts. Similar ideas have been expressed by Hotz (1953, p. 701). Ti combines first with Fe in ilmenite, then with Ca in sphene, and finally forms its own mineral, rutile. Mg at first unites with Ca and Fe in pyroxenes and hornblendes, but at lower temperatures commonly combines with K and some Fe in magnesian biotite, and finally Mg and minor Fe form chlorite. Ca forms pyroxenes and hornblendes with Mg and Fe, or builds plagioclase with Na and K. At lower temperatures Ca develops a series of its own minerals in, successively, tremolite, prehnite, Ca-zeolites, and finally calcite. The behavior and apparent high mobility of Ca during the alteration process implies migration of this element into the country rock, although this could not be verified. Na first combines with Ca and K in plagioclase, but subsequently forms albite rims around turbid oligoclase cores. The apparent tendency in this case is for Na to remain in the igneous melts and finally to form a highly mobile albitite magma. K at first unites with Na and Ca in oligoclase, later enters into the formation of biotite, but subsequently again builds its own mineral in sericite. Later formation of kaolinite may indicate migration of K into the country rocks.

Petrogenesis

Igneous Rocks

The present study has, of course, not solved the problem of the genesis of the spilitic kindred, ably summarized by Gilluly (1935). However, it contributes information on one of the rare examples (*e.g.*, Turner and Verhoogen, 1951, p. 203) of spilitic intrusives in which the albite is apparently directly crystallized from magma. The magma was probably spilitic at the time of emplacement, but further addition of hyperfusibles distilled from the country rocks accentuated the late magmatic and deuteric stages of crystallization. The abundance of gypsum in the Yeso formation indicates that various sulphur radicles were prominent among the hyperfusibles added to the magma, yet

only the high amount of barite in the residue from locality 7 furthers this possibility. Evidently the cover of the intrusion was insufficient to keep enough hyperfusibles in the residual melts to enter into the compositions of the major minerals. As they became concentrated by magmatic and deuteric crystallization, the bulk of the hyperfusibles migrated back into the country rocks, presumably accompanied by various elements from the rest magmas. Thus the presence of barite in the one spilitic dolerite possibly indicates the development of the same mineral also in the surrounding sediments. It is remarkable that the grain size of the rocks remains small throughout the series, in spite of the concentrations of hyperfusibles indicated by the deuteric alteration, metasomatism of country rocks, and the development and mobility of the residual albitite magma. The only phases with pegmatitic affinities are the rocks of Group 1c.

This may indicate that the thin cover of the intrusion prevented high concentrations of hyperfusibles, which instead migrated slowly by distillation from the surrounding rocks, additional streaming from below, and by escape upward as the magma consolidated. This process resulted in magmatic differentiation to albitite-residual liquids and even some Na and Fe metasomatism in the country rocks, producing the quartzofeldspathic rocks and small magnetite deposits.

Metasomatic and Mixed Rocks

The first metasomatizing solutions to be given off contained Na and Ca and probably some Al. These solutions resulted in the formation of the large oligoclase crystals in the quartzofeldspathic rocks (Fig. 2a, b). Later solutions from the intrusion apparently were more sodic with the result that albite formed in the country rocks at the expense of quartz. Earlier oligoclase was also attacked by the solutions and converted to albite (Fig. 2c, d, e). The discontinuous rims of fine opaque dust in quartz surrounding the oligoclase-albite centers (Fig. 2c) indicate that material, probably iron, diffused into solid quartz ahead of the metasomatizing solutions as miniature mafic fronts. Apparently the solutions were tenuous and incapable of carrying zircon, hence the quartzofeldspathic rocks contain only rounded zircons of sedimentary origin (Fig. 5f; Poldervaart, 1955). Meanwhile vapor pressures of the residual albitite magmas increased through crystallization, and the melts became unusually mobile (*c.f.* Spencer, 1938, p. 104). This ultimately resulted in their injection into the quartzofeldspathic rocks by brecciation and forcible intrusion. The albitite magma carried with it a few small zircons of magmatic origin which are now found in the breccias together with a majority of rounded zircons (Fig. 5g). One of the albitites (Fig. 5d) is evidently of the same origin. Without a study of the zircon concentrates, it would not have been possible to differentiate between the albitites and to identify one of them as being of mixed origin.

Conclusions

It is concluded from this study that:

(1) The intrusion has the shape of a partly discordant sheet or a dikelike body emplaced under a roof less than 3000 feet thick.

(2) The bulk of the igneous rocks can be classed as spilitic basalts and dolerites on the basis of their mineralogical and chemical composition.

(3) These rocks contain zircons comparable in form and amount to those recovered from normal basalts, dolerites, and gabbros.

(4) The rocks are associated with albitites most of which are of magmatic origin, as the sharply euhedral forms of the zircons recovered from them indicate. One albitite is of mixed origin and contains a majority of rounded zircons with only a few euhedral crystals. No evidence was found of resorption of zircons by the sodic residual magmas.

(5) The country rocks are siltstones and gypsum of the Yeso formation with thin beds of sandstone and limestone. Since they are not sodic in character, the spilitic kindred of the igneous rocks cannot be attributed to introduction of soda from the surrounding rocks (*c.f.* Waters, 1955, p. 707).

(6) The magma was probably spilitic at the time of emplacement, but late magmatic and deuteric stages of consolidation may have been accentuated by distillation of hyperfusibles, especially sulphur radicles, from the country rocks.

(7) High concentrations of hyperfusibles in the magma were probably prevented by escape through the relatively thin roof, but it is likely that there was continual slow migration of hyperfusibles through the magma, both by accession from below and by distillation from the wall rocks.

(8) Solutions given off by the magma locally metasomatized the Yeso siltstones to rocks consisting of quartz and sodic plagioclase. Oligoclase was formed first, but eventually both oligoclase and quartz were in part replaced by albite. A few of the rocks were finally brecciated and intruded by albitite veinlets of magmatic origin.

References Cited

Gilluly, J., 1935, Keratophyres of eastern Oregon and the spilite problem: Am. Jour. Sci., v. 29, p. 225–252, 336–352.

Hotz, P. E., 1953, Petrology of granophyre in diabase near Dillsburg, Pennsylvania: Geol. Soc. America Bull., v. 64, p. 675–704.

Kelley, V. C., and Wood, G. H., 1951, Lucero Uplift, Valencia, Socorro and Bernallilo counties, New Mexico: U. S. Geol. Survey Oil and Gas Inv. Prelim. Map. 47.

Poldervaart, A, 1955, Zircons in rocks. I. Sedimentary rocks: Am. Jour. Sci., v. 253, p. 433–461.

Spencer, E., 1938, The potash-soda feldspars. II. Some applications to petrogenesis: Mineralog. Mag. London, v. 25, p. 87–118.

Sundius, N., 1930, On the spilitic rocks: Geol. Mag. London, v. 67, p. 1–17.

Turner, F. J., and Verhoogen, J., 1951, Igneous and metamorphic petrology: N. Y., McGraw-Hill Book Co., 602 p.

Wager, L. R., and Mitchell, R. L., 1951, The distribution of trace elements during strong fractionation of basic magma—a further study of the Skaergaard intrusion, East Greenland: Geochim. Cosmochim. Acta, v. 1, p. 129–208.

Waters, A. C., 1955, Volcanic rocks and the tectonic cycle: Geol. Soc. America Special Paper 62, p. 703–722.

Department of Geology, Columbia University, N. Y. 27, N. Y.

Manuscript Received by the Secretary of the Society May 10, 1954

BULLETIN OF THE GEOLOGICAL SOCIETY OF AMERICA
VOL. 66, PP. 1109-1130, 3 FIGS., 4 PLS. SEPTEMBER 1955

VIOLENT MUD-VOLCANO ERUPTION OF LAKE CITY HOT SPRINGS, NORTHEASTERN CALIFORNIA

BY DONALD E. WHITE

ABSTRACT

During the night of March 1 and 2, 1951, an inconspicuous group of hot springs and small mud volcanoes in northeastern California burst into spectacular eruption, unequalled by other known mud volcanoes. The eruption cloud of steam, gases, and mud particles rose several thousand feet in the air and distributed fine debris to the southeast for a distance of at least 4 miles. More than 20 acres of the hot-spring area was intensely disturbed and greatly modified by the eruption, estimated to involve at least 6 million cubic feet or 300,000 tons of mud. Several days after the eruption, the area was barely active. The eruption appears to be unique in the history of the springs.

The hot-spring system is in deep fine-grained clastic sediments immediately east of the Surprise Valley fault bounding the Warner Range. The sediments of the spring area are saturated with near-neutral hot saline water. Previous temperatures and geothermal gradient of the area were probably high.

Mud volcanoes exist in similar physical environment near Gerlach in Washoe County, Nevada, and on the southeast shore of Salton Sea, Imperial County, California. Other mud volcanoes occur in acid thermal areas and are characterized by abundant volcanic gases and near-surface alteration by sulfuric acid; their eruptions involve only surficial material and not underlying competent bedrock.

Eruptions in deep fine-grained basin sediments are attributed to unstable or metastable temperature-depth relations existing in many high-energy thermal systems. Vapor pressure at depth may equal or exceed hydrostatic pressure. Great energy is stored in a thermal system of this type, but ordinarily is released slowly.

A mud-volcano origin is possible for some eruption deposits classed as phreatic or cryptovolcanic. Although near-boiling hot springs are considered phases of volcanism, true volcanic eruptions are distinct from mud-volcano eruptions. The former derive their energy directly from new volcanic rocks or magma, but the latter are caused by sudden release of energy stored in near-surface hydrothermal systems and do not involve direct release of energy from new volcanic magma. The energy of true volcanic eruptions, however, may be increased by release of energy from previously existing hydrothermal systems, for example in the Rotomahana phase of the great Tarawera eruption of 1886 in New Zealand.

CONTENTS

TEXT

	Page
Introduction	1110
Acknowledgments	1111
Lake City hot springs	1111
Previous activity	1111
Geologic setting	1111
Hot springs of the region	1111
Eruption of March 1 and 2, 1951	1112
Activity and observations on March 6, 1951	1113
Area nearly quiescent	1113
Major mud volcanoes	1116
Fissures in mud embankments	1116
Small mud volcanoes in major craters	1116
Intermediate mud volcanoes	1116
Areas of subsidence	1117
Small mud flows or extrusive mud volcanoes	1118
Large mud flow	1118
Airborne eruption debris	1118
Character of fragments	1119
Magnitude of the eruption	1119
Observations, September 16, 1951	1119
Observations, December 25, 1953	1119
Other mud-volcano areas	1120
General	1120
Gerlach hot springs, Washoe County, Nevada	1120
General description	1120
Mud pots and mud volcanoes	1120
Salton area, Imperial County, California	1121
General relations of hot springs and rhyolite domes	1121
Observations, April 1948	1121
Volcano Lake, Baja California	1123
Acid hot-spring areas	1123

	Page
Energy output of the Lake City eruption	1124
Computed mechanical energy	1124
Relation of mechanical energy to total energy	1125
Relative energy of eruption	1125
Lake City eruption	1126
Relative energy of geyser eruptions	1126
Mechanics of eruption of mud volcanoes	1126
General	1126
Cause of eruption	1127
Relation to volcanic eruptions	1128
Phreatic or cryptovolcanic eruptions	1128
Volcanic eruptions intensified by hydrothermal energy	1129
References cited	1130

ILLUSTRATIONS

Figure	Page
1. Pre-eruption sketch map of central portion of Lake City hot springs, showing outline of eruption area	1112
2. Sketch map of eruption area	1115
3. Temperature-depth relations of two thermal drill holes, compared to boiling-point curves	1122

Plate	Following page
1. Major mud-volcano vents about 12 hours after start of eruption	1116
2. Eruption area after major activity had ceased	1116
3. Mud-volcano craters and small mud flows	1116
4. Large and small mud flows	1116

TABLES

Table	Page
1. Partial analyses of thermal and meteoric waters from Lake City region and other mud-volcano areas	1114
2. Energy available in a thermal system with boiling-point temperature relations at depth and controlled by hydrostatic pressure	1124
3. Energy available in a thermal system of mud and water with boiling-point temperature relations at depth	1125
4. Energy available in a thermal system with boiling-point temperature relations at depth and controlled by lithostatic pressure	1127

Introduction

An extraordinary eruption of an inconspicuous group of hot springs occurred March 1, 1951, in Surprise Valley in the northeastern corner of California. No similar activity of comparable magnitude is recorded in geologic literature. The eruption was of a type best described as a mud volcano and was distinctly not a geyser nor true volcano.

The hot springs are located in sec. 23 and 24, T. 44 N., R. 15 E., about 2 miles north of Lake City and half a mile east of the front of the north-trending Warner Range. The springs were formerly so inconspicuous that they had no formal name. In this report they are called the Lake City hot springs.

The author first visited the scene of activity with R. G. Reeves, of the U. S. Geological Survey, on March 6, 1951, about 4½ days after the eruption started. On September 16, 1951, he revisited the area with G. A. Thompson and C. H. Sandberg, of the Geological Survey, and William Wise, of Carson City, Nevada.

DEFINITIONS: The terms mud pot and mud volcano have been used by several authors (Veatch, 1857; Day and Allen, 1925, p. 103; Barth, 1950, p. 113) to describe certain features of hot-spring areas, but the terms have not been clearly defined. The term mud pot is used to indicate a depression containing a fluid mixture of mud and water that is generally being agitated mildly by gases or steam. The term mud volcano is applied to those thermal features that erupt mud, either quietly or violently. The distinction between mud pots and many mud volcanoes is slight; a small change in type of activity may change one into the other, as Day and Allen (1925, p. 103) have indicated. Some of the mud volcanoes described in this paper, however, were not mud pots in the past nor are they likely to be in the future.

Although mud volcanoes are distinctly not true volcanoes, the comparison is appropriate in many ways. Most mud volcanoes propel blobs or clots of mud upward from a central crater by violent flow of gases and water vapor through mud in the floor of the crater. Mud falling outside the crater accumulates to form a cone comparable to a pyroclastic cone. A less common type of mud volcano is formed by quiet extrusion on the surface, unaccompanied by vigorous activity of gases. Some are comparable to shield volcanoes and to pahoehoe and aa lava flows.

Mud volcanoes of very different origin are associated with oil deposits of many regions, but are not likely to be confused with mud volcanoes of thermal areas.

Acknowledgments

Information on the first day of the eruption has been acquired largely from Mr. Joe Parman and Mr. Lloyd A. Rogers, editor of the Alturas Plaindealer, who visited the springs the morning following the eruption. Permission to use photographs taken by Mr. James Souther of Alturas is gratefully acknowledged. Particular appreciation is extended to Prof. Fred Humphrey of Stanford University, to whom the author is indebted for the sketch map of the eruption area. The author is also grateful to his associates for assistance and advice.

Lake City Hot Springs

Previous Activity

Little is known about the Lake City hot springs before their eruption in 1951. Waring (1915, p. 122–123) describes them briefly as

> "Hot springs near southwest side of Upper Lake. At points about 2 and 3 miles, respectively, north of Lake City, hot water rises in meadowland that borders Upper Lake. The quantity of flow and the temperature of the water are rather indefinitely known, as the water rises in tule-grown areas."

In a later report by Stearns *et al.* (1937, p. 118), a spring listed as California No. 14 is described as "near southwest side of Upper Lake, 12 miles north of Cedarville." Temperature is listed as 120° F (49° C) and discharge as 5 gallons per minute. The data on temperature, discharge, and number of springs are derived from some other source than Waring's earlier paper, and are of doubtful reliability. Of particular interest, in view of the lack of reliable data, are pre-eruption air photographs of the U. S. Forest Service (photos DEM-33-90 and -91, taken September 20, 1946). These photographs indicate a hot-spring area three-fourths of a mile long and as much as 800 feet wide, but only the central part contained many hot springs. Large pools and the cones of several mud volcanoes can be distinguished. The pre-eruption sketch map of the area (Fig. 1) has been constructed from these photos.

Although the temperatures of the springs were not known, some springs were reportedly hot enough for hog scalding and were therefore definitely hotter than the 120° F (49° C) reported by Stearns *et al.* (1937, p. 118). No direct evidence is available to indicate whether they had recently been at or near boiling, but near-boiling springs are believed to have existed in the inaccessible central portion of the marsh. The existence of small mud volcanoes, recognizable in the air photographs, is evidence that temperatures were at least periodically close to boiling.

According to other local reports, the springs have been quiet and inconspicuous since the area was first settled, although occasionally one of the mud volcanoes would erupt mildly and throw mud out on its banks. The 1951 eruption, however, was a very unusual and probably even a unique event in the life of these springs. No evidence on the ground or in the photographs indicates that comparable activity has occurred in the past.

Geologic Setting

Northeastern California has had a long and complex volcanic history extending through most of the Tertiary and Quaternary periods (Russell, R. J., 1928; Anderson, C. A., 1941; Powers, H. A., 1932). The Warner Range consists dominantly of gently dipping flows and agglomerates bounded on the east by a major fault of the basin-range type. This fault is about half a mile west of the Lake City hot springs. I. C. Russell (1884, p. 449–450) and R. J. Russell (1928, p. 466–467, 470) have discussed the fact that hot springs occur along the fault but neither author specifically mentions the Lake City springs.

The depth of alluvial fill under the springs and elsewhere in Surprise Valley is not known. A well a few miles south of Lake City and within a mile of the Warner Range was drilled through 835 feet of lacustrine sediments without reaching bedrock (R. J. Russell, 1928, p. 436).

Hot Springs of the Region

In the eastern half of Modoc County Stearns *et al.* (1937, p. 118–119, Pl. 15) have identified 18 springs and spring groups. Three of these groups discharge water at or near boiling, a fourth yields boiling water from wells, and two others, not including the Lake City group, are about 65° C in temperature. All these high-

temperature springs are believed to owe their heat and very probably a part of their water supply and mineral content to volcanism (White and Brannock, 1950, p. 567–572; Brannock *et al.*, 1948, p. 216–222).

Table 1 shows the chloride content, pH, and specific conductance of water samples collected from the Lake City hot springs, compared with selected samples from other areas.

The Lake City springs are similar chemically to many of the other thermal waters.

Eruption of March 1 and 2, 1951

The following account of the eruption of the Lake City hot springs was obtained from Mr. and Mrs. Joe Parman, on whose farm most of the activity occurred, and from Mr. Lloyd Rogers, editor of the weekly *Alturas Plaindealer*. Rogers and photographer James Souther arrived at the springs about mid-day of March 2 while the activity was still moderately strong. Their report and photographs of the eruption

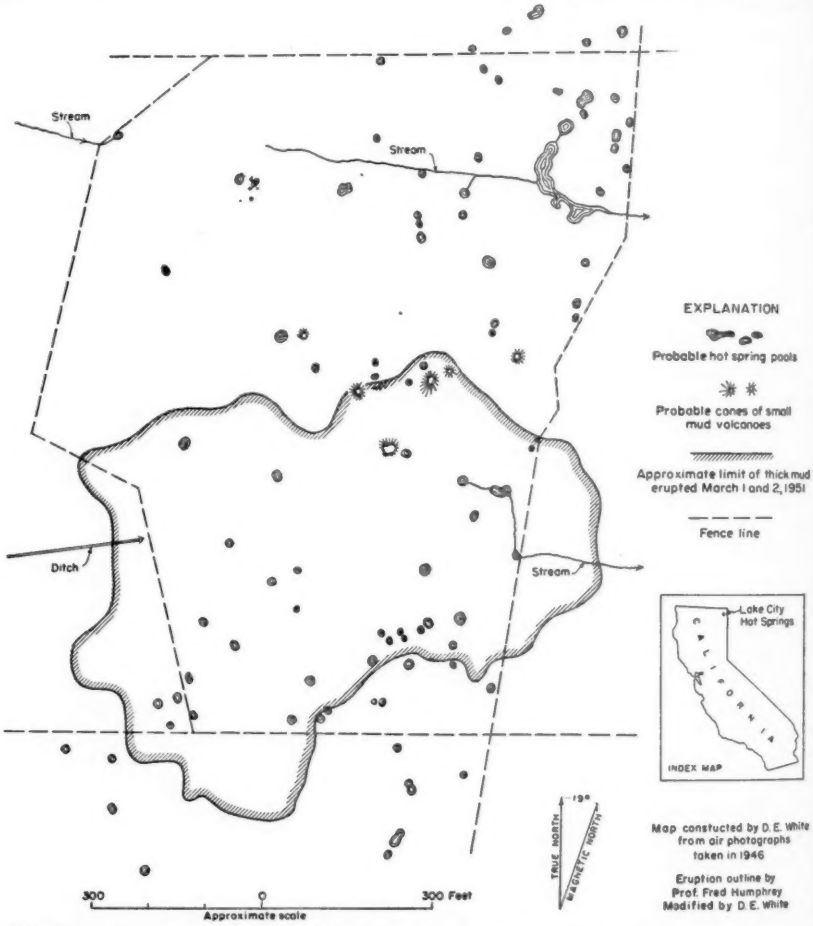

FIGURE 1.—PREERUPTION SKETCH MAP OF CENTRAL PORTION OF LAKE CITY HOT SPRINGS, SHOWING OUTLINE OF ERUPTION AREA

Map constructed from air photographs of September 20, 1946, U. S. Forest Service, with eruption outline by Prof. Fred Humphrey.

appeared in the Thursday, March 8 issue of the *Alluras Plaindealer*.

Apparently without warning on the night of March 1 at about 11.30 p.m. a large part of the spring area erupted, perhaps not en masse but at least in major part. Because of the darkness of the night, little could be seen, but the accompanying noise has been described as "terrific" and as a "grumbling and roaring sound accompanied by a loud whistling similar to rapidly escaping air." The erupting springs were said by some witnesses tc have formed a "tornadolike cloud with a long tail that reached down to the mud volcano." While this cloud was forming, the noise increased in volume and a series of tremors led many to believe an earthquake was occurring. The column of gases and mud was estimated to rise at least a mile in the air, drifting to the south and southeast under the influence of a strong wind.

Oddly enough, Parman and his family were asleep when the eruption started and were awakened only when friends telephoned from Lake City, about 2 miles to the south. However, the wind was blowing strongly to the southeast, and the springs are located nearly half a mile southeast of the Parman farm. The noise was so loud in Lake City that the local fire department was alerted in the belief that an explosion had occurred. A hail of frozen particles consisting largely of mud were falling on the town, and pellets about the size of peas were later reported from farms as far as 4½ miles from the spring. The local residents believed the pellets were erupted or blasted for those great distances. The eruption column, however, must have risen to considerable heights because of its contained steam and hot gases, and resultant low density, and not primarily because of explosive violence of the eruption. Evidence was later found to indicate that large blocks and boulders were erupted several hundred feet in the air. The mud pellets presumably formed fro n freezing water vapor, incorporating small particles of mud.

The activity is described as being greatest soon after the initial eruption, continuing very strongly but with decreasing vigor during the night. Early the next morning Parman found steam from vents rising perhaps 100 feet in the air. The fumarole discharge consisted almost entirely of vapors, but a little mud was being thrown nearly as high. The first known photographic record of the activity was obtained by Mr. James Souther about noon of March 2. Figure 1 of Plate 1 shows four small late-phase mud volcanoes in a much larger depression that was one of the major vents during the initial violent activity. Four or five other major vents, one of which is shown in Figure 2 of Plate 1 to be steaming with great vigor, were distributed in an area later determined to be nearly 700 feet long and as much as 700 feet wide. (*See* Fig. 2.) All surface and near-surface material in this large area of about 10 acres was completely churned up and thoroughly redistributed. Most of the activity had been localized in the major mud-volcano craters, each of which was 60–200 feet in diameter and was bounded by mud walls of ejected debris. Souther's photographs indicate that by noon of March 2 the activity in each large crater consisted of vigorously boiling mud pots and fluid mud volcanoes, occasionally blurping pellets and clots of mud to a height of 10–20 feet. At this time the eruption was essentially completed, but activity continued on a decreasing scale for several days.

Activity and Observations on March 6, 1951

Area nearly quiescent.—Nearly all activity had ceased by the morning of March 6, a little more than 4 days after the eruption started. The flow of energy from the thermal system was probably near its absolute minimum since the system first came into existence and may not be so low again until the system becomes extinct.

Masses of mud, still wet, hot and dangerous in many places, surrounded the disturbed area and rose up to 15 feet above the adjacent flat eastward-sloping alluvial plain. (*See* Pl. 2, fig. 1.) The previously existing springs apparently had discharged essentially on this plain.

Very little steam or vapor was rising from the springs. Nearly all mud-volcano craters, large and small, were drained of water though the bottoms of the deepest were below the surrounding plain, which was saturated with water. A small creek with a flow of about 3 second feet was discharging into the crater in one of the few

TABLE 1.—PARTIAL ANALYSES OF THERMAL AND METEORIC WATERS FROM LAKE CITY REGION AND OTHER MUD-VOLCANO AREAS

Springs	Description	Date	Temp. (°C)	Estimated discharge (gpm)	Cl (ppm)	pH	Specific conductance, K × 10⁶
Lake City	Preserved spring vent NE part of area	3/6/51	38	None	216	6.81	1,888
Lake City	Eruption crater, north-central part	3/6/51	49	None	224	6.38	1.825
Lake City	Boiling pool, NW part	9/16/51	96	None	212	7.77	1,680
Lake City	Boiling pool, east-central part	9/16/51	97.5	10–15	212	7.63	1,680
Lake City	Discharge from east-central part of area	9/16/51	Warm	100	202	7.83	1,745
Lake City	Artesian well ¼ mi. ESE of springs	9/16/51	21	¼	76*	....	....
N. end Lake City Group	About ⅜ mi. N of main group	9/16/51	55	None	233	6.67	1,855
Calif. No. 16†	12 mi. NE of Cedarville, SE of Lake City	9/16/51	65.8	50	212	7.96	1,645
Calif. No. 15†	2 mi. N of No. 16	9/16/51	87	40	228	7.76	1,630
Cedar Plunge	Erupting well E of Cedarville and SSE of Lake City	9/16/51	84	100	184	8.42	1,430
Kelly hot spring	About 35 mi. SW of Lake City	9/17/51	96.5	400	164	8.49	1,275
Kelly hot spring	Artesian well 500 ft. E of spring	9/17/51	28.9	½	4	8.51	265
Gerlach, Nev.	Geyser pool, border Black Rock Desert	8/6/47	94.7	50	2,136	7.13	6,850
Gerlach, Nev.	Mud volcano, inactive, 500 ft. to NE	8/6/47	27	None	4,500	6.29	15,740
Gerlach, Nev.	Hughes well, ½ mi. SE of springs	8/6/47	61.3	15	1,996	7.27	6,600
Gerlach, Nev.	Well ¾ mi. E of springs	8/6/47	21	Flowing	2,004	7.18	6,600
Salton, Calif.	Perpetual spouter, largely steam, near mud volcanoes	4/12/48	100.2	Small	69,560	6.97	130,600
Salton, Calif.	CO_2 well N of abandoned dry-ice plant	4/12/48	39.8	30–40	12,960	6.33	34,300
Salton, Calif.	Thermal well, Mullet Island	4/13/48	72.9	Periodic small discharge	59,720	5.83	115,500
Salton, Calif.	Salton Sea	4/13/48	Cold	....	14,320	7.96	40,850
Norris, Yellowstone	Phillips Cauldron	9/28/47	93.8	None	12	3.40	1,233

TABLE 1.—*Cont.*

Springs	Description	Date	Temp. (°C)	Estimated discharge (gpm)	Cl (ppm)	pH	Specific conductance, K × 10⁶
Norris, Yellowstone	Acid pool about 200 ft. NW of Norris drill-hole site	9/28/47	"Boiling"	Slight	12	1.86	6,105
Norris, Yellowstone	Congress Pool 100 ft. NW of acid pool	9/28/47	61	None	672	1.98	6,625
Boiling Lake, Lassen	Mud volcano	6/25/47	94.7	None	4	3.49	1,005
Boiling Lake, Lassen	Acid spring	6/25/47	94.4	Small	4	3.02	963

* Sample bottle broken, only sufficient quantity for chloride analysis.
† Numbers after Stearns *et al.* (1937, p. 118).

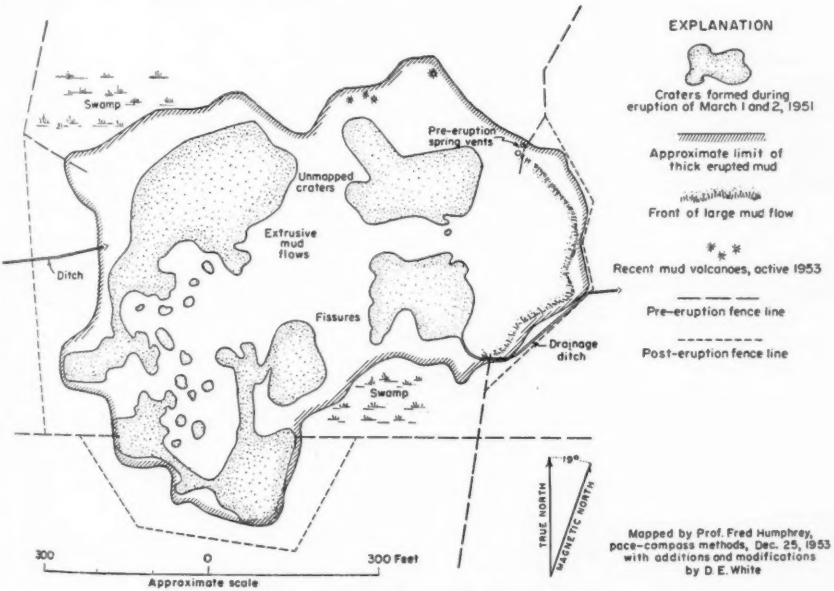

FIGURE 2.—SKETCH MAP OF ERUPTION AREA
Mapped by Prof. Fred Humphrey, pace-compass methods, December 25, 1953, with additions by White.

places where the bounding mud wall was insignificant. The creek water was disappearing underground, and no water was flowing out of the eruption area. One small mud pot in the western part contained a little water and was bubbling gently at a temperature of 47° C. A group of small mud pots in the northwestern part of the disturbed area was a little hotter, with temperatures of 60° C. Still farther to the northwest where the superficial layer of erupted mud had thinned to a foot or so, the most extensive activity of the area was taking place. This is believed to be an original part of the spring group not directly involved in the eruption, but its activity may have been in part induced in some complex way by the eruption.

The ground was hot, and so boggy that it could not be crossed safely, but many small hot pools and steaming vents were visible from the comparatively safe, well-drained mud embankments. No well-established pools lined with spring deposits were seen.

Major mud volcanoes.—The eruption area contains six large depressions or craters, very irregular in outline, and ranging from about 60 to 200 feet in diameter. These are surrounded by mud embankments generally rising 5–15 feet above the crater floors. These large depressions are believed to be the main vents for the initial and most violently active mud volcanoes. Mud walls are insignificant on the west sides of two southwestern craters and in two other depressed areas on the south side of the active area. These are probably craters of subsidence resulting from the eruption of mud and removal of support.

Fissures in mud embankments.—The mud embankments near several large depressions were cut by open fissures and cracks as much as 50 feet long and a foot wide. Some were at least 5 feet deep and were probably considerably deeper in spite of their occurrence in water-soaked mud. The fissures were concentrically arranged around at least one of the large depressions and probably resulted from settling of the over-steepened mud walls after activity had ceased. On March 6, vapor was rising quietly from many of the fissures, and in a few places considerable steam was flowing. The highest temperatures found in the area were measured in these fissures. Vapor from one vent discharged at 75° C, and steam escaping from a second vent under slight pressure had a temperature of 97.2° C (Pl. 2, fig. 2). The latter temperature is slightly above theoretical boiling point for the altitude of the springs (about 95.5° C at an altitude of approximately 4600 feet).

Small mud volcanoes in major craters.—Smaller mud pots and mud volcanoes are distinct from the larger depressions. These smaller features have a somewhat random distribution, but a large proportion are in the crater depressions of the large mud volcanoes. The small features are later than the depressions in which they occur and were active during the declining phases of the eruption. (*See* Pl. 1, fig. 1.) They were not over 5–15 feet in diameter and, because they formed in the soupy mud of the depressions, their cones are low and gently sloping. Larger mud volcanoes of this type probably existed during intermediate stages of activity but were not preserved.

The large mud volcanoes were probably deep, steep-sided craters during their maximum activity. When activity decreased, steep walls could not be maintained in soft water-saturated mud. The crater floors were probably built up considerably by collapsing and inflowing mud walls and by strong agitation of small mud volcanoes.

Intermediate mud volcanoes.—Other mud volcanoes of intermediate size, as much as

PLATE 1.—MAJOR MUD-VOLCANO VENTS ABOUT 12 HOURS AFTER THE ERUPTION STARTED

FIGURE 1.—A MAJOR MUD-VOLCANO CRATER SURROUNDED BY ERUPTED MUD EMBANKMENTS AND CONTAINING FOUR SMALL ACTIVE MUD VOLCANOES

The large crater is about 100 feet in diameter and was a center of intense activity the night of March 1 and 2, 1951; photographed by James Souther about noon, March 2, 1951

FIGURE 2.—VIGOROUSLY STEAMING CRATER OF A MAJOR MUD VOLCANO

Mud-erupted embankment, nearly water-saturated, in foreground; distance to edge of crater about 30 feet; photographed by James Souther about noon, March 2, 1951

PLATE 2.—ERUPTION AREA AFTER MAJOR ACTIVITY HAD CEASED

FIGURE 1.—FENCE BURIED BY ERUPTION DEBRIS ON THE SOUTHEAST BORDER OF THE ACTIVE AREA

Near source area for much of the mud flow of Figure 2 of Plate 4; fence poles about 5 feet high; photographed by White, March 6, 1951

FIGURE 2.—OPEN FISSURES IN ERUPTED MUD EMBANKMENT

Adjacent to a major mud volcano to the right of the photograph; probably caused by subsidence toward the crater. Temperatures as much as 97° C measured in these fissures. Photographed by White, March 6, 1951

FIGURE 1

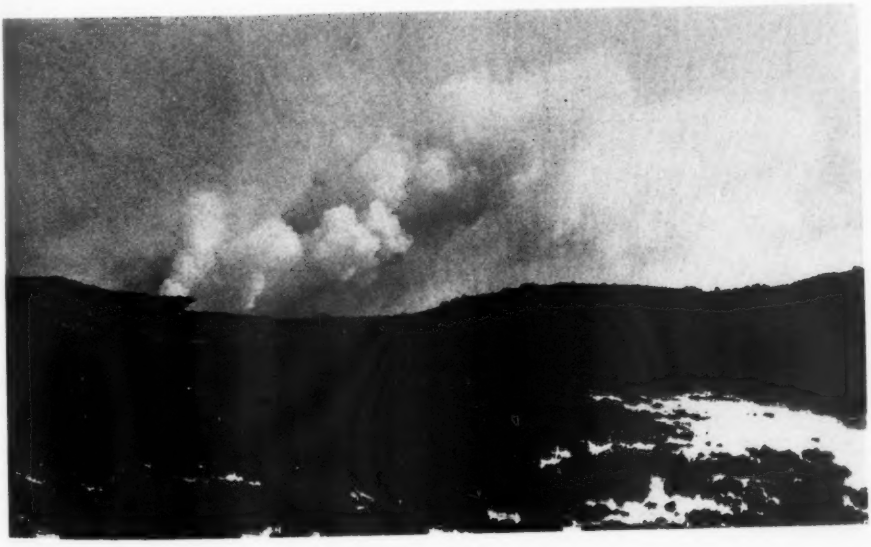

FIGURE 2

MAJOR MUD-VOLCANO VENTS ABOUT 12 HOURS AFTER THE ERUPTION STARTED

FIGURE 1

FIGURE 2

ERUPTION AREA AFTER MAJOR ACTIVITY HAD CEASED

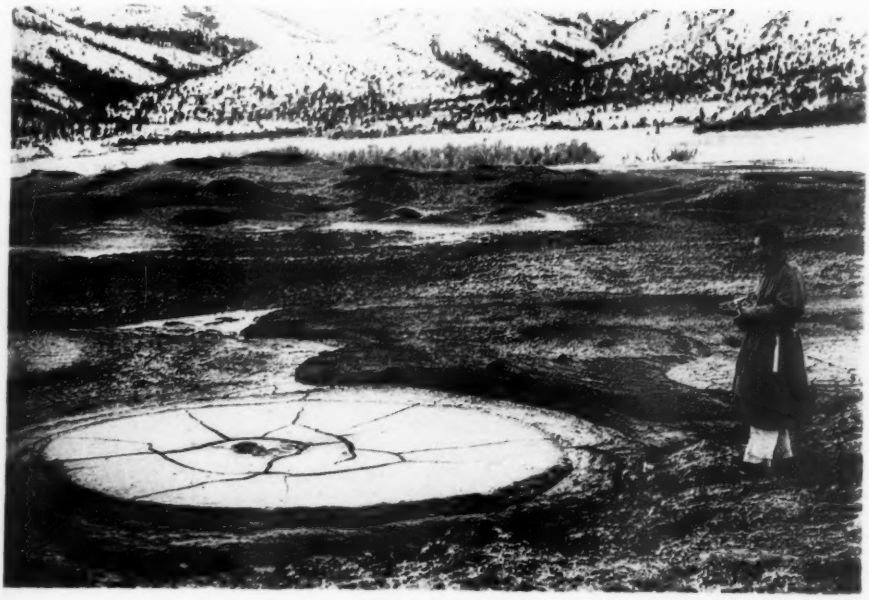

FIGURE 1

FIGURE 2

MUD-VOLCANO CRATERS AND SMALL MUD FLOWS

FIGURE 1

FIGURE 2

LARGE AND SMALL MUD FLOWS

25-30 feet in diameter (*see* Pl. 3), are irregularly distributed on the accumulations of mud separating the large depressions. In general their cones are high; inner as well as outer slopes are steep. The difference in altitude between crater floor and cone summit is as much as 15 feet, but 5–10 feet is more common. These mud volcanoes may grade into the major mud volcanoes, but the ones that have been preserved apparently formed after the most violent activity had ceased and are more closely related in time to the small mud volcanoes in the major craters. The differences between the small and intermediate types are believed to result principally from differences in the fluidity of their environment. Those in the major craters were erupting very fluid mud because water was concentrating in the depressions; only the latest of this type were preserved. On the other hand, the mud embankments containing the mud volcanoes of intermediate size were relatively high in altitude and were drained of excess water.

One mud volcano on an embankment was particularly instructive. Its cone was 7 or 8 feet in diameter, and the steep inner slopes revealed a cross section of the mud embankment. The lower part was brownish gray and coarse in texture without stratification, and had many randomly distributed stones and mud fragments or clots as much as 6 inches in diameter. The upper 2 feet was characterized by a gray color and a much finer texture, without conspicuous fragments other than small stones and mud clots that were probably semifluid when erupted. The contact between the two types of deposit is relatively sharp. The lower mud is believed characteristic of most of the disturbed material resulting from the more violent early phase of activity. The upper layer was deposited as a mantle on the lower mud by small mud volcanoes after the gross features of the area had been determined and the activity was tapering off. This particular mud volcano was distinctly later than the lower mud and apparently erupted through a part and perhaps all of the upper layer.

Areas of subsidence.—The large craters were formed primarily by the explosive eruption of mud. At least parts of some craters, however, are believed to have formed by subsidence because mud was removed from below by the extensive eruption. The three southwestern craters shown on Figure 2 are adjacent to the pre-eruption ground surface, with little or no intervening mud embankment. The scarcity of splatter near the western and southern borders of these craters is the principal evidence suggesting subsidence.

A swampy area southwest of the major mud flow (Fig. 2) appears to be about 1–2 feet lower in altitude than the ground surface to the south

PLATE 3.—MUD-VOLCANO CRATERS AND SMALL MUD FLOWS

FIGURE 1.—LATE-STAGE MUD FLOWS OR EXTRUSIVE MUD VOLCANOES, IN SOME RESPECTS RESEMBLING LAVA FLOWS

The pancake-shaped "pahoehoe" type of flow in the foregound was erupted from a vent under its center. Mud flows immediately beyond the observer were erupted from a single vent to the right of the photograph and are similar in some respects to aa lava flows. The crater-pocked embankment in the middle distance lies between major mud volcanoes.

FIGURE 2.—MUD-VOLCANO CRATERS OF INTERMEDIATE SIZE

Mud embankment formed by major mud volcanoes to right and left of photograph; craters of intermediate size were probably active after the most intense eruptions had ceased. The large angular block held by the observer consists of a ramifying network of calcite veins cutting a matrix of mud. This was the largest erupted fragment found in the area; photographed by White, September 16, 1951.

PLATE 4.—LARGE AND SMALL MUD FLOWS

FIGURE 1.—MINOR FLUID LATE-STAGE MUD FLOW

Still in motion when photographed by James Souther about noon, March 2, 1951; probably situated near the source area of mud flow of Plate 4, fig. 2; height of fence post about 3 feet

FIGURE 2.—SOUTHEAST BORDER OF MUD FLOW THAT MOVED EASTWARD FROM THE ERUPTION AREA AFTER DEEP ACCUMULATION OF ERUPTED DEBRIS

Flow is about 6 feet thick near border and 15 feet near center; rocks and mud pellets in foreground were erupted at least 300 feet from source vents; photographed by James Souther.

(Pl. 2, fig. 2). A small, general subsidence may have occurred here.

Small mud flows or extrusive mud volcanoes.—The mud volcanoes previously described are comparable in many ways to true pyroclastic volcanoes except for obvious differences in scale, temperature, and composition. Small mud flows or mud volcanoes of an extrusive type constitute a very late phase of the activity. These resemble extrusive lava flows unaccompanied by marked explosive activity. Figure 1 of Plate 4 shows a very fluid flow, photographed while still in motion. A somewhat more viscous flow of the same type was erupted from a vent in the central part of the disturbed area (Pl. 3, fig. 1). The flow was similar to a pahoehoe lava flow, spreading out on all sides from its vent to form a smooth-topped "pancake" about 15 feet in diameter and only a few inches high on its borders. This mud flow is very similar in general form to the "lily-blossom" pahoehoe lava, illustrated by Stearns and Macdonald (1946, Pl. 26A, p. 83) from Hawaii, and is also comparable in miniature to the pancake-like flow of recent dacite obsidian about half a mile north of Medicine Lake (Anderson, 1941, p. 372–373).

Another mud volcano, shown in the same photograph, erupted mud resembling an aa lava flow in some physical properties. The surfaces of its compound flows were rough with abrupt flow fronts 6 inches to a foot in height. These "aa" flows had moved farther from their vents and down steeper slopes than the "pahoehoe" flow, and they appeared to be initially more viscous. The original water content of the two contrasting types could not be determined, but presumably the differences resulted at least in part from a higher water content in the "pahoehoe" flow. The water content of the mud flow shown in Figure 1 of Plate 4 was very high.

The more-fluid mud flows were extruded through mud accumulations that were semisolid, and from the surface of which excess water had already drained. Compaction and settling of semisolid mud may have produced extrusion of entrapped masses of more-fluid mud that could rise and flow out at the surface because of its lower density. Eruption of the mud flows appears to be one of the late phases of activity. This is illustrated by the still-moving mud flow photographed about mid-day of March 2 after most of the explosive activity had ceased and is also supported by the fact that no exploded rocks or mud clots were found on the surfaces of the mud flows.

Large mud flow.—A much larger mud flow of different origin formed and moved eastward from the eruption area during or soon after the climax of activity (Pl. 4, figs. 1, 2). Viscous mud accumulated to a considerable thickness adjacent to the large mud volcanoes on the east and moved eastward down slope under the influence of its own weight. The photograph shows a jumbled irregular mass of mud blocks near the flow front, which indicates that the surface was broken up and disturbed during the last stages of movement in a manner strikingly comparable to that of block lava flows. The flow is approximately 320 feet wide at its base, and it advanced an average of 140 feet east of its base line. The average thickness of mud in the flow is about 12 feet, and its total volume is approximately 500,000 cubic feet. Its mass is nearly 30,000 tons, with an assumed density of 1.8.

Airborne eruption debris.—Blocks and fragments of mud and rocks as much as a foot in diameter have a significant distribution around the area. These fragments are most abundant on the east, southeast, and south sides of the eruption area and are as much as 300 feet from the nearest major center of activity. None were found lying on the surface of the latest mud near the small mud volcanoes. Few if any fragments were erupted on the surface of the large mud flow after movement had ceased, although blocks of comparable size are contained in the large mud flow and are abundant within the thicker accumulations of mud. The evidence clearly indicates that the large fragments were erupted into their positions during the most vigorous early activity. Blocks that fell near the main centers presumably were concealed under later deposits.

A block falling 300 feet from its source was probably erupted to a height of at least 100 feet and perhaps 200–300 feet, although precise estimates cannot be made without a knowledge

of their trajectories. Many of the blasts may have been inclined to the east or south, because even a very strong wind probably could not account for the existing distribution of large fragments 4–6 inches in diameter.

Character of fragments.—A variety of fragments was erupted. Mud, more or less indurated, is by far the most abundant, but most mud "blocks" were broken down into smaller fragments before or during impact. Fragments that were collected and identified are: (1) A large block about a foot in length, consisting dominantly of ramifying calcite veins. (*See* Pl. 3, fig. 2.) Adhering material proved that the veins had been deposited in cracks in fine clastic sediments. (2) Well-sorted sandstone consisting of rounded to subrounded grains of volcanic rocks cemented by zeolites and a little celadonite and clay minerals. The zeolites are largely heulandite(?), but stilbite(?) is also present. The volcanic fragments are almost unaltered, but a little feldspar has been replaced by zeolite. (3) A fine-grained aggregate of clay minerals (largely hydromica) and probably zeolite. (4) Fine-grained clays consisting mostly of hydromica but with considerable montmorillonite. Diatoms and zeolites are absent. (5) Fine-grained clays, largely montmorillonite, and clastic silicate grains, as well as a little zeolite cement. Diatoms are abundant, and most if not all are not the common hot-spring types. (6) Opaline masses with concretionary forms. The abundance of diatoms within the concretions and in the white powdery border material suggests that the concretions probably formed by introduction of opal into diatomite. Some of the diatoms are similar to types considered by the present author to be characteristic of hot springs, but so many other species are present that the diatomite is probably unrelated to hot springs.

Magnitude of the eruption.—The total volume of mud and hot water directly involved in the eruption is impossible to determine accurately. The eruption area measures about 600 by 500 feet. The average depth of the disturbance is unknown, but is at least 10 feet and probably 20–100 feet. If a depth of only 20 feet is assumed, the total volume is 6 million cubic feet and the mass, with an assumed density of 1.8, is approximately 330,000 tons.

Observations, September 16, 1951

The Lake City hot springs were visited again on September 16, 1951. The activity was greater at that time than it had been 5 days after the eruption. Water levels had risen almost to the levels of the surrounding fields, largely filling the major crater areas. The many small mud volcanoes in the large craters were submerged. Water was boiling vigorously in a number of pools and in two of these the intensity varied from time to time. One boiling pool in the east-central part of the area discharged into a larger nearby pool at rates estimated to range from 10 and 15 gpm. (*See* Table 1.) Although not a true geyser because it did not discharge intermittently, the pool was gradational between ordinary hot springs and true geysers.

Temperatures of 90°–97.5° C were not uncommon in the hot-spring pools in contrast to the maximum of 60° C measured in springs of the same area on March 6.

The muddy ground was almost as treacherous as in March, and many places were even more dangerous because of the higher water levels and poor drainage.

The total surface discharge from the hot-spring area was at least 100 gpm, in contrast to March 6 when about 1000–1500 gpm of surface water was flowing into the area and none was being discharged, presumably because the craters were being filled.

Observations, December 25, 1953

Professor Fred Humphrey of Stanford University visited the Lake City hot springs on December 25, 1953, and to him the author is most indebted for the following observations and for the post-eruption sketch map shown in Figure 1.

On December 25, 1953, the general activity probably equalled that of mid-September, 1951. The large craters were flooded with warm and hot water, and considerable vapor was being evolved. The stream from the west was flowing at an approximate rate of 150 gpm. At the western edge of the mud embankment, it disappeared under the mud and could be heard cascading downward for at least a few feet. The

ditch cut through the southeastern mud embankment to drain the area was discharging warm water at an estimated rate of 200 gpm.

Small mud volcanoes had formed during the preceding two years, probably in the fall of 1953. Four small cones are shown in Figure 2 on the northern fringe of the eruption area. The crater of the eastern cone is about 4 feet in diameter; the cone rises about a foot above the general surface and is surrounded by a ring of mud about 18 feet in diameter. This mud volcano is very near the former location of a conspicuous mud volcano shown on the pre-eruption 1946 air photos. The three new western mud volcanoes have craters about 2 feet in diameter; the cones rise about 6 inches above the nearby ground, and they are surrounded by mud rings approximately 10 feet in diameter. The fresh appearance of the mud indicates very recent activity, with no intervening heavy storm.

Other Mud-Volcano Areas

General

Activity similar to the Lake City hot spring eruption and comparable in magnitude has not been described from other areas. Most mud pots and mud volcanoes are relatively small and feeble in comparison with the Lake City mud volcanoes. The small mud volcanoes active during the late phases of the eruption are similar in energy relations to most mud volcanoes elsewhere.

Gerlach Hot Springs, Washoe County, Nevada

General description.—Mud volcanoes are found at Gerlach hot springs, about a mile northwest of Gerlach in northwestern Nevada. The spring area is approximately 1000 feet long and 200–300 feet wide. The environment is similar in many ways to that of the Lake City group of springs: (1) They are situated in a similar topographic position, about a third of a mile from the Granite Range and in the basin of the Black Rock Desert. (2) The range front is believed to be a fault scarp. (3) The spring group is elongated normal to the trend of the range front. (4) Fault scarplets are absent in the immediate vicinity of the springs. (5) The water table in the immediately surrounding area is at or very near the ground surface. (6) The springs emerge from probable deep-basin fill consisting dominantly of fine-grained lacustrine mud and silt.

Salinity in the Gerlach hot waters is high but only slightly higher than samples of warm and cool well waters near Gerlach. Ground water of the area obviously contains salines (Table 1) of the Black Rock Desert, a large playa lake and formerly a major arm of Pleistocene Lake Lahontan.

The only spring of the group with appreciable discharge is a pool about 20 feet in diameter at the southeastern end of the belt. It ordinarily discharges at a rate of about 50 gpm and at a temperature of 95° C, and is said to "boil up" periodically 1–4 feet above the general water level in geyserlike action.

Mud pots and mud volcanoes.—Many mud pots and mud volcanoes occur from 250 to 1000 feet northwest of the discharging pool. The ground surface rises gradually in the same direction toward the scarp on the front of the Granite Range. The altitude of the northwestern pool is about 15 feet higher than that of the geyser pool. The water table, as indicated by levels in the various pools, also rises to the northwest but less rapidly than the ground surface. In the northwestern pools the water levels are about 6 feet below the general land surface but were probably higher before trenches were cut to drain this part of the area.

Mud volcanoes are concentrated in the northwestern and particularly in the central parts of the belt. During the writer's visits no mud volcanoes were actively erupting mud. In fact, all appeared inactive or extinct, except that in some, gases were bubbling quietly through water in the crater floors. Temperatures in 1947 ranged from near air temperature to as much as 91° C. Evidence for recent activity in 1951 was found for only two mud volcanoes. One consisted of a pile of gray mud, only 5 or 6 feet in diameter, rising a foot above the surrounding grass-covered surface in a cone-shaped mound. The vent for the mud consisted of a summit crater about a foot in diameter. Mud near the crest of the cone was still damp, and fresh mud coated surrounding vegetation. Reportedly the small mud volcano had erupted the previous night, September 14, 1951, to a height of about

10 feet. The eruption column either was not vertical or a strong wind was blowing from the east, because mud was strewn to the west 10 or 15 feet.

Another larger mud volcano had also erupted since the previous rain. A pool 10–12 feet in diameter was surrounded on the north, east, and south by mud embankments as much as 3 feet high, and mud pellets were found more than 15 feet from the pool. The mud was light gray and dry. The pool was relatively cool, but fresh-looking mud coated all surrounding vegetation except to the south and had definitely been erupted after the most recent rain.

Other much larger mud pots and mud volcanoes exist in the area, but the magnitude or recency of activity is not known. At the time of the 1947 visit, a resident stated that he once saw one of the mud volcanoes erupt clots of mud to heights of at least 100 feet, an estimate similar to those made for the Salton mud volcanoes.

The Gerlach mud volcanoes are characterized by sporadic and apparently unpredictable intervals of activity separated by very much longer intervals of quiescence. Apparently a vent may have only a single period of eruptive activity and may then become extinct.

Salton Area, Imperial County, California

General relations of hot springs and rhyolite domes.—A group of hot springs, mud pots, and mud volcanoes are located near the southeast edge of Salton Sea not far from Niland, California (Le Conte, 1855; Veatch, 1857; Mendenhall, 1909; Waring, 1915; Kelley and Soske, 1936). The thermal features are closely associated with five relatively recent extrusive volcanic domes of pumiceous rhyolite, obsidian, and pyroclastic pumice. These domes rise 100–150 feet above the surrounding plain. The general relations of the thermal features and the domes are best described by Kelley and Soske (1936, p. 496–501).

Four groups of hot springs and mud pots occur within a distance of 2½ miles on a northwest line. The rhyolite domes lie on a second line nearly perpendicular to the hot-spring line. The springs, like those of Gerlach and Lake City, are situated in a basin containing fine clastic sediments of Quaternary age.

When the Salton Sea was flooded by the Colorado River from 1905 to 1907 the hot springs were submerged and the domes became islands (Mendenhall, 1909; Waring, 1915, p. 41). By the spring of 1935 the shore line of the sea had receded about 1½ miles from Mullet, the lowest dome (Kelley and Soske, 1936, p. 498). In recent years irrigation and drainage in Imperial Valley have resulted in another rise in lake level. When the area was visited on April 12 and 13, 1948, the Mullet dome was on the lake shore and the northwestern springs were again submerged. The main group of springs and mud volcanoes was covered by rising water shortly after 1948.

Wells were drilled near the rhyolite domes in a search for CO_2 (Kelley and Soske, 1936, p. 502). Abundant gas was found at high pressure and temperature, but associated steam was objectionable. Later wells were drilled east of Mullet Island and north of the line of mud pots, where temperatures were lower and the CO_2 was almost free of water vapor. Most production was from depths of 400–500 feet, and initial gas pressures were between 200 and 300 lbs. per square inch. (*See* Fig. 3.)

Observations, April 1948.—On April 12 and 13, 1948, the thermal features of the area about a mile southeast of the Mullet dome consisted of mud volcanoes, mud pots, muddy bubbling pools, perpetually spouting springs, steam vents, and at least one active geyser. The spouters and steam vents were particularly abundant near the center of the thermal area, which also included the geyser and many muddy pools but few mud volcanoes.

Many mud volcanoes are situated north and northwest of the steam vents and spouters. These mud volcanoes were formed by extrusion of mud flows, one on top of another similar to shield volcanoes, and not by explosive eruption. Although none of these was noticed in 1948, only the part of the area near board walks was examined because of the treacherous nature of much of the soft mud. Veatch (1857, p. 292) describes an eruption in 1857 similar to that of Gerlach, Nevada.

In addition to steam, the gases emitted from the area include CO_2 and some H_2S, as indicated by the presence of some sulfates and a little native sulfur

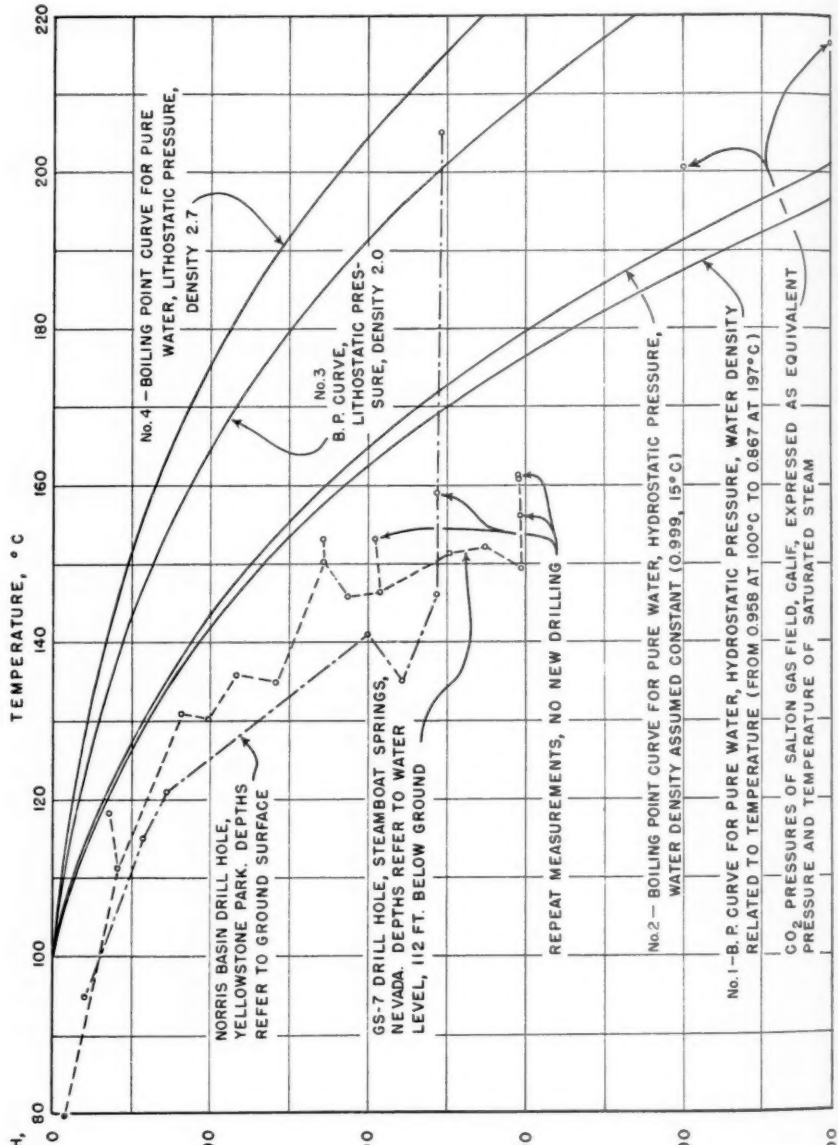
DEPTH, FEET
TEMPERATURE, °C
0
80
100
120
140
160
180
200
220
100
200
300
400
500
No. 4 — BOILING POINT CURVE FOR PURE WATER, LITHOSTATIC PRESSURE, DENSITY 2.7
No. 3 B.P. CURVE, LITHOSTATIC PRESSURE, DENSITY 2.0
NORRIS BASIN DRILL HOLE, YELLOWSTONE PARK. DEPTHS REFER TO GROUND SURFACE
GS-7 DRILL HOLE, STEAMBOAT SPRINGS, NEVADA. DEPTHS REFER TO WATER LEVEL, 112 FT. BELOW GROUND
REPEAT MEASUREMENTS, NO NEW DRILLING
No. 2 — BOILING POINT CURVE FOR PURE WATER, HYDROSTATIC PRESSURE, WATER DENSITY ASSUMED CONSTANT (0.999, 15° C)
No. 1 — B.P. CURVE FOR PURE WATER, HYDROSTATIC PRESSURE, WATER DENSITY RELATED TO TEMPERATURE (FROM 0.958 AT 100° C TO 0.867 AT 197° C)
CO_2 PRESSURES OF SALTON GAS FIELD, CALIF., EXPRESSED AS EQUIVALENT PRESSURE AND TEMPERATURE OF SATURATED STEAM

FIGURE 3.—TEMPERATURE-DEPTH RELATIONS OF TWO THERMAL DRILL HOLES, COMPARED TO BOILING-POINT CURVES

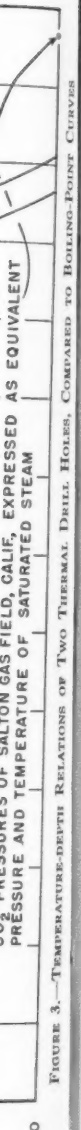

FIGURE 3.—Temperature-depth Relations of Two Thermal Drill Holes, Compared to Boiling-Point Curves

All the domes except Obsidian Butte show some recent acid alteration similar to the sulfuric acid alteration of many hot-spring areas. Some warm vapors are still being emitted from the two Pumice Buttes about a mile and a half south-southwest of the mud volcanoes, and Mullet Dome is even more active. A short distance southeast of the crest of this dome, pumiceous rhyolite is still being decomposed by acid attack. A temperature of 55.3° C was obtained at a depth of only 14 inches below the surface.

The old well on Mullet mentioned by Kelley and Soske (1936, p. 502) is on the south slope of the dome. The well was drilled through the dome and into sediments to a depth of 3500 feet, and in recent years the water rose in the well and erupted mildly three or four times a day to a height of several feet. No eruption was seen during the 1948 visit, but evidence of recent overflow was found. The water level in the well was surging between depths of 7.6–8.0 feet below the collar of the well, which was about 19 feet above the then-existing level of the Salton Sea. The temperature at water level was 72.9° C, only slightly less than the 73.3° C measured on the effective bottom, 18.8 feet below the collar.

An odor of H_2S was strong near the well, and a metallic film deposited on the steel tape used to measure temperature may have been native quicksilver.

Volcano Lake, Baja California

Mud volcanoes exist on the west shore of Volcano Lake 60 miles south-southeast of the Salton springs and about 20 miles south of the International Boundary. Mendenhall (1909, p. 14) states that the thermal features are similar to those of the Salton area but are on a larger scale.

The area is in the structural trench containing Coachella Valley, Imperial Valley, and Gulf of California and is presumably underlain by very thick and probably fine clastic sediments. The hot springs lie immediately southeast of Cerro Prieto, a prominent hypersthene andesite or dacite volcano of probable Pleistocene age. Only one small group of mud volcanoes were found during an investigation February 4, 1954, but others may have been disturbed or concealed by extensive levees that have been constructed in the area.

Acid Hot-Spring Areas

Mud volcanoes occur in some of the acid areas of Yellowstone Park (Allen and Day, 1935, p. 102–107), Lassen Park (Day and Allen, 1925, p. 103, 155), Coso hot springs, California, and in a number of localities in New Zealand (Grange, 1937, p. 89–95), Iceland (Barth, 1950, p. 113), and elsewhere.

The mud pots and mud volcanoes are largely restricted to localities where fine-grained clay and silica are abundant products of acid alteration. Sulfuric acid is produced by reaction of H_2S with atmospheric oxygen above and near the water table (Allen, 1934, p. 345–349). Complete disintegration to incoherent clays is therefore restricted to a near-surface zone. Steam and other gases stream up through fractured bedrock into the superficial mud deposits. If the gas-streaming is mild or if the mud is high in water content, the thermal feature is a mud pot, but if gas-streaming is violent and the mud is viscous and relatively low in water content, the thermal feature is a mud volcano. The underlying rocks are too competent to be erupted. Intense gas-streaming may erode and enlarge the channels, but generally the bedrock is not disturbed.

Mud volcanoes are rare in many acid areas because the pH of the environment is commonly too low (Table 1), or the original rocks were too high in silica to form abundant incoherent alteration products. The mud of some acid areas may not be dominantly a product of acid alteration. Deep residual soil at Boiling Lake in Lassen Park, and local clastic sediments in other places have supplied the fine-grained material necessary to mud volcanoes. The soil and sediments in these acid areas are commonly underlain at shallow depth by competent rock, in contrast to the deep fine-grained sediments of the Lake City thermal system.

Thermal activity in acid areas is ever-changing in intensity and in geographic position. Even the most vigorous of hot springs, fumaroles, or mud volcanoes eventually become less active, dormant, or extinct. Other similar fea-

TABLE 2.—ENERGY AVAILABLE IN A THERMAL SYSTEM WITH BOILING-POINT TEMPERATURE RELATIONS AT DEPTH AND CONTROLLED BY HYDROSTATIC PRESSURE (CURVE 1 OF FIG. 3)

One pound of water from the specified depth or temperature assumed to form appropriate proportions of water and steam at 100° C and 1 atm pressure

Depth ft.[1]	Temp. °C.[1]	Enthalpy[2] Btu	Excess Btu[3]	Steam[4] wt.%	Steam[5] cu.ft.	Total vol. cu.ft.[6]	Ratio, expanded to initial volume	Mech. energy ft.lbs.[7]
0	100.0	180.1	0	0	0	0.01672	1	0
4.7	103.5[8]	186.4	6.3	.65	0.174	0.191	11.4	368
25	115.6	208.3	28.2	2.91	0.78	0.80	47	1650
50	126.5	228.3	48.2	4.97	1.33	1.35	79	2810
100	142.8	256.8	76.7	7.91	2.12	2.14	123	4480
134.1	150.0	271.7	91.6	9.44	2.53	2.55	145	5350
200	162.3	294.6	114.5	11.82	3.17	3.18	180	6690
300	176.4	321.2	141.1	14.54	3.90	3.91	217	8230
500	196.6	359.7	179.6	18.5	4.96	4.97	269	10,500
541	200.0	366.3	186.2	19.2	5.14	5.15	278	10,900
	250.0	467	287	29.6	7.93	7.94	395	16,800
	300	578	398	41.1	11.0	11.0	489	23,300
	350	718	538	55.5	14.9	14.9	532	31,500
	374.0	903	723	74.6	20.0	20.0	400	42,300

[1] Most temperatures interpolated from curve 1 of Figure 3. Depths interpolated for temperatures of 103.5°, 150°, and 200° C. Depths not calculated for temperatures above 200° C.

[2] Keenan and Keyes, 1936, p. 31–32.

[3] Calculated from enthalpy of water at 100° C.

[4] From excess Btu relative to 970.3 Btu (heat necessary to convert 1 lb. water to steam at 1 atm pressure).

[5] Volume 1 lb. of saturated steam, 26.8 cu. ft. at 1 atm pressure.

[6] Calculated from initial specific volume of water, sp. vol. at 100° C, and final volume of water and steam.

[7] Mechanical work of expansion of steam in 1 atm pressure. Cubic feet of steam multiplied by 144 sq. in./sq. ft. and 14.7 lbs./sq. in. The mechanical energy is approximately 7½ per cent of total excess energy shown in column 4 (1 Btu = 778.3 ft. lbs.).

[8] Equivalent to maximum superheat recorded in natural thermal water at surface, 3.5° C in Giant Geyser (Allen and Day, 1935, p. 20).

tures come into existence, but the birth of one seldom coincides with the decline or extinction of another. The birth of a new "thermal feature" with many of the characteristics of mud volcanoes has been described from the Norris Basin area of Yellowstone Park (Turner, 1949, p. 526–527).

No evidence is available to indicate that mud volcanoes of acid areas ever erupt with the violence of the Lake City group or even the more vigorous of the Gerlach and Salton mud volcanoes, all of which are of the deep-sediment type. However, the total expenditure of energy from many of the acid mud volcanoes in time is probably much greater, because of continuous activity.

ENERGY OUTPUT OF THE LAKE CITY ERUPTION

Computed Mechanical Energy

Table 2 shows the total excess energy (above 100° C) stored in water under hydrostatic pressure at selected temperatures and depths. The per cent of steam and the available mechanical energy have been computed on the assumption that water of the indicated temperature (and corresponding saturation pressure) is suddenly exposed to a pressure of 1 atmosphere. Water is converted to steam until both phases reach a temperature of 100° C. Temperatures and corresponding depths of columns 1 and 2 are derived from curve 1 of Figure 3. This theoretical boiling-point curve is a very important

guide in predicting subsurface temperatures in vigorous thermal areas.

Under the assumed equilibrium conditions, all the mechanical energy is used in expanding the steam against air pressure. In an eruption a small part of the mechanical energy is used in lifting water or mud against gravity.

Relation of Mechanical Energy to Total Energy

In Table 2 the mechanical energy expressed in foot pounds is only about 7½ per cent of the total excess energy available above 100° C. Most of the total excess energy is used to convert water into steam, and most of the mechanical energy is actually utilized in expanding the steam against air pressure. If water is erupted directly from a depth of 100 feet to a height of 100 feet above the ground, 184 foot pounds of energy is required for 0.92 pound of water that remains from an original pound, or 200 foot pounds of energy for the original pound of water, including the part that is evaporated to steam. Friction, turbulence, air resistance, and evaporation below 100° C are neglected. This energy is only about 4½ per cent of the available mechanical energy or about 0.3 per cent of the total energy available above 100° C. The discrepancy is even greater if all energy available above atmospheric temperature is considered.

Table 3 shows the computed mechanical energy available in a thermal system of mud and water. The mud is assumed to consist of 20 per cent of water by weight or about 40 per cent by volume, depending on the mineralogy of the silicates and the temperature. The initial pressure on the mixture is assumed to be lowered abruptly to a pressure of 1 atmosphere. The differences between Tables 2 and 3 result from the low content of water, the difference in heat capacity of silicates relative to water, and the diversion of all excess heat above 100° C into the water fraction to form steam. A pound of mud erupted from a depth of 100 feet to a height of 100 feet above ground requires 200 foot pounds of energy, or about 12 per cent of the available mechanical energy (Table 3), as compared to only 4½ per cent for water. In actual eruptions, mud will probably not be erupted as high as water under similar circumstances.

The calculations demonstrate the abundant mechanical energy that is available in a thermal system with temperatures near boiling at depth.

TABLE 3.—ENERGY AVAILABLE IN A THERMAL SYSTEM OF MUD AND WATER WITH BOILING-POINT TEMPERATURE RELATIONS AT DEPTH AND CONTROLLED BY HYDROSTATIC PRESSURE (CURVE 1 OF FIG. 3)

One pound of material, 80 per cent silicates by weight and 20 per cent water*, assumed to form appropriate proportions of water and steam at 100° C and 1 atm pressure; density of silicate portion assumed 2.67, bulk density 2.0; heat capacity of silicates assumed 0.39 Btu per pound per degree C.

From		Excess Btu		Total steam, lbs.	Total steam, cu. ft.	Mechanical energy, ft. lbs.
Depth ft.	Temp. °C.	From water*	Silicates†			
25	115.6	5.6	4.9	0.0108	0.29	614
50	126.5	9.6	8.3	0.0184	0.49	1,045
100	142.0	15.3	13.1	0.0293	0.78	1,660
200	162.3	22.9	19.4	0.0437	1.17	2,470
300	176.4	28.2	23.8	0.0537	1.44	3,040
500	196.6	35.9	30.1	0.0681	1.82	3,860

* 20 per cent of corresponding values from column 4 of Table 2; 20 per cent by weight is approximately 40 per cent by volume, depending on the temperature.

† Heat available from silicates in cooling from indicated temperatures to 100° C.

Relative Energy of Eruption

Ordinarily data are inadequate to calculate directly the expenditure of energy by a mud volcano or a geyser in eruption. A useful quantity that can be calculated is here called the relative energy, and is defined as the product of the mass of material involved times the height that average water is erupted above ground. Calculations based on geysers and erupting wells at Steamboat Springs, Nevada, suggest that only about 5 per cent of available mechanical energy is actually utilized in erupting water to observed heights. The proportion of energy utilized in mud-volcano eruptions is probably of the same order of magnitude, al-

though energy loss owing to turbulence and friction may differ from geysers. Any error introduced by assuming equality is probably small compared to the errors introduced in determining the mass of material involved and the average height of eruption.

Lake City Eruption

The mass of mud involved in the Lake City eruption is estimated to be about 6 million cubic feet with a present density near 1.8 and a total mass of about 300,000 tons. The average height of eruption is completely unknown, but the morning after the most vigorous activity small amounts of mud were still being thrown to a height of 100 feet. The average height of eruption of all mud involved in the activity may have been 100 feet or more, but a conservative estimate of 20 feet is assumed in the following calculations. The relative energy of eruption is found to be 300,000 tons multiplied by 20 feet, or 1.2×10^{10} ft. lbs.

The actual expenditure of mechanical energy was probably about 20 times the relative energy, or 2.4×10^{11} ft. lbs., and the total excess energy above 100° C may have been 300 times as great, or 3.6×10^{12} ft. lbs. (See footnote 7, Table 2.)

Relative Energy of Geyser Eruptions

The chloride concentration of erupted water is ordinarily enriched significantly over that of water collected from the geyser vent prior to eruption. In the eruption process, some water is vaporized to steam and chloride is concentrated in the remaining water. If the water supply of the geyser prior to eruption is homogeneous in chloride content, the temperature of the water supply immediately prior to eruption can be computed from columns 5 and 2 of Table 2. The sample must be collected by a method that minimizes evaporation in the atmosphere below the boiling point. Actual measurements by the writer in geysers and erupting wells at Steamboat Springs, Nevada, have shown good agreement between computed and measured temperatures and depths. The total energy of the eruption can also be calculated from Table 2. When total discharge and height of eruption are measured or estimated, the relative energy of a geyser eruption can be calculated.

According to calculations based on data from Allen and Day (1935, p. 184, 187), the relative energy of an eruption of Old Faithful in Yellowstone Park is in the order of 8×10^6 foot pounds. (The height of eruption of average water is assumed to be 80 feet and the discharge per eruption, 1600 cu. ft.) Excelsior geyser (Allen and Day, 1935, p. 267–271) is now inactive, but it was by far the most vigorous of all Yellowstone geysers. From descriptions, the height of eruption of average water is assumed to be 100 feet and its discharge an average of 130 second feet for a duration of 10 minutes. With these assumptions, its relative energy of eruption was 5×10^8 foot pounds, or only $\frac{1}{25}$ that of the Lake City eruption.

Waimangu geyser in New Zealand (Grange, 1937, p. 114) erupted to a maximum height of 1000 feet or more from 1900 to 1917. This geyser was the largest that is known in recorded history. Its relative energy cannot be computed because no estimate of its discharge has been recorded. If the height of eruption of average water is assumed to have been 5 times as much, and its discharge 5 times as great as that of Excelsior, its relative energy may have been about equal to that of the Lake City eruptions.

Mechanics of Eruption of Mud Volcanoes

General

The source of energy of mud volcanoes, as well as of other high-temperature hot springs and fumaroles, is believed to be volcanic heat. The volcanic energy is transferred to the surface of the earth in part by conduction, but probably to a greater extent by circulation of water. Although some of the water of a hot-spring system is probably of volcanic origin, most is believed to be surface water heated in the thermal system (Allen and Day, 1935, p. 40–41; White and Brannock, 1950, p. 570–573). The energy of eruption of mud volcanoes is contained in the hydrothermal system near the surface. The principal evidence for this conclusion is the relatively small size and low temperature of mud volcanoes and the complete absence of new volcanic rock.

The mud volcanoes of sedimentary basins are characterized by fine-grained water-saturated clastic sediments, with no near-surface basement of competent rocks. The water table is at or very near the ground surface, gases are not conspicuous, and discharge of water is more

Table 4.—Energy Available in a Thermal System with Boiling-Point Temperature Relations at Depth, and Controlled by Lithostatic Pressure (curve 3 of Fig. 3)

Density of 2.0; other assumptions and calculations are similar to those of Table 2. One pound of water from specified depth assumed to form appropriate proportions of water and steam at 100° C and 1 atm pressure.

From		Enthalpy Btu	Excess Btu	Steam lbs.	Steam cu.ft.	Total vol. cu. ft.	Ratio, expanded to initial volume	Mech. energy ft. lbs.
Depth ft.	Temp. °C.							
0	100.0	180.1	....	....	....	....	....	....
25	127.4	230.1	50.0	0.0516	1.38	1.40	82	2,920
50	143.6	259.7	79.6	0.0821	2.20	2.22	128	4,650
100	164.9	299.4	119.3	0.123	3.30	3.31	187	6,980
200	191.4	349.7	169.6	0.175	4.68	4.69	255	9,900
300	209.6	385.0	204.9	0.211	5.65	5.66	301	12,000

abundant than in most acid areas. The sediments are relatively incompetent, and are fine-grained and low in permeability. They probably have the strength to resist stresses of short duration but have little strength to resist long-applied stresses. On the other hand the calcite veins in a matrix of mud found in the eruption debris indicate that fractures do exist and are maintained.

Most of the water normally discharged from the Gerlach and Salton areas, and presumably also from the Lake City area, is clear with little suspended sediment. This is evidence that the sediments of these thermal systems behave as solids and not as dense liquids. The semi-plastic nature of the sediments, however, is effective in producing a pressure gradient in the hydrothermal system that is probably intermediate between the pressure gradients of curves 1 and 3 of Figure 3.

Convection within the water system is probably absent or is greatly inhibited relative to that of well-fractured competent rocks. In a sufficiently vigorous thermal system, the temperature gradient is probably higher than the gradient of curve 1 in Figure 3 but is considerably less than the gradient of curve 3. The energies available for eruption are correspondingly intermediate between the values shown in Table 3 and those of Table 4.

Cause of Eruption

Thermal systems with temperature gradients close to the boiling point curve are highly unstable. If material is suddenly removed at the top of the system, the pressure is lowered throughout. Each point at depth, formerly just at its boiling point, is now above its boiling point. Boiling then starts throughout the column, or if mild boiling had previously existed, the rate of boiling rapidly increases. In competent fractured rock, water is displaced upward and out of the system by expanding gas bubbles, decreasing the hydrostatic pressure on the system and setting off a chain reaction that results in geyser action. The same unstable relations are also of critical importance in understanding mud-volcano eruptions in basin sediments.

Any sudden decrease in the pressure of the system is potentially the trigger for an eruption. The beginning phases of mud-volcano eruptions of the sedimentary-basin type have not been observed or described, so specific causes can only be postulated. These may include an unusual combination of gas bubbles erupting considerable mud from a pool that is ordinarily a mud pot; an unusually rapid lowering of barometric pressure; or some other ordinarily insignificant change. Regardless of the specific cause of the trigger action, not determinable from present evidence, there is no doubt that

abundant energy and the potentialities for eruption exist in the unstable temperature-depth relations of the thermal system.

If thermal systems are as unstable as the energy considerations suggest, major eruptions like the Lake City activity should be more common. However, the thermal system usually adjusts itself to minor change without incurring a major eruption. A slight decrease in pressure on the system probably results in a slight increase in boiling, insufficient in amount to exceed some critical value necessary to cause eruption.

The nature of the water solution also aids in the adjustment of a thermal system. In Figure 3 and Tables 2–4 the water of the system is assumed to be pure water. In actuality the water contains some dissolved substances tending to increase the boiling points and dissolved gases tending to decrease the boiling points. A solution of this type has no single boiling point, and its reaction to increasing temperature is best regarded as a boiling range. The temperature-depth curve of Steamboat drill hole GS-7, shown on Figure 3, is typical of the Steamboat drill holes in this respect: Equilibrium temperatures to depths of 200–250 feet below the water table generally lie below but very close to hydrostatic pressure curve 1 of Figure 3 and do not cross the curve. At greater depths the temperatures fall increasingly short of the theoretical boiling-point curve. The system is believed to be a single-phase liquid near the the base of the explored zone, but as the hot water rises and pressure decreases sufficiently, a vapor phase starts to form. The upper part of the temperature curve is determined to a major extent by boiling within the system. Actual temperatures lie below the theoretical curve because of the vapor pressures of gases in solution.

The significance of these relations in inhibiting eruption lies in the fact that the boiling point of the solution is raised as the quantity of dissolved gases decreases, in contrast to a pure-water system in which the boiling point is not affected by the quantity of steam that has formed. Stated in a different way, if a solution of water and gas is exposed to a constant temperature 1° above the temperature where vapor first forms, dissolved gas is selectively lost to the vapor and the solution soon comes to equilibrium at the new temperature because the boiling point has been raised. In contrast, if pure water is exposed to a constant temperature 1° above its boiling point, the water will continue to boil until all is evaporated, without reaching equilibrium.

The proposed explanation for the Lake City eruption assumes the energy for eruption is stored within the thermal system, and no major change in rate of flow or heat has occurred deep in the system. Calculations indicate that the thermal system does contain a very adequate source of energy, but complete answers for some of the vagaries of eruption are not apparent.

An alternative explanation assumes an increase in temperature or in rate of flow, relating the eruption to a surge of very hot water with vapor pressure considerably in excess of the near-surface pressure. This explanation may seem particularly attractive for the Lake City eruption because of its great vigor, unusual magnitude, and the fact that four or five major centers were active contemporaneously. An increase in temperature is believed to be unnecessary, but is not ruled out by present evidence.

Relation to Volcanic Eruptions

Phreatic or Cryptovolcanic Eruptions

Some eruptions or eruption products classed as phreatic or cryptovolcanic are closely related to the Lake City type of activity, if the energy for eruption were contained in water of hydrothermal systems at temperatures approximating the hydrostatic boiling-point curve. Reliable criteria are difficult to establish. The water table must have been at or very near the surface; the eruption products are characterized by local distribution, and probably by abundant fine-grained clay-rich particles; and no new volcanic fragments are involved. A search should be made for hydrothermal minerals known to be associated with shallow-depth hydrothermal systems. These include zeolites, montmorillonite and kaolinite clays, hydromicas, carbonates, opal, and probably chalcedony, chlorite, and pyrite. On the other hand, if the field evidence favors the derivation of the eruption products from competent rocks, volcanic

vapor pressures exceeding lithostatic pressures are indicated. New volcanic products such as scoria definitely eliminate hot springs systems as the principal or direct source of the energy that initiated eruption.

A breccia of late Pleistocene age at Steamboat Springs, Nevada, is distributed over an area 1000 feet long and 750 feet wide. The writer believes it is a mud-volcano deposit erupted on a scale at least equal to that of the Lake City eruption. The deposit consists of unsorted material ranging from clay-sized particles to boulders as much as 6 in. in diameter derived from the underlying alluvium and sinter. Many fragments were hydrothermally altered prior to eruption; on the borders of the area this heterogeneous material lies on unaltered alluvium. Similar deposits probably exist elsewhere.

Volcanic Eruptions Intensified by Hydrothermal Energy

The destructive power of true volcanic eruptions may be increased greatly by energy that has been stored in a vigorous hydrothermal system.

Much of the energy of the very destructive Tarawera, New Zealand, eruption of 1886 may have been derived from hydrothermal systems of Lake Rotomahana (Smith, 1886, p. 47–49). Grange (1937, p. 29, 36–37, 55, 78–85) has summarized the events and the eruption products. The activity first started early in the morning of June 10, 1886, on the northeast side of the Tarawera rhyolite domes and advanced rapidly to the southwest, forming a chain of craters 9 miles long. Within about 3 hours the whole chain was in maximum eruption, but after 2 hours the activity had almost ceased.

Basalt scoria and ash were erupted to the north and northeast from the craters on the Tarawera domes and from one of the southwestern craters, but a large volume of erupted material containing appreciable clay, known as Rotomahana mud, was derived from older material of the Lake Rotomahana thermal area in the south-central part of the chain of craters. The volume of Rotomahana mud is estimated to be about a fifth of a cubic mile (Grange, 1937, p. 29; Smith, 1886, p. 56). The mud was distributed to the north for a distance of at least 20 miles from its source, according to Grange's map of volcanic showers.

Prior to the eruption, the world-famous White and Pink Terraces containing hot springs and geysers had existed on the shores of the former Lake Rotomahana. Mud pots, mud volcanoes, and acid springs were abundant (Grange, 1937, p. 91–94). The terraces and all of the hot springs were completely destroyed or modified beyond recognition by the eruption.

Grange (1937, p. 83) states:

> "Besides being much lower than (Tarawera) mountain, the country round the old Rotomahana is formed of weaker rocks, some of them lake deposits, and much of them decomposed and altered to clays by the long-continued thermal activity. Across this low country the "fissure" widens out to a great, irregular crater-basin, three miles long and from half to one mile and a half wide. Here the weak surface rocks were shattered into sand and dust, and scattered over the surrounding country, leaving an excavation some three miles in area and bounded, at most places, by vertical walls from 200 to 300 feet high."

The southern part of the large basin contained numerous funnel-shaped depressions ranging up to 40 feet in diameter. Although not described in detail, they are suggestive of the mud-volcano vents of the Lake City area. The estimated average depth of material erupted from the basin is 300 feet. Fumaroles and other "points of activity" (mud volcanoes?) still existed in the Rotomahana crater 2 months after the eruption, although the craters on Tarawera were completely inactive.

A hydrothermal system with temperature-depth relations similar to those shown on Figure 3 probably cannot initiate a major eruption, but if vapor pressures in underlying magma are sufficiently high to disrupt and fragment the overlying cover, an important supply of stored energy is then made available to augment the direct volcanic energy. Of particular significance is the large volume of hot wall rocks and interstitial water that are involved in the eruption because of their stored thermal energy. In contrast the stable or passive wall rocks of most volcanic vents are involved only to a minimum extent in eruptions. The exceptional vigor of that part of the Tarawera eruption originating near Lake Rotomahana was probably due to energy from the hydrothermal systems of that area.

The energy of all explosive volcanic eruptions may be increased to some extent by energy from water-saturated rocks. The great vigor of some submarine eruptions and eruptions involving crater lakes may be due in considerable part to such stored energy, which becomes available following the initial disruption.

References Cited

Allen, E. T., 1934, Neglected factors in the development of thermal springs: Nat. Acad. Sci. Proc. v. 20, p. 345–349.

Allen, E. T., and Day, A. L., 1927, Steam wells and other thermal activity at "The Geysers," California: Carnegie Inst. Washington Pub. No. 378, p. 1–106.

—— 1935, Hot Springs of the Yellowstone National Park: Carnegie Inst. Washington Pub. No. 466, p. 1–525.

Anderson, C. A., 1941, Volcanoes of the Medicine Lake Highland, California: Univ. Calif. Pub., Bull. Dept. Geol. Sci., v. 25, p. 347–422.

Barth, T. F. W., 1950, Volcanic geology, hot springs, and geysers of Iceland: Carnegie Inst. Washington Pub. No. 587, p. 1–174.

Brannock, W. W., Fix, P. F., Gianella, V. P., and White, D. E., 1948, Preliminary geochemical results at Steamboat Springs, Nevada: Am. Geophys. Union Trans., v. 29, p. 211–226.

Day, A. L., and Allen, E. T., 1925, The volcanic activity and hot springs of Lassen Peak: Carnegie Inst. Washington Pub. No. 360, p. 1–190.

Grange, L. I., 1937, The geology of the Rotorua-Taupo Subdivision, Rotorua and Kaimanawa Divisions: Dept. Scientific and Industrial Research, Geol. Survey Br., Bull. No. 37, p. 1–138 (New Series) (New Zealand).

Keenan, J. H., and Keyes, F. G., 1936, Thermodynamic properties of steam: N. Y., John Wiley and Sons, p. 31–32.

Kelley, V. C., and Soske, J. L., 1936, Origin of the Salton volcanic domes, Salton Sea, California: Jour. Geology, v. 44, p. 496–509.

Le Conte, John L., 1855, Account of some volcanic springs in the desert of the Colorado in Southern California: Am. Jour. Sci., 2nd ser., v. 1[illegible] p. 1–6.

Mendenhall, W. C., 1909, Ground waters of the Indio region, California, with a sketch of the Colorado Desert: U. S. Geol. Survey Water Supply Paper 225, p. 13–14.

Powers, H. A., 1932, The lavas of the Modoc Lava Bed quadrangle, California: Am. Mineralogist v. 17, p. 253–294.

Russell, I. C., 1884, Reconnaissance in Oregon: U. S. Geol. Survey Fourth Ann. Rept., p. 449–450.

Russell, R. J., 1928, Basin Range structure and stratigraphy of the Warner Range in northeastern California: Univ. Calif. Pub., Bull. Dept. Geol. Sci., v. 17, p. 387–496.

Smith, S. Percy, 1886, The eruption of Tarawera: Wellington, New Zealand, Govt. Printer, 84 p.

Stearns, H. T., and Macdonald, G. A., 1946, Geology and ground-water resources of the island of Hawaii: Hawaii Div. Hydrography Bull. 9, p. 1–363.

Stearns, N. D., Stearns, H. T., and Waring, G. A., 1937, Thermal Springs in the United States: U. S. Geol. Survey Water-Supply Paper 679-B, p. 1–206.

Turner, D. S., 1949, Development of a new thermal feature in Yellowstone National Park: Am. Geophys. Union Trans., v. 30, p. 526–527.

Veatch, J. A., 1857, Notes of a visit to the mud volcanoes in the Colorado Desert in the month of July, 1857: Am. Jour. Sci., 2nd ser., v. 26, p. 288–295.

Waring, G. A., 1915, Springs of California: U. S. Geol. Survey Water-Supply Paper 338, p. 41, 122–123.

White, D. E., and Brannock, W. W., 1950, The sources of heat and water supply of thermal springs, with particular reference to Steamboat Springs, Nevada: Am. Geophys. Union Trans., v. 31, p. 566–574.

U. S. Geological Survey, 4 Homewood Place, Menlo Park, Calif.

Manuscript Received by the Secretary of the Society, September 7, 1954.

Publication Authorized by the Director, U. S. Geological Survey.

BULLETIN OF THE GEOLOGICAL SOCIETY OF AMERICA
VOL. 66 PP. 1131-1148 SEPTEMBER 1955

ISOTOPIC COMPOSITION AND DISTRIBUTION OF LEAD, URANIUM, AND THORIUM IN A PRECAMBRIAN GRANITE

By George R. Tilton, Claire Patterson, Harrison Brown, Mark Inghram, Richard Hayden, David Hess, and Esper Larsen, Jr.

Abstract

The isotopic compositions and concentrations of lead and uranium have been determined in some separated minerals and the composite of a granite from Monmouth township, Haliburton County, Ontario. The chemical and mass spectrometric methods that were used are described. The age of the zircon from the granite is 1050 million years. Much of the lead, uranium, and thorium exists in chemically unstable and presumably interstitial phases of the granite. A comparison of the observed amounts of uranium, thorium, and lead in the various minerals with those amounts that should have been present, had these three elements existed within the minerals as closed systems, shows a nonbalance of these elements in every case. It appears that the granite as a whole has closely approximated a closed system since it was formed with respect to uranium and its decay products, but has been an open system with respect to thorium and its decay products. Interpretations concerning the relationship of these data to lead ores are discussed.

CONTENTS

TEXT

	Page
Introduction	1131
Acknowledgments	1132
Rock description	1132
Chemical procedures	1134
Contamination	1134
Reagents and apparatus	1135
Isolation of lead	1135
Isolation of uranium	1136
Isolation of thorium	1137
Mass spectrometry of uranium and lead	1137
General	1137
Lead procedure	1138
Uranium procedure	1139
Accuracy	1139
Results	1139
Discussion	1141
Uranium-lead age of granite	1141
Potassium-argon age of the granite	1142
Loss or gain of uranium, thorium, and lead in the granite	1143
Distribution of uranium, thorium, and lead in the granite	1144
Material balance	1145
Internal transfer of uranium, thorium, and lead	1145
Relation to lead ores	1146
Conclusions	1147
References cited	1147

TABLES

Table	Page
1. Chemical analysis, norm, and mode of granite from near Tory Hill, Ontario	1133
2. Semiquantitative spectrographic analysis of granite from Tory Hill, Ontario, and of three minerals separated from the granite	1134
3. Uranium, thorium, and lead concentration and isotopic compositions of lead in various constituents of the granite	1140
4. Comparison of lead and thorium values obtained by different methods	1141
5. Ages for the granite and the Wilberforce pegmatite	1142
6. Contribution by each mineral to the uranium, thorium, and lead content of the total granite	1145
7. Comparisons between the observed and calculated amounts of radiogenic leads, in various constituents of the granite	1145
8. Calculated isotopic compositions of lead in the granite at various times	1146
9. Average composition of lead ores at various times	1147

Introduction

It has long been recognized that if techniques could be developed to determine precisely the isotopic compositions and concentrations of lead and uranium, when these elements are present in amounts of but a few parts per million, the range of materials amenable to precise radioactive dating would be enormously increased. In addition, such techniques would permit more detailed studies of the time and space relations

of radioactive elements and their decay products.

The isotope dilution technique of quantitative analysis, first described by Hayden, Reynolds, and Inghram (1949, p. 1500) and later applied (Inghram *et al.*, 1950, p. 916) to the study of calcium and argon in Stassfurt sylvite, has been applied in this work to lead, thorium, and uranium. The techniques described in this paper make possible both the precise determination of as little as 0.01 part per million of uranium and thorium and 0.1 part per million of lead in silicates, and the determination of the isotopic composition of lead totaling only a few micrograms in a sample.

Briefly, the isotope dilution method of analysis operates as follows: If the uranium content constituting about one part per million of a mineral is to be determined, approximately 5 grams of the mineral are dissolved and a few micrograms of U^{235} containing but a small fraction of U^{238} are added to the solution. The U^{235} becomes mixed with the uranium from the unknown which is primarily U^{238}. The mixture of uranium from the unknown and the uranium tracer is extracted from the solution, and the new ratio of U^{235} to U^{238} is determined. Knowing the initial sample weight, the weight of U^{235} tracer added, and the original and final ratios of U^{235} to U^{238}, one can readily compute the concentration of uranium in the unknown. The application of the technique to lead, although more complicated, is essentially the same.

The main obstacles to be overcome in this work were contamination during the isolation of such small quantities of material and difficulty in measuring accurately the isotopic composition of extremely small samples. Therefore extreme care was taken to control contamination and a combination of surface ionization and electron multiplier detection techniques were used in the mass spectrometer.

The techniques developed for uranium, thorium, and lead have been applied to a study of their distribution in a Precambrian granite. The studies were not exhaustive, but were undertaken primarily to test the method and demonstrate its applicability to geochemical and geochronological problems.

Acknowledgments

We wish to express our gratitude that the facilities of the Argonne National Laboratories, the Department of Terrestrial Magnetism of the Carnegie Institution, the U. S. Geological Survey, the Institute for Nuclear Studies of the University of Chicago, and the California Institute of Technology could be combined to make these studies possible. We are indebted to The Geological Society of America for a grant which has supported some of this work. The portion of the work undertaken at the California Institute of Technology was supported by the U. S. Atomic Energy Commission (Contract #AT-11-1-208). We sincerely thank Kenneth Jenson of the Argonne National Laboratories for the careful and precise potassium analyses, Claude Waring of the U. S. Geological Survey for making available the results of the spectrographic analyses for lead to which he has devoted considerable time and effort, and H. S. Armstrong of McMasters University for providing the sample of pegmatite perthite. We are grateful for the advice and criticism of our colleagues, in particular Gunnar Kullerud of the Mineralogisk-Geologisk Museum, Oslo, Norway, and Leon Silver, California Institute of Technology.

Rock Description

It was agreed that the granite to be used for this investigation should be of Precambrian age and should fulfill the following requirements: it should not have been altered or recrystallized, but it should be moderately radioactive; it should contain a moderate amount of lead and at least average amounts of the accessory minerals zircon, apatite, sphene, and magnetite; its potash feldspar should be rich in lead so that the isotopes of the lead of the original magma could be determined. The late Dr. H. V. Ellsworth supplied granite that satisfied most of these requirements from a source he described as follows:

> "On Map No. 52a, Haliburton area, Province of Ontario, (Satterly, 1943) the area between Tory Hill and Essonville marked with the symbol 'Ra' represents roughly the area from which the granite samples were taken and the symbols probably the actual openings. This granite is from the Brower-Simpson property."

The geology of the area between Tory Hill and Essonville is shown on a map by Adams and Barlow (1910) and on a modified map by Satterly (1943); both, on a scale of 2 miles to the inch, show metasedimentary rocks of the Grenville series at Tory Hill and Essonville and granite on the road between the two villages, with the contact between the Grenville and the granite about a mile east of the road. In October 1952, Larsen investigated the excellent new road cuts and found them to be chiefly in rocks of the Grenville series, with some small bodies of granite. There may be more granite to the west. The granite specimens used in this investigation undoubtedly came from some of the small bodies of granite. It is rather uniformly red and coarse-grained, with some gneissic structure. The microscopic texture is granoblastic with many grains of strained and broken plagioclase and quartz. Whether this is merely a protoclastic texture in early crystallized grains, or whether it reflects a post-crystallization deformation cannot be demonstrated. The larger grains of feldspar may be as long as 10 mm, with an average length of about 3 mm. Table 1 gives the chemical analysis, the norm, and the mode of the granite.

Semiquantitative spectrographic analyses of the granite and of apatite, sphene, and zircon separated from the granite are given in Table 2.

TABLE 1.—CHEMICAL ANALYSIS, NORM, AND MODE OF GRANITE FROM NEAR TORY HILL, ONTARIO
Chemical analysis by A. M. Sherwood, U.S. Geological Survey, Washington, D.C.

Chemical Analysis		Norm		Mode*	
SiO_2	72.55	Q	24.24	Quartz	24 ± 1
TiO_2	0.25	or	30.02	Perthite	52 ± 2
Al_2O_3	14.29	ab	41.39	Plagioclase	20 ± 1
Fe_2O_3	1.41	an	0.83	Hornblende	2 ± 1
FeO	0.54	C	0.41	Magnetite	0.4 ± 0.2
MnO	0.02	mt	1.16	Zircon	0.04 ± 0.01
MgO	0.06	il	0.46	Apatite	0.02 ± 0.01
CaO	0.17	hm	0.64	Sphene	0.4 ± 0.1
Na_2O	4.92	hy	0.20	Pyrite	0.02
K_2O	5.06			Calcite	trace
H_2O^-	0.09				
H_2O^+	0.14				
P_2O_5	0.01				
U	0.001				
Total	99.50				

*The mode was estimated from the chemical analysis, thin sections, and the amounts of separated minerals.

About 50 pounds of the granite were ground by hand to pass 15 mesh and sized. The minerals were separated by using bromoform, methylene iodide, and the Frantz Isodynamic separator with special precautions to avoid lead contamination (Larsen, Keevil and Harrison, 1952, p. 1047). The final zircon sample was hand-picked, and all mineral samples were more than 99 per cent pure.

The sphene, which is more abundant in this granite than in most granites, occurs in crystals, several mm long. It is reddish brown in transmitted light. Its optical properties are: $\alpha = 1.89$, $\beta = 1.90$, $\gamma = 2.01$, and 2V small, which indicate an ordinary sphene.

The zircon occurs in stout prisms that average about 1 mm in length. Several hundred mg of these grains were ground to approximately 200 or 300 mesh to obtain the powder used in analytical work. Optical examination of the powder revealed wide variations in refractive index (ω), which ranged from 1.92 to 1.82 and averaged about 1.85. Thin sections of several of the larger grains indicated exten-

sive zoning of the mineral. Some of the outer-zone zircon is very near ordinary fresh zircon with ω of about 1.915 and with strong birefringence. Some parts of a zircon crystal may be nearly or completely isotropic with n about 1.84. All intermediate indices of refraction seem to be present, as if mixtures in all proportions of the two end materials were present.

Hurley and Fairbairn (1953, p. 659) have found that the value of 2θ for diffraction from the lattice plane (112) of zircon is 35.635° for the undamaged mineral and approaches 35.1° for complete metamictization, accompanied by diminishing peak intensities and sharpness. An X-ray study of the present zircon gave a low, broad diffraction from the (112) plane with the maximum at about 35.3° indicating extensive metamictization in agreement with the optical data. The alpha activity of the zircon is 1100/mg/hr. The powdered mineral has been leached for 30 minutes in hot 1:1 aqua regia, and 35 per cent of the activity was removed.

Table 2.—Semiquantitative Spectrographic Analysis of Granite from Tory Hill, Ontario, and of Three Minerals Separated from the Granite

Analyses by C. S. Annell, U.S. Geological Survey, Washington, D.C.

	Over 10%	1–10%	0.1–1.0%	0.01–0.1%	0.001–0.01%	0.0001–0.001%
Granite	Al Si	Fe K Na	Ca Mn	Sr Ga Pb Mg V Ba Ti		Cu
Apatite	Ca P		Si Zr Fe Mn Na Sr Al Y La	Pb V Ti Mg	Yb Tm Ga Ho	Ba Cu Ag
Sphene	Si Ca Ti	Fe Al	Mn Th Na Zr Y La	Pb Mg Sr Sn V Yb	Ga Lu Tm Ba Ho Cu	Ba
Zircon	Zr Si		Fe Y Hf Al Pb	Mn Yb Tm Ho Lu Ti	Sr Ga Ba Mg	Ag Cu

Chemical Procedures

Contamination

Contamination was introduced from three sources: reagents, apparatus, and the laboratory air. The removal of lead, thorium, and uranium from the reagents and apparatus is discussed under Reagents and Apparatus. Contamination from the air was a critical factor in the case of lead. Air contamination was controlled as follows:

(1) The laboratory was mopped and vacuumed at frequent intervals. A positive pressure of filtered air was maintained in the laboratory and drafts were minimized.

(2) The bench tops and hoods were constructed of stainless steel and kept clean by frequent scrubbing and rinsing.

(3) All cleaned glassware and reagent bottles were sealed with a semiadhesive sheet plastic, "Parafilm".[1] The seals were broken only when materials were being transferred, and were immediately resealed after an operation.

(4) Hydrofluoric acid evaporations were carried out in a stainless steel box. Tank nitrogen, filtered through glass, was kept flowing through the box.

(5) All other evaporations were carried out in glass tanks. Fumes were swept out of the tanks by a continuous flow of filtered nitrogen.

Under these conditions, when the processing of a sample required 10–15 hours of evaporations and several days of handling, the lead contamination varied from a few tenths to slightly more than 1 microgram per sample. If air contamination during evaporation was not controlled, the amount of lead introduced per sample, varied erratically from 1 to more than 10 micrograms. The uranium and thorium contaminations were generally about .02 microgram or less per sample.

[1] Manufactured by Marathon Corp., Menasha, Wisconsin.

Reagents and Apparatus

Water was triple distilled. The final distillation was carried out through a Pyrex, triple cold wall reflux condenser. Nitric and perchloric acids were vacuum distilled in a transparent silica still containing a 60-cm vigreux column. Solid reagents were recrystallized and extracted repeatedly with dithizone in choloroform to remove lead. Organic liquids were extracted repeatedly with dilute nitric or hydrochloric acids and water. Hydrofluoric acid was prepared by passing the gas through a filter of fine "Teflon"[2] shavings and a "Teflon" tube bubbler into water in an ice-cooled platinum vessel.

Hydrochloric acid and ammonium hydroxide were prepared in the same manner as hydrofluoric acid except Pyrex and "Tygon" tubing, glass filters, and Pyrex vessels were used. Uranium, thorium, and lead tracer solutions were standardized both gravimetrically and by isotope dilution.

Pyrex glassware was used throughout. This was cleaned by scrubbing with scouring powder, rinsing with distilled water, complete immersion for 20 minutes in a 10 per cent solution of potassium hydroxide held near the boiling point, rinsing with distilled water, complete immersion for 20 minutes in concentrated nitric acid held near the boiling point, and rinsing with double distilled water. The glassware was handled only with stainless steel tongs that were kept clean and frequently rinsed. Stopcocks and ground stoppers were used without grease. Platinum-ware was cleaned by scrubbing with scouring powder, etching a fresh surface with aqua regia and rinsing with double distilled water. The lead gaskets encountered in tanks of compressed gases were removed, the fittings cleaned, and gaskets of "Teflon" substituted.

Isolation of Lead

The sample was dissolved and divided into two aliquots, a known amount of Pb^{208} tracer was added to one aliquot. The two aliquots were processed chemically to isolate the lead. A blank, consisting of a known amount of Pb^{208} tracer processed by the reagents, was isolated at the same time.

The feldspars and quartz were dissolved by heating first with hydrofluoric acid, and then with a mixture of borax and perchloric acid. Zircon and sphene were dissolved by fusing with borax, leaching with hydrochloric acid, and dissolving the residue in the same manner as for the feldspars and quartz. Magnetite and apatite were dissolved in hydrochloric acid and perchloric acid respectively. The granite composites were treated in the same manner as the feldspars and quartz, the insoluble residues being collected and treated in the same manner as the zircon and sphene.

The isolation of lead from these solutions consisted of complexing interfering ions with citrate and extracting lead dithizonate into chloroform at a pH of 9.5. When the iron content was high, as in the case of magnetite, the solutions were first oxidized with nitric acid and then ether-extracted. When some interfering anions were in large excess, as in the case of phosphate from apatite, large excesses of citrate and high dilutions were employed. The procedures are modifications of those developed by G. Lundell and H. B. Knowles (1920, p. 1440), P. A. Clifford and N. J. Wickmann (1936), K. Bamback and R. E. Burkey (1942), and E. B. Sandell (1950, p. 388–412) and were developed with the aid of radioactive tracers. The yields ranged from 30 to 80 per cent. A detailed discussion of some of the lead analytical work has appeared in a declassified Atomic Energy Commission document (Patterson, 1951). The specific analysis of the acid-washed granite was as follows:

(1) Ten grams of powdered rock were placed in a large centrifuge bottle, 50 ml of ether was added and the mixture swirled for 3 or 4 minutes. The ether was centrifuged off and discarded. This was repeated twice with ether, three times with 6 molar HCl, and four times with water.

(2) The cleaned material was dried at 110°C and weighed into platinum dishes. One hundred ml of concentrated hydrofluoric acid was added and evaporated to near dryness at low heat over a long period of time. One hundred ml of concentrated perchloric acid was added and the mixture warmed until HF fumes ceased

[2] Manufactured by E. I. duPont de Nemours and Co.

to evolve. Fifty ml of a saturated solution of borax was added and the mixture heated strongly until a cake was almost ready to form. It was then cooled, stirred with 200 ml of warm water, and centrifuged.

(3) The centrate was reserved and the residue transferred to the top of a 1-gram bead of fused borax in a platinum crucible. The bead was fused again, cooled, and dissolved in 50 ml of warm 3 molar HCl. This solution was made ammoniacal, centrifuged, the centrate reserved, and the residue transferred to a platinum dish.

(4) The residue was treated with hydrofluoric and perchloric acids and borax as described in (2), except that one-tenth of the quantities of reagents was used. There was no visible residue at this point. All solutions were combined and diluted to 500 ml in a volumetric flask.

(5) A 100-ml aliquot was withdrawn and mixed with an aliquot containing 25 micrograms of Pb^{208} tracer. This solution was treated as described below, the remaining 400 ml being treated in a similar manner except that proportionately larger amounts of reagents were used.

(6) Twenty-five ml of a 30 per cent citrate solution was added, then 10 ml of ammonium hydroxide. This solution was extracted with 50 ml of chloroform containing 2.5 mg of dithizone.

(7) The chloroform layer was separated and extracted with 50 ml of 2 per cent HNO_3.

(8) The water layer was separated and 10 ml of a solution containing 15 per cent concentrated ammonium hydroxide and 2 per cent KCN were added to it. This solution was then extracted with 10 ml of chloroform containing 0.2 mg of dithizone. The chloroform layer was separated and evaporated to dryness. One ml each of water, concentrated nitric acid, and concentrated perchloric acid was added and the solution evaporated to dryness. The yield was about 70 per cent.

Isolation of Uranium

Three methods of sample decomposition were employed: digestion in mineral acids (magnetite and apatite), fusion in borax followed by digestion in dilute hydrochloric acid (zircon and sphene), and treatment with hydrofluoric acid after which the insoluble fluorides were dissolved by fuming with perchloric acid in the presence of borate ion (feldspars and quartz).

After the sample was dissolved, the resulting solution was equilibrated with 30 micrograms of essentially pure U^{235}. The principal purification of uranium was then accomplished by hexone extraction of a nearly saturated solution of the nitrate salts (Blaedel *et al.*, 1945). The few remaining impurities were then precipitated on ferric hydroxide by ammonium carbonate, the carbonate ion holding the uranium in solution by complex ion formation. A final hexone extraction from 10 M ammonium nitrate solution gave uranium which apparently contained no more than a few micrograms of impurity and which was pure enough in all cases for good spectrometer runs.

In this study the contamination of a mineral analysis was obtained by comparing the results for two different weights of sample which were processed in an identical manner using identical quantities of reagents. In newer work straight blanks using ferric hydroxide as a carrier have been used since this has been found to be a superior method of measuring the small contaminations of 0.01–0.001 micrograms of uranium usually encountered in an analysis.

A detailed discussion of the uranium analytical work has appeared in a declassified Atomic Energy Commission document (Tilton, 1951).

The complete analysis of the acid-washed composite rock sample is as follows: Approximately 17 g of rock powder ground to pass 40 mesh was washed three times with ether, washed for three 5-minute periods in 6 M hydrochloric acid and finally rinsed three times with distilled water. The powder was dried at 115°C for 3 hours. The sample was weighed to the nearest mg into platinum and treated with 120 g of hydrofluoric acid at about 70°C for 3 hours until a moist paste remained. Eighty ml of perchloric acid and 40 ml of water were added and the solution was heated until it fumed on a hot plate at medium temperature and fumed for 15 minutes. Borax (7.5 g in 20 ml of water) and 100 ml of perchloric acid were then added. The solution was concentrated to acid fumes and fumed strongly for about 90 minutes at which point crystals began to separate from the thick syrup. Two hundred ml of

water was added and the mixture was steamed for 10 minutes. Five to ten mg of black and brown granules representing unattacked zircon and possibly other accessory minerals remained at this point. The solution was decanted into a 250 ml volumetric flask; the granules were washed into a beaker with water and the water evaporated off. The undissolved granules were fused 15 minutes in 3 g of borax at the maximum heat obtained from a Meeker burner (ca. 1200°C). The bead was digested 1 hour in 25 ml of 6 M hydrochloric acid. This solution was combined with that in the volumetric flask and the contents were diluted to the mark with water. Aliquots of 50.0 and 25.0 ml of this solution were pipetted into two 250 ml centrifuge bottles where they were equilibrated with 29.60 micrograms of uranium with a U^{235}/U^{238} ratio of 1752 by weight. Each sample was diluted to 1 liter and the hydroxides were precipitated by bubbling ammonia gas into the solution. The precipitate was dissolved in nitric acid and a second hydroxide precipitation was performed. This step was necessary to prevent the separation of perchlorates when the solution was later concentrated for extraction.

The second hydroxide precipitate was dissolved in 50 ml of concentrated nitric acid and each sample was concentrated to a volume of about 30 ml. Ammonia gas was passed into the solution until the ferric ion present turned from light yellow to deep orange in color (pH 2 to 3).

The salted nitrate solutions were each extracted three times with 35 ml of hexone (4-methyl-2-pentanone). The hexone was then extracted twice with 25 ml of water. The aqueous extract was concentrated to 10 ml and 0.5 mg of Fe^{+++} as ferric nitrate was added. The iron was precipitated by dropwise addition of a saturated solution of ammonium carbonate, adding one to two drops in excess. The ferric hydroxide with occluded impurities was centrifuged off and discarded.

Each supernate from the carbonate treatment was acidified and concentrated to a volume of a few drops. Fifteen ml of 10 M ammonium nitrate solution was added and the resulting solution was extracted twice with 15 ml of hexone. The hexone was washed with 2–10 ml portions of water. This aqueous extract was concentrated, taking to final dryness in a 5 ml beaker. The residue was heated a few minutes with the hot plate at high temperature to destroy the ammonium nitrate present. A thin black film of uranium oxide then remained.

Isolation of Thorium

The thorium chemistry has been described elsewhere (Tilton *et al.*, 1954). Briefly, the work was carried out as follows: Approximately 1 mg of thorium with a Th^{230}/Th^{232} ratio of four was isolated from a Colorado Plateau uranium ore. This material served as a carrier to determine the thorium content of the minerals (which consisted solely of the isotope Th^{232}), as the U^{235} served for the uranium determinations. Chemical concentrations of thorium were accomplished by various combinations of three procedures: precipitation of thorium on lanthanum oxalate as carrier; extraction at a pH of two into a benzene solution of trifluorothenoylacetone (TTA) (Hagemann, 1950, p. 769); and extraction into hexone from a nearly saturated solution of aluminum nitrate containing 10 per cent nitric acid (Levine and Grimaldi, 1951).

The mass spectrometric determinations were checked colorimetrically using the sodium salt of 2-(2-hydroxy-3, 6-disulfo-1-napthylazo) benzene-arsonic acid (Thorn) using the procedures described by Thomason, Perry and Byerly (1949, p. 1240) and the 24.1 day beta activity of Th^{234}-Pa^{234} as a tracer to correct yield losses in processing. The two methods checked within the limits of error.

Mass Spectrometry of Uranium and Lead

General

The isotopic analysis of lead and uranium from separated minerals of granites has not been previously attempted, largely owing to the fact that the minimum sample size which can be readily handled using the classical techniques is of the order of several mg. Thus, in order to obtain sufficient lead from a mineral containing one part-per-million of the element, several kg of sample would have to be processed. In view of the difficulties of preparing satisfactory mineral separates and of undertaking the

special chemical porcedures here outlined, the amount of work involved in processing such large quantities would be prohibitive. The alternative was chosen of developing techniques of micro mass spectrometry such that only gram quantities of mineral separates are required.

The sample size necessary for an isotopic analysis by use of the lead iodide evaporation method (Nier, 1939b, p. 155) is prescribed by several factors. Many mass spectrometers can satisfactorily resolve the isotopes of lead in the Pb^+ ion position, but few operate satisfactorily in the PbI^+ position. But in the former position the spectrum is complicated by the presence of the mercury isotope of mass 204, if mercury pumps are used, and the sample size must be such as to swamp this peak. Mass spectrometers in which oil pumps are used do not suffer from this limitation since the background peak at this mass is much smaller, but the advantage is partially cancelled by the fact that the hydrocarbon background is variable with time, thus making corrections difficult to apply. In principle, however, the lead iodide evaporation method could be utilized for smaller samples than are now required if a machine of sufficient resolving power were used to permit operation in the PbI^+ region where the backgrounds are much smaller.

The limitation in sample size with the $Pb(CH_3)_4$ method (Collins *et al.*, 1951, p. 966) is largely one of preparing the volatile compound in sufficient quantity and purity for satisfactory analysis. The recent work using this method indicates that several mg are necessary. This is little improvement over the sensitivity obtained by Aston (1933, p. 535) in his early studies of radiogenic leads using $Pb(CH_3)_4$ as the source gas. The method does not appear to be extendable to micro-samples.

After several possible ion sources were considered, the surface ionization source was selected because it is very selective in its ionization. It will not ionize mercury, and hydrocarbons are ionized only very weakly. The resultant spectrum is quite clean, thus removing partially one of the major limitations of the lead iodide evaporation source.

Although the surface ionization source gives a cleaner spectrum than the older sources, ion currents are small, thus necessitating the use of an ion detector of high sensitivity. For this reason the usual ion detector was replaced with an internally placed electron multiplier similar to that used by Cohen (Cohen, 1943; Allen, 1939).

The standard 60° sector deflection instrument, in which transmissions of several per cent are obtainable, was selected, but the size was increased to improve both resolution and transmission. The mass spectrometer finally evolved is a 12-inch radius of curvature single focussing instrument using the surface ionization source of Inghram and Chupka (1953, p. 519). For large samples of 10^{-6} g, only the central filament is used. For smaller uranium samples, it is operated with the sample loaded on a side filament. The advantages of the multiple filament assembly have not to date been realizable with lead.

The machine is equipped with differential pumping to shorten the pump-down time between samples. The time required is about 1 hour instead of 6–8 hours as is required with a single pump. Both permanent magnets and electromagnets have been used to produce the 7000 gauss field. Either is satisfactory. With the machine finally evolved it is possible to detect isotopes of lead if present to 10^{-10} g, and of uranium to 10^{-13} g.

Lead Procedure

Three compounds were used in the surface ionization source: the oxide, the sulfide, and the sulfate. Either of the first two compounds give reliable results, although all samples in the present work used the oxide. In particular:

(1) The sample of $Pb(ClO_4)_2$ is placed in a 5 ml beaker, evaporated to dryness, and heated for one-half hour at 350°C to remove all traces of acid.

(2) A sample of borax weighing one-half as much as the lead sample is dissolved in 25 microliters of water and added to the above.

(3) Concentrated HNO_3, sufficient to neutralize the borax, is added and the 25 microliters is swished about the beaker to dissolve the lead.

(4) The sample is taken up in a pipette and transferred to the 0.030 inch x 0.001 inch tung-

sten filament of the surface ionization source, evaporated to dryness, inserted in the mass spectrometer, and pumped down.

(5) The temperature of the filament is raised slowly to about 600°C where emission of Pb^+ ions starts. At first the spectrum is complicated by the peaks of WO^+ resulting from tertiary processes, (Hess *et al.*, 1951, p. 838), but this clears up with time if the acid concentration has been kept sufficiently low. Data must either be taken on a ratio recorder or plotted on a linear time scale so that the slow drift in ion intensity can be calculated from the data.

(6) After the data is calculated, corrections must be applied for the nonlinearity of the source and electron multiplier ion detector. These corrections must be determined by running a standard isotope mixture.

The sulfide procedure is less reliable from the transfer standpoint since the sulfide must be transferred as a slurry from the bottom of a centrifuge tube. The sulfate can be formed by adding weak sulfuric acid to the filament after the nitrate is loaded, but care must be taken to avoid excessive attack of the filament.

Uranium Procedure

The uranium procedure is similar to that given for lead except that no borax is used and the filament material consists of outgassed tantalum instead of tungsten. The most intense peaks are UO_2^+, when the single filament source is used, and U^+, when the multiple assembly is used. Uranium ions are emitted at much higher temperatures than are lead ions, and the currents are much more stable.

Accuracy

With great care, the accuracy of isotopic analysis of uranium and lead by use of a mass spectrometer equipped with a surface ionization source is about 0.5 per cent of the abundance of an isotope. This gives less accuracy than does a gas source, since rapid intercomparison with identical ion geometries is not possible. This disadvantage, however, is counteracted by several factors: (1) There is no "memory" whereby measurement of one sample is affected by previous samples, a serious problem in the case of gas sources, usually limiting a machine to a narrow range of isotopic compositions; (2) The sample sizes required are a million or more times less than with gas sources.

One of the most important factors limiting accuracy is the background correction. The presence of thallium, bismuth, and WO^+ ions complicates the correction of the lead data. In general the background was determined in the region above Bi^{209} and interpolated under the lead peaks. In most cases the corrections were less than 2 or 3 per cent of the Pb^{204} peak and were accurate to about 10 per cent.

The ion intensity from a surface ionization source drifts with time. To correct this the spectra are recorded on a linear time base so that intensities can be interpolated. A ratio-recording system (Stevens and Inghram, 1953, p. 987) has also been used on samples other than those reported here.

The problem of isotopic fractionation during the evaporation process is less serious, for with refractory salts evaporation takes place from a solid rather than from a liquid surface. Thus, little mixing takes place and the fractionation is very small compared with the theoretical maxima.

Results

The uranium, thorium, and lead data are listed in Table 3. Assigned errors in the values for the composition of the lead and the amounts of uranium and thorium in the composite granite samples are due to possible losses in dissolving sphene and zircon, which comprise less than half of one per cent of the sample. Measured isotope ratios have been assigned absolute errors of one per cent which are the result of uncertainties in absolute corrections. An uncertainty of ±50 per cent was assigned to the amount of lead contamination introduced in processing a sample. When the ratio of sample lead to contamination lead was small, probable errors in the measured lead concentrations were due mainly to uncertainties in the amounts of lead contamination.

Independent analyses of the lead in three samples were made by C. L. Waring, of the U. S. Geological Survey, using emission spectrography. Independent analyses of the thorium in three samples were made by use of

TABLE 3.—URANIUM, THORIUM AND LEAD CONCENTRATIONS AND ISOTOPIC COMPOSITION OF LEAD IN VARIOUS CONSTITUENTS OF THE GRANITE

Sample[c]	Mineral abundance (weight per cent)	Total U in PPM[a]	Total Th in PPM[a]	Total Pb in PPM	Pb^{206} in PPM[a]	Isotopic composition of lead[b] (atom ratios)			Isotopic composition of lead (atomic per cent)			
						$\frac{Pb^{206}}{Pb^{204}}$	$\frac{Pb^{207}}{Pb^{204}}$	$\frac{Pb^{208}}{Pb^{204}}$	Pb^{204}	Pb^{206}	Pb^{207}	Pb^{208}
Zircon	0.04 ± 0.01	2650 ± 40	2180 ± 20	461	392 ± 10	.....	.....	.....	<0.01	85.35 ± 1.5	6.39 ± 0.1	8.26 ± 0.15
Sphene I[d]	0.4 ± 0.1	303 ± 5	.....	240	68.4 ± 3	39.13	17.11	79.38	0.732	28.65	12.52	58.10
Sphene II[e]	0.4 ± 0.1	.....	2205[g]	113	39.9 ± 1	108.6	22.18	146.2	0.360	39.07	7.98	52.59
Acid washings sphene II[f]	.....	[n]	3170[h]	222	44.5 ± 1	21.78	15.73	69.30	0.928	20.20	14.59	64.28
Magnetite	0.4 ± 0.2	2.57 ± 0.04	.....	1.4[i]	0.325 ± 0.1	36.7 ± 3	16.8 ± 1	97.4 ± 8	0.658	24.2	11.1	64.1
Apatite	0.02 ± 0.01	90.5 ± 1.3	.....	136[k]	34.5 ± 4	31.9 ± 5	16.3 ± 3	76.3 ± 10	0.797	25.4	13.0	60.8
Pyrite	0.02	.....	.....	370[l]	.....	20.34	15.92	54.34	1.09	22.21	17.38	59.32
Quartz	24 ± 1	0.13 ± 0.01	.....	5.5[m]	1.36 ± 0.05	.....	.....	.....	.....	.....	.....	.....
Plagioclase	20 ± 1	0.20 ± 0.02	.....	3.8	0.94 ± 0.1	18.16	15.48	40.02	1.34	24.32	20.74	53.60
Perthite	52 ± 2	0.22 ± 0.03	0.410 ± 0.008	9.5	2.35 ± 0.1	18.58	15.74	39.52	1.34	24.82	21.03	52.81
Unwashed composite	.....	2.74 ± 0.05	41.88 ± 0.60	9.3	2.18 ± 0.05	20.25	15.65	48.73	1.17	23.65	18.27	56.91
Washed composite	.....	1.80 ± 0.20	24.33[j]	5.6	1.35 ± 0.1	21.20	15.56	49.35	1.15	24.33	17.89	56.63
Pegmatitic perthite crystal	.....	.....	.....	8.4	2.05 ± 0.05	16.81	15.28	36.02	1.45	24.32	22.11	52.12

(a) The errors assigned to the concentrations result from errors in the mass spectrometric and chemical procedures, uncertainties in the amounts of contamination, and nonreproducibility of leaching procedures.

(b) Except where indicated, the absolute errors of the lead ratios are about one per cent of the values.

(c) All the samples, except the unwashed composite, have been stirred with 6 M HCl, centrifuged, and rinsed with water.

(d) A coarse, heterogenous sample; uranium and lead determinations were made on aliquots of single dissolved sample.

(e) A finely ground, homogenous sample; thorium and lead determinations were made on separate solid samples.

(f) Concentrations are given in terms of micrograms leached per gram of sphene.

(g) Obtained by difference of thorium in acid leachings and thorium in untreated sample (5375 ± 75 ppm).

(h) Colorimetric determination; yields determined with radioactive tracer.

(i) Obtained by difference of thorium in acid leachings (17.55 ± 0.25 ppm) and thorium in untreated sample.

(j) Errors are the result of low sample lead to contamination lead ratios.

(k) Errors result from uncertainties in estimated corrections for unshielded electron multiplier and indirect measurements of composition. All of the sample was sacrificed during these initial and less accurate runs. At the time, it was thought that lead tracer was needed as a carrier as well, and two samples containing different proportions of tracer were used.

(l) Colorimetric determination; yields determined with radioactive tracer.

(m) The lead composition was assumed to be identical to that in the perthite. All of a large sample of highly purified material was sacrificed for a single concentration run before it was discovered that the lead concentrations were so high. In an initial run, in which a highly discriminating electron multiplier was used on a sample suspected of being contaminated, the quartz lead composition was different from the compositions of perthite and plagioclase lead samples run under the same conditions.

(n) Fluorometric uranium determinations of unleached and acid-leached sphene (finely ground) showed approximately 20 per cent of the uranium to be removed by the acid treatment. Analysts: F. Cuttitta, F. Scott and M. Delevaux, U. S. Geological Survey, Washington, D. C.

colorimetric procedures. The spectrographic, spectrophotometric, and isotope dilution values are compared in Table 4.

A determination of the U^{238}/U^{235} ratio in uranium isolated from sphene was made for the purpose of ascertaining whether uranium in granite possesses the same isotopic composition as uranium in ore deposits. In sphene, the following ratio was found:

$$U^{238}/U^{235} = 138.4 \pm 0.6$$

a value which agrees within experimental error with the best values for ore uranium (Nier, 1939a, p. 151; Inghram, 1946, p. 35).

Discussion

Uranium-Lead Age of the Granite

The ages of pegmatitic uraninites from Wilberforce, Haliburton Co. have been determined by Nier (1939b, p. 159) and by Collins, Lang, Robinson, and Farquhar (1952, p. 21). These are listed in Table 5 together with the ages for zircon and sphene which were calculated by assuming the isotopic composition of the lead in sphene at the time it was formed was that found in the macro pegmatitic perthite crystal. The following constants were used:

$T_{\frac{1}{2}}U^{235} = 7.13 \times 10^8$ yrs. (Fleming *et al.* 1952, p. 642).

$T_{\frac{1}{2}}Th^{232} = 13.9 \times 10^9$ yrs. (Kovarik and Adams, 1938, p. 413).

$T_{\frac{1}{2}}U^{238} = 4.51 \times 10^9$ yrs. (Fleming *et al.*, 1952, p. 642).

$U^{238}/U^{235} = 137.8$ (Inghram, 1946, p. 35).

The errors associated with the lead data for apatite and magnetite are so large that ages calculated from these values are not considered significant.

The close agreement of the U^{238}/Pb^{206} age for zircon with the U^{235}/Pb^{207} and Pb^{207}/Pb^{206} ages is quite significant in view of the highly metamict character of the zircon. These differences are within the effect of combined experimental errors, which include an uncertainty of 2 per cent in the half-life of U^{235}. The obvious discrepancy of the Th^{232}/Pb^{208} age for zircon requires that there has been either addition of thorium without any significant addition of uranium or loss of Pb^{208} without any loss of Pb^{206} or Pb^{207}.

The studies that have been made on the sphene may, perhaps, be related to those of the zircon. The loss of Pb^{208} from the dilute-acid-washed sphene is extreme. The analysis of the acid washings, given in Table 4, conclusively demonstrates that small amounts of uranium lead and major amounts of thorium and thorium lead are very loosely bound, chemically, and that there is a net deficiency of Pb^{208} in the mineral. These mineral grains are doubtlessly heterogeneous, and the mass of the phase containing loosely bound thorium and lead is small compared to the mass of the entire grain.

TABLE 4.—COMPARISON OF LEAD AND THORIUM VALUES OBTAINED BY DIFFERENT METHODS

Sample	Total lead (ppm)		Total thorium (ppm)	
	Isotope dilution	Emission spectrography	Isotope dilution	Colorimetric analysis
Zircon	461	449	2170	2180
Sphene I	240	245	...	...
Sphene II	...	...	5375	5550
Composite granite	...	...	41.9	44.0
Perthite	9.5	5	...	...

The low thorium-lead age for the zircon could have been the result of addition of thorium to the mineral, which would not affect the uranium-lead age seriously, since the Th/U ratio of the interstitial material of the rock is about 24. The sphene data indicate, however, that the cause may be the loss of Pb^{208} instead. Selective loss of Pb^{208} is possible if there has been a segregation of thorium and uranium in some regions of the mineral grains. Probably part of the thorium is concentrated in the skin or surface inclusions of the mineral where Pb^{208} has been lost. Preliminary studies have shown that the powdered mineral loses 35 per cent of its radioactivity and 30 per cent of its lead when it is leached for 30 minutes in hot 1:1 aqua regia[3]. It may be noted in this connection that Buttlar and Houtermans (1951, p. 43) have demonstrated a fractionation of

[3] Recent studies at the California Institute of Technology have demonstrated that substantial fractions of the radioactive elements can be leached from granites with acid strengths as low as 0.1 M.

thorium and uranium within a zircon crystal 5 cm in diameter from Renfrew County, Ontario, in which the Th/U ratio ranged from zero to two in different regions.

TABLE 5.—AGES FOR THE GRANITE AND THE WILBERFORCE PEGMATITE

(In millions of years)

Sample	$\frac{Pb^{207}}{Pb^{206}}$	$\frac{U^{235}}{Pb^{207}}$	$\frac{U^{238}}{Pb^{206}}$	$\frac{Th^{232}}{Pb^{208}}$
Uraninite (a)	1015	1055	1060	1000
Uraninite (b)	1025	....	....	....
	1032	....	....	....
	1090	....	....	....
Zircon	1090	1060	1030	390
Sphene I	(c)	(c)	910	....
Sphene II	1090	....	....	450

(a) Cardiff Township, Haliburton County, Ontario (Wilberforce); Nier (1939)

(b) Same location as (a); Collins, Lang, Robinson, and Farquhar (1952)

(c) The fraction of radiogenic Pb^{207} was too small to warrant age calculations involving that isotope.

Previous thorium-lead age determinations have been lower for the most part than uranium-lead age determinations where the two methods have been applied to the same mineral. In Nier's earlier work (1939b) and (1941), the two methods agree for only three samples the thorium-lead ages are lower for seven and samples. However, Holmes, Leland, and Nier (1950, p. 87) have summarized four additional analyses in which the thorium-lead ages are higher in three cases. It is perhaps significant that all monazite minerals studied by Nier *et al.* (1941) have given, as has the present work, radically lower thorium-lead ages where comparison with uranium-lead ages is possible.

Because the substantial differences which occur among some of the age values are well outside experimental error, the existence of loosely bound Pb^{208} demonstrated, and the Pb^{207}/Pb^{206} ages for all of the minerals agree well, we have concluded that: either (1) uranium, thorium, and their decay products have existed only with varying degrees of approximation to closed systems within each mineral since its formation; or (2) these elements have a heterogeneous distribution in several phases of widely different chemical and physical properties which are associated with each mineral, and as a result, different amounts of these elements have been lost during the isolation of each mineral in the laboratory. The U^{235}/Pb^{207} age of the zircon, 1060 m.y., is the most probable age of the granite and this agrees with the ages determined for associated pegmatites. Formation of the red granite which marks the end of major igneous activity involving the Grenville sediments (*see* Engel and Engel, 1953) occurred 1060 m.y. ago and the associated pegmatites were formed at about the same time.

Potassium-Argon Age of the Granite

Measurement of the amount of K^{40} and the amount of radiogenic A^{40} in a rock together with the known values of the half life and branching ratio of K^{40} allows the potassium-argon age of the rock to be calculated. Assuming there has been no subsequent leakage or leaching of argon or of potassium from the rock, this age gives the length of time since the crystallization of the potassium-containing phases of the rock. If potassium crystallizes in comparable amounts and at different times in several phases of the rock, the potassium-argon age of the gross rock is a weighted average of the ages of the components.

To measure the amount of radiogenic A^{40} in the Haliburton Co. granite, the gases in the granite were first released by adding, in a vacuum, 9.24 g of granite into 30 g molten NaOH which was contained in a nickel tube. The resultant gases were mixed with 6.10×10^{-5} cc at stp tracer argon which was 96.5 per cent A^{38} and 3.5 per cent A^{40}. The resultant mixture was then purified by passing successively in a greaseless system through traps of anhydrous $Mg(ClO_4)_2$, heated CuO, vacuum moistened NaOH, anhydrous $Mg(ClO_4)_2$, and finally through a calcium vapor furnace. The remaining gases were collected on 1.2 g of activated coconut charcoal at liquid nitrogen temperature.

The argon so collected and so purified was introduced from a greaseless sample system into a 60° deflection, 6-inch radius of curvature gas analysis mass spectrometer, and its isotopic composition was measured. Results of

the analysis were, after correction for spectrometer discriminations but not for possible impurities, that the relative amounts of the various argon isotopes collected were:

$$\frac{A^{36}}{A^{38}} = 0.0153; \qquad \frac{A^{38}}{A^{40}} = 0.0436$$

Two gravimetric analyses of different samples of the granite by Kenneth Jensen of the Argonne National Laboratory gave values of 4.82 per cent and 4.86 per cent for the amount by weight of K_2O extracted from the granite. The average value of 4.84 per cent was used.

In addition it was assumed that the relative abundance of K^{40} in potassium is 0.0119 per cent (Nier, 1950, p. 793), that the half life of K^{40} is 1.27×10^9 yr (W. F. Libby, personal communication, 1952), that the branching ratio $\frac{\text{(number of K-captures)}}{\text{(number of beta decays)}}$ for K^{40} is 0.085 (Wasserburg and Hayden, 1955, p. 51), and that the normal abundances of the argon isotopes are $A^{36} = 0.337\%$, $A^{38} = 0.063\%$, $A^{40} = 99.600\%$ (Nier, 1950, p. 792). These normal abundances were checked to 1 per cent on the mass spectrometer with which the analyses were made. These data indicated that the age of the sample is 800 m.y. Approximately 80 per cent of the A^{40} measured by the mass spectrometer was radiogenic.

Possible sources of error are numerous. First, A^{40} and/or K^{40} may have leaked or been leached out of the rock over periods of several hundreds of millions of years. Argon leakage would make the observed age too low; loss of potassium would make the observed age too high. Secondly, although almost no rock residue was found in the NaOH after the gas extraction, still all the rock argon might not have been able to mix with the tracer argon owing to occlusion in the nickel, in the molten NaOH, or on the glass of the vacuum system. This would lower the apparent age. Thirdly, the small 36 peak observed in the mass spectrometer might in part be due to ions other than A^{36+}. For example, HCl^{35+} frequently gives peaks at this mass. This particular contamination seems unlikely in this instance since no Cl^+ peaks were observed. The 36 peak was observed to decay with time proportionately to the 38 and 40 peaks, but this is not a positive proof that it was composed solely of A^{36}. If part of the 36 peak is due to some other ion the calculated value is once more too low. In addition to these possible errors, all tending to lower the observed age, small errors in either direction could be introduced in the measuring (using mass spectrometric isotope dilution techniques) of the tracer argon sample, in the chemical analysis, and in the mass spectrometric analyses.

If the age of this sample as determined by the lead-uranium method is assumed correct, and if no argon or potassium has been lost, this data may be used to compute an apparent K^{40} branching ratio of 0.0587. This is well below the most reliable measured values and indicates that leakage of argon is probably the source of the discrepancy between this age and the lead-uranium ages.

Loss or Gain of Uranium, Thorium, and Lead in the Granite

If there has been no transfer or exchange of uranium, thorium, and their decay products between the granite and its surroundings, the isotopic composition of lead in the granite at the time it was formed can be calculated from the total concentrations of uranium, thorium, and lead and the isotopic composition of lead now present in the rock. The initial composition of the lead, after correcting for decay over a period of 1050 m.y., is calculated to be:

$$Pb^{206}/Pb^{204} = 16.4$$
$$Pb^{207}/Pb^{204} = 15.4$$
$$Pb^{208}/Pb^{204} = 30.2$$

Of all the constituents of the rock that were completely studied, only the perthite and the plagioclase have ratios of uranium and thorium to lead such that no appreciable addition of radiogenic lead would occur in a billion years. The average isotopic composition of the lead in these minerals is:

$$Pb^{206}/Pb^{204} = 18.3$$
$$Pb^{207}/Pb^{204} = 15.6$$
$$Pb^{208}/Pb^{204} = 39.8$$

which values are considerably more radiogenic than the initial ones calculated. This marked discrepancy cannot be resolved by analytical errors and can only result from either the loss of uranium and thorium and the gain of lead by the granite, or the internal transfer of ura-

nium, thorium, and their decay products among the mineral constituents of the granite. To discover the cause, some lead isolated from an associated pegmatite mineral was studied. If both the granite and the associated pegmatites in this area originated from a common source and were formed at nearly the same time, the initial isotopic composition of lead in both should have been the same. Furthermore, the amount of internal transfer of trace constituents among very large pegmatitic minerals should be much less than among the relatively fine-grained granitic minerals. Lead, isolated from a single large perthite crystal which was taken from an associated pegmatite,[4] was found to have an isotopic composition of:

$$Pn^{206}/Pb^{204} = 16.81$$
$$Pb^{207}/Pb^{204} = 15.28$$
$$Pb^{208}/Pb^{204} = 36.02.$$

Determinations of the amounts of uranium and thorium in this mineral are in progress; however by analogy with previous data they are presumed to be insignificant. As an indication that the isotopic composition of this pegmatitic lead is not anomalous, a comparison may be made with the isotopic compositions of some lead ores formed at the same time in this general region. The mean composition of the Tetreault, Ontario lead ore (Nier *et al.*, 1941, p. 115) and the Frontenac County, Quebec, lead ore (Collins *et al.*, 1953, p. 410), both formed 1000 m.y. ago, is:

$$Pb^{206}/Pb^{204} = 16.53$$
$$Pb^{207}/Pb^{204} = 15.28$$
$$Pb^{208}/Pb^{204} = 35.55$$

The relationship among the leads in the pegmatitic perthite, in the ores, and in the granite may be quite complicated; indeed the differences between the isotopic compositions of these leads may be highly significant. However, there is a general agreement between the observed isotopic compositions of uranium leads formed in this region 1000 m.y. ago and those calculated for the lead originally present in the granite when it was formed, and a corresponding disagreement for the thorium leads. It would appear that the sample of granite studied has closely approximated a closed system since it was formed with respect to uranium and its decay products, but has been an open system with respect to thorium and its decay products.

Distribution of Uranium, Thorium and Lead in the Granite

Marked differences exist in the distribution of uranium, thorium, and lead in the granite. Most of the stably bound uranium and thorium was concentrated in the accessory minerals zircon, sphene, and apatite. This result is consistent with the observations of previous workers, notably Larsen, Keevil, and Harrison (1952) who measured the distribution of radioactivity in mineral separates from a number of granitic rocks. In contrast, most of the stably bound nonradiogenic lead, indicated by the concentration of Pb^{204}, was found to reside in the feldspars and quartz, resisting strongly any tendency to concentrate in zircon or magnetite. Thus, there are enormous variations in the ratios of uranium and thorium to nonradiogenic lead in the various minerals of the granite. The ratios range from values so low that the isotopic composition of the lead would not have been altered appreciably by radioactive decay in a billion years, to values so high that the lead found is almost entirely of radiogenic origin.

A substantial fraction of the uranium and even greater fractions of thorium and nonradiogenic lead were found to exist in chemically unstable environments in the rock. Uranium, thorium, and lead thus present are so loosely bound that they can be removed from the pulverized rock by a 5 minute stirring with 6 M hydrochloric acid in the cold. The fractions of the uranium, thorium, and lead in the composite rock observed to be extracted by this weak acid treatment were approximately 34 per

[4] The perthite specimen was collected in June of 1952 by H. S. Armstrong while in charge of a field party for the Ontario Department of Mines. The crystal was about 2 inches in diameter and 6 inches long and was taken from a pegmatite cutting a crystalline limestone-biotite paragneiss complex north of Tory Hill, Monmouth Twp., Ontario.

This locality is a new (summer, 1952) road clearing and can be located on Satterly's map, No. 52a, Haliburton Area, published by the Ontario Department of Mines. It is immediately adjacent to the road shown on this map. The specimen was taken a few hundred feet north of the jog in the road between the double "l" in "Hill" of Tory Hill and the "R" of the "Ra" occurrence, the red dot of which is superimposed on two black squares representing houses.

cent, 42 per cent, and 40 per cent, respectively. The different uranium and thorium concentrations found in the untreated and in the acid-washed granite agree with the observations of Hurley (1950, p. 3), and Picciotto (1950, p. 175). Picciotto, using refined radio-autographic techniques, has found that a large fraction of the radioactive elements present in some granitic rocks reside in the mineral interstices and intra-crystalline fractures, most of the remaining fraction residing in accessory minerals, and on this basis it may be assumed that the loosely bound uranium, thorium, and lead originate from the inter-crystalline interstices. The presence in the interstices of such large fractions of trace elements with contrasting lattice distributions suggests that interstitial material, like pegmatitic veins, may contain high concentrations of other trace elements.

Table 6.—Contribution by Each Mineral to the Uranium, Thorium and Lead Content of the Total Granite

(Parts per million of total rock)

Acid washed minerals	Pb^{204}	Pb^{206}	Pb^{208}	U^{238}	Th^{232}
Zircon	0.0000	0.157	0.02	1.06	0.87
Sphene	0.0069	0.273	0.24	1.21	8.8
Apatite	0.0002	0.007	0.16	0.02	...
Magnetite	0.0000	0.001	0.00	0.01	...
Perthite	0.0652	1.222	2.61	0.11	0.21
Plagioclase	0.0103	0.189	0.41	0.04	...
Quartz	0.0178	0.326	0.70	0.03	...
Total.....	0.1004	2.18	4.14	2.48	(9.9)
Acid-washed rock	0.0629	1.35	3.16	1.80	24.33

Material Balance

Table 6 shows the contribution made by each mineral to the uranium, thorium, and lead content of the total granite, as determined by multiplying the concentrations of uranium, thorium, and lead in each mineral by the weight-fraction of the mineral in the original rock. In all cases the sums of the contributions of lead, uranium, and thorium in the individual acid-washed minerals are different from the lead, thorium, and uranium concentrations in the acid-washed rock. This lack of material balance may have resulted from one or more effects. Errors in estimating mineral abundances could cause the discrepancy for uranium or thorium, but it is not possible to reduce the calculated concentrations for lead sufficiently by changing the mineral abundances by any reasonable amount. The discrepancies may be related to the fact that the mineral separates consisted of particles that were considerably larger on the average than the same unseparated minerals in the composite. There may be a variation either in trace element concentration or in leaching effects with particle size. The small composite samples may not have been representative of the very large sample which was the source of the separated minerals.

Table 7.—Comparisons between the Observed and Calculated Amounts of Radiogenic Leads in Various Constituents of the Granite

Sample	Ratio of radiogenic Pb^{206} found to radiogenic Pb^{206} calculated from uranium present	Ratio of radiogenic Pb^{208} found to radiogenic Pb^{208} calculated from thorium present
Leachings from sphene (II)	.....	0.45
Sphene (II)	.....	0.43
Sphene (I)	0.84	.....
Zircon	0.97	0.36
Leachings from composite rock	0.60	0.62
Plagioclase	2.3	.....
Perthite	6.4	17.1
Pyrite	.....	(Probably $\gg 1$)[a]

[a] The amount of radiogenic Pb^{208} present in the acid washed mineral would require about 0.2 per cent thorium, which is improbably high.

Internal Transfer of Uranium, Thorium, and Lead

One may calculate the amount of lead generated in 1050 m.y. by the decay of the uranium and thorium in each mineral and compare these values with the observed radiogenic lead in each mineral which is found by subtracting

the nonradiogenic lead originally present. The composition of this nonradiogenic lead was assumed equal to that in the pegmatitic perthite. The comparisons listed in Table 7 are made by dividing the amount of radiogenic lead found in each mineral by the corresponding amount of radiogenic lead that should have been generated by the uranium or thorium present in each mineral.

All these ratios deviate from unity, and it is clear that in no single constituent of the rock that has been isolated in the laboratory and examined, has radioactive decay operated within a completely closed system. Both deficiencies and excesses of radiogenic lead are demonstrated for systems of uranium, thorium, and lead existing in stably bound, or supposedly intra-crystalline environments. Similarly, deficiencies of radiogenic lead are demonstrated for systems of uranium, thorium, and lead existing in chemically unstable, loosely bound, or supposedly interstitial environments that have very small masses relative to the masses of the minerals or the rock as a whole. A satisfactory explanation of these effects is not known at present; however, it seems apparent that either complete chemical systems were not isolated in the laboratory from various parts of the granite or transfer of uranium, thorium, and lead has occurred on a micro scale within the granite. It is probable that extensive transfer on a macro scale has also occurred for thorium or its decay products.

Relation to Lead Ores

In connection with discussions of the world-wide variations of the isotopic composition of lead ores with time, a number of writers, notably Holmes (1947), Houtermans (1947), Bullard and Stanley (1949), and Collins, Russell, and Farquhar (1953), have assumed that lead ores are products of representative isolation of lead at different times from rocks where, in any given area, the relative ratios of uranium and thorium to lead have not changed except by decay processes since the earth's crust was formed. If the relative ratios of uranium and thorium to lead and the isotopic composition of the lead now present in the granite are used to determine the variation of the isotopic composition of the lead, both in the rock to the time it was formed and at earlier times in the material from which the rock was derived, it is found that lead ores formed from representative samples of this lead would have the compositions at various times given in Table 8.

TABLE 8.—CALCULATED ISOTOPIC COMPOSITIONS OF LEAD IN THE GRANITE AT VARIOUS TIMES

Time (m.y. ago)	Pb^{206}/Pb^{204}	Pb^{207}/Pb^{204}	Pb^{208}/Pb^{204}
0–50	20.3	15.7	48.7
1060	16.4	15.4	30.2
3500	4.7	11.1	(<0)

The average composition of lead ores formed within the last 50 m.y., formed 1050 m.y. ago, and formed 3500 m.y. ago (determined by least squares analyses of the variations of the isotopic compositions of lead ores with time; Collins *et al.*, 1953, p. 413), and the isotopic composition of meteoritic lead (Patterson *et al.*, 1953, p. 1234) are given in Table 9.

Since it is improbable that a sample of terrestrial lead can be less radiogenic than primordial lead, and since the Pb^{206}/Pb^{204} and Pb^{207}/Pb^{204} ratios, as well as the Pb^{208}/Pb^{204} ratio, are improbably low for lead isolated from the granite source material 3500 m.y. ago, it is apparent that much lower ratios of uranium and thorium to lead were present for a considerable period of time in the granite source material as a whole than now exists in the granite itself. In effect, a pronounced enrichment of uranium and thorium relative to lead occurred when the granite was formed. It is possible that ore leads may be representative of the isotopic composition of the lead in the material which was a source of both the ores and their associated rocks at the time they were formed, but it is obvious that the isotopic compositions of the ore leads and leads from this granite are not directly related after the time of formation of the granite. Such differentiation processes may invalidate the assumption that lead ores, which are formed at different times at different places in the earth's crust, may be directly correlated by a single genetic history.

The physical and chemical processes by which an ore lead is formed may be extremely impor-

tant in relation to its isotopic composition, in view of the marked variations of the isotopic composition of lead found to exist in the different components of this granite and the large variations in the chemical stabilities associated with these components. The large variations of the isotopic composition of the Sudbury ore leads, reported by Russell, *et al.* (1954, p. 307), may illustrate the result of the discriminatory action of such processes upon a system similar to the one studied here. Considerable caution should be exercised in assuming mechanisms of ore formation that ignore these possibilities.

TABLE 9.—AVERAGE COMPOSITION OF LEAD ORES AT VARIOUS TIMES*

Time (m.y. ago)	Pb^{206}/Pb^{204}	Pb^{207}/Pb^{204}	Pb^{208}/Pb^{204}
0-50	18.5	15.6	38.4
1060	16.7	15.5	36.3
3500	11.4	13.5	31.1
Meteoritic troilite	9.4	10.3	29.2

*Ore values calculated from the data of Collins, Russell, and Farquhar (1953)

CONCLUSIONS

The present work has demonstrated that a study of the amount of uranium, thorium, and the isotopes of lead in granites and their mineral constituents may help to trace rock histories and to explain related geochemical phenomena. Since the U/Pb and Th/Pb ratios may vary widely from one mineral to another, the various leads will develop different isotopic compositions with time. This "labels" the lead in one phase of the rock with respect to that in another, and thus provides internal lead tracers. This makes it feasible to apply criteria and study aspects of problems which are impossible with elements that are not involved in radioactive decay processes.

A co-ordinated study of uranium, thorium, and lead in a variety of igneous and sedimentary rocks by the same methods will permit conclusions concerning the past history of these elements in geochemical cycles and possible magmatic fractionations which have taken place in the earth's crust.

REFERENCES CITED

Adams, F. D., and Barlow, A. E., 1910, Geology of the Haliburton and Bancroft areas, Province of Ontario: Ottawa Govt. Print. Bur., Canada Dept. of Mines Mem. No. 6, 419 p.

Allen, J. S., 1939, The detection of single positive ions, electrons and photons by a secondary electron multiplier: Phys. Rev., v. 55, p. 966–971.

Aston, F. W., 1933, The isotopic constitution and atomic weight of lead: Proc. Roy. Soc. Lond., v. 140A, p. 535.

Bamback, K., and Burkey, R. E., 1942, Micro determination of lead by dithizone: Anal. Chem., v. 14, p. 904–907.

Blaedel, W. J., Post, Walling, and Sedlet, 1945, Atomic Energy Comm., Rept. CN 2766.

Bullard, E. C., and Stanley, J. P., 1949, The age of the earth: Veroffentl. d. Finn. Geodatischen Institutes No. 36, p. 33–40.

Buttlar, H. V., and Houtermans, F. G., 1951, Photographische Messung des U and Th gehaltes nach der Auflage methode: Geochim. et Cosmochim. Acta, v. 2, p. 43–62.

Clifford, P. A., and Wickmann, N. J., 1936, Dithizone methods for the determination of lead: J. Assoc. Official Agr. Chem., v. 19, p. 140–145.

Cohen, A. A., 1943, The isotopes of cerium and rhodium: Phys. Rev., v. 63, p. 219.

Collins, C. B., Freeman, J. R., and Wilson, J. T., 1951, A modification of the isotopic lead method for determination of geological ages: Phys. Rev., v. 82, p. 966–967.

Collins, C. B., Lang, A. H., Robinson, S. C., and Farquhar, R. M., 1952, Age determinations for some uranium deposits in the Canadian Shield: Proc. Geol. Assoc. Canada, v. 63, p. 15–41.

Collins, C. B., Russell, R. D., and Farquhar, R. M., 1953, The maximum age of the elements and the age of the earth's crust: Can. Jour. Physics, v. 31, p. 402–418.

Engel, A. E. J., and Engel, C. G., 1953, Grenville Series in the N. W. Adirondack Mountains, N. Y.: Geol. Soc. America Bull., v. 64, p. 1013.

Fleming, E. H., Jr., Ghiorso, A., and Cunningham, B. B., 1952, The specific activities and half-lives of U^{234}, U^{235}, U^{236}: Phys. Rev., v. 88, p. 642–652.

Hagemann, French, 1950, The isolation of actinium: J. Am. Chem. Soc., v. 72, p. 768–771.

Hayden, R. J., Reynolds, J. H., and Inghram, M. G., 1949, Reactions induced by slow neutron irradiation of europium: Phys. Rev., v. 75, p. 1500–1507.

Hess, D. C., Weatherill, G., and Inghram, M., 1951, Suppression of spurious ions in the mass spectrometer: Rev. Sci. Inst., v. 22, p. 838–839.

Holmes, Arthur, 1947, A revised estimate of the age of the earth: Nature, v. 159, p. 127–130.

Holmes, A., Leland, W. T., and Nier, A. O., 1950, The age of uraninite from Gordonia, S. Africa: Am. Jour. Sci., v. 248, p. 81–94.

Houtermanns, F. G., 1947, Das Alter des Urans: Zs. f. Naturforschung, v. 2a, p. 322–328.

Hurley, P. M., 1950, Distribution of radium in granites and possible relation to the age measurement: Geol. Soc. America Bull., v. 61, p. 1–7.

Hurley, P. M., and Fairbairn, H. W., 1953, Radiation damage in zircon: A possible age method: Geol. Soc. America Bull., v. 64, p. 659–674.

Inghram, M. G., 1946, Vol. 14, Manhatten Project Technical Series, Div. 2, Gaseous Diffusion Project, Chap. V., p. 35.

Inghram, M. G., Brown, H., Patterson, C., and Hess, D. C., 1950, The branching ratio of K^{40} radioactive decay: Phys. Rev., v. 80, p. 916.

Inghram, M. G., and Chupka, W. A., 1953, Surface ionization source using multiple filaments: Rev. Sci. Inst., v. 24, p. 518–520.

Kovarik, A. F., and Adams, H. L., Jr., 1938, The disintegration constant of thorium and the branching ratio of ThC: Phys. Rev., v. 54, p. 413–421.

Larsen, E. S., Keevil, N. B., and Harrison, H. C., 1952, Method for determining the age of igneous rocks using the accessory minerals: Geol. Soc. America Bull., v. 63, p. 1045–1053.

Levine, H., and Grimaldi, F. S., 1951, Application of mesityl oxide to the determination of thorium: Atomic Energy Comm. Rept. AECD 3186.

Lundell, G. E. F., and Knowles, H. B., 1920, The determination of zirconium and titanium in zirconium ores: J. Amer. Chem. Soc., v. 42, p. 1439–1448.

Nier, A. O., 1939a, The isotopic composition of uranium and the half-lives of the uranium isotopes. I: Phys. Rev., v. 55, p. 150–153.

— 1939b, The isotopic composition of radiogenic leads and the measurement of geological time. II: Phys. Rev., v. 55, p. 153–163.

— 1950, A redetermination of the relative abundances of the isotopes of carbon, nitrogen, oxygen, argon and potassium: Phys. Rev., v. 77, p. 789–793.

Nier, A. O., Thompson, R. W., and Murphy, B. F., 1941, The isotopic composition of lead and the measurement of geological time: Phys. Rev., v. 60, p. 112–116.

Patterson, C. C., 1951, The isotopic composition of trace quantities of lead and calcium: Atomic Energy Comm., Rept. AECD 3180.

Patterson, C. C., Brown, H. S., Tilton, G. R., and Inghram, M. G., 1953, Concentration of uranium and lead and the isotopic composition of lead in meteoritic material: Phys. Rev., v. 92, p. 1234–1236.

Picciotto, E. E., 1950, Distribution de la Radioactivité dans les Roches Éruptives: Bull. de la Soc. belge de Geol. de Paleontol. et. d'Hydrol., v. 59, p. 170–199.

Russell, R. D., Farquhar, R. M., Cumming, and Wilson, J. T., 1954, Dating galenas by means of their isotopic compositions: Trans. Am. Geophys. Union, v. 35, no. 2, p. 301–309.

Sandell, E. B., 1950, Colorimetric determination of traces of metals: N. Y., Interscience Publishers, Inc., 673 p.

Satterly, J., 1943, Mineral occurrences in the Haliburton area: Ontario Dept. of Mines, 52nd Ann. Rept., v. 52, pt. 2, IV.

Stevens, C. M., and Inghram, M., 1953, Ratio recording in isotopic analysis: Rev. Sci. Inst., v. 24, p. 987–989.

Thomason, P. F., Perry, M. A., and Byerly, W. M., 1949, Determination of microgram amounts of thorium: Anal. Chem., v. 21, p. 1239–41.

Tilton, G. R., 1951, The distribution of trace quantities of uranium in nature: Atomic Energy Comm. Rept. AECD 3182.

Tilton, G. R., Aldrich, L. T., and Inghram, M., 1954, Mass spectrometric determination of thorium: Anal. Chem., v. 26, p. 894–898.

Wasserburg, G. J. and Hayden, R. J., 1955, A^{40}-K^{40} Dating, Geochim. et Cosmochim. Acta, v. 7, no. 1, p. 51–60.

DEPARTMENT OF TERRESTRIAL MAGNETISM, CARNEGIE INSTITUTION OF WASHINGTON, WASHINGTON, D. C.; CALIFORNIA INSTITUTE OF TECHNOLOGY, PASADENA, CALIF.; CALIFORNIA INSTITUTE OF TECHNOLOGY, PASADENA, CALIF.; DEPARTMENT OF PHYSICS, UNIVERSITY OF CHICAGO, CHICAGO, ILL.; ARGONNE NATIONAL LABORATORIES, CHICAGO, ILL.; ARGONNE NATIONAL LABORATORIES, CHICAGO, ILL.; U.S. GEOLOGICAL SURVEY, WASHINGTON, D. C.

MANUSCRIPT RECEIVED BY THE SECRETARY OF THE SOCIETY, APRIL 24, 1954.

BULLETIN OF THE GEOLOGICAL SOCIETY OF AMERICA
VOL. 66, PP. 1149-1198, 30 FIGS. 1 PL. SEPTEMBER 1955

DEFORMATION OF THE NORTHEASTERN PACIFIC BASIN AND THE WEST COAST OF NORTH AMERICA

By Henry W. Menard

Abstract

Four great bands of unusually irregular topography named "fracture zones" have been discovered in the northeastern Pacific basin, and three have been traced into western North America. Individual zones range from at least 1400 to 3300 miles long and average 60 miles wide. The zones follow great circles for most of their lengths, and all are roughly parallel. Topography within the fracture zones is characterized by great seamounts, deep narrow troughs, asymmetrical ridges, and escarpments. Two escarpments are about 1 mile high and more than 1000 miles long. Two fracture zones separate regions which differ in depth by a quarter or half a mile.

The fractured area includes 8,000,000 square miles (5 per cent of the earth's surface), and the parallel trends of the fractures indicate a single origin. It is tentatively concluded that an annular convection current rising near the Hawaiian Islands and sinking near North America stressed the crust and produced the fracture zones by plastic deformation. The San Andreas fault marks a complementary zone of plastic deformation, and the California Coast Ranges lie within the zone. The Channel Islands and Transverse Ranges of California, and the Revilla Gigedo Islands and Volcanic province of Southern Mexico lie within continental extensions of the deep-sea fracture zones and parallel the zones. Some geomorphic provinces on the sea floor are bounded by fracture zones as are the Sierra Nevada, the Great Valley of California, the Baja California Peninsula (including the Peninsular ranges), and the Gulf Trough. Evidently the provinces were formed either with or after the fracture zones, and the stresses which formed them did not transect the zones. The zones appear to cut Mesozoic structure; they contain more active volcanoes and earthquakes than is normal for the northeastern Pacific area.

CONTENTS

TEXT

	Page
Introduction	1150
Acknowledgments	1152
Regional bathymetry	1152
Generalized description	1152
Criteria for geomorphic provinces	1153
Gulf of Alaska seamount province	1154
Ridge and Trough province	1155
Deep Plain of northeastern Pacific	1158
Baja California seamount province	1158
Description of fracture zones	1162
Mendocino fracture zone	1162
Murray fracture zone	1164
Clarion fracture zone	1167
Clipperton fracture zone	1170
Other fracture zones (?)	1172
Origin of fracture pattern	1172
Plastic deformation in earth's crust	1172
Possible origins	1173
Shift in poles	1174
Change in earth's flattening	1177
Shrinking of earth's crust	1178
Composite origin	1178
Local convection current	1179
Pacific-wide convection current	1179
Preferred hypothesis	1182
Origin of topography within fracture zones	1182
Generalized characteristics	1182
Deformation within plastic zones	1183
Elastic bending	1183
Origin of regional differences in depth	1184
Composition of Pacific crust	1184
Deep Plain and Baja California seamount province	1184
Deep Plain and Ridge and Trough province	1187
Implied crustal deformation	1188
Fault displacements	1188
Crustal shortening	1188
Age of fracturing	1189
Present seismicity and vulcanism	1189
Geologic dating	1190
Origin of some gross structures of western North America	1192
Correlation between geologic provinces and fracture zones	1192
Speculations regarding interrelations and origins	1193
General	1193
Structures within fracture zones	1193

Page
Structures between fracture zones..... 1193
San Andreas fracture zone..... 1193
Guatemala trench..... 1194
California Coast Ranges..... 1194
Garlock and Big Pine faults and bend in San Andreas fault..... 1195
Summary of tentative conclusions..... 1196
References cited..... 1197

ILLUSTRATIONS

Figure Page
1. Track chart..... 1151
2. Fracture zones and seamounts..... 1152
3. Seamount GA-1..... 1153
4. Seamount GA-3..... 1154
5. Seamount GA-4..... 1155
6. Gilbert seamount..... 1156
7. Pratt seamount..... 1157
8. Jasper seamount..... 1159
9. Crest seamount..... 1160
10. Henderson seamount..... 1161
11. Profiles of Mendocino fracture zone..... 1162
12. Fracture zones plotted on great circle projection..... 1163
13. Profiles of Murray fracture zone..... 1164
14. Relation between geomorphic and structural provinces, and fracture zones..... 1166
15. Block diagram of Clarion and Clipperton fracture zones..... 1168
16. Profiles of Clarion fracture zone..... 1169
17. Relation of fracture zones to transcurrent faults in Caribbean area..... 1170
18. Profiles of Clipperton fracture zone..... 1171
19. Displacement by shearing in band of plastic yielding..... 1173
20. Surface deformation in Luder's lines..... 1173
21. Relation between fracture zones and proposed shear pattern resulting from polar shift from India..... 1175
22. Relation between fracture zones and proposed shear pattern resulting from polar shift from Greenland..... 1176
23. Map of convection cell pattern..... 1181
24. Section of convection cell pattern..... 1182
25. General types of topography in fracture zones..... 1183
26. Possible origin of fracture zones and regional differences in depth..... 1186
27. Profiles of continental slopes..... 1187
28. Earthquake epicenters and volcanoes in northeastern Pacific area..... 1190
29. Stress and strain pattern in northern California..... 1195
30. Deformation pattern at junction of two zones of plastic yielding compared to pattern at junction of San Andreas and Big Pine-Garlock faults..... 1196

Plate Facing page
1. Bathymetric chart of Murray fracture zone 1198

TABLES

Table Page
1. Relief of Murray Escarpment..... 1165
2. Depth and relief in western section of Murray fracture zone..... 1165
3. Relief of Clarion fracture zone..... 1167
4. Energy of submarine earthquakes in and out of northeastern Pacific fracture zones 1191

Introduction

Scripps Institution of Oceanography and the Navy Electronics Laboratory explored the sea floor of the northeastern Pacific Ocean with five expeditions and many shorter cruises in the period 1948–1953 (Fig. 1). Three expeditions, *Northern Holiday* in 1951 and *Shuttle* and *Shellback* in 1952, were largely confined to these waters, but on the *Mid-Pacific* Expedition in 1950 and the *Capricorn* Expedition in 1952–1953 the exploration of the northeastern Pacific was incidental to the study of the central and southern Pacific. As of March 1953, about 44,000 miles of sounding lines with recording echo sounders or spot sounding spaced a few miles apart had been obtained in the northeastern Pacific by these expeditions.[1] Twenty-one seamounts have been surveyed by several crossings, and 11 have been dredged in this area. The principal emphasis of the bathymetrical phases of the exploration, however, has been on the great escarpments and troughs (Fig. 2).

The near-shore portion of the Mendocino Escarpment, discovered by H. W. Murray (1939), was discussed in detail by Shepard and Emery (1941, p. 35–41). Colbert (1949, p. 898) and Studds (1950, p. 787) mentioned that the continuity of the scarp had been confirmed for 300 miles west of Cape Mendocino. Twenty-two crossings by the Scripps Institution of Oceanography research ship Horizon, in 1950 and 1951, showed that the scarp was continuous for at least 1200 miles and possibly more than 1400 miles (Menard and Dietz, 1952, Fig. 1). The scarp was again crossed and dredged in two places about 120 miles from shore by USS Epce(r) 857 in 1952.

The existence of the Murray fracture zone

[1] By January 1955, *Trans-Pac*, *Cusp*, *Hawaii '53*, and *Hawaii '54* had been added to the roster of expeditions crossing this area (Fig. 1), and the length of sounding lines amounted to about 80,000 miles.

was suggested by Menard and Dietz (1952, p. 270). The first planned reconnaissance was made in the late summer of 1951 by HORIZON as the concluding part of the *Northern Holiday* time the trough was considered an isolated depression. HORIZON and EPCE(R) 857 operating in company on the *Mid-Pacific* Expedition in 1950 crossed the trough twice, but the pairs of

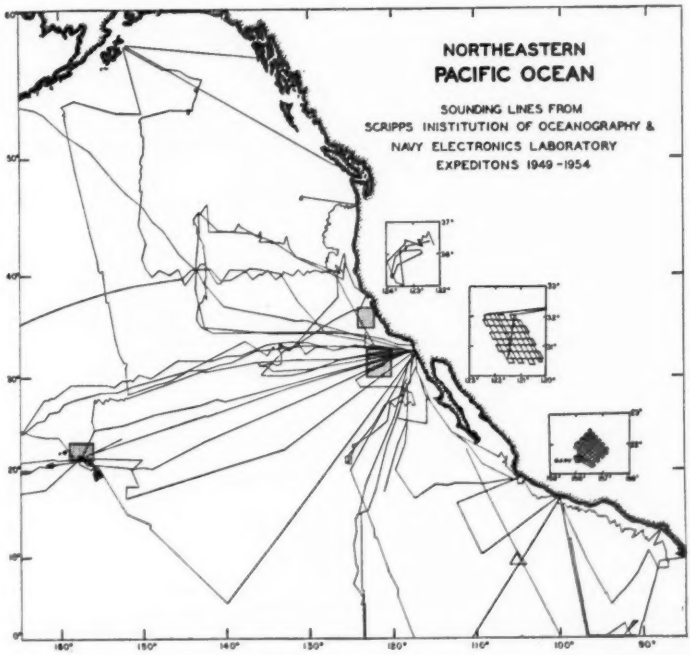

FIGURE 1.—TRACK CHART OF VARIOUS SCRIPPS INSTITUTION OF OCEANOGRAPHY AND NAVY ELECTRONICS LABORATORY EXPEDITIONS IN OR PASSING THROUGH NORTHEASTERN PACIFIC

Expedition. Ten crossings of the zone were spread over a distance of 1200 miles. However, eight crossings were concentrated relatively near shore so that the outer 800 miles remained poorly defined. More detailed exploration was made in the fall of 1952 in the initial stage of the *Capricorn* Expedition. Expedition plans required that both BAIRD and HORIZON proceed from San Diego to the Marshall Islands without undue delay en route. Fortunately for ease of exploration, the Murray fracture zone lies along a great circle between San Diego and the Marshall Islands, and 17 new crossings showed the zone continuous for more than 1900 miles.

The first crossing of the Clarion Trough with a recording echo sounder was made by USS SERRANO in conjunction with the Navy Electronics Laboratory SOFAR program. At that crossings were so far apart that any connection seemed doubtful. Older spot soundings, however, showed that a line of anomalous deep spots connected the two pairs of *Mid-Pacific* Expedition crossings and the one by SERRANO. The line of deep spots closely corresponded to a great circle, and the great circle closely approximated the trend of the Murray fracture zone and the outer part of the Mendocino fracture zone. The supposed continuity of the Clarion Trough was tested by laying out the courses of subsequent expeditions to cross unexplored areas. Such crossings were made by HORIZON and EPCE(R) 857 in the *Shuttle* and *Shellback* expeditions in 1952 and by HORIZON and BAIRD on the *Capricorn* Expedition in 1953.

Both HORIZON and EPCE(R) 857 crossed the Clipperton fracture zone during the *Mid-Pacific*

Expedition, and its existence was confirmed after six more crossings during the *Shuttle* and *Shellback* expeditions. The course of the Swedish *Albatross* Expedition also crossed this area and located the zone in a previously unexplored area. HORIZON and BAIRD also made two crossings of other unexplored sections of the zone during the *Capricorn* Expedition.

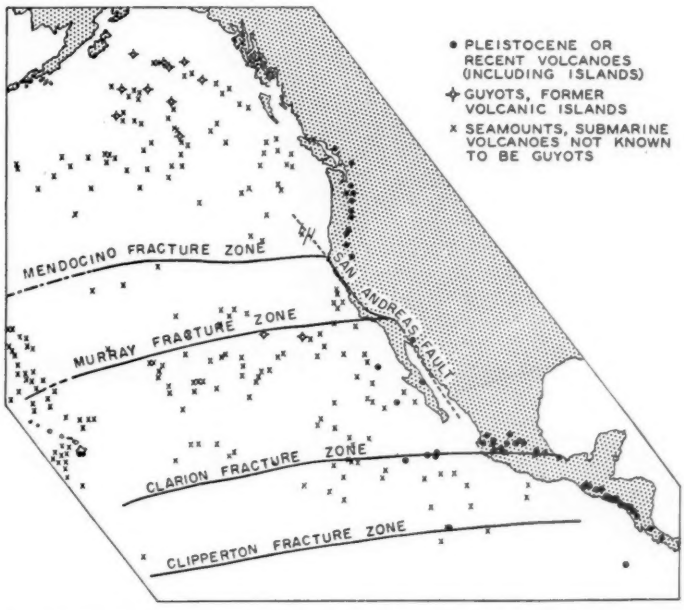
• PLEISTOCENE OR RECENT VOLCANOES (INCLUDING ISLANDS)
GUYOTS, FORMER VOLCANIC ISLANDS
× SEAMOUNTS, SUBMARINE VOLCANOES NOT KNOWN TO BE GUYOTS
MENDOCINO FRACTURE ZONE
MURRAY FRACTURE ZONE
SAN ANDREAS FAULT
CLARION FRACTURE ZONE
CLIPPERTON FRACTURE ZONE

FIGURE 2.—MERCATOR PROJECTION OF NORTHEASTERN PACIFIC SHOWING FRACTURE ZONES, SAN ANDREAS FAULT, AND VARIOUS KINDS OF MAJOR VOLCANOES

ACKNOWLEDGMENTS

The writer is indebted to his colleagues at the Navy Electronics Laboratory and the Scripps Institution of Oceanography for the months spent monitoring echo sounders to collect the soundings on which much of this paper is based. The Coast and Geodetic Survey and the Hydrographic Office have provided unpublished soundings.

E. C. Buffington, Robert S. Dietz, A. J. Eardley, Edwin L. Hamilton, Harry H. Hess, Peter Misch, Roger Revelle, George Shumway, and F. A. Vening Meinesz have read all or parts of the manuscript. Their discussions and comments have contributed greatly to its development. Ozalid copies of the echograms of the Swedish *Albatross* Expedition were made available by Gustaf Arrhenius.

REGIONAL BATHYMETRY

Generalized Description

The floor of the northeastern Pacific is part of a broad bowl centered north of Midway Island. Continental slopes form the steep sides of the bowl, and the abyssal sea floor forms the gently sloping bottom. Fracturing and vulcanism on a vast scale have deformed the contours of the bowl, and both the deformed and undeformed parts of the bowl have been covered by sediment in many places. This realm of the north Pacific may once have been one uniform topographic province, but now the topography is uniform only in relatively small areas. Several areas have been identified as topographic provinces (Eardley, 1951, p. 501–511; Menard and Dietz, 1951, p. 1268–1274, 1952, p. 268–270; Arrhenius, 1952, p. 190, Fig. 3d; Menard, 1955, Fig. 2), but recent soundings permit more

detailed descriptions of these provinces and some shifting of province boundaries as well as the delineation of new provinces such as the fracture zones.

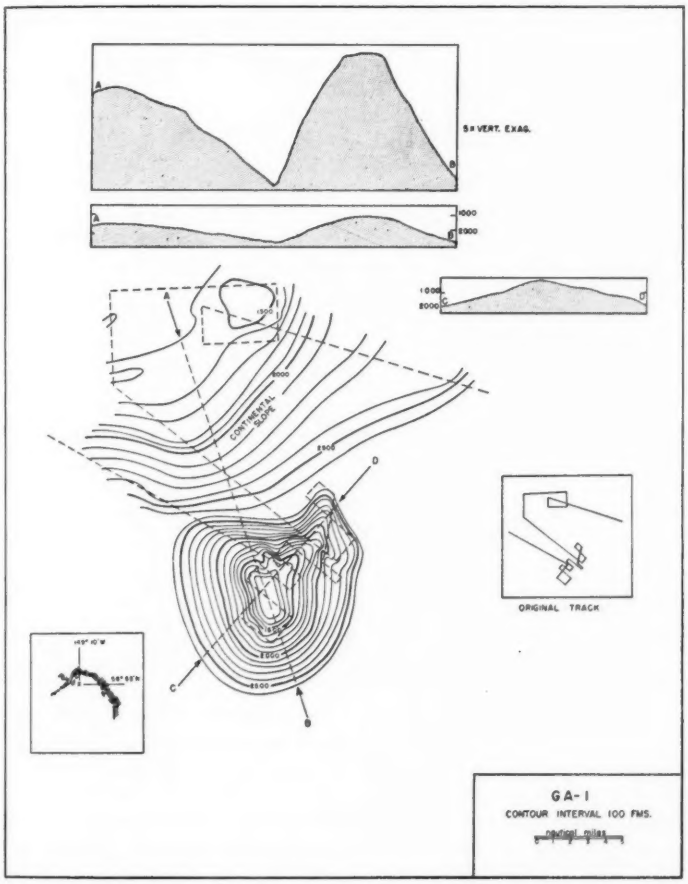

FIGURE 3.—SEAMOUNT GA-1, A GUYOT RISING FROM AXIS OF ALEUTIAN TRENCH

Description of the submarine topographic provinces is highly pertinent to this paper because the fracture zones form province boundaries related in origin and age. Moreover, the topography of the provinces is structural, and an understanding of the structures is essential to an understanding of the great fractures.

Criteria for Geomorphic Provinces

Important topographic characteristics for distinguishing submarine geomorphic provinces are: (1) relief of the continental slope (if the province borders a continent) and of the transition zone between the base of the continental slope and the relatively level deep-sea floor, particularly whether a trench or trough, or a smooth continental rise is at the base of the slope; (2) average depth and slope of the sea floor; (3) microrelief of sea floor, whether smooth or irregular; (4) number and distribution of oceanic islands and submarine volcanoes, minimum depths of the peaks, and occurrence of guyots; (5) occurrence, orientation, and distribution of fault blocks; (6) present seismicity and vulcanism (inasmuch as the relief is of structural or volcanic origin).

Gulf of Alaska Seamount Province

The northernmost geomorphic division is the Gulf of Alaska Seamount province (Menard and Dietz, 1951, p. 1268–1274). Its northern boundary is the Aleutian Trench, but to the north and northeast the province approaches shore. The continental slope bordering the province is only about 1½ miles high, and submarine canyons dissect it deeply. Below the steep continental slope the continental apron is steep near the continental slope but flattens farther seaward. Leveed channels of the type now known in many places in the oceans (Menard and Ludwick, 1951, p. 5–6; Buffington, 1952; Dietz, 1953) and usually ascribed to the action of turbidity currents meander across the rise to an unknown distance from shore (Menard, 1955, Fig. 2). The constant westward slope appears to be a graded profile. The continental rise and the deep-sea floor are unusually smooth compared with most other places in the Pacific but closely resemble the sea floor off the eastern United States (Heezen, Ewing, and Ericson, 1951); the continental slope in both areas is mature (Dietz, 1952, p. 1810).

Rising from the smooth alluvial plain, 36 majestic submarine volcanoes make the province distinctive. Some have been described from spot soundings (Murray, 1941) and single lines of recorded echo soundings (Menard and Dietz, 1951, p. 1268–1274), but the *Northern Holiday* Expedition made bathymetric surveys and dredged the seamounts. Figures 3–7 show typical Gulf of Alaska seamounts discovered by the Coast and Geodetic Survey and surveyed by HORIZON.

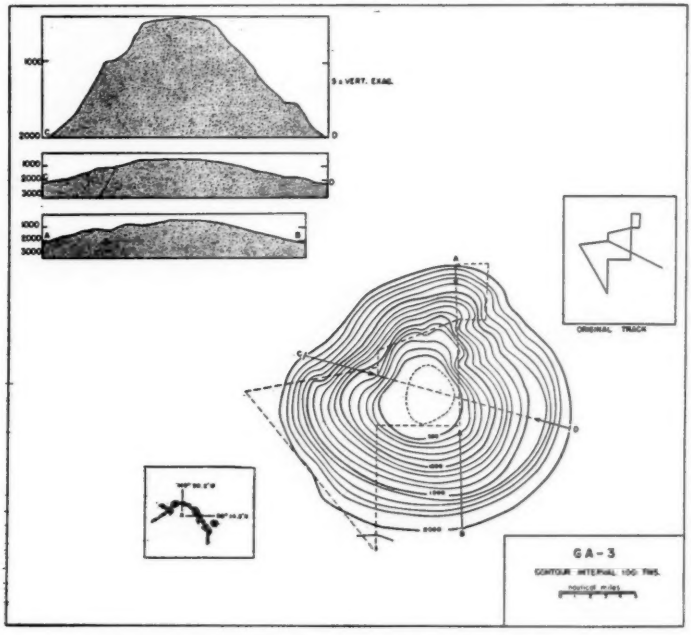

FIGURE 4.—SEAMOUNT GA-3, A GUYOT IN GULF OF ALASKA

No islands interrupt the surface of the Gulf of Alaska, and no known seamount is shoaler than 227 fathoms. However, 11 seamounts are guyots with typical flat tops indicating they were once subject to wave truncation at sea level (Hess, 1946, p. 785; Menard and Dietz, 1951, p. 1283; Hamilton, 1951, p. 204–206). Most of the truncated tops are now about half a mile below sea level, and several are much deeper. The province is not seismically active.

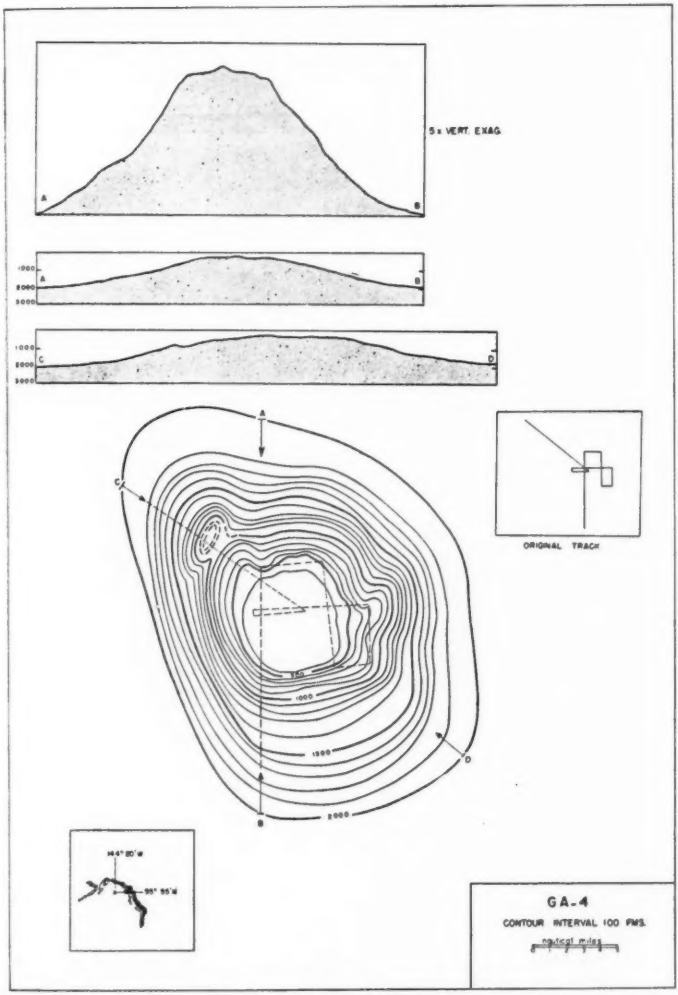

FIGURE 5.—SEAMOUNT GA-4, A GUYOT IN GULF OF ALASKA

Note differences between original and corrected track. Corrections determined by solving maneuvering board problem which gives drift with uniform speed and direction capable of making depth agree at all crossings.

and no records of discolored water suggest recent volcanic eruptions.

This topography is old in every respect. A thick apron of sediment apparently has covered the base of the continental slope and has spread southwest across the whole width of the Gulf of Alaska. Former islands have sunk to great depths, the considerable depth of other submarine mountains plus the lack of known seismic or volcanic activity suggest that no new islands are forming.

Ridge and Trough Province

The Ridge and Trough province to the south shows strong evidence of comparative youth (Menard and Dietz, 1951, p. 1284–1285). The continental slope is about 1½ miles high and

is dissected by several well-known submarine canyons. An apron of sediment spreads from the base of the slope off Queen Charlotte Island and in the northern part of the province, but a long, narrow, seismically active trough lies between the apron and the base of the slope. Evidently the top of the apron has been faulted down so recently that sediment moving out from the continent has not yet filled the trough to re-establish an even gradient seaward. In the southern part of the province, off the northwestern United States, a smooth, and (in a seaward direction) level plain extends for a few scores of miles from the base of the slope (Menard, 1955, Fig. 4). The plain slopes gently toward the south parallel to the trend of the continental slope but perpendicular to its slope. This unusual relationship is explained by the topography of the deep-sea floor.

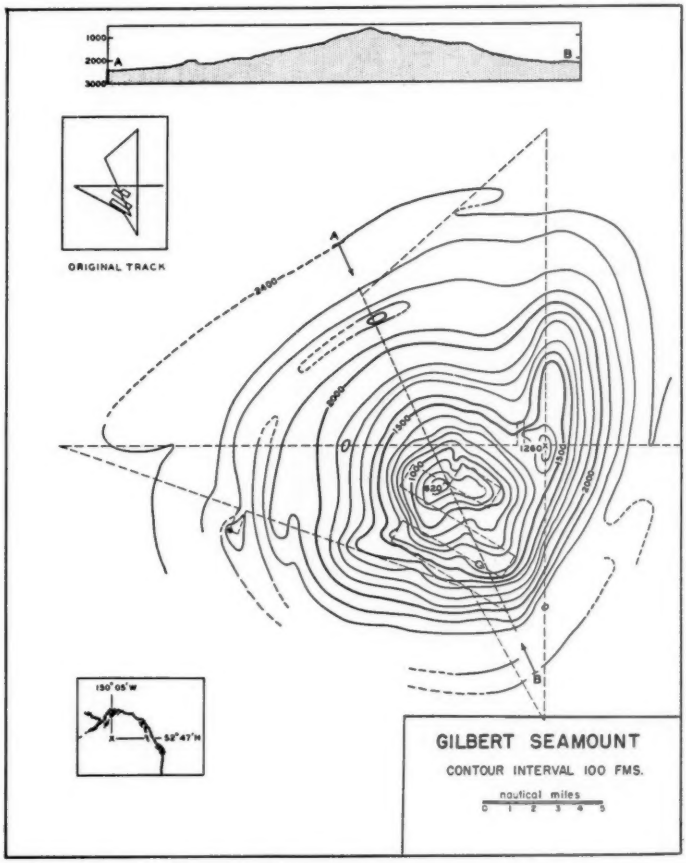

FIGURE 6.—GILBERT SEAMOUNT, A SEAPEAK IN GULF OF ALASKA
Pointed top may be compared with truncated tops of guyots

The sea floor presumably was block-faulted into long thin ridges which trend northeast or north. From the ridges rise a few submarine volcanoes some of which are only a few fathoms below the surface, but most crossings of the ridges indicate steep-sided, low blocks, unlike volcanoes (Menard and Dietz, 1951, Pl. 5). The concentration of Coast and Geodetic Survey sounding lines in this area made it

possible to prepare a bathymetric chart (Menard and Dietz, 1952, Fig. 1), but several interpretations were possible. For two weeks in September 1952 EPCE(R) 857 was used for a geological reconnaissance of the southern part of the Ridge and Trough province to check the bathymetry at critical points. The sounding lines confirm the existence of the long ridges.

The long ridges roughly parallel the continental slope and guide the flow of turbidity currents moving sediment out from the continent. One of several leveed channels on the otherwise smooth plain at the base of the continental slope off Oregon, was traced southward for almost 200 miles. Apparently the turbidity currents cannot surmount the ridges to flow west (direction of the regional slope) but are diverted southward to a divide through which they again flow westward or fan out to fill low spots on the downstream side of the ridges. A few basins appear entirely ringed by high ridges so that turbidity flows moving along the bottom cannot fill them with sedi-

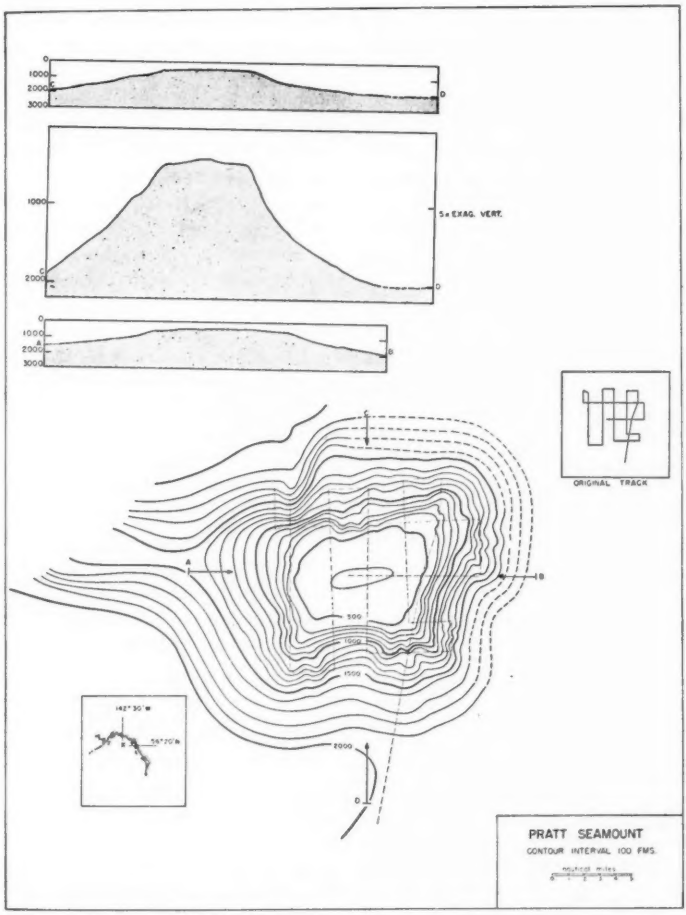

FIGURE 7.—PRATT SEAMOUNT, A GUYOT IN GULF OF ALASKA
Note gradual shoaling toward center of truncated top

ment. These basins are thousands of feet below the level of the surrounding alluvial plains formed by deposition from turbidity currents; their bottoms are irregular, which suggests that deposition from suspension in the main mass of the ocean may be much slower than deposition from turbidity currents moving in concentrated clouds along the bottom.

The deep depressions may have an origin unrelated to varying rates of deposition, however. About a third of the earthquakes in the California region occur in the southern part of the Ridge and Trough province (Gutenberg and Richter, 1949, p. 34). The epicenters form a wide band with the trend and position of an extension of the San Andreas fault (Menard and Dietz, 1952, p. 272). The submarine depressions may be actively subsiding blocks.

The southern boundary of the Ridge and Trough province is formed by the Mendocino and Gorda escarpments. The long thin ridge which caps the escarpments forms a barrier to sediment movement along the deep-sea floor so that none of the leveed channels in the Ridge and Trough province extend into the deep area south of the escarpments.

Deep Plain of Northeastern Pacific

South of the Mendocino escarpment the sea floor is about half a mile deeper than it is to the north. The unusually deep area is bounded on the south by the Murray escarpment, and the sea floor is roughly a quarter of a mile higher south of the Murray escarpment than it is to the north. The nearshore part of this area has a distinctive topography and is here named the Deep Plain of the Northeastern Pacific. Spot soundings taken prior to 1940 suggest that the Deep Plain has many irregularities but echograms from recent expeditions show a smooth, deep plain sloping gently southwest for several hundred miles from shore.

The continental slope off central California forms the eastern boundary of the Deep Plain. It drops off abruptly to a depth of more than 2 miles, and large submarine canyons dissect it (Shepard and Emery, 1941, p. 69–81). Below the abrupt slope are three great deep-sea fans (Menard, 1955, Fig. 6) which grade imperceptibly into the gently sloping Deep Plain at a depth of about 2½ miles. Crossing the fans are leveed and unleveed channels; those which have been explored in some detail lead out from submarine canyons (Dill, Dietz, and Stewart, 1954).

Like most topographic provinces in the northeastern Pacific, the deep area between the Mendocino and Murray fracture zones including the Deep Plain contains no islands or shoals, but it is unique in that it appears to contain few seamounts. Five seamounts—submarine volcanoes—rise from the continental slope bordering the area, but they trend parallel to the coast and may be genetically unrelated to the deep-sea floor. Eleven seamounts are indicated by the older spot soundings, and one other was found on *Northern Holiday*. However, the location of two of the seamounts indicated by spot soundings was crossed on *Capricorn*, and the seamounts were not there. The concentration of seamounts per unit area is only slightly below average for the northeastern Pacific if the concentration of sounding lines is considered. However, none of the seamounts is more than 1 mile high, and most are barely half a mile high. Only two seamounts are documented by more than one line of spot soundings, most of the seamounts are indicated by only one sounding; and many of the sounding lines are demonstrably unreliable elsewhere.

Baja California Seamount Province

South of the Murray fracture zone and north of the Clarion fracture zone a mountainous area studded with volcanoes forms a geomorphic province. The general area within a few hundred miles of shore is called the Plateau de Californie on the charts of the International Hydrographic Bureau of Monaco, and the whole area off Baja California was tentatively called the Mexican rise by Menard and Dietz (1952, p. 269–270). When the soundings from the *Shuttle* and *Shellback* expeditions became available (1952) it was apparent that neither rise nor Plateau was an acceptable term because much of the sea floor south of the Clarion fracture zone stands at the same depth as the sea floor to the north. Consequently the area is here named the Baja California Seamount province.

Off almost all shores the zone between the shore and the continental slope is the geneti-

cally controversial but topographically monotonous continental shelf. Along the eastern border of the Baja California Seamount province, however, this zone has irregular topography and a less controversial origin. Shepard and Emery (1941, p. 9–29) described and named the continental borderland off southern California, a wide zone of islands and banks separated by deep basins. They ascribed the origin of the islands and basins to block faulting. Exploration shows that the continental borderland extends as far south as the middle of Baja California and that topography is similar in the southern part of the Gulf of California. Inasmuch as Baja California and the Gulf of California also contain fault blocks (Beal, 1948, p. 99–100; Shepard, 1950, p. 12–19), the whole continental border of the Baja California Volcanic province has a distinctive ridge-and-trough topography.

The continental slope west of the continental borderland drops off abruptly to a depth of about 2 miles. It is irregular but does not appear deeply dissected by canyons. A smooth apron a few tens of miles wide lies at the base of the slope in some places. Off the southern half of Baja California the continental slope drops abruptly for 2–2½ miles into a series of long thin troughs a few hundred fathoms below the general level of the deep-sea floor to the west. The troughs are flat-bottomed indicating a fill of sediment.

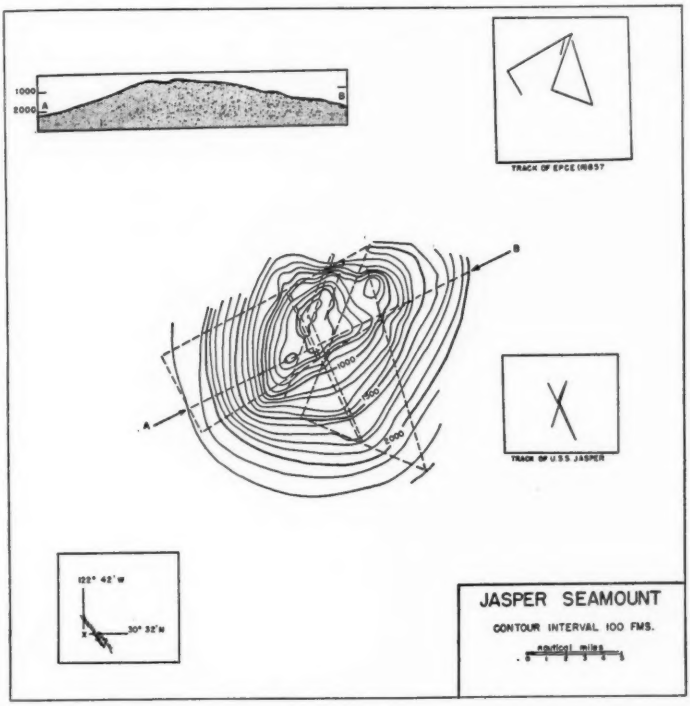

FIGURE 8.—JASPER SEAMOUNT, A SEAPEAK IN BAJA CALIFORNIA SEAMOUNT PROVINCE

The abyssal sea floor of the Baja California Seamount province is too irregular to permit generalization regarding depth. The province slopes generally westward except for a band about 300 miles wide near shore which averages about 2200 fathoms deep. The province is roughly a quarter of a mile shallower than the Deep Plain to the north.

Widespread vulcanism, particularly recent vulcanism, characterizes the province. Guada-

lupe Island comprises a group of eroded Late Tertiary or Quaternary volcanoes (Johnson, 1953, p. 236). Alijos Rocks are three steep-sided remnants of a large volcanic cone. Volcanic islands are so rare in the northeastern Pacific basin that these deserve special consideration, but the evidence supporting unusual vulcanism comes chiefly from submarine volcanoes. Of 51 seamounts, 15 are more than 1 mile high, and every expedition crossing the province finds new seamounts. Seven seamounts have been surveyed, and Jasper and Henderson have been dredged. The volcanoes are typical isolated cones with steep sides and pointed tops (Figs. 8, 9). None are guyots with wide flat tops. Henderson Seamount (Fig. 10) appears to have a flat top at 220 fathoms, but the area is only half a square mile, and this is too small to demonstrate that a sharp peak has been planed off. However, hundreds of pounds of coarse, basaltic gravel were dredged from the top of this seamount, and a large fraction of subrounded and subangular pebbles and cobbles suggests wear in the surf zone.

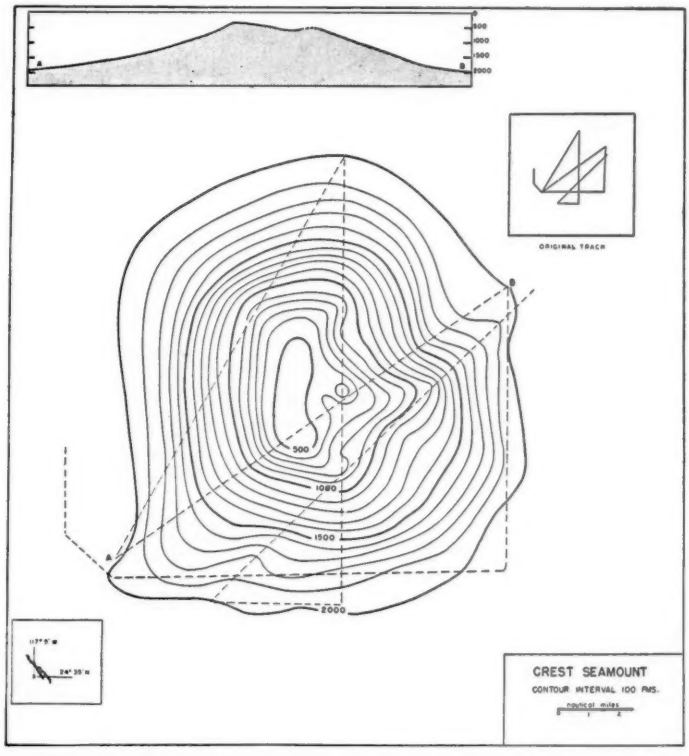

FIGURE 9.—CREST SEAMOUNT IN BAJA CALIFORNIA SEAMOUNT PROVINCE
Top has not been surveyed and it is not known whether seamount is guyot or seapeak

Contrasting strongly with the smooth floor of the Deep Plain to the north, the Baja California Seamount province is irregular. Recorded echo soundings show thousands of miles of jagged bottom in which the irregularities have a relief of 100–200 fathoms. The relief must be tectonic, but it is uncertain whether it is caused by vulcanism or faulting. The lack of a smooth blanket of sediment suggests either that the topography was formed relatively recently or that the rate of sedimentation is unusually slow. No large rivers carry sediment

from southern California and Baja California into the ocean, and even the limited amount introduced by intermittent small rivers is trapped in the basins of the continental borderland or in the troughs off Baja California (Menard, 1955, p. 241).

The deep-sea floor is not seismically active, but the continental margin in the province has been faulted into blocks, and many faults are still active (Clements and Emery, 1947).

The area between the Clarion and the Clipperton fracture zones has been divided into the East Pacific Ridge and the East Eupelagic area (Arrhenius, 1952, p. 190). Division is based on the topography and sediments as observed by the Swedish *Albatross* Expedition. The topography of the East Pacific Ridge resembles the topography of the Baja California Seamount province but is shallower. Farther from shore the topography becomes more subdued in the East Eupelagic area. The maximum of a few hundred meters of sediment (Raitt, Personal communication) in this area suggests that the topography never was irregular.

South of the Clipperton fracture zone, the

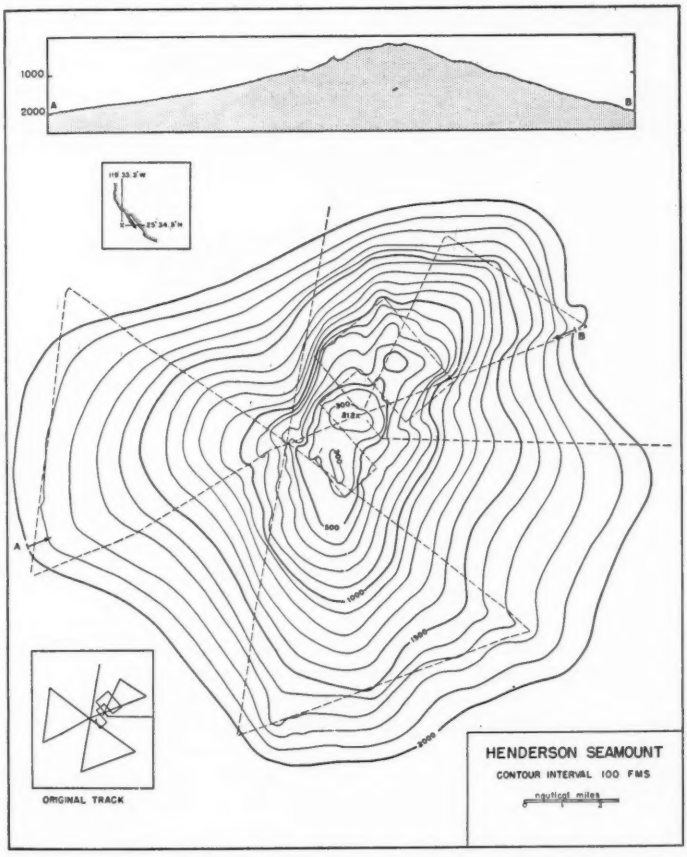

FIGURE 10.—HENDERSON SEAMOUNT IN BAJA CALIFORNIA SEAMOUNT PROVINCE

Small platform at depth of 220 fathoms covered with subangular and subrounded gravel which may be evidence for former wave truncation, but from topography alone it is not possible to tell whether this seamount is a guyot.

information available from *Shellback* and *Capricorn* permits only a few generalizations regarding topography. From the northern limit of the southeastern Pacific Plateau to the Clipperton fracture zone, the sea floor slopes gently long, and has a maximum height of 6000 feet. From 75 to 200 miles from shore the principal feature is a great ridge (Fig. 11). The much higher and slightly steeper south side is the Mendocino Escarpment with a maximum

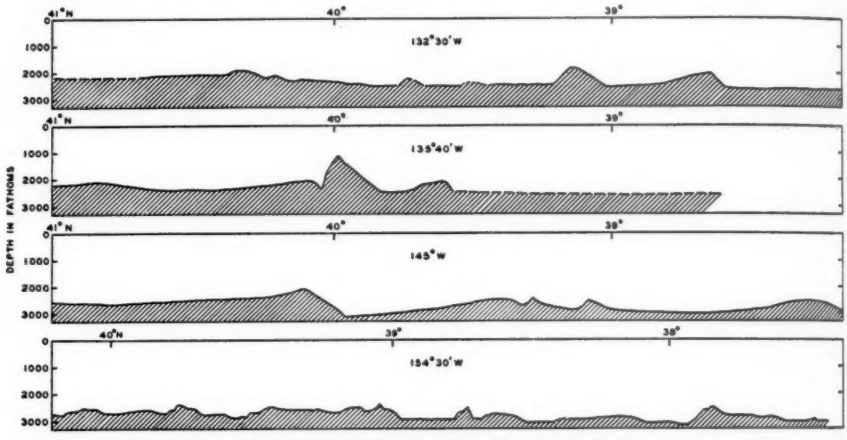

FIGURE 11.—NORTH-SOUTH PROFILES OF MENDOCINO FRACTURE ZONE
Vertical exaggeration approximately 6/1

northward. Seamounts have not been found, although minor hills are not uncommon. The one important topographic feature is at 4°N., 124°W. where an asymmetrical ridge flanks a narrow deep. The ridge and deep strike northwest for at least 20 miles, and the maximum relief is almost a mile. This feature closely resembles a fracture zone except in trend. It lies about 240 miles south of the Clipperton fracture zone.

DESCRIPTION OF FRACTURE ZONES

Mendocino Fracture Zone

The Mendocino fracture zone was the first discovered in the northeastern Pacific and is the best known (Menard and Dietz, 1952). Prior to 1952 the Gorda Escarpment had been surveyed by the Coast and Geodetic Survey for 70 miles from shore, and the outer 1330 miles of the fracture zone had been crossed 12 times by older survey ships, and 22 times by HORIZON.

The near-shore Gorda Escarpment (Shepard and Emery, 1941, p. 35–37) lies on the north side of an asymmetrical ridge, is about 75 miles height of 10,500 feet. The topography is more complex from 200 to 380 miles from shore. A northeast-trending lineation intersects the main ridge and scarp which decreases in elevation westward from 8400 feet to 3300 feet. Two ridges separated by a deep, steep-sided, narrow trough are found between 380 and 560 miles from shore. The Mendocino Escarpment has a maximum height of 8580 feet, and the south side of the narrow trough is as high as 7560 feet and has an extraordinary average slope in one place of 28°. A regular escarpment is found on the south side of an asymmetrical ridge from 560 to 1200 miles from shore. The average height is about 5000 feet, and the maximum is 8420 feet. Parallel asymmetrical ridges lie south of the main escarpment.

A 200-mile gap separates the westernmost sounding line from the next one to the east so that the topography of the fracture zone between 1200 and 1400 miles from shore is not known. The main escarpment, about 3700 feet high, lies about 60 miles south of the due west trend which it follows for 1200 miles from shore, so that a connection is not certain (Menard and Dietz, 1952, p. 271). However,

the connecting link would trend parallel to the three other fracture zones in the northeastern Pacific, which tends to confirm its presence. Considering all the fracture zones, the trend "parallelism" with the great-circle trends of the Murray, Clarion, and Clipperton fracture zones. Quite possibly the irregular topography along this course is part of the Mendocino

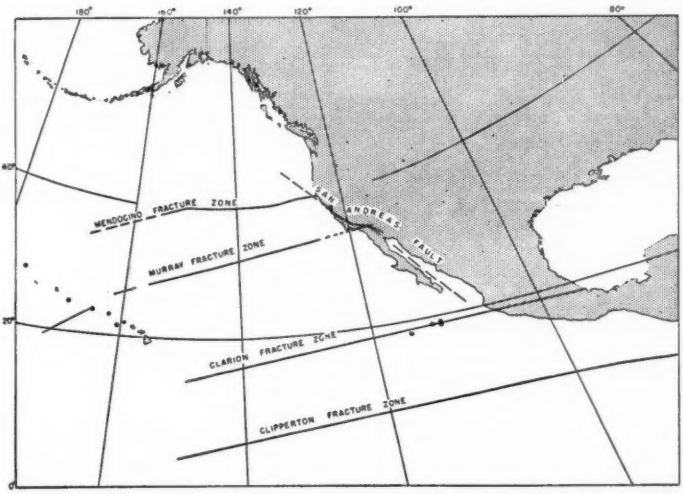

FIGURE 12.—FRACTURE ZONES OF NORTHEASTERN PACIFIC PLOTTED ON GREAT CIRCLE PROJECTION
Straight lines on earth's surface are straight lines on this type of projection

of the inner 1200 miles of the Mendocino fracture zone is anomalous, and the connecting link is normal.

No lines of closely spaced soundings cross the probable trend of the Mendocino fracture zone more than 1400 miles from shore. The few lines of spot soundings, mostly by USS RAMAPO, show some evidence for a continuation toward the west-southwest but it is not compelling. Another form of evidence comes from the echogram made by HORIZON on a great-circle course from north of Midway Island toward 40°N., 145°W. during the concluding part of the *Mid-Pacific* Expedition. The topography shown on this echogram is irregular with a relief of 200–500 fms along this course. The intersecting line made by HORIZON on a southerly course during Expedition *Northern Holiday* shows that the sea floor is smooth for hundreds of miles except near the point of intersection, which is in the southern part of the Mendocino fracture zone. Purely by coincidence the great-circle course followed during the *Mid-Pacific* Expedition is only 2° from fracture zone which, consequently, would extend from North America to the Hawaiian Islands (near Midway Island) like the Murray and Clarion fracture zones.

The Mendocino is the only fracture zone that offsets the continental slope, yet it has no large-scale topographic continuation on the continent. A gouge and fracture zone about 3 miles wide in the sea cliffs just north of Cape Mendocino has been traced eastward for 15 miles (Ogle, 1952). The faulting which formed the gouge zone may be related to the Mendocino fracture zone.

A more tenuous extension of the fracture zone is suggested by the alignment of the boundaries of topographic provinces east of Cape Mendocino. The long line of the Cascade volcanoes stops at a point east of Cape Mendocino as does the long block of the Sierra Nevada. This penetration of the continent by the Mendocino fracture zone, although not demonstrated, would not be unexpected because both the Murray and Clarion fracture zones penetrate similar distances.

Murray Fracture Zone

The Murray fracture zone is a 1900-mile gash which follows a great circle across the sea floor and into California (Fig. 12). The name comes from the Murray Deep, the only well-known related geographical feature in the Pacific. It consists of long narrow ridges and depressions, with a parallel line of majestic submarine volcanoes to the south (Pl. 1). An asymmetrical ridge forms the south side of the zone (Fig. 13). The steep north side of the ridge is the Murray Escarpment. At the base of the escarpment a parallel trough opens to the west but has local depressions. In some places the sea floor just north of the trough is relatively level, but elsewhere another asymmetrical ridge—steep on the south side—faces the trough. For hundreds of miles south of the fracture zone the sea floor is about a quarter of a mile shallower than it is for hundreds of miles to the north.

The fracture zone may have an extension on the continent, but its effect on the topography at the transition between continent and deep sea—the continental slope—is not obvious. The Patton Escarpment (Shepard and Emery, 1941, Chart 1) is the long, straight, continental slope between the continental borderland off southern California and the deep sea. The Santa Lucia Escarpment is a similar slope which follows the trend of the Patton Escarpment but is 50 miles from it. The zone trends through this 50-mile gap and may have produced it. Rodriguez Seamount, a submarine volcano, in this gap may be related to the faulting in the zone. However, several other submarine volcanoes lie along the continental slope off California (Shepard and Emery, 1941, p. 33–35) and all of them, including Rodriguez Seamount, may be genetically related to the continental slope.

Between Long. 122°W. at the base of the Patton Escarpment and Long. 128°W. the sounding density is too limited for accurate

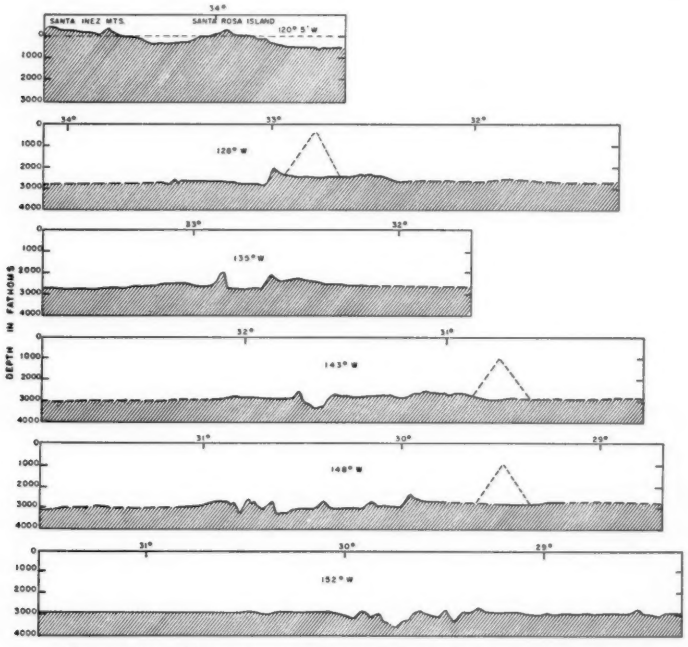

FIGURE 13.—NORTH-SOUTH PROFILES OF MURRAY FRACTURE ZONE

Vertical exaggeration approximately 6/1. Dashed cones are submarine volcanoes located slightly east or west of the line of profile.

contouring within the fracture zone. The asymmetrical ridge, clearly defined to the west may continue almost to the Patton Escarpment, but seven echograms show irregular and complex topography in the fracture zone. In contrast the sea floor north of the fracture zone

TABLE 1.—RELIEF OF MURRAY ESCARPMENT

Average longitude	Depth of top (fathoms)	Depth of bottom (fathoms)	Relief (feet)
129°40′	2360	2680	1920
130°40′	2270	2750	2880
133°	1900	2870	5820
135°	1830	2970	6840
137°	1890	2820	5580
137°50′	2370	2670	1800
139°	2380	2920	3240
140°30′	2550	2930	2280
142°30′	2670	3310	3840

is a smooth plain sloping gently westward. The plain is about 200 fathoms deeper than the sea floor south of the fracture zone. Fieberling Seamount (Carsola and Dietz, 1952) and an unnamed seamount lie about 60 miles south of the Murray Escarpment and rise about 2 miles above the surrounding sea floor.

From Long. 128°W. to 141°W. the Murray Escarpment is the most prominent feature of the zone. HORIZON and BAIRD have crossed the escarpment in 15 places in this section, and the available echograms and essentially continuous lines of spot soundings make this the best-known part of the fracture zone. The relief is almost 7000 feet in the middle of this section where a high ridge about 5 miles wide drops into an elongate depression about 10 miles wide and 200 fathoms deep (Table 1). The depression is absent in the eastern part of the section, possibly because it has been filled by the same flood of sediment which formed the smooth floor of the Deep Plain to the north. Between 137°W. and 138° 30′W. Long. the depression is much shallower than elsewhere, and the ridge is also unusually low, suggesting that the faulting had little vertical expression.

A ridge about 30 miles south of the Murray Escarpment parallels it. Locally it is 1500 feet high, but soundings are too few for accurate description. Erben Guyot rises above Murray Escarpment at Long. 132° 30′W. (Carsola and Dietz, 1952, p. 481). The guyot is itself about 2 miles high, and the total relief to the bottom of the scarp is more than 15,800 feet.

TABLE 2.—DEPTHS AND RELIEF IN WESTERN SECTION OF MURRAY FRACTURE ZONE

Average longitude	Minimum depth of northern ridge (fathoms)	Maximum depth of northern trough (fathoms)	Maximum depth within irregular zone (fathoms)	Maximum depth of southern trough (fathoms)	Minimum depth of southern ridge (fathoms)	Relief of southern scarp (feet)
143°	2540	3310	?	2830	2500	1980
147°	2645	3200	3200	2850 (?)	2350	3000 (?)
150°	2630	3160	3210	3000 (?)	2450	3300 (?)
152°	2760	3000	3530	3250	2650	3600
154°	?	?	3270	3150	2850	1800
156°	?	?	3330	3290	2910	2280

At about 141°W. Long. the fracture zone changes from a rather simple escarpment with a depression at the base to a broad irregular trough bordered by two asymmetrical ridges (Fig. 13). From 141°W. Long. there is little variation to 157°W., the westernmost part of the zone explored. The northern slope of the southern ridge is an escarpment which has the same general position as the Murray Escarpment has with relation to the whole fracture zone. The two escarpments may be connected, but existing soundings favor an echelon arrangement. The sounding line made during *Northern Holiday* crosses the whole fracture zone in two places, and the two *Capricorn* sounding lines zig-zag along ridges or deeps within the zone. Combining these lines, generalized profiles of the zone between 141°W. and 151°W. indicate the following sequence of topography from north to south: an asymmetrical ridge with the steep side on the south, a trough 3–10 miles wide, a 20-mile-wide irregular area of ridges and troughs (which cannot be contoured with any confidence at present), a trough about 5 miles wide, and an asymmetrical ridge with a prominent escarpment on the south side (Table 2).

The continuity of both the southern and

northern troughs deserves special mention. Although it is less than 10 miles wide, the northern trough has been traced (four crossings) for 250 miles. It appears to connect with the trough at the base of the Murray Escarpment and thus extend several hundred miles farther east. Moreover, it may also continue far to the west; older spot soundings permit such an interpretation, but the interval between soundings and the errors of position are much too large for accurate definition of such a narrow trough. The southern trough, which is equally narrow, has been traced for 700 miles (five crossings) and may extend even farther both east and west.

The fracture zone is not known west of 157°W. Long., but a zone of irregular topography follows the same trend almost to the Hawaiian Islands. The topography is complicated by the intersection of a line of seamounts trending south-southeast so that interpretation of the bathymetry is not reliable. However, either a closely spaced line of seamounts or a narrow ridge trends southwest along the line of the Murray fracture zone. Beyond the Hawaiian Islands the eastern part of the Mid-Pacific Mountains also trends southwest in a long narrow ridge from Necker Island. This ridge lies about 50 miles south of the great circle which follows the Murray fracture zone, but the trends are only slightly divergent. The zone may have been displaced by cross shearing along the Hawaiian Islands (Betz and Hess, 1942, p. 111), or it may bend where it crosses the Hawaiian structure as the San Andreas fault bends in crossing the Murray fracture zone. In any case the eastern Mid-Pacific Mountains are probably related to the Murray fracture zone.

The Murray fracture zone has been traced across the sea floor for 1800 miles in a straight line as far east as the base of the continental slope off southern California. The Channel Islands and the Transverse Ranges are located where the extended trend of the Murray fracture zone would cross the margin of the conti-

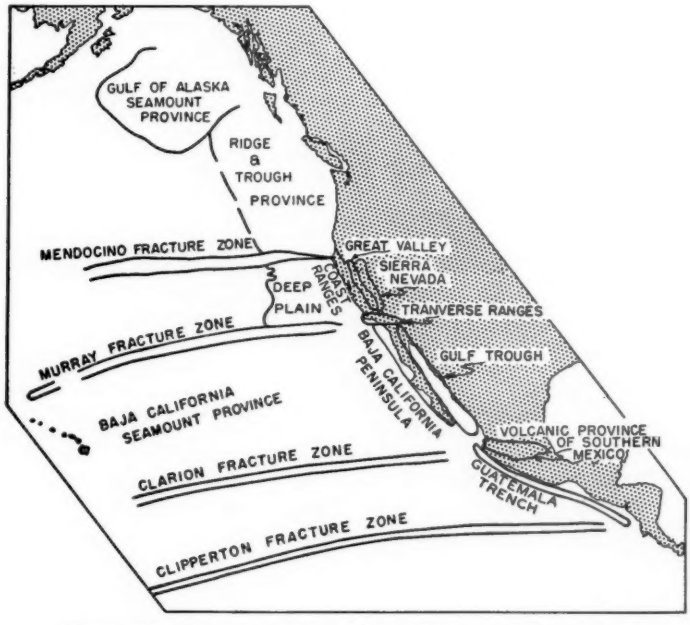

FIGURE 14.—CONTINENTAL AND MARINE GEOMORPHIC PROVINCES
Note that most provinces lie within or are bounded by fracture zones

nent (Fig. 14). These islands and ranges trend eastward in contrast to the southeasterly trends found elsewhere in California but coinciding exactly with the trend as well as the position of the Murray fracture zone. A profile across the Santa Inez Mountains, Santa Barbara Basin, and Santa Rosa Island shows that the width and general relief of the east-trending continental zone resemble the western part of the fracture zone (Fig. 13). A regional change in depth also occurs on the two sides of the transverse structures just as it does elsewhere across the Murray fracture zone except that on the continent the sense of the vertical movement is reversed. North of the transverse structures the continent is above sea level, but to the south it has been submerged and forms the continental borderland dotted with islands of continental rock at a general level of a few hundred fathoms below sea level (Shepard and Emery, 1941, p. 9–19).

TABLE 3.—RELIEF OF CLARION FRACTURE ZONE

Average longitude	Type of sounding line	Maximum depth of trough (fathoms)		Minimum depth of ridge (fathoms)		Relief of North Trough (feet)
		North	South	North	South	
118° 30′	echogram	.....	.....	.....	.....	none
120° 50′	echogram	2500	2450	2190	2110	1860
121° 30′	spot	2550		1970		3480
122°	echogram	none		1265 (seamount)		none
123° 10′	echogram	2510		2025		2910
123° 30′	spot	2630		2175		2730
124° 20′	echogram	2380		2060		1920
127° 30′	spot	2590		2160		2580
129° 30′	spot	2920		2420		3000
130° 30′	echogram	2830	2910	2200	2170	3780
133°	spot	3200	2800	2320	2240	5280
136° 30′	spot	3060		2500		3360
138°	spot	2975		2600		2250
140°	spot	2905		2420		2910
141°	spot	2890		2350		3240
142° 30′	spot	3400		2450		5700
146° 30′	spot	2920		2640		1680
149°	echogram	3320		2420		5400

Clarion Fracture Zone

The Clarion fracture zone is named after Clarion Island, the westernmost of the Revilla Gigedo group, which lies in the zone and marks its transition from a submarine to a subaerial feature. The zone may be divided into three sections. From Long. 149°W. to Long. 127°W. it is characterized by irregular topography featuring a long narrow trough. Between 127°W. and 118° 30′W. intermittent troughs are separated by volcanoes and possibly unfaulted areas of the sea floor. Between 118° 30′W. and 96°W. is a line of Quaternary volcanoes many of which are still active. The main narrow trough may be traced for 1700 miles if the intermittent deeps in the transition section are included, and for that distance it deviates from a great circle by no more than 15 miles (Fig. 12). The volcanic section is wider but follows a great circle, so that the total length of the fracture zone is 3000 miles.

The outer trough section of the Clarion fracture zone (149°W.–127°W.) is crossed by 11 lines with closely spaced soundings; two are echograms. The section is 1350 miles long, the average spacing is more than 100 miles, and the maximum spacing is 240 miles. All lines show both the trough and the flanking ridge characteristic of this section (Table 3), and both are probably continuous. However, the trough is not continuous in the adjacent

transition section where the sounding lines are more closely spaced, and possibly more sounding lines would also show interruptions in the trough to the west.

vertical movement which produced it may have been intermittent in the fracture zone and died out to the east. If so the discontinuities in the trough may be sections of the

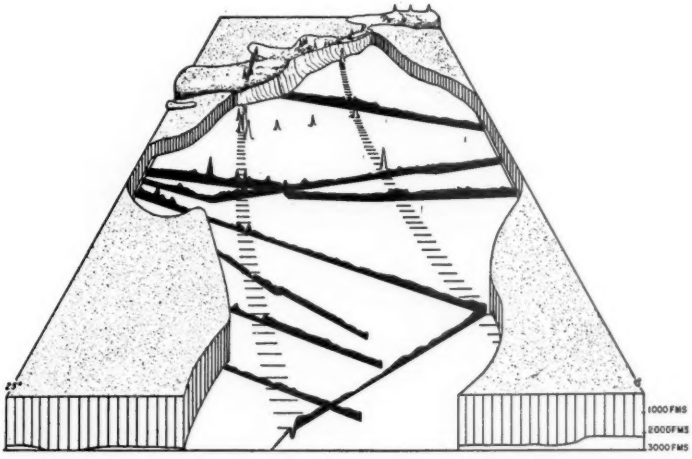

FIGURE 15.—BLOCK DIAGRAM OF CLARION AND CLIPPERTON FRACTURE ZONES
Not all sounding lines indicating fracture zones are shown because several trend along line of sight

Figure 15 shows a perspective drawing of some of the sounding lines crossing the fracture zone, but several have been omitted because they cross the zone at an acute angle and consequently lie along the line of sight of the figure. The zone of irregular topography is 60–100 miles wide, and no regional change in depth occurs across the zone (Fig. 16). The Clarion fracture zone thus differs from the three other fracture zones in the northeastern Pacific area.

The western end of the fracture zone has not been found. The westernmost crossing at 149°W. shows that the trough is 5400 feet below the top of the adjacent ridge and about 2400 feet below the general level of the sea floor. This great relief suggests that the trough continues to the west, but it has not been found on the few spot-sounding lines in the area, and no echograms are available.

The transition zone (127°W.–118° 30′W.) is crossed by five echograms and two spot-sounding lines. The topography is irregular, but the trough does not extend along the whole section. The trough has not been found in the fracture zone anywhere east of 118° 39′W., and the fracture zone which have not been vertically displaced. On the other hand several small seamounts have been found in the transition section of the fracture zone. The lava which produced these volcanic cones may have filled the trough locally and so produced the discontinuities.

In addition to the smaller seamounts—none of which is more than 1 mile high—within the fracture zone, the great cone of California Seamount rises 2 miles above the surrounding sea floor about 30 miles south of the center of the fracture zone. It has a pointed peak showing no evidence of wave planation.

From the Revilla Gigedo Islands to the east coast of Mexico the Clarion fracture zone is dotted with 25 volcanoes, 21 in the Volcanic Province of Southern Mexico (Eardley, 1951, p. 585–587, Fig. 342, p. 595) and four in the Revilla Gigedo Islands. Of these, six in Mexico are active (Gutenberg and Richter, 1949, Fig. 9, p. 37), and one on San Benedicto Island became active in 1952. The seven form the only line of active volcanoes in the western hemisphere not parallel to a coast line or island-arc structure. Considering the gradual transi-

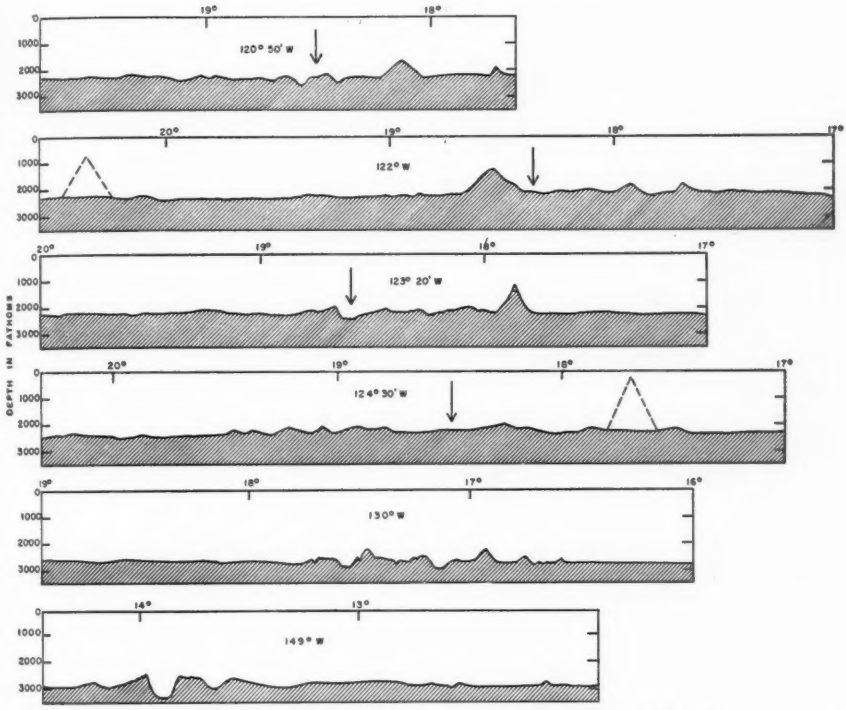

FIGURE 16.—NORTH-SOUTH PROFILES OF CLARION FRACTURE ZONE

Vertical exaggeration approximately 7/1. Dashed cones are seamounts located slightly east or west of profile line. Top four profiles are in middle section of fracture zone where Clarion Trough is not continuous. Arrows indicate where extrapolated great circle trend of western part of trough intersects line of profile.

tion along a straight line from a continuous trough to a trough interrupted and bordered by volcanoes to a line of volcanic islands to a line of continental volcanoes, there is no doubt that all these features are related and form a part of the Clarion fracture zone.[2]

The boundaries of the fracture zone in the vicinity of the Revilla Gigedo Islands cannot be determined from the few soundings available. The extended line of the great circle followed by the Clarion Trough passes midway through the group—slightly north of Clarion Island and slightly south of San Benedicto Island—indicating that the islands lie near the center of the fracture zone like the smaller seamounts to the west. This trend is supported by an echogram taken along a southerly course between the Revilla Gigedo Islands and the coast of Mexico. It shows some unusually deep holes which, in the absence of other soundings, may be unrelated to the Clarion Trough but lie on the same great circle.

The Clarion fracture zone may continue eastward into the Caribbean basin. Earthquake epicenters in the Caribbean basin trend in a curved band which links with the circum-Pacific earthquakes through the Volcanic

[2] Almost 150 years ago Humboldt observed that the volcanoes from Oribaza to Colima trend across the general structure of Mexico and that the trend may continue out to sea. "Do not these analogies give us reason to suppose that there exists in this part of Mexico, at a great depth within the Earth, a fissure stretching from east to west through a space of 137 leagues (343 miles), and through which the volcanic fire has made its way at different times, bursting the outer crust of porphyritic rocks, from the coasts of the Gulf of Mexico to the South Sea? Is this fissure prolonged to that little group of islands, called by Colluet the Archipelago of Regigedo, and round which, in the same parallel with the Mexican volcanoes, pumice stone has been seen floating?" (*in* Mather and Mason, 1939, p. 182).

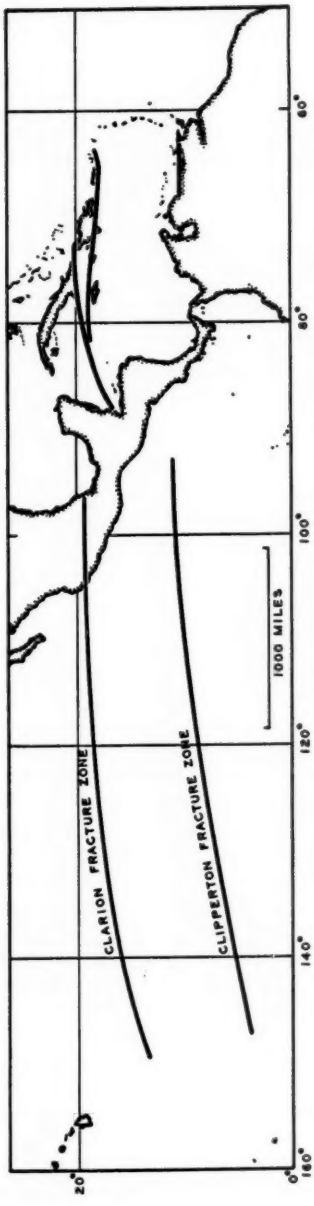

FIGURE 17.—RELATION OF CLARION AND CLIPPERTON FRACTURE ZONES TO GREAT TRANSCURRENT FAULTS OF CARIBBEAN AREA
Faults from Hess and Maxwell (1953, p. 4) and Hess (1938, p. 88)

Province of Central Mexico (Gutenberg and Richter, 1949, p. 37) which is a part of the Clarion fracture zone. If the fracture zone crosses Yucatan along this band of epicenters, it might connect with the Cayman or "Bartlett" Trough (Hess, 1933, p. 34–35) which exhibits much of the characteristic topography of a fracture zone although with unusually great relief. From this area the fracture zone might follow the great east-trending transcurrent fault indicated by Hess and Maxwell (1953, Fig. 2, p. 4) (Fig. 17). The left-lateral movement shown by Hess and Maxwell agrees with the direction of movement on the Clarion fracture zone deduced by the writer from the stress pattern in the northeastern Pacific basin. The writer's preferred hypothesis of fracture-zone origin is seriously weakened if this extension of the fracture pattern exists.

Clipperton Fracture Zone

Clipperton fracture zone is named after Clipperton Island which lies within the fracture zone and is the only island near it in the Pacific basin. The fracture zone lacks the great relief of those to the north, and it has been crossed in comparatively few places. Even the existence of the zone would be questionable were it not that its position can be predicted before an area is sounded. After the discovery of the Mendocino, Murray, and Clarion fracture zones, other parallel trends were sought at distances equivalent to the spacing between the known zones. A few spot-sounding lines and the *Mid-Pacific* Expedition fathograms indicated a 200-fathom regional change in depth across a line with the proper trend and position. This line, extended, passed by Clipperton Island which previously had been unrelated to any known structural trend. These relations suggested a fracture zone, and its position was predicted by assuming a great-circle trend. The course of the *Shellback* Expedition intercepted the proposed trend midway in a 1400-mile gap between previous sounding lines and Clipperton Island. Despite the length of the interpolation, a zone of exceptionally rough topography separating regions with different depths was found at the expected position. The northern limit of the zone of rough topography (fracture zone) was

about 10 miles north of the great-circle trend. The position of the fracture zone has since been predicted and confirmed in three other widely separated positions.

The ridges have about 300 fathoms relief. The regional depth changes from about 2150 fathoms south of the fracture zone to 2350 fathoms north of it.

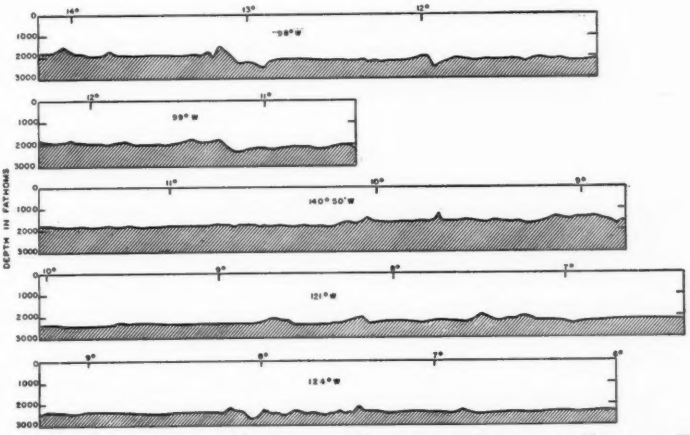

FIGURE 18.—APPROXIMATELY NORTH-SOUTH PROFILES OF CLIPPERTON FRACTURE ZONE
Vertical exaggeration about 7/1

On the basis of bathymetry, the fracture zone has been traced for 3300 miles. In its western part from 153°W. to 125°W. Long. it appears on four spot-sounding lines and on the echograms of the Swedish *Albatross* and the *Mid-Pacific* expeditions. No steep scarp or asymmetrical ridge has been found; merely a gradual change in depth of about 200 fathoms (Fig. 18, profile at 140°W.). The absence of the typical topography of a fracture zone may not be significant, because the *Mid-Pacific* track barely entered the fracture zone and then changed course for Hawaii, and the other sounding records give no details of the topography in the fracture zone.

At 124°W. the fracture zone consists of a band of irregular topography about 50 miles wide (Fig. 18). Two peaks, possibly ridges, rise about 200 fathoms above the regional depth, and a trough is about 300 fathoms below regional depth. The maximum relief in a continuous slope is 410 fathoms. The regional depth does not change across the fracture zone.

At 121°W. Long. the zone of irregular topography is about 80 miles wide. Two asymmetrical ridges about 40 miles apart may form the boundaries of the fracture zone (Fig. 18).

East of Clipperton Island the topography is complicated by a north-trending swell with irregular relief. An echogram at 105°W. shows a 200-fathom change in regional depth at the expected position of the fracture zone (Fig. 18), but the position coincides with the approximate boundary of the north-trending swell and the change in depth may not be related to the fracture zone. Another echogram 60 miles to the east shows irregular topography but no regional change in depth. Echograms at 99° and 97° 30'W. show irregular topography with pronounced deeps (Fig. 18) near the expected position of the fracture zone, and a band of anomalous deeps is shown farther east by spot soundings. The band is roughly 120 miles wide or almost double the usual width of a fracture zone. This may merely reflect inaccurate positioning, but the fracture zone may branch.

The Clipperton fracture zone has not been traced east of 97°W., but if the trend is extended into the Caribbean region (Fig. 17) it coincides approximately with a great fault along the northern edge of South America (Hess, 1938, p. 88). If this fault is a continuation of the fracture zone, the zone closely follows a great circle for 5600 nautical miles

(6400 statute miles) or about a quarter of the circumference of the earth.

Other Fracture Zones (?)

Four fracture zones have been discovered, and others may be found as more echograms become available from other regions in the Pacific. Possible locations are about 600 miles north of the Mendocino fracture zone, midway between the Murray and Clarion fracture zones, and about 600 miles south of the Clipperton fracture zone. These positions are suggested by the regular spacing of the known zones. The small number of echograms and spot-sounding lines now available justifies only a brief discussion, but they indicate that all three possible fracture zones may have some local topographic expression. An east-west line of seamounts (or a ridge) at the expected distance south of the Clipperton fracture zone (Shumway, 1953) can be traced for about 600 miles but does not appear on any of the three available echograms between 110° and 125°W. A line of seamounts (or a ridge) trends roughly parallel to the Mendocino fracture zone at the expected distance north of it, but the line does not continue as far east as the Gulf of Alaska. Regional depth does not differ on the two sides of this line.

The most probable position for another fracture zone is midway between the Murray and Clarion fracture zones. A zone at this location would give a regular unit spacing for all the zones from Mendocino to Clipperton rather than a unit spacing between the northern and southern pairs and double the unit spacing between the middle pair. A linear deep, with accompanying ridges and seamounts, which trends about N. 80°E. through 27°N., 119°W., probably marks a fracture zone. This band of irregular topography has been found on six echograms giving a known length of 250 miles. Near 119°W., the main trough is about 3 miles wide and about 400 fathoms below regional depth of 2150 fathoms. An asymmetrical ridge on the south side of the trough rises to 1450 fathoms and has a relief of 1100 fathoms. Elsewhere in the zone the relief is not so great. The trough is only 100–150 fathoms deep at 121°W., and it is not found at 122° 30′W.; instead the zone of rough topography is marked by four peaks 200–300 fathoms high. The zone of rough topography has not been traced west of 122° 30′ nor east of 117° 30′. In both directions spot soundings suggest that the sea floor is about as irregular as in the Baja California Seamount province. Echograms might permit tracing the zone to the west, but none are available.

Origin of Fracture Pattern

Plastic Deformation in Earth's Crust

The mode of deformation of the earth's crust in response to tangential stress varies with depth. Near-surface rocks are relatively brittle and deform according to Mohr's law so that planes of maximum shear are symmetrically disposed around the direction of principal stress at angles less than 45°. Deeper in the crust, rocks are subjected to high temperatures and pressures and tend to flow plastically. Evidence suggests that if the whole thickness of the crust is stressed the resulting primary deformation is plastic, and the pattern accords with the theory of plastic deformation wherein the planes of maximum shear are symmetrically disposed around the direction of principal stress at angles that may exceed 45°. Bijlaard (1936) and Vening Meinesz (1947, p. 6–28), for example, use the theory of plastic deformation to explain the pattern of island arcs and of shear patterns in the earth's crust respectively. This theory permits relating the northeastern Pacific fracture zones to the great strike-slip San Andreas fault as a system of complementary shears, and no hypothesis of brittle fracture supports such a relationship. The writer considers this evidence that the primary deformations of the crust are plastic.

The theory of local plastic deformation is based on laboratory tests of stress. In a compression or tension test a polished surface of a piece of mild steel is suddenly marred by a network of dull lines when the yield stress is reached (Van Iterson, 1947, p. 114). These Hartmann or Lüders' lines mark narrow zones of plastic deformation within the main body of stressed but undeformed material. Continued stressing after the yield stress is reached produces shearing in the plastically deformed zones (Fig. 19 after Sully, 1949, Fig. 36), but

a pattern of zones of plastic deformation does not necessarily imply shearing in all zones. Commonly shearing is restricted to one or two complementary zones. Both the theory of plastic deformation and experimental observations show that between two zones the angle that incloses the principal stress may exceed 90°. Experimentally, angles of about 110° are common. The angles depend on the difference in the magnitude of the stresses rather than in their absolute magnitude.

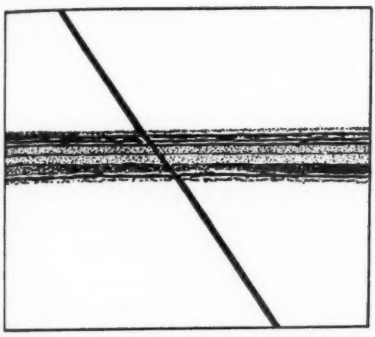

FIGURE 19.—DISTORTION OF STRAIGHT LINE BY SHEARING IN ZONE OF PLASTIC DEFORMATION

A copy of photograph (Sully, 1947, Fig. 36) of surface of stressed sample. Straight scratch appears refracted in deformed zone because of very small strike-slip movement on large number of shear planes.

Nadai (1931, p. x-xi) suggested that gross structures in the earth's crust are the equivalents of Lüders' lines:

> "The flow or slip lines, which frequently appear as a pattern with an astonishingly regular symmetry on the surface or in sections of solid bodies stressed above the plastic limit, have proved an extremely interesting object of investigation and a valuable means for analyzing the stress distributions under which they were produced. . . . In the hands of the geologists, who in their faults have observed similar phenomena on a large scale for a long time, these surfaces might serve to decipher the riddles in the formation of high mountain chains, just as their smaller relatives have helped to describe more precisely the plastic states in permanently deformed bodies."

Various experimental observations regarding Lüders' lines may provide clues in the interpretation of the deformation of the earth's crust by local plastic zones: (1) The zones may be a surface phenomena or may cut through the entire test piece depending on the type of stress. (2) Compression may produce a narrow welt in the plastic zone, and tension a narrow furrow (Nadai, 1931, p. 88), so that tension and compression may be differentiated even though the angles are the same; however, either stress may produce a gentle slope (Fig. 20). (3) The spacing between lines in some materials is a function of the rate of stressing (Nadai, 1931, p. 111). Rapid stressing produces a denser network of lines. (4) The lines are narrow zones, and the width of the zones may be a function of the shape of the material. The width of the zones is of the same order of magnitude as the thickness of the plate if a thin plate is plastically deformed (Bijlaard, 1951, p. 518).

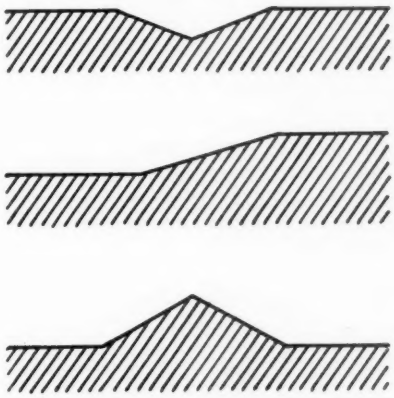

FIGURE 20.—PROFILES OF SURFACE DISTORTIONS PRODUCED IN ZONES OF PLASTIC YIELDING BY VARIOUS STRESSES (from Nadai, 1931, p. 88)

Top, furrow caused by tension; *middle*, slope caused either by tension or compression; *bottom*, welt caused by compression.

Possible Origins

Any acceptable origin must have been competent to produce the observed pattern of deformation. If several origins seem acceptable, one that can produce other major structures may be preferred. Inasmuch as the San Andreas fault is one of the most important structures on the continent adjacent to the northeastern Pacific, it may be used to test hypotheses. In addition, the simplest hypothesis may be preferred on philosophical grounds.

Individually the fracture zones of the northeastern Pacific are among the major tectonic features of the earth's crust; as a group they are spread over an area as great as North America. Even so vast a deformation may have a local cause, or it may be only a part of world-wide deformation with a planetary cause. The working hypotheses of origin include a shift in the poles, a change in the earth's flattening, shrinking of the earth, and local or Pacific-wide convection currents.

If the beginning of the fracturing could be accurately dated the number of working hypotheses could be reduced. The change in flattening and the shift in the poles were in early Precambrian time, the shrinking of the earth is continuing, and the local or Pacific-wide convection currents probably existed in Mesozoic-Cenozoic time. The writer has found no evidence that the fracture zones existed prior to the Cretaceous Period; however, the evidence for dating is meager, and in any event the possibility of Cretaceous rejuvenation of Precambrian faults cannot be excluded.

Shift in Poles

The spinning earth is slightly flattened at the poles and bulges at the equator. If the whole crust should shift over the relatively plastic mantle, the shape of the crust and the mantle would no longer coincide, and the crust would be stressed. The former equatorial region of the crust would be too large for the underlying mantle, and the stress would be compressional. Conversely, the stress in the former polar regions would be tensional.

Vening Meinesz (1947, p. 19–24) has determined equations for the values and orientations of such stresses. Drawing on a theory of Bijlaard's (1936, p. 7–10) regarding the plastic deformation of thin plates, he has also shown the orientation of the lines of deformation (shear net) resulting from various angular displacements of the poles. A polar shift of 70° along the 90° meridian would produce a shear net that shows a statistically significant correlation with the observed topography and inferred structures of the crust. Vening Meinesz has advanced the hypothesis that such a shift has occurred and that the north pole was once near Calcutta—probably in Precambrian time. He believes that a gradual shift of the whole crust produced stresses which plastically deformed the crust and eventually sheared it. Further, he finds little positive correlation with any other shear net caused by polar shifting and deduces that the shearing has occurred but once, and that subsequently the energy which shifted the crust may have been expended in friction between the fractured blocks.

The strength of Vening Meinesz' argument lies in the correlation between the observed topography and the computed shear net. However, as he observes, the possibility of some bias in measuring orientation of topography cannot be excluded. The fracture zones of the northeastern Pacific were unknown in 1947 so that no element of bias enters into a comparison of the topography of these zones with the various shear nets proposed by Vening Meinesz. (This does not apply to any new shear net proposed by the writer.) In other respects the fracture zones individually and as a group are ideal for testing the existence of any unique world-wide shear net. They are essentially linear (length to width ratio is about 30/1), and three of them follow great circles for distances of more than 1000 miles. Further, unlike many proposed lineations on the continents, the topography has not been materially altered by erosion, sedimentation, or later tectonic deformation. Their orderly configurations strongly suggest that the individual fracture zones represent single lines of deformation and that, as a group, they form a pattern. The pattern is spread over such a large area that whole curved sections of hypothetical shear nets (on Mercator Projection maps) may be tested at once rather than dealing with short, straight, local sections.

Vening Meinesz correlated his computed shear net and observed topographic and tectonic lines by determining the ratio between the length of topographic lines correlated with the net and the length correlated with some random directions. A deviation within 12° was considered a positive correlation. The bisectors of the angles between the lines of the net were taken as the random directions in any given area.

This method is hardly applicable to the northeastern Pacific because almost all well-

defined linear topography is within the fracture zones and is subparallel. However, the method gives an infinite correlation ratio for the Mendocino and Murray fracture zones and a zero correlation ratio for the Clarion and correlation with topography (Umbgrove, 1947, p. 305). Consequently, any such hypothesis must appear to be supported by the preferred orientation of the topography. Vening Meinesz (1947, p. 28–48) has attempted to eliminate

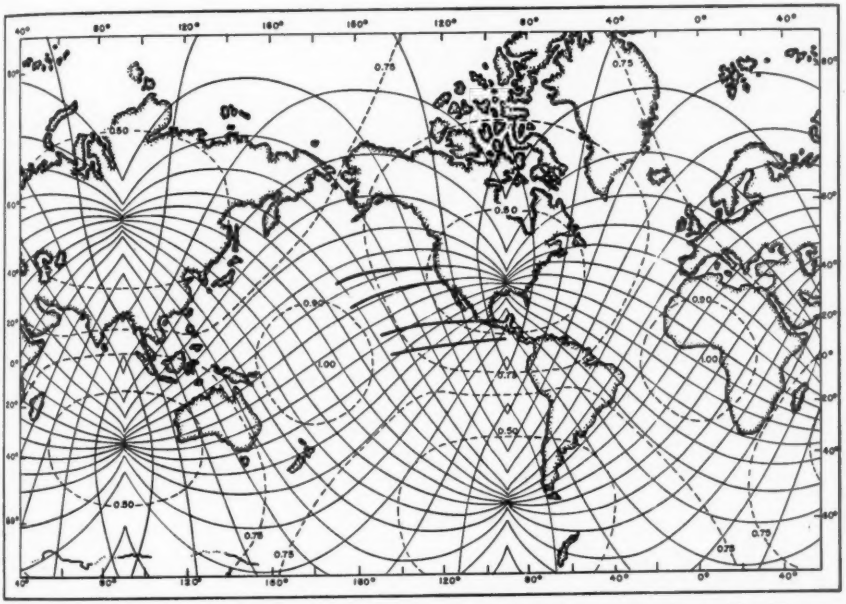

FIGURE 21.—COMPARISON OF PATTERN OF FRACTURE ZONES AND WORLD-WIDE SHEAR NET WHICH WOULD BE PRODUCED BY MIGRATION OF NORTH POLE FROM NEAR CALCUTTA TO ITS PRESENT POSITION
(According to Vening Meinesz, 1947)

Clipperton fracture zones (Fig. 21). The Mendocino fracture zone does not deviate from Vening Meinesz' preferred shear net by more than 12° anywhere along its 1400-mile length, and it follows the shear net exactly for about 700 miles. The correlation between the shear net and the Murray fracture zone is even more extraordinary. For 1700 miles the deviation between the two scarcely exceeds 5° although the bearing of the net itself changes by about twice that amount. Clarion and Clipperton fracture zones show a no less remarkable lack of correlation with the shear net. Neither trends within 12° of the net anywhere in a total distance of about 6000 miles.

The main trends of the earth are diagonal so that any mainly diagonal hypothetical shear net inevitably shows a better than random this spurious correlation by making a quantitative comparison of the degree of correlation of shear nets produced by all plausible planetary stresses. He measured correlation ratios for the topography of almost half the world; for the polar-shift hypothesis he obtained values of 325,700 km which correlate with the net, and 139,000 km which correlate with the random directions. Adding the fracture zones to these lengths does not materially affect the ratio between them.

Nevertheless, the lack of correlation between the shear net and the Clarion and Clipperton fracture zones appears fatal to at least part of Vening Meinesz' hypothesis. If an integrated fracture pattern, such as exists in the northeastern Pacific, in part agrees with the proposed shear net and in part conspicuously dis-

agrees, it suggests that the partial agreement is fortuitous. However, a shift in the poles can account for the trends of all four fracture zones if that part of the hypothesis which proposes

(1) In Precambrian time the north pole migrated from the vicinity of Calcutta toward central Greenland. When the pole had moved through an angle of 70° the resulting stresses

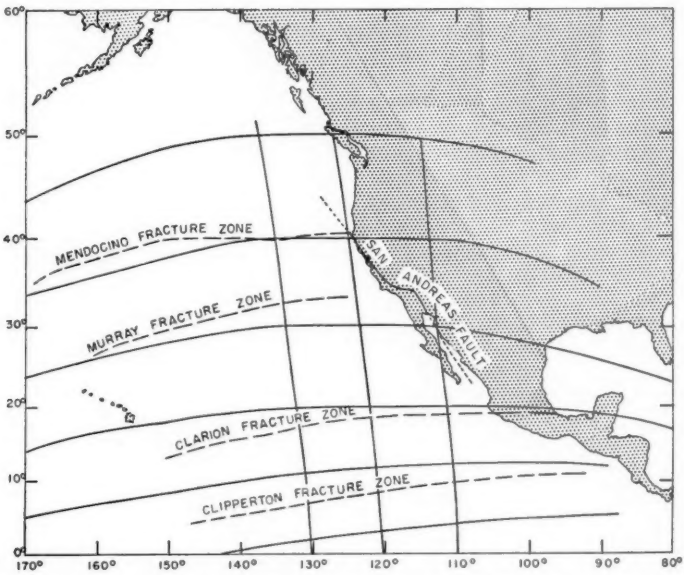

FIGURE 22.—COMPARISON OF FRACTURE ZONES WITH SHEAR NET WHICH WOULD BE PRODUCED BY MIGRATION OF NORTH POLE FROM GREENLAND TO ITS PRESENT POSITION

only one fracturing is discarded. The trends of the Clarion and Clipperton fracture zones agree closely with a shear net which would result if fracturing occurred after the pole had moved from 76°N. Lat., 40°W. Long. (in central Greenland) to its present positon (Fig. 22). Vening Meinesz' hypothesis places stringent restrictions on the possible movement of the north pole from the vicinity of Calcutta in order to obtain the same agreement between the calculated shear net and observed topography and geological structures. The movement of the pole cannot have exceeded 70° at the time or fracture, nor have deviated much from the 90°E. meridian. The proposed position of 76°N., 40°W. for the north pole lies at an angle of less than 2° to the left of the 90° meridian; according to this hypothesis it is one of the possible intermediate positions of the migrating pole. The distance of migration is more than 70°, however, and a somewhat complicated sequence of events is required:

produced crustal deformation in some places including the Mendocino and Murray fracture zones. The complementary shear lines in Vening Meinesz' net trended about N.20°W. in central California; the San Andreas fault which trends about N. 30°W. may also have been formed at this time.

(2) The migration continued along the same bearing until the pole reached central Greenland, but no new shear net was formed because the shear net did not deviate significantly from the existing fractures. The energy produced by the movement was dissipated as friction between the crustal blocks.

(3) The pole migrated from central Greenland to its present position during Precambrian time. No new fractures were formed where the shear pattern corresponding to this movement trended roughly parallel to the earlier fractures, but they were formed in some previously unfractured areas or where the new shear pattern was at a large angle to the earlier one. The

Clarion and Clipperton fracture zones were formed in such an area.

Although the path of migration is more complicated than required by Vening Meinesz' basic hypothesis, the cause of the migration he proposed is adequate to account for the complication. If subcrustal currents could slide the rigid crust over the mantle so that the pole moved from Calcutta to its present position, one set of currents might move it to central Greenland, and then another set might become dominant and move it to its present position.

A shift in the poles with two periods of fracture gives the observed pattern of the northeastern Pacific fracture zones and may explain the orientation of the San Andreas fault. It remains to be seen whether the stresses are adequate to deform the crust. Vening Meinesz (1947, p. 21) has computed that the maximum possible stress resulting from a shift in the poles would be 2230 kg/cm² assuming that the ellipticity of the earth was 1/297—its present value. Vening Meinesz concludes that stresses no smaller than half the maximum can deform the crust. For a shift of 70° the maximum value would be 2160 kg/cm², and in the vicinity of the Mendocino and Murray fracture zones it would range between about 0.75 times the maximum to the west and 0.5 times the maximum to the east (Fig. 21). A shift in the pole from central Greenland to its present position would yield a maximum stress of 540 kg/cm², and the value would range from 1.0 on the west to 0.75 times the maximum on the east of the area of the Clarion and Clipperton fracture zones. Values of this magnitude are not adequate to produce world-wide fracturing, but localized deformations seem possible. Much larger stresses would result if the pole migrated in the early history of the earth, when the moon was closer to the earth and consequently the earth was flatter.

Change in Earth's Flattening

According to Sir George Darwin's theory the moon separated from the earth, and tidal friction between the two bodies slowed the earth's rotation around its axis and caused the moon to recede to its present orbit. The origin of the moon from the earth is not now accepted (Jeffreys, 1952, p. 234–235), but the slowing down of the earth's rotation and the recession of the moon from the earth are retained. If the earth is spinning more slowly than it did in the past it was formerly flatter. The change in shape has stressed the crust-producing compression in the equatorial region, which decreased in diameter, and tension in the polar regions, which increased in diameter.

Vening Meinesz (1947, p. 28–47) finds that the shear pattern produced by this stress shows little correspondence to the topography and major structures of the earth, and that the stress probably is not great enough to have deformed the crust in the last $1.6 \cdot 10^9$ years, according to Jeffrey's values for the change in flattening in that time. The stress is much greater if an earlier time and a greater flattening are considered, but some question exists regarding the earliest time at which the crust could develop permanent stresses.

The pattern of the northeastern Pacific fracture zones argues against the hypothesis of a change in flattening around the present axis. The possibility remains that fracturing resulted from a change in flattening at a time when the poles were not in their present position. Two possible positions of the pole deserve brief discussion. If the north pole were at 50°N., 50°W., in early Precambrian time, a change in flattening would give a shear pattern corresponding closely to all four northeastern Pacific fracture zones but with no correspondence with the trend of the San Andreas fault. If the pole were at 66°N., 78°W., the shear pattern would correspond to the Mendocino and Murray fracture zones and the San Andreas fault but not to the Clarion and Clipperton fracture zones. A composite hypothesis is required to explain the origin of the southern fracture zones; a movement of the north pole from central Greenland to its present position, which has already been proposed to explain the pattern of these fracture zones, offers a possible solution.

It is doubtful whether either hypothesis is adequate to produce the required deformations. The maximum stresses caused by a change in flattening during the early history of the earth may have deformed the crust in some places,

but in the eastern half of the northeastern Pacific the stresses were less than half the maximum value. The only reason for proposing a change in flattening and the polar-shift hypothesis was to explain the origin of the San Andreas fault as well as the fracture zones, but the fault lies at the latitude where the stresses would be a minimum. Consequently, this hypothesis may be discarded.

Shrinking of Earth's Crust

Compression caused by the shrinking of a cooling earth is considered a plausible hypothesis of mountain building. The writer is unable to relate the world-wide stress pattern produced by contraction to the local strain pattern of the fracture zones, but Wilson's (1951, p. 94–96) proposed variation of the contraction hypothesis yields a stress orientation in the fractured area. In addition to finding several new and significant relations in structural geometry, Wilson has extended observations by Sollas (1903) and Lake (1931) and integrated them with the physical theory of Scheidegger and Wilson (1950). His argument regarding island arc formation is:

(1) The centers of the arcs of small circles described by island arcs and mountain ranges of the present fall on two great circles at approximately right angles, one around the Pacific and one across the length of Asia.

(2) The great circles mark tension cracks or flaws produced below the surface of no strain by cooling of the earth.

(3) Above the level of no strain (about 100 km deep) compression produces faults at points of crustal weakness in the shape of sections of cones. The surface outcrops of the faults are the sites of island arcs.

(4) Sections of cones correspond to one of the few ways in which a spherical shell can fail around a local weak point.

The hypothesis of crustal shortening may be questioned on general grounds as well as with regard to the formation of the fracture zones. The sufficiency of crustal shortening caused by cooling has been questioned repeatedly, but a re-examination of estimates of shortening in mountain ranges (Jeffreys, 1952, p. 306–309) indicates they are exaggerated, and that the total shortening is not greater than that which might be produced by cooling. The shortening of the crust required by the formation of fracture zones is uncertain but probably is no greater than the shortening in any single major mountain range, so only a small increase in total crustal shortening is required to explain the fracture zones.

For Wilson's hypothesis in particular, the reality of the tensional great circle around the Pacific may be questioned. The scattering of the centers of small circles may be too great for a significant relationship. The center of the Marianas arc, to take the extreme example, is more than 1000 miles from the proposed great circle. Cause and effect may perhaps be expressed equally accurately by saying that island arcs occur around the Pacific, and the shape of the Pacific Ocean approximates a great circle.

The westernmost parts of the fracture zones are about 3600 miles from Wilson's great circle which crosses North Dakota, Alabama, Cuba, and Colombia. If tension along this great circle produced compression in the upper 100 km of the crust, the stress would have to be transmitted in the crust around the curve of the earth for 60° of arc to form the fracture zones. This appears improbable but need not be argued because the geometry of the stress pattern is impossible. Localized plastic deformation, which gives the only explanation of the pattern of the fracture zones and the San Andreas fault, requires that the principal stress lie at an angle of about 55° to the band of deformation. Assuming the principal stress is perpendicular to Wilson's great circle, this condition is met for the Mendocino fracture zone, but the Clarion and Clipperton fracture zones are almost perpendicular to the great circle. The fracture zones were not produced by this cause.

Composite Origin

A composite origin of polar shift followed by combined contraction and change in flattening (Bijlaard, 1948, p. 6–7) may explain the common north-south and east-west lineations in the crust which—if unexplained—weaken the significance of Vening Meinesz' hypothesis of polar movement (Umbgrove,

1947). According to this hypothesis, the superposition of stresses caused by contraction and change in flattening forms meridianal deformation. The deformation decreases the intensity of part of the stress pattern so that the principal and intermediate stresses are interchanged, and deformation is produced along east-west lines.

The hypothesis gives a better agreement with the alignment of all four fracture zones than a hypothesis of polar shift or change in flattening alone; however, the agreement is not so good as with the hypothesis of two polar shifts or nonplanetary compression.

Local Convection Current

The possibility that the earth's crust may be deformed by subcrustal convection currents was advanced by Vening Meinesz *et al.* (1934) with reference to the formation of island arcs. His hypothesis is that convection cells with horizontal axes exert drag on the bottom of the crust. The drag produces a compression in the crust which leads to deformation. The presence of convection currents in the upper part of the mantle is supported by mathematical developments which show that a horizontal temperature gradient would produce sufficient stress to start convection in uniform material (Brooks, 1941, p. 548). The existence of the earth's magnetic field can be explained by convection currents in the core (Elsasser, 1950, p. 27–29), and the drag of these currents may induce counter-rotating currents in the mantle. Convection currents probably were formed near the surface in the early thermal history of the earth (Jeffreys, 1952, p. 331–332), but the ease of convection in the upper few hundred kilometers of the mantle has since decreased because the material has become nonuniform (Birch, 1951, p. 534). One compelling argument for convection just below the solid crust is advanced by Hess (1951, p. 524). Tectogene roots persist without uplift for periods as great as 50 million years. Stresses acting in the crust could not prevent rising in areas with such high negative gravity anomalies, so a downward drag on the tectogene root is required, which in turn demands a convection current.

With so much evidence for the existence of convection currents, it is reasonable to look to one for the origin of fracture zones (without enquiring how it chanced to exist in the northeastern Pacific.) Judging only by the four known fracture zones, the convection current was roughly equidimensional and had a surface area about 5 per cent as great as the earth. If some suspected fracture zones exist and if all the zones had the same origin, the convection current may have been much larger. The pattern of the marine fracture zones could have been produced by either a northeast-southwest or a northwest-southeast compression. A northeast-southwest compression is required, however, if the San Andreas fault is a complementary shear. The angle between the San Andreas fault and the Mendocino and Murray fracture zones is 120°–125°, which is more than the common angle of 110° measured between Lüders' lines, but it is possible, provided some secondary stress is acting perpendicular to the principal stress. The origin of the secondary stress need not be the same as the primary stress. A world-wide compression caused by crustal shrinking, for example, would produce a secondary stress and increase the principal stress.

Pacific-wide Convection Current

The orientation of the principal stress required to produce the marine fracture zones and the San Andreas fault as complementary shears is about N. 25°–30°E. or 20°–30° from perpendicular to the continental margin. The stress, therefore, is a compression roughly perpendicular to the margin of the Pacific Basin. Around most of its periphery the Pacific Ocean is ringed by oceanic deeps, island arcs, folded mountains, and earthquake epicenters—all evidence of Mesozoic and Cenozoic compression perpendicular to the margin of the Pacific basin. The major exceptions are the seismically stable coast of Antarctica and the central coast of North America which is seismically active but in many ways unlike the other areas. Mesozoic arcuate mountain ranges may have existed, but not Cenozoic island arcs. The fracture zones lie off the central coast of North America and indicate that a post-Mesozoic compression perpendicular to the margin

of the Pacific basin has acted there as well as where island arcs have been formed.

The writer agrees with Griggs (1939, p. 618) and Scheidegger (1953, p. 148) that the only plausible hypotheses for the origin of island arcs are compression caused by shrinking of a cooling earth and compression caused by the drag of subcrustal convection currents. Crustal shrinking (at least in the form proposed by Wilson, 1951) could not have produced the fracture zones. Consequently if island arcs and fracture zones are produced by the same cause, the cause is subcrustal convection currents.

Granting convection currents and their ability to produce the cross section of an island arc, the arcuate plan remains to be explained, and it is only in plan that island arcs and fracture zones can be compared because the cross section of the fracture zones is essentially unknown. Scheidegger (1953, p. 144) has indicated it is difficult to account for an arcuate failure of the crust by convective drag because of the necessary continuity of vortex lines in the currents. Vening Meinesz (1948) has overcome some difficulties by proposing that the plan of the East Indies has been determined in part by a world-wide fracture pattern formed in Precambrian time by a migration of the poles.

Bijlaard (1936; 1938; 1951) has proved that the initial failure of the crust occurs in zones of plastic deformation oriented at angles of about 55° to the principal stress, and that both the angles at the junctions between island arcs and the maximum angles tangent to the arcs approximate 110°. He proposes (1951, p. 519) that a subcrustal current acting from Asia toward the Pacific produced zones of plastic deformation followed by a plastic downbuckling and the subsequent development of an island arc in much the same manner as proposed by Vening Meinesz *et al.* (1934). This process accounts for the pattern and also the cross section of the island arc, although the disagreement between the present and past stress patterns implies that the direction of the current has shifted since the initial plastic failure of the crust. According to this hypothesis, deep-focus earthquakes form along a plane of maximum stress dipping 45° below the zone of plastic deformation. The hypothesis does not explain the reverse movement of deep-focus earthquakes nor the persistence of roots for tens of millions of years without rising.

Only Bijlaard's hypothesis gives a plausible explanation of the plan of both island arcs and the fracture zones of the northeastern Pacific area. Both are produced by plastic failure of the crust in relatively straight zones. Local conditions determine whether island arcs are produced at the intersections of the zone. Bijlaard's hypothesis also indicates that the scale of the required convection currents on two sides of the Pacific is about the same because the area from the Marianas arc to Asia is about the same size as the fractured area of the northeastern Pacific, whereas the areas of individual island arcs are an order of magnitude smaller. This relation suggests that the arcs are relatively local phenomena and that they owe their origin to some secondary effect which has not developed since Mesozoic time in the northeastern Pacific area.

Brooks (1941) proposes that, if initial cooling occurs in the middle of the Pacific basin, a downward movement of the mantle will ensue. This movement generates a circular convection current which in turn produces other convection currents in an annular pattern.

> "This is different from the polygonal pattern usually observed in plane convection, not only because we are here dealing with the spherical case, but primarily because there exists a region of maximum cooling which provides a center from which the convection-system originates. Now, every convection-problem can be analyzed into fundamental modes of motion, each of which, in the presence of an initial superdiabatic gradient, grows exponentially with the time, but each with a different exponential factor depending on the size of the corresponding convection-cell. In every case there is one particular cell-size that grows more rapidly than any other" (p. 550).

The optimum cell size produces a convergence at the center, a divergence 40° from the center, and a convergence 73° from the center. The outer convergence corresponds roughly to the margin of the Pacific Basin, and it is in this annulus that island arcs are found. "No tectogene occurs in the center of the ocean-basin, because of the absence of light continental material on which the currents could act" (p. 551). The period of the cycle of convection is about 12 million years which is taken to be about the right order of magnitude considering the uncertainty of the constants involved in the computation. In the later stages of the flow the

main convection tends to break up into a number of small cells. A high heat flow is predicted under the Pacific Basin.

opposite direction from the one proposed by Bijlaard, but either could produce the initial pattern of deformation.

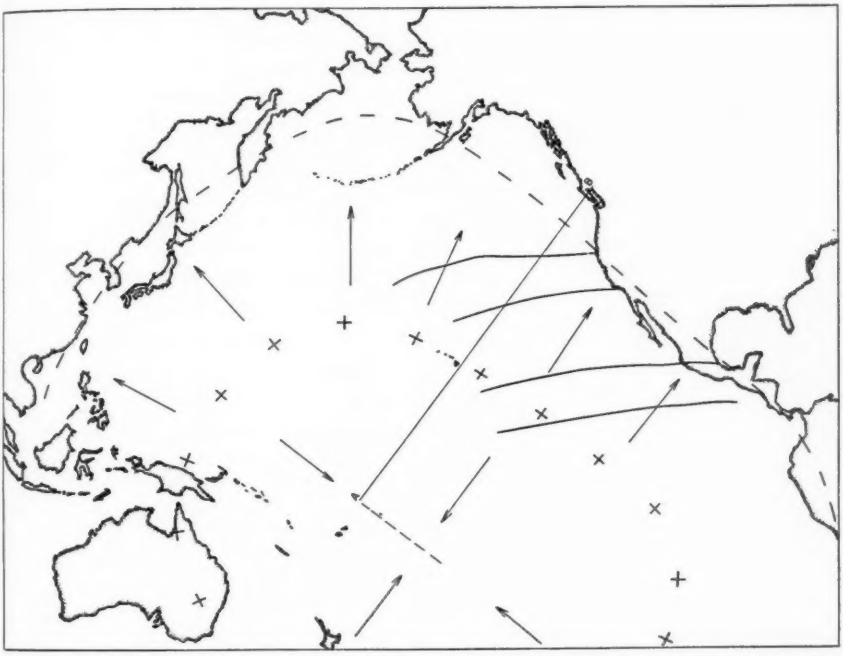

FIGURE 23.—ANNULAR CONVECTION CELLS PRODUCED BY COOLING IN CENTRAL PACIFIC AREA
Minus signs mark convergences, plus signs mark divergences, and arrows show horizontal movement. Fracture zones show good correlation with location and direction of movement of outer annulus. A profile along A-B appears in Figure 24 (drawn from data in Brooks, 1941).

This theory explains almost all the pertinent geological and geophysical features of the northern and southeastern Pacific basin, which is particularly impressive because many facts were not discovered until almost a decade after the theory was published. These are:

(1) A horizontal current acting under the whole area of the fracture zones, and which is properly oriented to produce the fracture zones and the San Andreas fault according to Bijlaard's theory of local plastic deformation (Fig. 23).

(2) A similar horizontal current under the Bonin-Marianas-Palau area which would be necessary for the widespread initial local plastic deformation required by Bijlaard's theory (1936) of the formation of island arcs in the western Pacific. The current is moving in the

(3) A divergence under the Hawaiian Islands which agrees with independent deductions (Dietz and Menard, 1953, p. 110) regarding the origin of these islands as indicated by the regional bathymetry (Fig. 24).

(4) The unexpectedly high heat flow through the floor of the Pacific Basin measured by Revelle and Maxwell (1952).

The theory shows no such high degree of correlation with the geology and geophysics of the southwest Pacific, possibly because continental Australia interrupts the otherwise circular plan of the Pacific basin. However, the anomalous arcs of the Solomon and New Hebrides islands, which face away from the Pacific, face toward the convection current which Brooks' theory would place under this area. The Tonga-Kermadec arc remains the major

unexplained feature in the Pacific. However, it lies near the central convergence proposed by the theory and may have been formed by it although the orientation is anomalous.

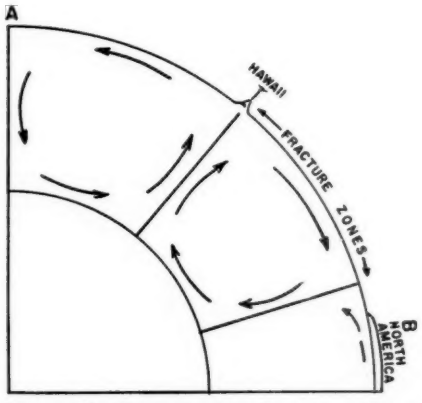

FIGURE 24.—PROFILE ACROSS CONVECTION CELLS

Showing how Hawaiian Islands are located along divergence and fracture zones are in area of crust which would be stressed by horizontal movement of cell (proposed by Brooks, 1941).

Even if the pattern of major structures in the north Pacific was determined by local plastic deformation in response to the crustal stress generated by annular convection currents, the occurrence of island arcs in some areas and not in others remains unexplained. Eddies form during the decay of the primary convection, and they may account for the formation of island arcs (Griggs, 1951, p. 518). The absence of island arcs in the northeastern Pacific might indicate that the primary current still prevails in the area, but some sort of secondary convection pattern seems required to explain the differences in regional depth on opposite sides of the Mendocino and Murray fracture zones. It is more plausible to assume that eddies formed in both areas. The principal difference in the initial deformation of the two areas is that many complementary sets of zones of plastic deformation were formed in the western Pacific, and only one set was developed in the northeastern Pacific. No explanation for this is evident, but similar relations have been observed in smaller fault patterns on land. This difference may account for the localization of island arcs if it is assumed that the root produced by the initial deformation favors the formation of an eddy. Intense eddies might form in the western Pacific where zones of plastic deformation intersect, and less intense eddies might elevate the sea floor on one side of a fracture zone in the northeastern Pacific. If no other factor had influence, island arcs would also be expected at the intersection of the San Andreas fault zone and the Mendocino and Murray fracture zones. Their absence suggests that convection under the continent or some outward movement of hot material from under the continent (Hess, 1951, p. 530) may also be required for the formation of island arcs, and that this is not occurring under North America.

Preferred Hypothesis

Both the hypothesis of two systems of fracturing caused by a shift in the poles and the hypothesis of fracturing caused by the drag of a convection current (either local or Pacific-wide) can explain the orientation of the fracture zones of the northeastern Pacific and of the San Andreas fault. A choice between them can be made only on the principle of simplicity. The polar-shift hypothesis requires two stress patterns to produce the fracture pattern, Precambrian fracturing by a process not now acting, and subsequent rejuvenation by other processes to explain Tertiary and present-day deformation, seismicity, and vulcanism; the convection-current hypothesis requires only one stress pattern and may still be active. The writer therefore prefers the origin by a convection current, and subsequent discussion in this paper will be related only to this origin.

Future field mapping on land and at sea may demonstrate that only one origin for the fracture zones is possible. If, for example, the fracture pattern of the northeastern Pacific is but a small part of a world-wide pattern, origin by a local or Pacific-wide convection current would be eliminated. On the other hand, if fracture zones are confined to the northeastern Pacific, a planetary cause would be improbable.

ORIGIN OF TOPOGRAPHY WITHIN FRACTURE ZONES

Generalized Characteristics

Sea-floor topography can provide an insight regarding tectonics which is not matched by

topography on land. In deep-ocean basins all the topography is constructional because the effect of erosion is negligible. Consequently a profile of the sea floor may be considered a structural profile except that sedimentation tends to fill depressions.

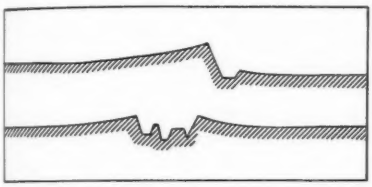

FIGURE 25.—PROFILES OF IDEALIZED TYPES OF TOPOGRAPHY FOUND IN FRACTURE ZONES

The topography within the fracture zones is distinguished from unfractured areas by the magnitude and character of the relief. It is of two general types (Fig. 25): (1) an escarpment on the steep side of an asymmetrical ridge separating regions with considerably different depths; examples are the eastern portions of the Mendocino and Murray fracture zones and most of the Clipperton fracture zone; and (2) two facing escarpments on the steep sides of asymmetrical ridges separated by linear ridges and deeps; examples are the western portions of the Mendocino, Murray, and Clarion fracture zones. Broad, shallow depressions flank the gentle slope of asymmetrical ridges of both types.

The principal aspect of origin which can be deduced from topography alone is whether fracture zones in cross section are elevated welts or depressed furrows in relation to the undistorted sea floor. A quantitative evaluation of the relative vertical movement within fracture zones is necessarily subjective because of the difficulty of establishing an average regional depth, but the fracture zones are welts. All 23 profiles of the four fracture zones show that the average depth of the sea floor in the zones is less than in the adjacent relatively smooth areas. In all but a few places, even the central band of linear deeps and ridges has an average depth above the floor of the region. The uplift of the asymmetrical ridges far surpasses the sinking of the central band in the few places where it has sunk.

Deformation within Plastic Zones

When Luders' lines are formed because the plastic-yield limit is exceeded, the surface in the zones of yielding becomes deformed (Fig. 20). The surface may be forced upward into a welt in case of compression, downward into a furrow in case of tension, or into a slope in either case (Nadai, 1931, p. 88). The fracture zones seem to be large equivalents of Lüders' lines, and their relief should be similar.

Inasmuch as the average profile of a fracture zone shows its elevation above the regional depth of the sea floor, the generating stress was compressional. This confirms the deduction of a compressional origin based on the strain pattern relating the fracture zones and the San Andreas fault as complementary shears.

Because deformation of the crust is not accomplished under the same conditions as in a testing machine, certain differences may be expected: (1) The crust rests on the mantle which buoys it up; any downward movement of the crust must displace the mantle and result in an upward movement elsewhere, and later isostatic adjustments may be expected. (2)The top of the crust probably is brittle and should deform by fracturing when the bottom of the crust and the mantle respond by plastic flow. Specific topographic features such as an asymmetrical ridge may be produced by this superficial fracturing, perhaps in response to vertical movements resulting from the lateral displacement of the mantle or isostatic adjustments within a fracture zone.

Elastic Bending

The relief of the East Indies has been explained in terms of elastic bending of a layered crust (Vening Meinesz, 1948). Inasmuch as the narrow ridges, deeps, and volcanoes of the fracture zones are in many ways similar to the relief of an island arc, possibly elastic bending could have produced this relief.

Vening Meinesz believes a compressional stress in the crust produces elastic instability so that waves are formed with wave lengths of a few hundred kilometers. The strain resulting from continued compression is concentrated in the trough of a wave which coincides with an incidentally weak part of the crust. Thus a

downbuckle is formed and with it an oceanic trench with ridges on one or both sides.

The existence of elastic bending in the crust has been dismissed by Bijlaard (1938, pp. 4–15) and Jeffreys (1952, pp. 311–314) on independent grounds. Bijlaard finds that the crust deforms plastically under a stress an order of magnitude smaller than required for elastic buckling, and local plastic deformation of the type proposed for the origin of the fracture zones precedes even plastic buckling. Jeffreys considers the possibility of elastic bending prior to failure of the crust and finds (p. 314) that "the combined effect of elasticity and gravity is such as to prevent elastic instability unless the thickness of the crust is less than something of the order of 12 m". As he further points out, the magnitude of models used for tests in laboratories results in bending, but the tests are irrelevant to the problem of the behavior of the crust.

Origin of Regional Differences in Depth

Composition of Pacific Crust

Those parts of the Mendocino and Murray fracture zones characterized by single great escarpments separate regions of the sea floor with significantly different average depths. Regional differences in depth are commonplace on the earth and are usually explained by differences in density in the underlying rocks. The problem is to explain why regions with different depths should be bounded by fracture zones. The differences in depth could not have antedated the fracture zones.

Isostasy prevails in any large area of the sea floor (Vening Meinesz *et al.*, 1934; Ewing, 1952, p. 89), therefore the differences in depth are caused by differences in the distribution of density in the crustal and subcrustal materials. Speculation regarding these differences is enlightened by recent geophysical studies of the structure of the sea floor. Refraction shooting in the Atlantic and Pacific has found only unconsolidated sediment, consolidated sediment or lava, sima, and ultra-sima (Raitt, 1949, 1951; Officer and Ewing, 1952; Officer, Ewing, and Wuenschel, 1952, pp. 793–800; *Capricorn* Shipboard Rept., 1953, pp. 21–27), and no other types of rocks are indicated in the Pacific by studies of seismic waves (Gutenberg, 1951, p. 438; Ewing, 1952, p. 88). Moreover the Mohorovičić discontinuity between sima and ultra-sima shows little significant variation in depth below the sea floor except where it is bowed down by loads of sediment near the continents (Officer and Ewing, 1952) or by seamounts or islands (Officer, Ewing, and Wuenschel, 1952, p. 800; Raitt, 1952, p. 23) or other structural topography. Exceptional crustal material may lie under the sea floor of the Easter Island Swell and the Ridge and Trough province (Gutenberg and Richter, 1935, p. 315, 324), although recent studies suggest this is unlikely (Oliver, Ewing and Press, 1953; *Capricorn* Shipboard Rept. 1953, p. 26).

Before the fracture zones were formed, turbidity currents spreading out from North America could deposit sediment wherever the sea floor was deepest. With enough time this process would have produced coalescing alluvial fans and a smooth, gently sloping sea floor such as is now found off the east coast of North America (Heezen, Ewing, and Ericson, 1951, p. 1407). After the formation of the fracture zones, the asymmetrical ridges stood as dams to the north-south movement of turbidity currents. Different rates of sedimentation on opposite sides of the fracture zones may have produced part of the differences in regional depth. Any roots under the fracture zones may also have dammed the convection current in the mantle which formed them. If so, secondary convection currents, or eddies, might have been established under the sea floor between the dams. If the rate of overturn of the eddies differed, some parts of the mantle would be heated more than others, and the resulting expansion may have produced part of the differences in regional depth.

Deep Plain and Baja California Seamount Province

The crustal structure of the eastern part of the Baja California Seamount province was studied by refraction shooting during the Mid-Pacific Expedition. The Mohorovičić discontinuity is about 5 km. below the sea floor, and above the layer of sima (velocity 6.7 km/sec) sediment is 10–700 m thick (Raitt, 1949). Refraction shooting in other parts of the Pacific during the *Capricorn* Expedition suggests that

the travel-time curves in the Baja California Seamount province can be interpreted to include a few hundred meters of volcanic material with a corresponding decrease in sediment thickness (Raitt, Personal communication).

This province is about 250 fm shoaler than the Deep Plain north of the Murray fracture zone. Even if no sedimentary cover existed in the Deep Plain, the maximum allowable thickness of 380 fm of sediment in the Baja California Seamount province is inadequate to explain this difference in depth because isostatic adjustment would reduce the elevation of the sea floor caused by the sediment to about 190 fm. Moreover, the topography in the two regions indicates that the sediment is thicker north of the Murray fracture zone than to the south. The smooth, graded profile of the Deep Plain suggests thick sediment, and the irregular topography of the Baja California Seamount province suggests a thin cover. Sediment spreading out from the continent in turbidity currents off Baja California and southern California is barred from reaching the deep sea by a band of troughs in the continental borderland and at the base of the continental slope and no thick blanket of sediment would be expected (Menard, 1955, pp. 239–242).

The many volcanoes and the irregular topography in the Baja California Seamount province suggest that a layer of lava may have elevated the sea floor relative to the Deep Plain which contains comparatively few volcanoes. However, Raitt's results show that the effect would be small. The lava dredged from seamounts in the province is vesicular to dense olivine basalt. The velocities in such basalts measured at Guadalupe Island off Mexico and at Bikini Atoll range between 3 and 4 km/sec. (Raitt, 1952, p. 20), suggesting a relatively low density. If the lava is formed from the underlying material and is less dense, the province is out of isostatic adjustment and rises with a net result that the elevation of the sea floor is about 1⅓ times the increase in thickness of the lava. Even so a layer of lava 1 km thick with a density of 2 gm/cc is required to produce the 250-fm difference in regional depth. Travel-time curves allow for less than half that thickness, and a reasonable minimum density is about 2.7 gm/cc; these values give an elevation of less than 100 fm. Consequently the formation of an appreciable thickness of lava is not sufficient to explain why the Baja California Seamount province rises above the Deep Plain.

Variations in the thickness of the simatic layer would produce corresponding variations in regional depth, but the sima below the Deep Plain would have to be very thin or absent to cause the depth difference below the Baja California Seamount province. An initial difference in depth of about 400 fm is required assuming (1) 300 fm of sedimentary fill in the Deep Plain producing a 200-fm elevation after isostatic subsidence, and (2) a 250-fm layer of lava in the Baja California Seamount province producing an elevation of approximately 70 fm after isostatic rise. Prior to the formation of lava and the deposition of sediment the weight of 4100 m of density 1.0 gm/cc plus about 5000 m of sima of density 3.0 gm/cc in the Seamount province was equal to the weight of 4800 m of water plus some thicknesses of sima and ultra-sima (3.3 gm/cc) with a total value of 4300 m. A layer of 4300 m of ultra-sima is required to balance the weights; therefore an absence of sima is indicated. A negligible thickness of sima under the Deep Plain has been suggested to explain the differences in regional depth (Menard and Dietz, 1952, p. 274), but the many recent geophysical measurements widely distributed in the Atlantic and Pacific show that the thickness of the simatic layer is relatively constant. The writer is reluctant to appeal to extraordinary conditions to explain the depth of the Deep Plain, and the possibility of no sima is dismissed.[3] Seismic waves which cross the entire Pacific including the length of the Deep Plain indicate an average thickness of 11 km of sima for the whole distance (Evernden, 1952). Assuming that 3 km is a reasonable minimum value for the thickness, the Deep Plain would initially be 150 fm below the Seamount province; 250 fm of initial relief remain to be accounted for.

Having considered the effect of sediment, lava, and sima, the only remaining variable is the density of the ultra-sima below the Mohorovičić discontinuity. The crustal structure in

[3] Field examination of refraction shooting records obtained during the *Cusp* Expedition suggests that the crustal thickness in the northeastern Pacific is not conspicuously different from elsewhere in ocean basins (Russell Raitt, Personal communication).

the Melanesian subcontinent which was measured during the *Capricorn* Expedition allows no explanation for the unusually shoal depth of the region except that the ultra-sima is less dense than in the deep ocean to the east, according to Russell Raitt and Roger Revelle (Personal communication). Consequently a similar difference in density may have produced most of the difference in regional depth between the Deep Plain and the Baja California Seamount province. Convective overturn related to the origin of the fracture zones offers a plausible explanation for the origin of density differences in the ultra-sima. The principal difficulty is to explain why the boundaries of the areas of relatively different overturn should coincide with the Murray fracture zone, which trends at 55° to the movement of the subcrustal current. Subcrustal currents may be capable of skimming off portions of the crust and so producing regional differences in depth (Griggs, 1939, p. 642–643), but the boundaries of the skimmed or thickened regions should be roughly perpendicular to the movement of the current. The formation of the deep area between the Mendocino and Murray fracture zones would require skimming the crust from an area about 2500 miles long and 600 miles wide oriented at an angle of 55° to the direction of the current. This appears impossible. A possible explanation results if it is assumed that the root pushed down below the fracture zone is relatively deep. The root under the fracture zone would be composed of material only slightly more dense than the surrounding mantle because the gravity anomaly is negligible (Vening Meinesz *et al.*, 1934, p. 90). Granting such a root, the subcrustal flow which formed the fracture zone would be confronted with a relatively rigid dam oriented at an angle to the flow. The dam would impede the flow and might generate counter eddies or rollers with horizontal axes and a direction of movement contrary to the unimpeded flow below (Fig. 26). Rollers are indicated by the first movement of deep-focus earthquakes associated with oceanic trenches (Hess, 1951, p. 530), although the cause of the rollers is not necessarily the one suggested here. If the rate of overturn of the rollers varies between

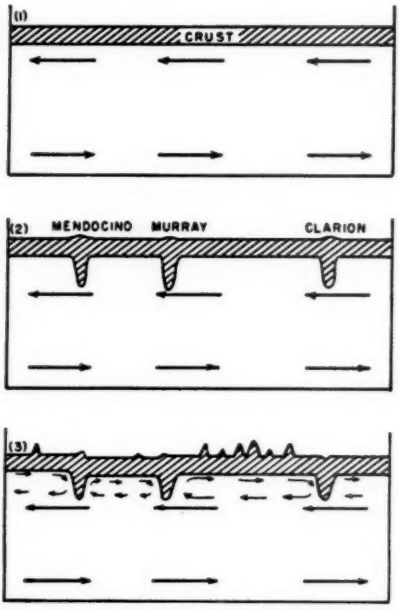

(1) Crust stressed by drag of a convection current. (2) Yielding of the crust in narrow bands of plastic deformation forms the fracture zones and, possibly, deep roots below them. (3) Supposed roots act as dams interrupting flow of convection current and forming eddies. Relatively faster flow and heat transmission in eddies below Ridge and Trough Province and the Baja California Seamount province expand top of mantle and elevate provinces above Deep Plain. Same heating produces more volcanoes in elevated provinces than in Deep Plain.

FIGURE 26.—POSSIBLE DEVELOPMENT OF REGIONAL DIFFERENCES IN DEPTH AND CONCENTRATIONS OF SEAMOUNTS BY CONVECTIVE EDDIES

different pairs of fracture zones, the temperature and consequently the density of the material immediately beneath the crust would also vary. A comparatively rapid rate of overturn is suggested by the comparatively less dense ultra-sima of the Baja California Seamount province. The heat available from this relatively rapid overturn may explain why volcanoes are common in the seamount province and rarer elsewhere.

Deep Plain and Ridge and Trough Province

If variations in the regional depth of the northeastern Pacific resulted solely from variations in the density of ultra-sima, the density of the high Ridge and Trough province should be less than the density of the Baja California Seamount province, and according to the preceding hypothesis the number of volcanoes should be greater. More volcanoes are found in the seamount province; consequently either the number of volcanoes is not significant or some of the difference in elevation is caused by a process unrelated to differences in density of ultra-sima. Such a process is deposition by turbidity currents.

Gutenberg and Richter (1935, p. 324) conclude that the area between northern California and Alaska is continental in nature, presumably because of an unusual thickness of sediment or of sima. This "continentality" (no sial is indicated) may have caused the region of the Ridge and Trough province to be shoaler than the rest of the northeastern Pacific before the formation of the fracture zones. A more recent study of earthquakes recorded at Hawaii indicates that the crust in the area is not significantly different from normal for the Pacific (Oliver, Ewing, and Press, 1953). Prior to the development of a hypothesis for the origin of the fracture zones, it was suggested that the Mendocino Escarpment was similar to a continental slope at the margin of the continental area of the sea floor (Menard and Dietz, 1952, p. 273). This hypothesis should be re-evaluated. Even though some regional differences in depth may have existed before the formation of the Mendocino fracture zone, it is improbable that the continental region had a southern boundary which exactly coincided with the future position of the fracture zone. The Mendocino fracture zone in this

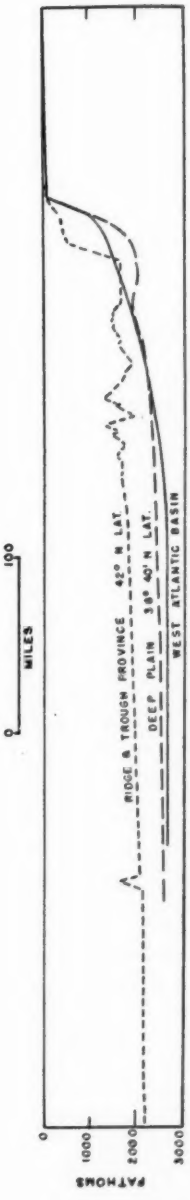

FIGURE 27.—PROFILES OF SEA FLOOR IN THREE AREAS OFF NORTH AMERICA
Note similarity of continental slope angles but differences in height

area shows the only significant deviation from a great circle of any of the fracture zones and its trend may have been determined in part by differences in crustal structure, but the Mendocino Escarpment is too long and straight to be the boundary of a pre-existing crustal block.

Cause and effect must be reversed. Part of the difference in depth found everywhere across the Mendocino fracture zone may have resulted from the formation of rollers in subcrustal currents, and part from the formation of the continuous ridge at the top of the Mendocino Escarpment. Much of the uniform difference in depth probably is caused by sedimentation. The truth of this hypothesis can be established only by reflection or refraction shooting, now not available. However, both the Deep Plain and the Ridge and Trough province exhibit a smooth, concave-upward graded profile which suggests that sediment deposited by turbidity currents blanketed any initial topography except for a few volcanoes and the narrow ridges and troughs (enclosed by ridges) in the Ridge and Trough province. The profiles are strikingly similar (Fig. 27) except that the continental slope across the eastern edge of the Deep Plain is higher, and the whole profile of the Deep Plain is several hundred fathoms deeper. In a north-south profile across the escarpment, the two regions appear flat with no gradation between them. Turbidity currents north of the escarpment are dammed from flowing into the deeper area to the south by the ridge at the top of the escarpment. Both profiles closely resemble profiles of the sea floor off the Atlantic side of North America (Fig. 27) where the smooth graded slopes have also been ascribed to deposition by turbidity currents (Ericson, Ewing, and Heezen, 1951, p. 964). Such a slope south of Nova Scotia has been studied by geophysical shooting (Officer and Ewing, 1952), and the sediment in the continental rise (the apron at the base of the continental slope) is 33,000 ft. thick above a sima layer which is of average thickness but is bowed downward. It may be assumed that this crustral structure is approximately duplicated in the Ridge and Trough province and the Deep Plain, at least to the extent that the sima is bowed down and the sediment is unusually thick at the base of the continental slope (Dietz, 1952, p. 1810).

Two origins of the present graded profiles at different depths are reasonable: (1) The rate of sedimentation in the two regions has been relatively constant, and sediment has filled the low areas and produced a graded profile over a sea floor which was initially very different in average depth in the two regions. (2) The rate of sedimentation has been significantly faster in the Ridge and Trough province so that a thicker blanket of sediment has produced the difference in regional depth although the depth was about the same before the Mendocino Escarpment was formed. The choice between the origins will be made by future geophysical studies. However, the volume of sediment-laden water introduced directly into the deep sea by the Columbia and other rivers north of the escarpment is much greater than the volume introduced by the Sacramento and the San Joaquin, the only major rivers to landward of the Deep Plain; therefore (2) may be more important.

Implied Crustal Deformation

Fault Displacements

Lüders' lines may be formed without fracturing a test block, but, if stressing is continued after the lines are formed, shear fractures usually are produced along one or several lines. The fracture zones including the San Andreas fault mark bands of plastic deformation analogous to Luders' lines, but by the same analogy fracturing by strike-slip movement need not have occurred in all the fracture zones. All the strike-slip movement may have taken place along the San Andreas fault zone.

No conclusive evidence for strike-slip movement along the four marine fracture zones can be adduced. The asymmetrical ridges and narrow troughs within the fracture zones were probably produced by faulting of the relatively brittle material in the upper part of the crust. The type of relief indicates that the faulting had a vertical component. The very straight trends of the ridges and troughs suggest some horizontal component.

Crustal Shortening

During plastic deformation the crust was shortened perpendicular to the trend of the

fracture zones. The amount of the shortening is an inverse function of the thickness of the crust and a direct function of the local thickening that formed a root. The Mohorovičić discontinuity in at least part of the northeastern Pacific area is only 5 km below the sea floor (Raitt, 1951), but the reduction of gravity anomalies in the Pacific suggests that relatively rigid material is 20–30 km thick. A value of 15 km for the thickness of the material is plausible for computations. The thickness of the root is unknown, but isostatic compensation for even the most elevated parts of the Clarion fracture zone requires that the material above the Mohorovičić discontinuity be thickened by only 1 km—20 per cent of the average thickness in the region. A similar thickening in the lower part of the relatively rigid crust would form a root only 3 km thick. If the underlying mantle has some strength which decreases downward, the formation of a crustal root might be accompanied by the formation of a corresponding root in the mantle. The root would be characterized by higher than average strength for a given depth in the mantle, although the difference in density would be negligible.

The average width of the four fracture zones is 60 miles. Assuming that the 15-km crust was thickened to 18 km, the total shortening was 48 miles. If the possible fracture zone exists midway between the Murray and Clarion fracture zones, the total shortening was 60 miles. The deformed area of the northeastern Pacific is roughly 3000 miles wide in the direction of the shortening, thus the shortening was about 2 per cent. The shortening may have been much more if the roots below some of the fracture zones were deeper than required to support the present topography.

Age of Fracturing

Present Seismicity and Vulcanism

Gutenberg and Richter (1949, Fig. 8, p. 35; Fig. 9, p. 37) show many submarine epicenters within the area of the northeastern Pacific fracture zones (Fig. 28). Most of them may be correlated with the San Andreas fracture zone and the Acapulco-Guatemala Trench, but a significant portion remain unexplained. In this section it is shown to what degree the epicenters are geographically related to the fracture zones and whether the zones are seismically active. The number and energy of submarine earthquakes within 200-mile-wide bands centered on the zones are compared with the earthquakes in the larger areas between the bands. The width of the bands takes into account the width of the fracture zones and the errors involved in locating epicenters. The earthquakes considered lie either on the continental slope or the deep-sea floor. Data on locations and magnitudes are from Gutenberg and Richter (1949), and energies are computed from their equation (p. 19).

$$\log E_{(\text{ergs})} = 1.8M + 12 \quad \text{where } M \text{ is the magnitude.}$$

Results of the quantitative comparison are shown in Table 4. The ratio of number of earthquakes within the zones to those without is 1.6/1, and the ratio per unit area is 3.9/1. The ratio of seismic energy expended within and without the fracture zones is far more significant than the number of earthquakes; this ratio is 99/1 in favor of the fracture zones. The ratio per unit area is more than 200/1. The zones, therefore, are significantly more active seismically than is normal for the deep-sea floor in the northeastern Pacific.

Earthquake epicenters are concentrated seaward of Cape Mendocino in the fracture zone. Some may be related to Mendocino faulting, but the San Andreas fault extends out to sea through this area, and it is impossible to separate most earthquakes caused by movement along the San Andreas fault from those caused by other faults in the same area. First motion of at least one of these earthquakes indicates a correlation with the San Andreas fault (Byerly, 1938, p. 3) but is unreported for most earthquakes. The ratio between seismic energy in the fracture zones and out of them would be considerably increased if the Mendocino fracture zone were included.

Most active volcanoes in the coastal zone bordering the fractured area of the northeastern Pacific are associated with the Acapulco-Guatemala Trench (Fig. 28). Of the remaining 12 shown to be active or probably active (Gutenberg and Richter, 1949, Fig. 8, p. 35; Fig. 9, p. 37), 6 lie in an east-west band across

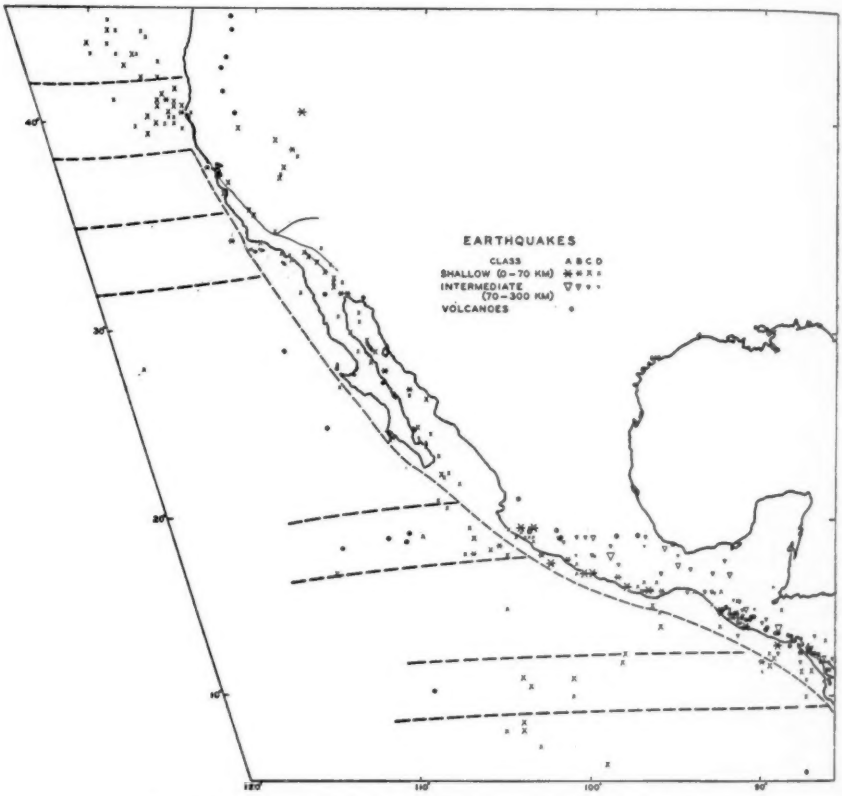

FIGURE 28.—EARTHQUAKES AND VOLCANOES IN FRACTURED AREA

Of the volcanic islands, only San Benedicto has an active volcano (from Gutenberg and Richter, 1949, Figs. 8, 9).

central Mexico in the Clarion fracture zone. The eruption on San Benedicto Island in the Revilla Gigedo group, which formed a new volcano (Dietz and Richards, 1953) named Bárcena, added a seventh active volcano to this zone.

The Clarion fracture zone is marked both by earthquake epicenters and by active volcanoes, indicating that tectonic forces are still active although not necessarily the forces which produce the fracturing. The other three fracture zones show a degree of seismic activity far above normal for the deep-sea floor although the earthquakes in the Mendocino fracture zone may be caused solely by the intersecting San Andreas fault. In all probability all the racture zones are active.

Geologic Dating

Earthquakes and active volcanoes show that some, and probably all, the fracture zones are now active. Very little dating of beginning of activity can be done from samples collected along the fracture zones at sea, and the interpretation of the fracture zones on land is somewhat tentative. Consequently no attempt at precise dating is made at this time. On the other hand the approximate date of the fracturing has an important bearing on the origin of the fractures. If it began in Precambrian time, an origin connected with a change in the position of the poles is more likely if it did not begin until Mesozoic or Cenozoic time the origin is more probably related to a convection current.

The writer finds no indication that the frac-

TABLE 4.—ENERGY OF SUBMARINE EARTHQUAKES IN AND OUT OF NORTHEASTERN PACIFIC FRACTURE ZONES

Area location	Epicenter location		Magnitude	Energy (10^{22} erg)
	N. Lat.	W. Long.		
WITHIN FRACTURE ZONES				Total energy $6100 \cdot 10^{22}$ ergs Total width perpendicular to fracture zones 600 miles
Murray fracture zone	34½	121½	7.3	1300
Clarion fracture zone	17	115	6¾	140
	19	110	5½	0.8
	20½	108	5¾	2.2
	19½	107¼	5½	0.8
	18	107½	5½	0.8
	18	107	7.0	400
	19	107	6¾	140
	18¼	106	6½	50
	18½	105½	7.0	400
	18	105	6	6.3
Clipperton fracture zone	11	104	6	6.3
	10½	103½	6¾	140
	11	101	6¾	140
	10	101	5½	0.8
	12½	98	6	6.3
	12	90	7.5	3200
	11¾	89½	6.9	250
	10	87	6	6.3
OUTSIDE FRACTURE ZONES				Total energy $67 \cdot 10^{22}$ ergs Total width perpendicular to fracture zones 1480 miles
Between Mendocino and Murray fracture zones	None	.....	.....	.....
Between Murray and Clarion fracture zones	28	126½	5½	0.8
	27	115	5½	0.8
	21	109	5¾	2.2
Between Clarion and Clipperton fracture zones	15	105	6	6.3
	14¾	96	6	6.3
	14	96	6¼	18
Between Clipperton fracture zone and latitude 5°N	8	105	5½	0.8
	8½	104	6¼	18
	8	104	6	6.3
	7	104	5½	0.8
	6	99	6	6.3
	6	99	5½	0.8

ture zones existed in pre-Mesozoic time, but various lines of evidence suggest tectonic activity in the fracture zones during Mesozoic and Cenozoic time. Dating of submarine topography by fossils is available for only one place in the whole eastern Pacific. Carsola and Dietz (1952, p. 491) found Miocene (?) Foraminifera encased in a calcareous cement capping Erben Guyot, one of the line of great seamounts in the Murray fracture zone. This submarine volcano grew upward to form an island, was truncated, and became submerged by Miocene time. The date of the vulcanism is not known, but the geologically brief life of volcanic islands in the Pacific suggests that it was not pre-Tertiary.

No Pre-Cretaceous fossils have been found in the Pacific basin. The implication is that the sea-floor topography, including the fracture

zones, of the Pacific basin is all Cretaceous or younger. However, geological and paleontological research by dredging and by drilling on islands has just begun. Only on Kita-Daito-Shima and Bikini (Ladd, Tracey, and Lill, 1948, p. 53) and Eniwetok atolls (Ladd, 1952) has drilling reached pre-Pleistocene rocks; and only the Mid-Pacific Mountains (Hamilton, 1953, p. 204) and Erben Guyot (Carsola and Dietz, 1952, p. 491) have been dredged of pre-Pleistocene rocks.

The continental parts of the fracture zones can be dated more accurately. The Transverse Ranges of California, a part of the Murray fracture zone, were formed in the Tertiary; the Volcanic Province of Southern Mexico, a part of the Clarion fracture zone, contains no pre-Tertiary lavas (Eardley, 1951, p. 585). The San Andreas fault, as a complementary shear, may be the same age as the fracture zones. The date of initial movement on the fault is in doubt. Hill and Dibblee (1953, p. 446–449) have tentatively proposed correlations of strata on opposite sides of the fault which, if accepted, indicate the movement may be at least as old as Cretaceous.

Peter Misch has suggested a significant line of reasoning for dating the fracture zones. The dominant Mesozoic structures of the western Cordillera extend from Alaska to Baja California with but a few minor interruptions. There is no reason to believe that these interruptions existed when the structures were formed. One interruption occurs at the intersection with the Murray fracture zone, and, presumably, the fracture zone is younger. On the other hand much of the Tertiary faulting and folding superimposed on the original Mesozoic structures is confined between pairs of fracture zones and occurred with the formation of the fracture zones or after it. For example, the Mesozoic Sierra Nevada batholith has its counterpart south of the Murray fracture zone, but the pattern of Tertiary block faulting in the Sierra Nevada does not. This reasoning indicates a late Mesozoic or early Tertiary age for the formation of the fracture zones.

No single bit of evidence for dating the fracture zones is compelling, but all point to a Mesozoic-Cenozoic age. Mesozoic-Cenozoic rejuvenation along more ancient fractures remains a possibility but is unnecessary to explain any features of the fracture zones.

Origin of Some Gross Structures of Western North America

Correlation Between Geologic Provinces and Fracture Zones

Almost all the major geologic provinces along the Pacific coast of North America have northerly or northwesterly trends. Two prominent exceptions are the Transverse Ranges of southern California (including the Channel Islands) and the Volcanic Province of Southern Mexico (including the Revilla Gigedo Islands). These lie, respectively, along the Murray and the Clarion fracture zones, and the northern and southern boundaries of the provinces correspond approximately to the limits of the fracture zones.

None of the other provinces lie within the fracture zones, but none transect the zones (Fig. 14) except possibly the Guatemala Trench and the northern limit of the California Coast Ranges. The Mendocino fracture zone forms the southern limit of the Ridge and Trough province, and, if its trend is extrapolated eastward for but a fraction of its length, it also forms the southern boundary of the Cascade Range. The Deep Plain province is bounded on the north by the Mendocino fracture zone and on the south by the Murray fracture zone. The Murray fracture zone also forms the approximate southern boundary of the Great Valley and the Sierra Nevada in California, and the Mendocino zone may form the northern boundary. The Baja California Seamount province, the Baja Calijornia Peninsula (including the Peninsular Ranges and continental borderland), and the Gulf Trough (Beal, 1948, p. 98–99) are bounded on the north by the Murray fracture zone and on the south by the Clarion fracture zone. The Guatemala Trench crosses both the Clarion and Clipperton fracture zones, but it is relatively shallow in the zones, and its ends are only a few miles beyond the fracture zones. All but one of the active volcanoes associated with the trench, and all associated shallow-and intermediate-focus earthquakes are bounded by the Clarion and Clipperton fracture zones.

The surprising feature of the correlation be-

tween the fracture zones and the various submarine and continental provinces is not so much that the boundaries coincide but that so many provinces extend from one fracture zone to the next. This may be somewhat a matter of definition for the submarine provinces because the existence of the fracture zones was known when the provinces were delineated. However, the remarkable differences in regional depth, number of seamounts, and smoothness of the bottom, which distinguish the Deep Plain from the Ridge and Trough province and the Baja California Seamount province, leave little doubt that the Mendocino and Murray fracture zones bound the Deep Plain. This possible bias cannot have affected the delimitation of provinces defined before the fracture zones were discovered. It is particularly significant, therefore, that the Great Valley, the Sierra Nevada, the Baja California Peninsula, the Gulf Trough, and the Guatemala Trench all extend from one fracture zone to the next despite a considerable variation in the length and trend of the various provinces. A fracture zone may exist halfway between the Murray and Clarion fracture zones although it has only a relatively minor topographic expression. It has the proper position to determine the southern boundary of the California continental borderland but apparently does not extend across Baja California.

Speculations Regarding Interrelations and Origins

General.—The discovery of unsuspected major elements in a tectonic pattern justifies speculation regarding their significance. The writer believes a great northeast-southwest compression has produced plastic deformation in very long, thin zones in the crust and fracturing in the more brittle rocks at the surface. The San Andreas fault and associated structures are considered a fracture zone with a trend complementary to the submarine fracture zones.

Structures within fracture zones.—Faulting of all types may be expected within the fracture zones. The dominant movement subsequent to the formation of lines of weakness by plastic flow probably is strike slip, but the submarine topography indicates that normal faulting is common, and open fissures may be required for the upward movement of lava which formed the volcanoes of the Revilla Gigedo Islands and the Volcanic Province of Southern Mexico. Contrariwise, thrust faulting is prominent in the Transverse Ranges of southern California. The type of faulting found locally within a fracture zone, therefore, may have no regional significance. The trend of topography and structures in the Transverse Ranges and the Volcanic Province of Southern Mexico is related to the general trend of the Murray and Clarion fracture zones, but the type of fracturing may be incidental to the local variations in the plastic distortion of the lower part of the crust.

Structures between fracture zones.—The Sierra Nevada, Great Valley of California, Gulf Trough, Baja California Peninsula, and Deep Plain of the northeastern Pacific all lie wholly within and extend across the area between a pair of fracture zones. These spatial relations cannot be coincidences; they require some general explanation. Several conclusions may be drawn:

(1) The crust between pairs of fracture zones has behaved like a block since the zones were formed, and geologic structures tend to cut across the whole width of each block.

(2) The faults or folds within the blocks cannot cross the fracture zones which bound the blocks to north and south.

(3) The various provinces must have been formed at the same time or after the fracture zones.

The deformation of each block of the crust depends on the relative amount of movement on the faults in the bounding fracture zones, and the combination of movement on the San Andreas fault may produce a complicated structural pattern within each block.

San Andreas fracture zone.—The San Andreas fault unquestionably presents the outstanding structural puzzle of California. Detailed mapping in various areas (Taliaferro, 1943; Wallace, 1949) produces more questions regarding age and displacement than answers. Although it is the longest and most active fault in the area (perhaps in the world) it cuts the surrounding structures at various angles and seems to have singularly little relation to them in many places. Perhaps the San Andreas and related faults mark a great fracture zone produced by the same stress as the submarine fracture zones and complementary to them.

Including the submarine extensions indicated by earthquake epicenters, the San Andreas

fault zone extends from a point west of Oregon to the southern end of the Gulf of California and perhaps beyond. Unlike any other post-Mesozoic structure it crosses the Mendocino and Murray fracture zones. Consequently its origin is more directly related to the fundamental stress acting in the region than is the origin of the structures which are confined within separate blocks. The angle between the San Andreas fault zone and the Mendocino and Murray fracture zones is 120°–125° which is an allowable value for plastic deformation although somewhat larger than the angle of 110° ordinarily produced by a testing machine. One may assume, therefore, that the San Andreas fault zone and the submarine fracture zones mark lines of weakness caused by plastic deformation, and that they are complementary and were produced by the same stress—probably at the same time. Seen as a part of a fracture zone, the San Andreas fault is exceptional only in its seismicity. All the fracture zones trend contrary to the surrounding structures, and all are extremely long. Even with its submarine extensions the San Andreas fault is only two-thirds as long as the Clarion fracture zone.

Guatemala Trench.—The trench is an exceptional, topographic-structural feature because it transects two fracture zones. It begins where the submarine extension of the San Andreas fault appears to end, and the deviation in trend is only about 30°. These relations suggest that the trench may be an extension of the San Andreas fracture zone. The trench has associated shallow- and intermediate-depth earthquakes, nonvolcanic coastal mountains, and a line of volcanoes and in many respects appears to be a normal Pacific arc (Gutenberg and Richter, 1949, p. 36–37). In other ways the arc is somewhat unusual: (1) The trench is relatively straight although the shore line is arcuate. (2) In Mexico the volcanoes and intermediate-depth earthquakes follow the Clarion fracture zone rather than the trench; Gutenberg and Richter (1949, p. 37) attribute this to the branching of the Caribbean loop. (3) The trench is 1–2 miles shallower than most trenches. (4) Gravity anomalies show no root under the trench off Mexico (Vening Meinesz, 1948). Vening Meinesz finds that the gravity anomalies indicate a regionally compensated bend downward suggesting that the continent is riding over the sea floor—possibly incidental to a general strike-slip movement. He has found similar anomalies and topography off the west coast of Sumatra where strike-slip movement is prominent on land, and the compressional component perpendicular to the coast causes it to push against the sea floor. Off Java the trend of the trench is more nearly perpendicular to the regional stress so that a normal deep trench with a root is formed. Thus the southern part of the Guatemala Trench off Central America might be similar to the trench off Java because it is more nearly perpendicular to the regional compression. The trend varies by no more than 5° from perpendicular to the regional compression proposed by the writer.

California Coast Ranges.—The possible width of the proposed San Andreas fracture zone is worthy of consideration. The submarine fracture zones (including the asymmetrical ridges) are 60–100 miles wide in most places, and the complementary fracture zone on land might be expected to have a similar width. This width is not evident. The San Andreas rift is a fraction of a mile wide, and even if the Hayward and San Jacinto faults are part of the fracture zone the width is only about 20 miles. A zone 60 miles wide would include most of the Coast Ranges, and much of the complexity of structure in these ranges may be due to their presence within a fracture zone.

One of the most puzzling aspects of the stress pattern in California is how a compression perpendicular to the axes of folds in the Coast Ranges could also produce strike-slip shearing along the San Andreas fault which intersects the folds at an acute angle. For example, the primary stress acting from S.25°–30°W., which the writer proposes to explain the origin of the submarine fracture zones and the San Andreas fault, would not produce the folds. Bijlaard (1936, p. 16–17) analyzed the possible patterns of deformation which would be produced in a zone of local plastic deformation, and his analysis can be applied to explain the orientation of folds in the Coast Ranges. Professor Bijlaard (Personal communication) calculated the relative values of stresses required to produce the observed angle of 120°–125° between the San Andreas fracture zone and the Mendocino and Murray fracture zones. With the angle at 120°, his theory of local plastic deformation shows that a secondary stress with about a third of the value of the principal stress is acting at

right angles to principal stress. If the principal stress is S_1, the resolution of stresses yields a component of 0.2 S_1 parallel to the San Andreas fault and acting in the proper direction to give the observed movement. The maximum compression has a value of 1.02 S_1 and is oriented about S. 40° W. The axes of folds produced by this compression would trend N. 50° W. The trends of folds in the Coast Ranges cannot be established accurately because most of them are somewhat curved. The average trend of 40 Coast Range folds that are more than 10 miles long and are shown on the Structural Map of the United States is N. 48° W. In relation to a theoretical trend of N. 50° W., 20 per cent deviate by no more than 2°, 58 per cent by no more than 10°, and 88 per cent by no more than 20°. These values compare favorably with the 10 per cent, 48 per cent, and 75 per cent (respectively) agreement with the trend of folds which would result if the secondary stress were zero and, hence, independently confirm Bijlaard's analysis of the relative values of the principal and secondary stresses which formed the fracture zones and the San Andreas fault in this area (Fig. 29).

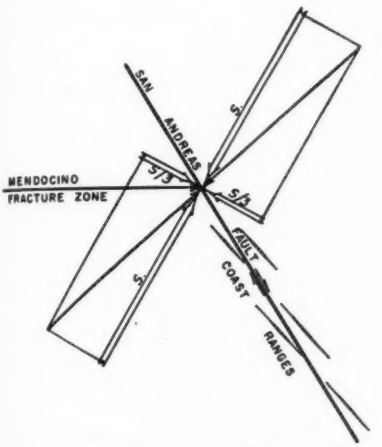

FIGURE 29.—ORIENTATION AND RELATIVE MAGNITUDES OF STRESSES CAPABLE OF PRODUCING SAN ANDREAS FAULT AND MENDOCINO FRACTURE ZONE AS COMPLIMENTARY ZONES OF PLASTIC YIELDING

Maximum compression approximately perpendicular to axes of folds in Coast Ranges.

The origin of the secondary compressional stress is not related to the origin of the principal stress by annular convection currents under the Pacific basin. If the currents produced any stress perpendicular to the principal stress, it would be a tension because of the lateral spreading of material required for continuity as the current moved from the inner to outer part of an annulus. The secondary stress may be caused by some unrelated process localized at the margin of the continent, or by some planetary cause such as the shrinking produced by cooling. If the latter, a third of the principal stress would also result from the same cause.

Garlock and Big Pine faults and bend in San Andreas fault.—The Garlock and Big Pine faults are the two parts of one major fault 200 miles long with a left-lateral, dominantly strike-slip movement (Hill and Dibblee, 1953, p. 452). This major fault is offset by the San Andreas fault and, in turn, produces a sharp change in trend in the elsewhere straight San Andreas fault. All the faulting is essentially contemporaneous. The Garlock-Big Pine and San Andreas faults are considered conjugate shears produced by one of three possible stresses, a north-south compression, a northwest-southeast clockwise couple, or a northeast-southwest counterclockwise couple. The last stress is favored as most closely related to the northwest-trending folds of the Coast Ranges.

Hill and Dibblee considered only about 120,000 square miles, but the stress pattern they deduced is about the same as the pattern the writer proposes is acting in the 8,000,000 square miles affected by the fracture zones of the northeastern Pacific area. This substantiates their conclusion that the Garlock-Big Pine and San Andreas faults are primary strain features in California. The differences in the proposed stress patterns apparently arise because Hill and Dibblee based their analysis on the fault trends at one of the points of intersection of fracture zones where the trends are abnormal. Considering this much larger area, the Garlock-Big Pine fault forms the northern margin of the easternmost tenth of the Murray fracture zone. For the trend of the whole length of the San Andreas and Murray fracture zones, a compressive stress from about S. 25°–30° W. is required.

The theoretical pattern of intersection of two active zones of plastic deformation is given by Nadai (1931, Fig. 369, p. 302). It agrees closely

with the structures produced locally at the intersection of the Garlock-Big Pine fault and the San Andreas fault as shown by Hill and Dibblee (1953, Fig. 6 p. 456) (Fig. 30). Considering the fracture zones as a whole, however, the pattern at the intersection shows no obvious agreement with this theory. Where it crosses the Transverse Ranges the San Andreas fault has a more westerly trend than elsewhere along its great length, and this change in trend conforms with theoretical expectations. However, the Murray fracture zone exhibits no corresponding bend toward the southeast. On the contrary, the Garlock fault, which appears related to the fracture zone, bends northeast.

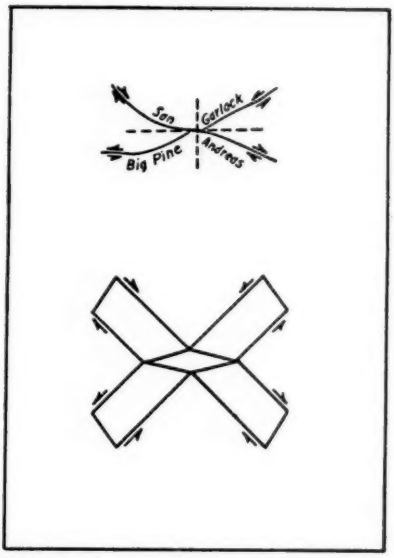

FIGURE 30.—COMPARISON OF PLAN OF INTERSECTION OF SAN ANDREAS FAULT AND BIG PINE-GARLOCK FAULT (HILL AND DIBBLEE, 1953, FIG. 6) AND THEORETICAL PLAN OF INTERSECTION OF ZONES OF PLASTIC DEFORMATION AS GIVEN BY NADAI (1931, FIG. 369)

The bend in the San Andreas fault as it crosses the Murray fracture zone may be explained if the fractures zones are intermittently or alternately active. If the San Andreas fracture zone was active first, the San Andreas fault may have been relatively straight along its whole length. If the fault then became inactive, and plastic deformation began in the Murray fracture zone, the section of the fault traversing the Murray fracture zone would be bent to the west by a number of cross faults with strike-slip movement. Straight scratches on a piece of metal become bent in the same way when the metal yields in bands of local plastic deformation (Fig. 19 after Sully, 1949, Fig. 36). Renewed movement on the San Andreas fault would reconnect the slightly displaced segments of the fault.

SUMMARY OF TENTATIVE CONCLUSIONS

(1) The fracture zones were produced by plastic deformation of the crust.

(2) The fracture zones and the San Andreas fault are complementary shears formed by the same stress. The Guatemala Trench may be a continuation of the San Andreas zone of deformation, although the type of deformation may be different.

(3) The deformation was caused either by a double migration of the poles or by a local or Pacific-wide convection current. The convection current origin is preferred.

(4) An integrated system of annular convection currents may have produced the fracture zones, island arcs, and the Hawaiian Islands. The direction of movement under the fracture zones was about N. 25°–30° E.

(5) The zones are seismically and volcanically more active than is average for the northeastern Pacific area.

(6) Fracturing probably began in Mesozoic-Genozoic time.

(7) Differences in regional depth in the northeastern Pacific area were produced at the same time or after the fracturing.

(8) The relatively shallow depth of the Baja California Seamount province compared to the Deep Plain requires a difference in the density of the mantle below the two areas. Density differences may result from varying rates of heating by convective eddies localized by the roots of fracture zones. The unusually large number of volcanoes in the Baja California Seamount province may have been caused by the same heating which elevated the sea floor.

(9) At least part of the difference in regional depth of the Ridge and Trough province and the Deep Plain is caused by different depths of sedimentary fill. The asymmetric ridge within the Mendocino fracture zone acts as a dam separating turbidity currents in the two provinces.

(10) The California Coast Ranges are within the San Andreas fracture zone. The trend of folds in the ranges is caused by a principal stress, which produced the San Andreas fault and the fracture zones, and a secondary stress at right angles to the principal stress and with about a third of its value.

(11) The Channel Islands and Transverse Ranges of California mark the continental extension of the Murray fracture zone; the Revilla Gigedo Islands and the Volcanic Province of Southern Mexico bear the same relation to the Clarion fracture zone.

(12) The Clarion and Clipperton fracture zones may connect with the great transcurrent faults postulated by Hess in the Caribbean region. If so, the proposed hypothesis of origin by a convection current under the Pacific is seriously weakened.

(13) The sections of the crust between fracture zones have been deformed as blocks since the zones were formed, and geological provinces extend the entire width of the blocks. The stresses within the blocks are secondary compared to the stress which formed the fracture zones and no post-Mesozoic structure within a block crosses a fracture zone.

(14) A few echograms from sparsely sounded areas indicate other fracture zones in the Pacific basin.

References Cited

Arrhenius, G., 1952, Sediment cores from the east Pacific: Repts. Swedish Deep-sea Expedition 1947–48, v. 5, Goteborg, 227 p.

Beal, C. H., 1948, Reconnaissance of the geology and oil possibilities of Baja California, Mexico: Geol. Soc. America Mem. 31, 138 p.

Betz, F., and Hess, H. H., 1942, The floor of the North Pacific Ocean: Geog. Rev., v. 32, p. 99–116.

Bijlaard, P. P., 1936, Theorie des deformations plastiques et locales par rapport aux anomalies negatives de la gravitation, aux fosses oceaniques, aux geosynclinaux, au volcanisme, a l'orogenie et a la geologie de l'ocean pacifique occidental: Assoc. Geodesie, Cong. d'Edinbourg.

—— 1938, A theory of plastic buckling with its application to geophysics: K. Ned. Akad. v. Wet. Amsterdam Proc., v. 41, p. 3–15.

—— 1948, On the linear patterns of the earth's crust: K. Ned. Akad. Wet. Amsterdam Proc., v. 51, p. 450–456.

—— 1951, On the origin of geosynclines, mountain formation, and volcanism: Am. Geophys. Union Trans., v. 32, p. 518–519.

Birch, F., 1951, Remarks on the structure of the mantle, and its bearing upon the possibility of convection currents: Am. Geophys. Union Trans., v. 32, p. 533–535.

Brooks, H., 1941, Cyclic convection-currents: Am. Geophys. Union Trans., v. 22, p. 548–551.

Buffington, E. C., 1952, Submarine "natural levees": Jour. Geology, v. 60, p. 473–479.

Byerly, P., 1938, The earthquake of July 6, 1934: amplitudes and first motion: Seismol. Soc. America Bull., v. 28, p. 1–13.

Capricorn Expedition, Shipboard Rept., 1953, Scripps Inst. Oceanography Ref. 53–15, 60 p.

Carsola, A. J., and Dietz, R. S., 1952, Submarine geology of two flat-topped northeast Pacific seamounts: Am. Jour. Sci., v. 250, p. 481–497.

Clements, T., and Emery, K. O., 1947, Seismic activity and topography of the sea floor off southern California: Seismol. Soc. America Bull., v. 37, p. 307–313.

Colbert, L. O., 1949, Oceanographic activities of the U. S. Coast and Geodetic Survey: Am. Geophys. Union Trans., v. 30, p. 897–899.

Dietz, R. S., 1952, Geomorphic evolution of continental terrace (continental shelf and slope): Am. Assoc. Petroleum Geologists Bull., v. 36, p. 1802–1819.

—— 1953, Possible deep-sea turbidity-current channels in the Indian Ocean: Geol. Soc. America Bull., v. 64, p. 375–378.

Dietz, R. S., and Menard, H. W., 1953, Hawaiian Swell, Deep, and Arch, and subsidence of the Hawaiian Islands: Jour. Geology, v. 61, p. 99–113.

Dietz, R. S., and Richards, A. F., 1953, Volcanic eruption of San Benedicto Island, Mexico (Abstract): Geol. Soc. America Bull., v. 64, p. 1503.

Dill, R. F., Dietz, R. S., and Stewart, H. B., 1954, Deep-sea channels and delta of the Monterey submarine canyon: Geol. Soc. America Bull., v. 65, p. 191–194.

Eardley, A. J., 1951, Structural geology of North America: N. Y., Harper and Bros., 624 p.

Elsasser, W. M., 1950, Earth's interior and geomagnetism: Rev. Modern Physics, v. 21, p. 1–35.

Ericson, D. B., Ewing, M., and Heezen, B. C., 1951, Deep-sea sands and submarine canyons: Geol. Soc. America Bull., v. 62, p. 961–966.

Evernden, J. F., 1952, Love wave dispersion and the structure of the Pacific Basin (Abstract): Geol. Soc. America Bull., v. 63, p. 1352.

Ewing, M., 1952, The Atlantic Ocean Basin: Am. Mus. Nat. History Bull., v. 99, p. 87.

Griggs, D., 1939, A theory of mountain-building: Am. Jour. Sci., v. 237, p. 611–650.

—— 1951, Summary of convection-current hypotheses of mountain building: Am. Geophys. Union Trans., v. 32, p. 527–528.

Gutenberg, B., 1951, Crustal layers of the continents and oceans: Geol. Soc. America Bull., v. 62, p. 427–440.

Gutenberg, B., and Richter, C., 1935, On seismic waves (2nd paper): Gerlands Beitr. Geophys., v. 45, p. 280–360.

—— 1949, Seismicity of the earth: Princeton, N. J., Princeton Univ. Press, 273 p.

Hamilton, E. L., 1951, Sunken islands of the Mid-Pacific Mountains (Abstract): Geol. Soc. America Bull., v. 62, p. 1502.

—— 1953, Upper Cretaceous, Tertiary, and Recent planktonic Foraminifera from mid-Pacific flat-topped seamounts: Jour. Paleontology, v. 27, p. 204–237.

Heezen, B. C., Ewing, M., and Ericson, D. B., 1951, Submarine topography in the North Atlantic: Geol. Soc. America Bull., v. 62, p. 1407–1409.

Hess, H. H., 1933, Interpretation of geological and geophysical observations, in the Navy-Princeton gravity expedition to the West Indies in 1932: U. S. Navy, Hydrog. Office, p. 27–54.

—— 1938, Gravity anomalies and island arc structure with particular reference to the West Indies: Am. Philos. Soc. Proc., v. 79, p. 71–96.

—— 1946, Drowned ancient islands of the Pacific Basin: Am. Jour. Sci., v. 244, p. 772–791.

—— 1951, Comment on mountain building: Am. Geophys. Union Trans., v. 32, p. 528–531.

Hess, H. H., and Maxwell, J. C., 1953, Caribbean research project: Geol. Soc. America Bull., v. 64, p. 1–6.

Hill, M. L., and Dibblee, T. W., Jr., 1953, San Andreas, Garlock, and Big Pine Faults, California: Geol. Soc. America Bull., v. 64, p. 443–458.

van Iterson, F. K. Th., 1947, Plasticity in engineering: London, Blackie and Son Ltd., 174 p.

Jeffreys, Harold, 1952, The earth: Cambridge, Cambridge Univ. Press, 392 p.

Johnson, C. W., 1953, Notes on the geology of Guadalupe Island, Mexico: Am. Jour. Sci., v. 251, p. 231–236.

Ladd, H. S., 1952, Foundation of Eniwetok Atoll (Abstract): Geol. Soc. America Bull., v. 63, p. 1273.

Ladd, H. S., Tracey, J. I., and Lill, G. G., 1948, Drilling on Bikini Atoll, Marshall Islands: Science, v. 107, p. 51–54.

Lake, P., 1931, Island arcs and mountain buildings: Geog. Jour., v. 78, p. 149–157.

Mather, K. F., and Mason, S. L., 1939, A source book in geology: N. Y., McGraw-Hill Book Co., Inc., 702 p.

Menard, H. W., 1955, Deep-sea channels, topography and sedimentation: Am. Assoc. Petroleum Geologists Bull., v. 39, p. 236–255.

Menard, H. W., and Dietz, R. S., 1951, Submarine geology of the Gulf of Alaska: Geol. Soc. America Bull., v. 62, p. 1263–1285.

—— 1952, Mendocino submarine escarpment: Jour. Geology, v. 60, p. 266–278.

Menard, H. W., and Ludwick, J., 1951, Applications of hydraulics to the study of marine turbidity currents: Soc. Econ. Paleontology Mineralogy Spec. Pub., no. 2, p. 2–13.

Murray, H. W., 1939, Submarine scarp off Mendocino, California: Field Engineers Bull. 13, p. 27–33.

—— 1941, Submarine mountains in the Gulf of Alaska: Geol. Soc. America Bull., v. 52, p. 333–362.

Nadai, A., 1931, Plasticity: N. Y. McGraw-Hill Book Co., 349 p.

Officer, C. B., and Ewing, M., 1952, Geophysical investigations in the emerged and submerged Atlantic coastal plain. Pt. VII: The continental shelf, continental slope, and continental rise south of Nova Scotia: (Abstract) Geol. Soc. America Bull., v. 63, p. 1287.

Officer, C. B., Ewing, M., and Wuenschel, P. C., 1952, Seismic refraction measurements in the Atlantic Ocean. Pt. IV: Bermuda, Bermuda Rise, and Nares Basin: Geol. Soc. America Bull., v. 63, p. 777–808.

Ogle, B. A., 1952, Major shear zone at False Cape, Humboldt Co., California: Geol. Soc. America Bull., v. 63, p. 1341.

Oliver, J., Ewing, M., and Press, F., 1953, Crustal structure and surface wave dispersion Pt. IV the Atlantic and Pacific Ocean Basins: Lamont Geol. Observatory Tech. Rept. no. 26, 39 p.

Raitt, R. W., 1949, Studies of ocean-bottom structure off Southern California with explosive waves (abstract): Geol. Soc. America Bull. v. 60, p. 1915.

—— 1951, Seismic refraction studies of the Pacific Ocean Basin: Paper delivered at Annual Meeting, Seismol. Soc. America, March 23–24.

—— 1952, The 1950 seismic refraction studies of Bikini and Kwajalein Atolls and Sylvania Guyot: Univ. Calif., Scripps Inst. Oceanography, Ref. 52–38, 25 p.

Revelle, R. R., and Maxwell, A. E., 1952, Heat flow through the floor of the eastern North Pacific Ocean: Nature, v. 170, p. 199.

Scheidegger, A. E., 1953, Examination of the physics of theories of orogenesis: Geol. Soc. America Bull., v. 64, p. 127–150.

Scheidegger, A. E., and Wilton, J. T., 1950, An investigation into possible methods of failure of the earth: Geol. Assoc. Canada Proc., v. 3, p. 167–190.

Shepard, F. P., 1950, 1940 *E. W. Scripps* Cruise, Pt. III: Submarine topography of the Gulf of of California: Geol. Soc. America Mem. 43, p. 1–32.

Shepard, F. P., and Emergy, K. O., 1941, Submarine topography off the California coast: Geol. Soc. America Spec. Paper 31, 171 p.

Shumway, G. A., 1953, Galapagos Islands regional bathymetric trends (Abstract): Geol. Soc. America Bull., v. 64, p. 1514.

Sollas, W. J., 1903, The figure of the earth: Geol. Soc. London Quart. Jour., v. 59, p. 180–188.

Studds, R. F. A., 1950, Oceanographic activities of the U. S. Coast and Geodetic Survey: Am. Geophys. Union Trans., v. 31, p. 786–788.

Sully, A. H., 1949, Metallic creep: N. Y., Interscience Pub. Inc., 278 p.

Taliaferro, N. L., 1943, Geologic history and structure of the central coast ranges of California: Calif. Min. Bur. Bull. 118, p. 119–162.

Tolstoy, I., and Ewing, M., 1949, North Atlantic hydrography and the Mid-Atlantic Ridge: Geol. Soc. America Bull., v. 60, p. 1527–1540.

Umbgrove, J. H. F., 1947, The pulse of the earth: The Hague, 2nd ed., Martinus Nijhoff, 358 p.

Vening Meinesz, F. A., 1947, Shear patterns of the earth's crust: Am. Geophys. Union Trans., v. 28, p. 1–61.

—— 1948, Gravity expeditions at sea, 1923-1938, v. 4: Pub. Neth. Geod. Comm., Delft, 223 p.

Vening Meinesz, Umbgrove, J. H. F., and Kuenen, Ph. H., 1934, Gravity expeditions at sea: Pub. Neth. Geod. Comm., v. 2, Delft, 208 p.

Wallace, R. E., 1949, Structure of a portion of the San Andreas rift in southern California: Geol. Soc. America Bull., v. 60, p. 781–806.

Wilson, J. T., 1951, On the growth of continents: Royal Soc. Tasmania Papers and Proc. 1950, p. 85–111.

U. S. Navy Electronics Laboratory, Code 552, San Diego 52, California

Manuscript Received by the Secretary of the Society October 27, 1953

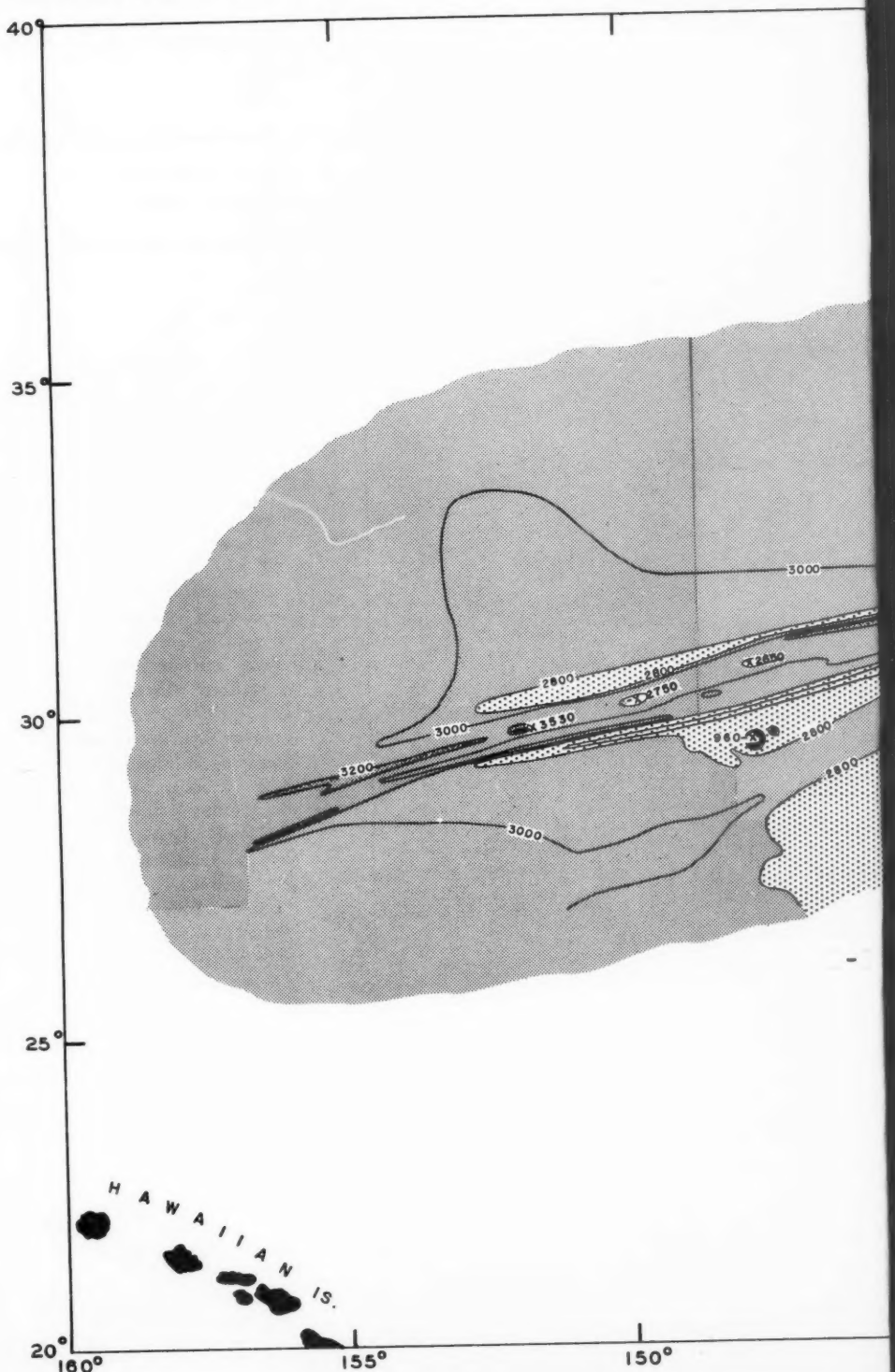
40°
35°
30°
25°
20°
160°
155°
150°
3000
2800
2800
X2850
X2760
3000
X3530
3200
2800
2800
3000
HAWAIIAN IS.

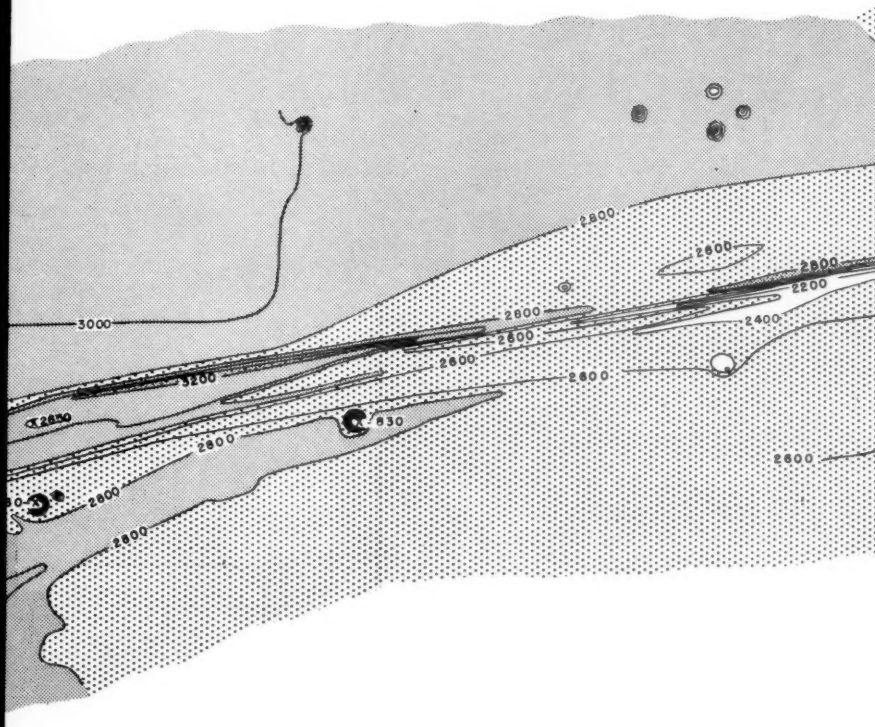

0 100 200 300 400

NAUTICAL MILES

145° 140° 135°

(BATHYMETRY IN VICINITY OF M
(Contour interval 20

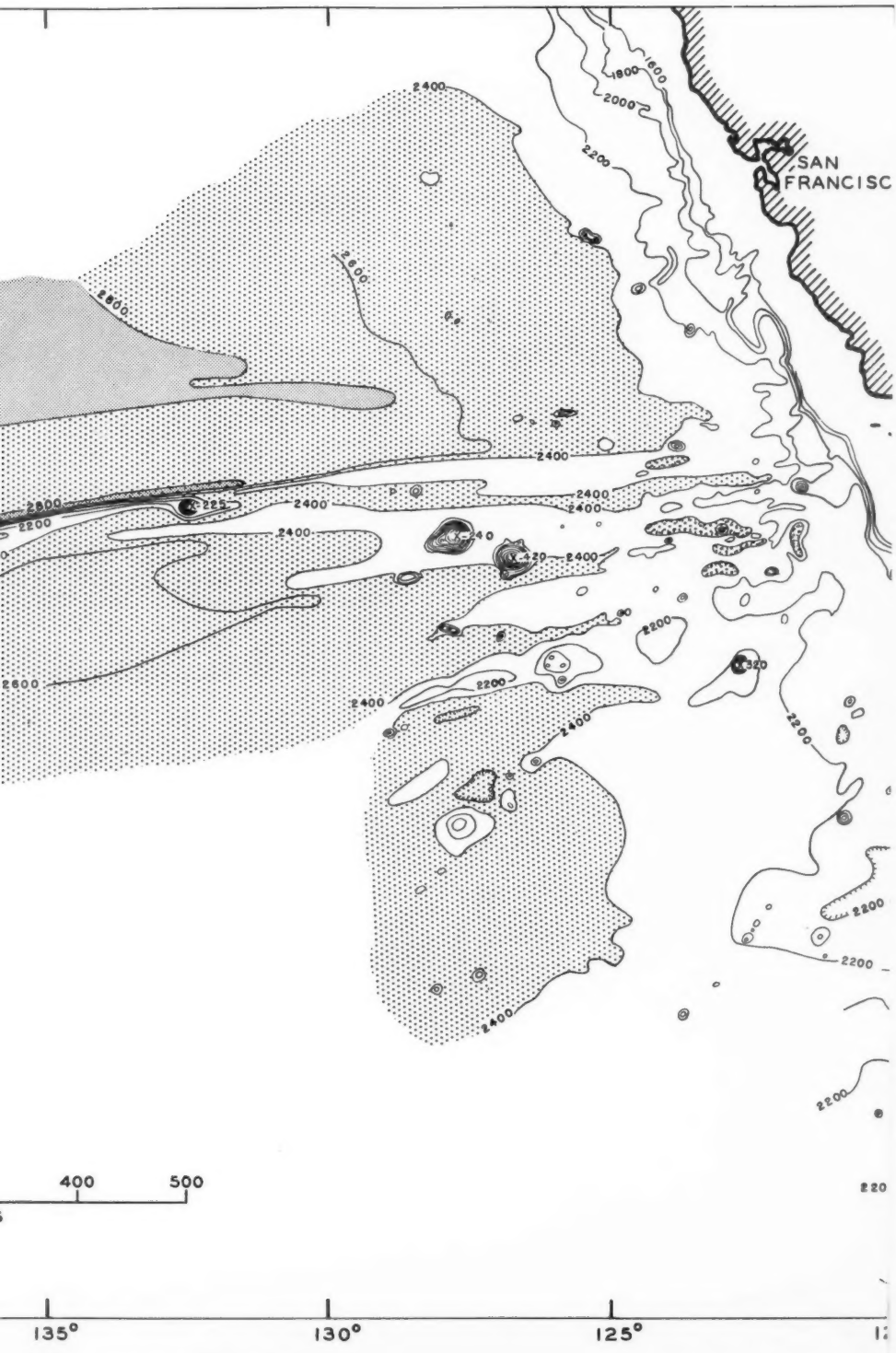

INITY OF MURRAY FRACTURE ZONE)
our interval 200 fathoms)

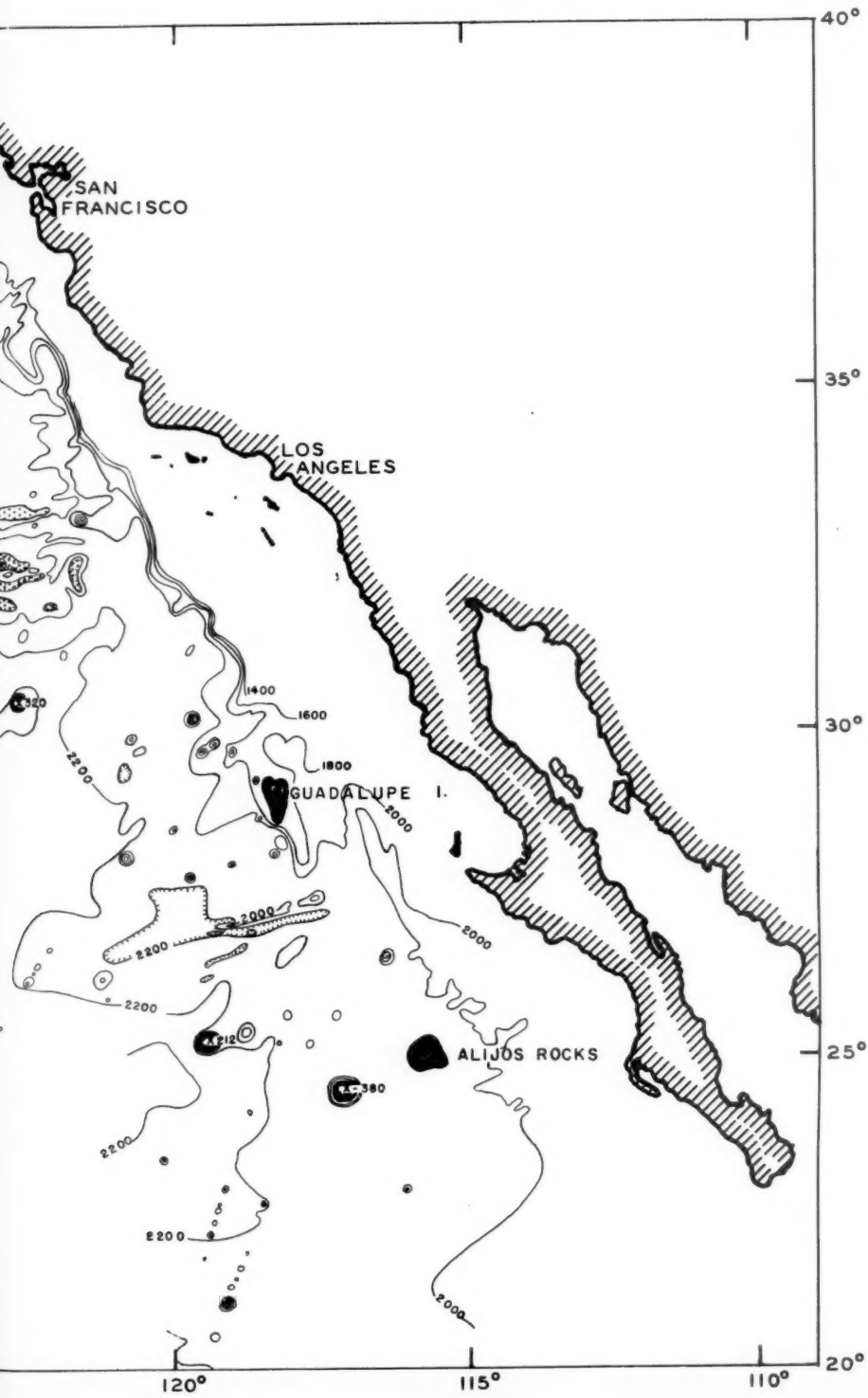
40°
35°
30°
25°
20°
120°
115°
110°
SAN FRANCISCO
LOS ANGELES
GUADALUPE I.
ALIJOS ROCKS
1400
1600
1800
2000
2200
2000
2200
2200
2200
2200
2000
2000
320
212
380

Short Notes

BULLETIN OF THE GEOLOGICAL SOCIETY OF AMERICA
VOL. 66, PP. 1199–1202 SEPTEMBER 1955

INTERPRETATION OF GUTENBERG'S LOW-VELOCITY LITHOSPHERE CHANNEL

By M. H. P. Bott

Introduction

Two recent papers by Gutenberg (1951; 1954) have brought to attention a problem concerning elastic-wave velocities in the upper lithosphere. Near-earthquakes have provided long-standing evidence for an upper crustal layer, apparently present at least under Europe and North America, characterized by longitudinal-wave velocity (P_g) of about 5.6 km/sec. On the other hand longitudinal waves propagated from surface explosions, rock bursts, etc., which have mainly been recorded in Germany and North America, travel in the subsedimentary rocks with velocities usually exceeding 6.0 km/sec.

This apparent discrepancy has been attributed to misinterpretation of near-earthquake velocities (Leet, 1936; Tatel, Adams, and Tuve, 1953) or alternatively to local bodies of high-velocity rock. However, abundant repetitive near-earthquake evidence from places like California (Gutenberg, 1943) together with numerous recent reports of high velocities from surface shocks have led Wood (1948) and Gutenberg (1951; 1954) to consider the discrepancy as a real feature of regular continental occurrence.

Gutenberg's Geometrical Interpretation

In geometrical explanation of these findings Gutenberg (1951) reconstructed the seismological model of the upper crustal layer to include an upper division with longitudinal elastic-wave velocity increasing with depth from 6.0 to 6.5 km/sec, overlying a low-velocity lithosphere channel in which waves from near earthquakes are transmitted with a longitudinal velocity of 5.6 or perhaps 6.0 km/sec. This model apparently resolves the problem and has the added advantage of accounting for certain other discrepancies including the anomalous time of origin observed for some transverse waves from near earthquakes.

Physical Interpretation

The downward decrease of velocity, assuming it to be a reality, might be accounted for by either or both of the following two basic hypotheses:

(1). *Physical hypothesis:* The upper crust is considered to be chemically and lithologically homogeneous, and the downward decrease of velocity is taken as being caused by physical changes arising from increasing temperature and pressure with depth. This hypothesis was proposed in a general way by Wood (1948). Gutenberg (1951) subsequently elaborated, suggesting that the velocity distribution depends on the α-β quartz transition. In a later paper Gutenberg (1954) attributed the phenomenon to phase changes without specific mention of quartz.

Yoder (1950) criticized the quartz hypothesis because the rock at transition depth will be low in quartz or quartz free. Gutenberg (1951) partially resolved this difficulty by showing that the decrease of velocity expected from the variation of Young's Modulus with temperature takes place well below the transition temperature.

(2). *Mineralogical hypothesis:* The alternative hypothesis is that the upper layer consists of two lithologically and chemically distinct divisions, the upper of which transmits elastic waves faster. This hypothesis was suggested by Wood and Richter (1933) and by Gutenberg (1943). Later this explanation was rejected by both Wood (1948) and Gutenberg (1951), mainly because of the geological difficulties

involved in postulating a regional, rather than local, body of high-velocity rocks.

However, it is suggested here that this difficulty does not exist. Surface sedimentary and metamorphic rocks are often thought of as being granitic. This is not so as they show an average *intermediate* chemical composition and when consolidated an intermediate density as revealed by sample-density measurements and gravity surveys over granites (Bott, 1953). Below these rocks some geologists, including the writer, think there is a truly acidic layer which provides material for granite magma or granitization. Indeed, an increased proportion of sodium at some depth seems indispensable whatever the origin of granite is thought to be. For this situation a downward decrease of velocity seems to be inevitable. An increased sodium content disproportionately increases the theoretical compressibility (Adams *in* Gutenberg *et al.*, 1951), and hence either this or greater acidity suggests lower velocities. In experimental support seismic surveys usually yield longitudinal velocities of less than 5.6 km/sec in various exposed granites in contrast with the higher velocities in regionally metamorphosed rocks under the same conditions.

While a downward decrease of velocity is consistent geologically and seismologically with the mineralogical hypothesis just described, it is still not obvious how the velocity in the acidic or soda-rich layer could be as low as 5.6 km/sec. For laboratory velocity determinations on samples of granite agree with calculations from measured elastic constants in giving a longitudinal velocity of 6.0–6.2 km/sec at pressures corresponding to depths of 10 or 15 km. A similar difficulty exists in the correlation of the intermediate layer of seismology with basic material (Jeffreys, 1952) in that the predicted velocities for basalt and gabbro are higher than the observed velocities for this layer.

If the identification of layers is correc tthese unexpectedly low velocities may be accounted for either by unreality of laboratory determinations or by crustal changes which would be grouped in the physical hypothesis. In possible support of the former it is pointed out that the seismic-field velocities for granite seem also to be lower than expected, and also lower than 5.6 km/sec, although this may be caused by feldspar alteration.

Jeffreys (1952) suggests that the actual velocities may be reduced by the widespread presence of glass in both upper and intermediate layers, although there seems to be no geological support for his thesis (Gutenberg *et al.*, 1951). Phase changes may be of importance although the quartz hypothesis of Gutenberg cannot be applied to basalt. Another possibility which is in accord with petrological knowledge is that the greater abundance of water expected for the sources of igneous rocks (up to 10 per cent for the source of granite) may be responsible for the lower velocities.

Conclusion

It is suggested that the main decrease of velocity with depth of Gutenberg's lithosphere channel is caused by the downward change from intermediate to acidic bulk composition or possibly merely by an increasing sodium content. The acidic layer may have an unexpectedly low velocity because of increased water content or other changed physical properties at depth. Hence the seismological and geological concepts of crustal structure under the continents are satisfied by a combination of the physical and mineralogical hypotheses.

The boundary region is best understood if it separates the primary outer acidic layer of the earth below from the overlying rocks subsequently derived by geological processes which have formed a metasedimentary layer of intermediate bulk composition.

References Cited

Bott, M. H. P., 1953, Negative gravity anomalies over acid "intrusions" and their relation to the structure of the earth's crust: Geol. Mag., v. 90, p. 257–267.

Gutenberg, B., 1943, Earthquakes and structure in southern California: Geol. Soc. America Bull., v. 54, p. 499–526.

—— 1951, Crustal layers of the continents and oceans: Geol. Soc. America Bull., v. 62, p. 427–440.

—— 1954, Low-velocity layers in the earth's mantle: Geol. Soc. America Bull., v. 65, p. 337–348.

Gutenberg, B., *et al.*, 1951, Internal constitution of the earth: 2d ed., New York, Dover Publications, Inc., p. 50–80.

Jeffreys, H. H., 1952, The earth, its origin, history, and physical constitution: 3d ed., Cambridge University Press, p. 81–85.

Leet, L. D., 1936, Seismological data on surface layers in New England: Seismol. Soc. America Bull., v. 26, p. 129–145.

Tatel, H. E., Adams, L. H., and Tuve, M. A., 1953, Studies of the earth's crust, using waves from explosives: Am. Philos. Soc. Proc., v. 97, p. 658–670.

Wood, H. O., 1948, A possible layer for the transmission of fast P waves from surface disturbances: Seismol. Soc. America Bull., v. 38, p. 33–39.

Wood, H. O., and Richter, C. F., 1933, A second study of blasting recorded in southern California: Seismol. Soc. America Bull., v. 23, p. 95–110.

Yoder, H. S., 1950, High-low quartz inversion up to 10,000 bars: Am. Geophys. Union Trans., v. 31, p. 827–835.

Department of Geology, Science Laboratories, South Road, Durham, England

BULLETIN OF THE GEOLOGICAL SOCIETY OF AMERICA
VOL. 66, P. 1203-1204 SEPTEMBER 1955

LOW-VELOCITY LITHOSPHERE CHANNEL

BY B. GUTENBERG

In composing the note, *Interpretation of Gutenberg's low-velocity lithosphere channel*, Mr. M. H. P. Bott did not have access to three additional contributions by Gutenberg (1954; 1955a; 1955b). According to these publications, the increase in temperature with depth is the main cause for two low-velocity channels (Fig. 1) in the upper lithosphere (one in the "granitic" layer, another in the "gabbro" layer) as well as for the channel extending downward from the Mohorovičić discontinuity deep into the asthenosphere. In a paper presented in the Symposium, *The crust of the earth* at Columbia University on October 15. 1954, this temperature effect was discussed in detail (Gutenberg, 1955a). Effects of phase changes may be superposed. The note of Mr. M. H. P. Bott shows that changes in composition may produce an additional decrease in wave velocity with depth.

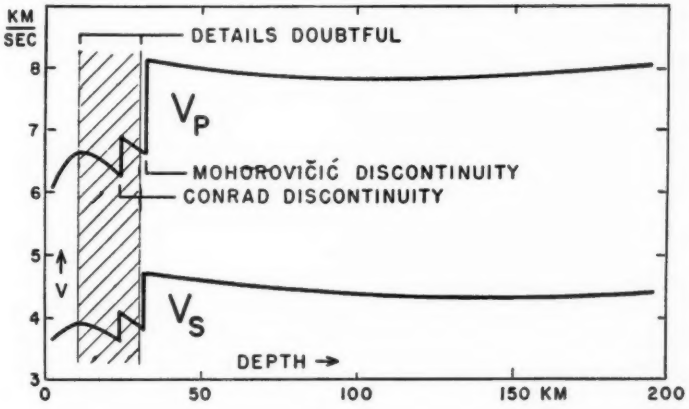

FIG. 1

References Cited

Gutenberg, B., 1954, Effects of low velocity layers: Geofisica Pura e Applicata, v. 28, p. 1–10.
—— 1955a, Wave velocities in the earth's crust: Geol. Soc. America, Special Paper 62, p. 19–34.
—— 1955b, Channel waves in the earth's crust: Geophysics, v. 20, p. 283–294.

BULLETIN OF THE GEOLOGICAL SOCIETY OF AMERICA
VOL. 66, PP. 1205-1206 SEPTEMBER 1955

CANONS OF LANDSCAPE EVOLUTION—A DISCUSSION

By H. D. THOMPSON

In his brilliant and stimulating paper King (1953) has done a great service to geologists. His challenge to some of the Davisian concepts is a much-needed and welcome contribution. Discussion and testing of his "canons" no doubt will lead to further advances in the field of geomorphology. This comment concerns itself with canon Number 1—namely, the relative importance of process, stage, and structure, as basic factors in a landscape.

Without arguing their relative importance, Davis listed the basic factors as structure, process, and stage. This seems to be a logical and sequential order; for the destructional forces must have a landmass, *structure*, on which to work. The action of these forces, *process*, proceeds in more or less systematic order so that certain features are typical of each *stage*.

Although Davis listed structure first, he failed to emphasize this factor sufficiently. He considered structure in a large and general way only, such as stratified rocks or crystalline rocks, folded structure or faulted structure, homogeneous or nonhomogeneous rocks. In fact it is reported that Davis said one need not be a geologist at all in order to understand his system. That may be true insofar as the mental exercise is concerned. But the geologist finds that many aspects of landscape forms are best understood when the structure is known. If structure is considered in its detailed aspects as well as in its general features, it should rank first among the factors of landscape characteristics.

On the basis of relative importance King proposes process, stage, and structure. Why is a mesa steep-sided and flat-topped? Why does a cuesta have a steep and a gentle side? Why is a hogback steep on both sides? Why is the drainage pattern in one region dendritic while in another region it is trellis?, or radial?, or annular? Why are the ridges clean-cut, linear, and parallel in one region whereas they are irregular and sprawling in another? Why is this a valley and that a ridge? Why is the gap in the ridge here instead of somewhere else? Why is this ridge high and the other low? Why does this hill have gentle slopes while the slopes of the other are precipitous? Structure, of course.

As King confined his canons and his discussion to the forms resulting from subaerial processes, the importance of process is greatly restricted, for glaciation, wave action, etc., are not considered. Also, in view of his belief, with which my observations agree, that stage has little, if any, effect on steepness of slope and shape of profile, whereas structure is important, it seems odd that he should place stage above structure. In my opinion, gained from observations in various parts of North America, structure, both general and detailed, should not be assigned a tertiary, or even a secondary role, but should be recognized as the primary factor in landscape evolution.

Reference Cited

King, Lester C., 1953, Canons of landscape evolution: Geol. Soc. America Bull., v. 64, p. 721–752.

HUNTER COLLEGE, NEW YORK 68, N. Y.

Reply to Comment by H. D. Thompson

By LESTER C. KING

Re process, stage, and structure: (1) The great continental erosion cycles are developed independently of structure and depend primarily upon the stand of continents above sea level. They transgress many different structures in different parts of the continents, and upon each structural terrain appropriate details of landscape may develop; but the major phenomenon is the broad cycle and not any local assemblage of detail. So process is more widespread and important than structure.

(2) Thus the mesa which my correspondent

quotes exists not because it is capped by a resistant stratum but because an erosion cycle of a certain type produces scarps. Flat-topped, steep-sided hills, sometimes accordant in level, occur normally and independently of structure —*e.g.*, in two-cycle landscapes.

(3) Structural effects are accentuated at that stage of a cycle when relief is increasing, or when high relief is being maintained. Even then a favorable process is necessary to etch out the structures. At other stages, both early and late in the cycle, process destroys structural effe even to obliteration.

(4) The chief agents of continental erosi are ice, running water, and wind, each of whi moulds its characteristic topography, whate the structure. In the ice-worn shield of Cana the great pediplains of Africa, and in the des sand seas details reflecting structure may present, but the main impress on the topog phy that makes these regions distinctive is th of *process*, and *stage* before structure.

Reply by H. D. Thompson

Re structure, process, and stage:

After reading King's reply to my comments I find that we still are not in agreement on the point in question. Since it would not be appropriate here to enter into extended debate, permit me to suggest a compromise—namely that one's conviction on the relative importance of structure and process will depend in large measure on his point of view and his objecti in the study of geomorphology. To one who primarily interested in the mechanisms of su aerial weathering and erosion the process w seem to be paramount. On the other hand, o who looks for structural explanations of lan scape features will usually find them, and him the structure factor is of prime importan

BULLETIN OF THE GEOLOGICAL SOCIETY OF AMERICA
VOL. 66, PP. 1207-1212 SEPTEMBER 1955

CANONS OF LANDSCAPE EVOLUTION—A DISCUSSION

By JOHN R. SCHULTZ

Lester King (1953) has made one of the most fundamental and stimulating contributions to geomorphology to appear in a long time. However, some of the concepts questioned or disproved are very dear to many geomorphologists and geologists, and it is hardly to be expected that the changes this paper foreshadows will occur over night. But it is almost certain to cause even the staunchest followers of the orthodox school to admit other possibilities and thus cannot fail to have a beneficial effect even in quarters where it is least accepted. Inasmuch as it may be predicted with considerable confidence that some will judge the paper as having gone too far, this discussion is largely confined to pointing out that in some respects Professor King's paper does not go far enough.

The concept of the erosion cycle is firmly rooted in geomorphology and geology, and it cannot be denied that it has a certain value. Regarded strictly as a concept, no criticism is possible, but a great deal of criticism may be levelled against the manner in which it has often been applied to explain the mechanics of landscape formation. Professor King's paper contains numerous examples of errors or oversimplifications that have resulted from facile deductions based on the erosion-cycle concept, but no really thorough examination of the uses and abuses of the concept is made. Therefore, the writer has taken it on himself to examine the subject a little deeper, and to judge the erosion cycle concept as applied to the mechanics of landscape formation by its fruits. When so judged, the following shortcomings immediately become apparent.

(1) As Davis repeatedly maintained, he always regarded himself as a geographer; that is, as one whose chief interest is in describing landscapes in terms that are concise, readily understood, and easily remembered. There is no question that the erosion-cycle concept suits these purposes admirably, but the generality of the concept has tended to discourage any real investigation into what may be called the dynamics of the subject; that is, in finding out just how flowing water and other natural agencies actually operate to produce a landscape. It is probably chiefly because of their obsession with "stage" rather than "process" that geomorphologists of the Davis school have contributed little or nothing to an understanding of the mechanics of natural agencies involved in landscape formation. The best work along these lines has been done by men who either did not regard themselves as geomorphologists or were not completely satisfied with deductions based on the erosion cycle. Bagnold's excellent work, *The physics of blown sand and desert dunes*, is a case in point. This shortcoming in the erosion-cycle concept is felt more keenly in applied geology, geologic-engineering work particularly. The geologist working with civil engineers is often called upon to say something about rates; that is, just how long did it take a river to accomplish a certain task and what will it do in the future, and also something about the thickness of alluvial deposits. Very little help is to be obtained from appealing to the erosion cycle, and the only possible method of approach is to go into such basic subjects as hydraulics, physics, and soil mechanics. The hydraulic engineer can tell the geomorphologist much more about flow conditions in a river than he is able to deduce (accurately) from the erosion cycle, and soil mechanics is far ahead of geomorphology in the analysis of slope stability, landslides, the flow of underground water, etc., as almost any good book on the subject will indicate. Furthermore, civil engineers seem to be taking the lead in application of aerial photographs to the study of geomorphology. One does not have to pursue hydraulics, soil mechanics, and allied subjects very far in order to appreciate that they are basic to geomorphology, and if the dynamics of landscape sculpture are ever to be adequately understood it will be necessary for geomorphologists to be firmly grounded in these fields. Deductions from the erosion-cycle concept give us a great deal of information as to how rivers and other natural agencies forming landscapes

ought to act, but if we wish to know how they really act we must follow the basic approach of hydraulics supplemented by actual observations of rivers, physics, soil mechanics, and allied subjects. Time alone will tell if the present deductive approach will be modified along these basic lines, or if this suggestion (which has also been made in the publications of this society by such outstanding geomorphologists as R. P. Sharp and A. N. Strahler) will be merely regarded as an attempt to drive geomorphologists out of the paradise created for them by Davis.

(2) When used as an instrument of research, the concept of the erosion cycle is all too often applied in a purely deductive manner. Davis' work contains many brilliant examples of the power of deduction actually to predict hidden geomorphic features, which is about the sole reason for believing that a conclusion based on deduction has any validity. Perhaps the best example is his deduction that upraised marine terraces should have both a marine and nonmarine cover, both of which were actually observed later by Woodring in his work in Palos Verdes Hills. Nevertheless, deduction is a dangerous tool in geomorphic research and has led to numerous errors some of which are cited by Professor King and a few more of which are listed below.

A. It is probable that most geomorphologists today tend to favor the meteorite hypothesis for origin of the Carolina Bays simply because they are unable to visualize these features as a part of a "normal" erosion cycle and have insufficient acquaintance with hydraulics and soil mechanics to conceive of their having been formed by the more prosaic process of groundwater leaching of calcium carbonate from the essentially unconsolidated deposits of the Coastal Plain, accompanied by piping of the clay and silt constituents as the rate of groundwater movement increased with increased removal of soluble materials. LeGrand's (1953) recent paper on the subject is a step in the right direction. Another recent paper by Wolfe (1953) attributing the origin of similar features in New Jersey to thawing of permafrost also has merit and may well be correct. If so, about the only problem remaining with regard to the Carolina Bays is just how far south do the permafrost effects extend?

B. The so-called pimple mounds of the western Gulf Coastal Plain and other regions are another example of a geomorphic feature which does not fit well into the deductive school's scheme of things, and deduction has come up with about 50 different explanations. Recently, the suggestion has been made that they too are related to permafrost, another subject in which deduction has been unable to accomplish very much. Certainly, the key to understanding of permafrost phenomena lies in a detailed study of the physics of water, water vapor, and ice, correlated with soil mechanics and soil physics, subjects which are at present pursued mainly by civil engineers.

C. Perhaps the most outstanding example of the limitations of the deductive school is found in H. N. Fisk's (1944; 1952) and R. J. Russell's (1940) work in the lower Mississippi River Valley, which shows conclusively that the so-called "old age" lower Mississippi River Valley has not much in common with what deduction seems to indicate. First, it is not "old" but very young, and is probably one of the youngest major relief features on the face of the earth. Second, the alluvium forming the valley is not a thin layer laid down on an eroded and peneplained bedrock floor, but a thick deposit extending below sea level filling a deep gorge cut during a time when sea level was about 400 feet lower than now. Third, the Mississippi in forming its tremendously wide alluvial valley has not migrated gradually and uniformly from one valley wall to another, but has built up a series of meander belts which confined it for a certain length of time, and the shift from one meander belt to another was a rather sudden and not a gradual process. It may be argued that this is an exceptional case, but it is not improbable that when other large rivers are known in a detail comparable to that of the Mississippi their behavior will also be found to depart considerably from deductions made from the erosion-cycle concept.

D. This phase of the subject should not be dropped without some mention of meanders. Deduction has done little or nothing to explain the origin of these important geomorphic features and has even perpetrated certain errors. For example, meanders are almost certainly not caused by small local obstructions

neither do all meandering streams flow so slowly as to be easily deflected. The exact opposite may be the case; that is, meanders may actually result from the tremendous momentum of flowing water, which far from being readily deflected from one course to another actually cuts into the outside bank and in so doing takes the initial step in a complicated sequence of cause and effect leading to meanders. That some such process is at work is indicated by Friedkin's (1945) laboratory studies and the abandoned meander loops cut into the hard rocks forming the walls of the lower Moselle River Valley. These abandoned meanders are found at two distinct levels above the present river, and in one case a cutoff has been formed. The relationship of these abandoned meanders to the present river seems to make the conclusion inescapable that both the abandoned and the incised meanders of the present river were formed during a single cycle of uplift and erosion. Whether or not the surface was peneplained before uplift cannot be determined from the data in hand. In any event, we have here a clear illustration that uplift was not rapid in comparison with the rate of erosion.

E. The above illustrations may be summarized in the statement that the deductive approach has tended to take the study of geomorphology from the field and laboratory and into the realm of pure thought. It has also tended to retard a truly analytical study of natural agencies through the application of such fundamental sciences as hydraulics, physics, and soil mechanics. The erosion-cycle concept is an excellent teaching device, which is all that Davis really intended it to be, but it has often been used as a substitute for actual detailed study of the processes at work. It appears that future progress in geomorphology depends largely on a better understanding of the dynamics of landscape formation which can be gained only through application of the fundamental sciences.

(3) Another shortcoming in deducing everything from the concept of the erosion cycle is that it may easily prejudice field observations. This procedure tends to influence the observer to see what he was trained, or expects, to see, rather than what is actually there. King's paper contains numerous illustrations of such faulty observations.

(4) As King so forcibly brings out, the concept of a "normal" geomorphic cycle is unnecessary, impossible to substantiate, and probably fallacious. Geomorphology and geology are over-generalized and at the same time somewhat provincial in outlook. On a world scale, arid regions are certainly as "normal" as humid ones. As King states, all the unglaciated landscapes we know in humid regions have concave residuals. The landscape of the driftless area in southern Wisconsin, for example, except for more or less soil creep, green woods, and grass, resembles that of certain parts of the arid west so strongly that those who wish to keep the concept of an arid and humid type of erosional topography will be forced to assume an arid climate in Wisconsin during relatively recent geologic time in order to bolster their view. The writer of this discussion strongly concurs with King that leaving out certain uplifted more or less flat areas and certain buried more or less flat surfaces marking major unconformities, it would be interesting to be shown a peneplain. Pediplains there are, but no peneplains. This raises the question: should the term "peneplain" be retained, or should it be redefined to indicate what is now meant by a pediplain? The latter course should probably be followed, for the term "peneplain" is too strongly entrenched in the literature to be dropped without causing considerable confusion.

(5) It is gradually becoming apparent that Penck's approach has much to recommend it, and an English translation of *Die Morphologische Analyse* (1924) would constitute an important contribution to geomorphology.* This translation is much more urgently needed than usual, for Penck's style is very difficult to follow, and only those thoroughly conversant with German are capable of understanding his contributions in the original.

(6) This portion of the discussion would be misleading if it gave the impression that the writer wishes to derogate in any way the importance and magnitude of Davis' achievements. On the contrary, as a former student of

* An excellent translation appeared while this note was in press.

Davis, he would like to observe that Davis dominated American geomorphology so completely during his lifetime that his successors appear to have no choice but to do over what he did so incomparably better, or strike out in search of new paths. It might also be observed that the truest followers of a great figure are often those who contribute most to the continuing vitality of the field in which he worked.

Having stated his views on what he considers the uses, and more particularly the abuses, of the erosion-cycle concept, the writer would like to make a few remarks concerning certain rather detailed aspects of King's paper.

The term "thalweg" appears to be used throughout in the sense of what a civil engineer would call the "valley profile", or simply "profile". It is certainly not used to designate the line joining the deepest points of the stream channel, which is the meaning long attached to it by civil and hydraulic engineers. This brings to mind the suggestion that geomorphologists use the term "thalweg" only in the engineering sense, and adopt the engineers' term "profile" for the slope of the valley floor, or axis. What geomorphologists call a "cross profile", or "cross section", then becomes simply "section", meaning as it does to engineers a profile at right angles to the valley axis. Adoption of these engineering terms would not only eliminate misunderstandings, but would also tend to add precision to geomorphic terminology.

The discussion of pedimentation and hillslope evolution is perhaps the most stimulating part of the paper. King's on-the-spot observations of flow over the pediment and escarpment are a real contribution to geomorphology. His analysis of flow conditions in terms of turbulence is generally sound, but it is possible that it does not go far enough. Flow over the escarpment during torrential rains is probably closely analogous with flow over the spillway of a dam, and an important phenomenon (well described in numerous books and treatises on hydraulics) may have been overlooked. This phenomenon is known as the hydraulic jump, and the remainder of this discussion is devoted to an attempt to point out its possible importance in pediment sculpture.

Water flowing over any small segment of a spillway, or an escarpment, falls at an ever-increasing rate, and as the velocity increases the sheet of falling water becomes thinner, for the volume passing over the rim at any instant must closely approximate that striking the base. If the velocity becomes high enough, the water may actually leave the face of the escarpment and fall with the acceleration of gravity. When the water reaches the base, the velocity is abruptly checked, and the segment of water under consideration becomes correspondingly thicker. Under some conditions the sheet of water formed at the base flows in a laminar manner, as stated by King, until the addition of water derived from rainfall on the pediment surface converts it into turbulent flow. Under other conditions, however, the water may pile up at the base of the escarpment to form a hydraulic jump. The position of the hydraulic jump is seldom fixed, but tends to oscillate through a certain range. Flow conditions within the hydraulic jump are extremely turbulent, and if much air is mixed in the water (as is likely to be the case in flow over high and steep escarpments) the ordinary erosive effects of turbulent water may be greatly reinforced by cavitation. Cavitation erosion may also occur along the zone where the falling water leaves the escarpment face.

It is, therefore, possible that the agency causing the extremely abrupt change in slope between the base of the escarpment and the top of the pediment is the hydraulic jump. This explanation cannot be appealed to directly in situations where loose detritus extends to the very base of the escarpment, but inasmuch as very heavy rains capable of forming a hydraulic jump are probably extremely rare, it is possible that alluviation of pediments takes place mainly between the deluges that actually form the rock-cut surfaces underlying the alluvium.

No one conversant with the subject would wish to deny that formation of pediments is probably a rather complex process. It is becoming increasingly apparent, as King so ably demonstrates, that channeled flow cannot, except perhaps in very restricted situations, account for the trimming back of the escarpments over distances of hundreds of miles. Some form of sheet flow seems to be necessary to account for this, and it may well be that the best starting point for analysis of the processes at work

is the flow of water over spillways, a subject concerning which a wealth of information has been compiled by hydraulic engineers.

Acknowledgments

Flow conditions over the escarpment and upper levels of the pediment have been discussed with Dr. Lorenz G. Straub, Director, St. Anthony Falls Hydraulics Laboratory. Minneapolis, Minnesota, and Messrs. Joseph B. Tiffany, Jr., Assistant Director, Waterways Experiment Station, and W. B. Tanner, Waterways Experiment Station, Vicksburg, Mississippi. When given the relationships of the escarpment and pediment, Doctor Straub actually gave the same picture of flow conditions that King observed during very heavy rains, but Doctor Straub also agrees that under certain conditions a hydraulic jump may be formed. This discussion was read in manuscript by Mr. W. J. Turnbull, Chief, Soils Division, Waterways Experiment Station. Mr. Charles R. Kolb, Geologist, Waterways Experiment Station, offered many helpful suggestions during preparation of this discussion.

References Cited

Bagnold, R. A., 1941, The physics of blown sand and desert dunes, New York, William Morrow & Co.

Davis, W. M., 1933, Glacial epochs of the Santa Monica Mountains, California: Geol. Soc. America Bull., v. 44, p. 1041–1133.

Fisk, H. N., 1944, Geological investigation of the alluvial valley of the Lower Mississippi River, Mississippi River Commission, Vicksburg, Mississippi.

——, 1952, Geological investigation of the Atchafalaya basin and the Problem of Mississippi river diversion, Mississippi River Comm., Vicksburg, Miss.

Friedkin, J. F., 1945, Laboratory study of the meandering of alluvial rivers: Waterways Experiment Sta., Vicksburg, Miss.

King, Lester C., 1953, Canons of landscape evolution: Geol. Soc. America Bull., v. 64, p. 721–752.

Knechtel, Maxwell M., 1952, Pimpled plains of eastern Oklahoma: Geol. Soc. America Bull., v. 63, p. 689–700.

LeGrand, H. E., 1953, Streamlining of the Carolina bays, Jour. Geology, v. 61, no. 3, 263–274.

Penck, Walther, 1924, Die morphologische Analyse, Stuttgart, J. Engelhorn.

Russell, R. J., 1940, Quaternary history of Louisiana: Geol. Soc. America Bull., v. 51, p. 1199–1234.

Sharp, R. P., 1950, Needs of modern research in physical geomorphology, Geol. Soc. America Bull., v. 61, p. 1502.

Strahler, A. N., 1952, Dynamic basis of geomorphology, Geol. Soc. America Bull., v. 63, p. 923–938.

Wolfe, Peter E., 1953, Periglacial frost-thaw basins in New Jersey, Jour. Geology, v. 61, no. 2, p. 133–141.

Woodring, W. P., Bramlette, M. N., and Kew, W. S. W., 1946, Geology and Paleontology of Palos Verdes Hills, California, U. S. Geol. Survey, Prof. Paper 207, 145 p.

WATERWAYS EXPERIMENT STATION, VICKSBURG, MISS.

BULLETIN OF THE GEOLOGICAL SOCIETY OF AMERICA
VOL. 66, PP. 1213-1214 SEPTEMBER 1955

PENEPLANATION AND PEDIPLANATION

By C. A. COTTON

In a short note there is not scope for a discussion of the question whether true pediplanation (so well exemplified in Africa, as King's (1947) studies have shown) operates as a worldwide process, under the climatic conditions now prevailing, to the exclusion of a "cyclic" dissection to maturity followed by "peneplanation"—*i.e.*, a late cycle-stage process that involves a combination of valley widening with reduction in steepness of slopes. Attention may be directed, therefore, to one portion only of King's *Canons of landscape evolution* (1953)—namely, his claim that W. M. Davis had in 1930 temporarily abandoned what King calls "old ideas of progressively flattening hill slopes." Whether the concurrence of Davis at this stage would lend support to the pediplanation thesis is beside the point. It may not need such support. One must, however, avoid reading more between the lines of a classic work than the author intended.

It is clear that Davis, in 1930, recognized the fact that processes analogous to or characteristic of pedimentation operate to some extent in every landscape. At the stage of peneplanation and even earlier he notes that valley floors have become so wide that their lateral parts have much in common with pediments. He describes them as "slowly lowering", but so, it has been shown, are pediments. He does not go so far, however, as to attribute much of the progressive reduction, "as old age comes on", in the bulk of the residuals comprising groups of "mounts and hills already well subdivided and subdued" to retreat of marginal scarps. Far from recognizing a general process of scarp retreat across the landscape, or even of very vigorous pedimentation along valley sides, which implies the presence of a more or less sharp re-entering angle at the base of retreating scarps, he points out that now "the convex profiles of the residual hills gradually become concave as they are continued down the broad valley floors." The hills have already been worn "down" to moderate relief. From now on, because all streams "will assume fainter and fainter gradients, . . . the degradational processes working on the interstream hills must continually strive to reduce them to grade . . .".

Thus the whole emphasis is on *down*wearing, which affects the whole landscape, valley floors and interfluves alike, but which is at the same time *differential, reducing relief.*

It is regrettable that in this article by Davis (1930), the text of which is wholly admirable and undoubtedly expresses his meaning clearly, some of his drawings are misleading, lending themselves to the interpretation that they convey more "advanced" views than the author held. Ambiguity seems to have crept in because of the difficulty of transferring to the graphic presentation the concepts the author had in mind. Line drawing, usually his faithful ally, failed Davis on this occasion. Each of the three figures reproduced from Davis by King (1953, Figs. 6, 7, 8) shows a re-entering angle in the valley-side slope, which Davis himself did not claim to find in nature. That it has been only unintentionally drawn into the diagrams is obvious. It is due to the artificiality of the conventional device adopted to indicate an approach to flatness in valley-floor strips, which Davis wished to emphasize and succeeded in overemphasizing. No sharp re-entering angle appears in his *profiles*, however. (*See especially* Figure 6.) Davis tended at this time to exaggerate in his drawing some insignificant differences of slope, as is shown by his absurd caricatures of flood-plain convexity in the same diagrams. That it was not his intention to show the re-entering angle he drew in Figure 7 is proved by his text, for he describes a "curved [contrasting with abrupt] change of slope to valley floor in humid mountains." (Davis, 1930, p. 149.)

Figure 6 shows no more than valley widening in a little-dissected plateau. In designing this drawing Davis improved but little on its prototype, Figure 23 of his *Erklärende Beschreibung* (1912), and it shows no change in his point of view between 1912 and 1930. Retreat of the valley side is shown, but it is by no means

parallel retreat. In Figure 7, which depicts valley development across an upland that is by this time well dissected, far more downwearing is shown to be in progress than valley-side retreat.

It is of interest to note that Professor Henri Baulig, a champion of the theory of progressive reduction of land slopes to gentler declivity, has criticized the drawing reproduced as King's Figure 7, specifically disapproving the re-entering angle it shows on the slope. His comment is that instead of this a "gradual passage from convexity to concavity is the rule for mature slopes in homogeneous structure" (1950, p. 141).

In Figure 8, used by King (who has borrowed it from Davis) to illustrate his conception of a pediplain, not only has the re-entering angle on the slope been introduced—though, it seems, unintentionally—but the flood plains of minor streams (which must have flood plains in the "humid" landscape Davis sets out to depict) are not shown at all, nor is their valley form indicated. ("Delicate modulation of valley-floor slopes is not shown"—Davis, 1930, p. 138). So much detail is omitted that the incipient peneplain introduced with no other indication of its form (relief or slopes) than a few subparallel lines cannot be claimed as embodying a revision of Davis' generalization. The original caption (Davis, 1930, Fig. 7) describes this figure as showing only "a late stage of valley-floor widening in a humid region."

References Cited

Baulig, Henri, 1950, Essais de géomorphologie: Paris, Les Belles Lettres.

Davis, W. M., 1912, Die erklärende Beschreibung der Landformen: Leipzig, Teubner.

——, 1930, Rock floors in arid and in humid climates: Jour. Geology, v. 38, p. 1–27, 136–158.

King, Lester C., 1947, Landscape studies in South Africa (Presidential address): Geol. Soc. South Africa Proc., v. 50, p. xxiii–lii.

——, 1953, Canons of landscape evolution: Geol. Soc. America Bull., v. 64, p. 721–752.

VICTORIA UNIVERSITY COLLEGE, WELLINGTON, NEW ZEALAND

REPLY TO PROFESSOR COTTON

By L. C. KING

Professor Cotton is concerned to show that W. M. Davis in 1930 did not temporarily abandon his earlier ideas of hillslope development, and regrets the "misleading" nature of some of his drawings.

The master stands in no need of apologetics. Both in his text and figures (which I quoted) Davis described accurately what he saw—and what I see.

Where I opined (p. 738) that Davis saw truly but did not fully understand because of his fixed idea of the peneplain, Professor Cotton's note implies that he neither saw nor understood.